Chapter 3

Hydrogeology

The Study on Groundwater Resources Assessment
in the Rift valley Lakes Basin in Ethiopia, Final Report (Supporting Report)

JICA
KOKUSAI KOGYO CO., LTD.

3 Hydrogeology

3.1 Satellite image analysis

3.1.1 Satellite image

The interpretation of surface information on satellite imagery to grasp the hydrogeological condition and geological structure was conducted using the following satellite imagery (Table 3.1).

Table 3.1: Satellite Image for Interpretation

Satelites	Information	Main Purpose
LANDSAT	TM(1986-1990), ETM+(2000), seven bands, ortho-rectified, 30m resolution	Surface interpretation.
SRTM	1994-, 30m resolution	Extract DEM to create contours
ASTER	2006, 3 bands, ortho-rectified	Extract DEM, Interpretation on 3D model
SPOT	2006-2007, Pacromatic, 0.5m resolution	Surface interpretation

The true color image of Spot satellite has been presented in Figure 3.1.

3.1.2 Surface interpretation

The surface interpretation of satellite imagery is explained based on the report "Rift Valley Lakes Basin Integrated Resources Development Master Plan Study Project, June 2008, Halcrow Group Limited and Generation Integrated Rural Development Consultants, Ministry of Water Resources, The Federal Democratic Republic of Ethiopia" (Hereinafter referred to as Halcrow 2008), as the Spot imagery was obtained in the middle of July 2010. Here are described basic findings extracted from Halcrow 2008. The Halcrow Report includes extensive work in the review of the interpretation using the following satellites.

Landsat MSS – 1970, (all four bands ortho-rectified)

Landsat TM - 1986-1990 (all seven bands ortho-rectified)
Landsat ETM - 2000 (all eight bands ortho-rectified)
MrSid composite images for 1987-90 (colour composite bands from bands 7, 6, 5 and 2) ortho-rectified)
MrSid composite images for 2000 (colour composite bands from bands 7, 6, 5 and 2) ortho-rectified)
Aster Imagery for 2006 (3 bands, partially orthorectified).

The land cover mapping of the RVLB at 1:250,000 has been achieved by a combination of automatic (unsupervised) imagery classification, visual (supervised) classification and ground truthing.

In terms of land cover and land use change by land cover category the following general conclusions can be drawn in reference with Halcrow 2008.
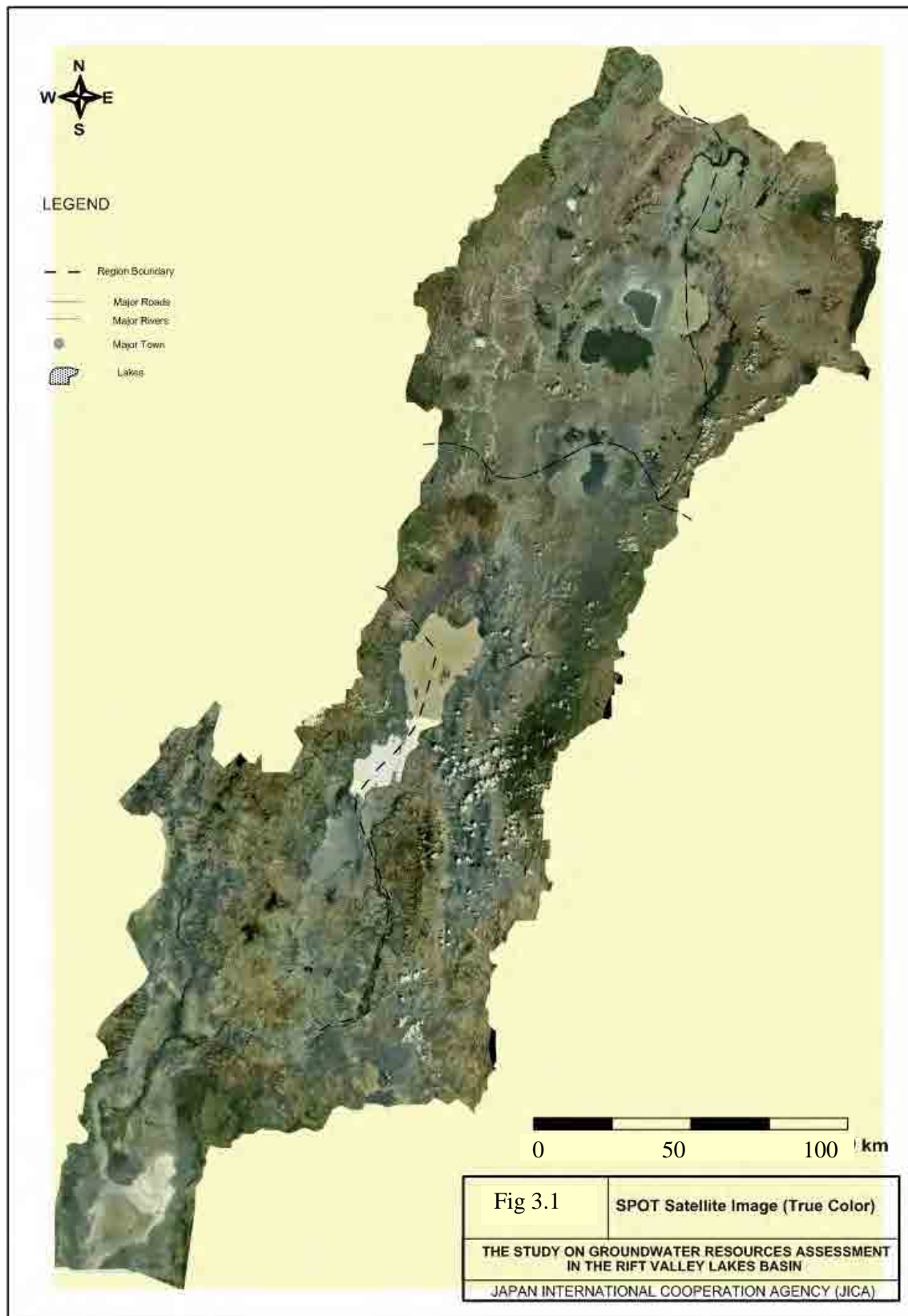
Figure 3.1: SPOT Satellite Image (True Color)

Urban: There is an evidence of expansion in urban and peri-urban land cover in the whole RVLB.

Cultivation: The extent of cultivated land is increasing but at a slower pace than in the past as the most suitable areas are already used.

Afro-alpine vegetation: The extent of afro-alpine vegetation is gradually being diminished as cultivation encroaches into this land cover type in Arsi. An intensification of cultivation on the plains could help to reverse this trend since converted lands are marginal for cultivation.

Forest: Forested areas have generally remained the same as in 1992 with some areas of expansion and some of contraction. There is evidence though of forest degradation as trees are cut down on farmland and not replaced. Forestry plantations and on-farm tree planting has been practiced in some areas but fuel wood is still in short supply in many areas.

Woodland: Areas of woodland have suffered degradation rather than deforestation in the past 20 years and there is little evidence for the expansion of woodlands.

Shrubland: Shrubland is generally confined to areas of shallow stony soils in the moister parts of the basin and these areas have not been encroached upon by cultivation. In the drier southern areas though there has been a conversion of shrubland to cultivation, particularly in flood plains close to major rivers.

Riverine Vegetation: There is little evidence for any land use change in riverine vegetation.

Grassland: There is some evidence for the conversion of grassland to cultivation in the north of the basin although the areas are very small.

Marshland: Marshlands are dynamic and can be expected to change and there is evidence of slight changes in marshlands in the past 20 years. These often include the appearance or disappearance of water bodies within the marshland and an increase in vegetative cover in former water areas.

Bare Land: There has been an increase in bare land within the basin although this is more linked to lake level change than soil erosion.

Lakes: The main changes in the lakes are confined to Lake Abiyata, the level of which has fallen dramatically between 2000 and 2006 and the former lake Chew Bahir which is now mainly a salt flat with very little water remaining.

The conclusions that can be taken from the land cover/land use study are that the pattern of land cover has not changed significantly or dramatically in the past 21 years. However, the nature of land use has changed in that an ever increasing population is reliant on a similar area of land to feed itself, which, without an increase in productivity, is becoming increasingly difficult to do. This problem is compounded by the fact that, through being in continual use, the ability of the land to produce is declining.

3.1.3   Digital elevation model

The Digital Elevation Model (DEM) was generated from the SRTM and Aster Satellite imagery. The data was applied to create contours and shaded relief model to understand the surface characteristics of the study area. The shaded relief model was generated to assess the lineaments and other geomorphological marks (such as volcanic craters) to support the structural evidence in relation to its geological setting and history. Shaded relief model and the major lineaments are presented in Figure 3.2 and Figure 3.3.
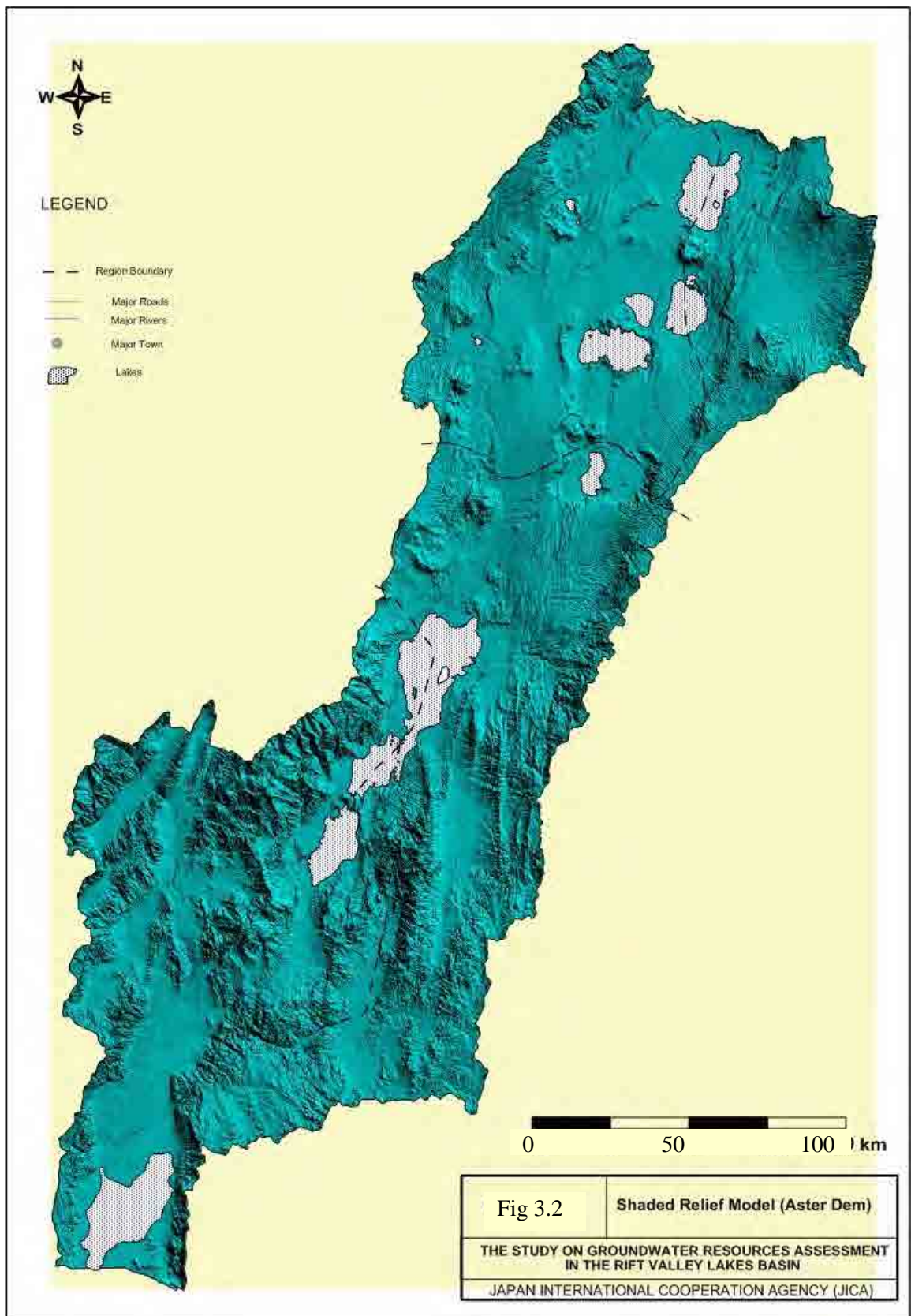
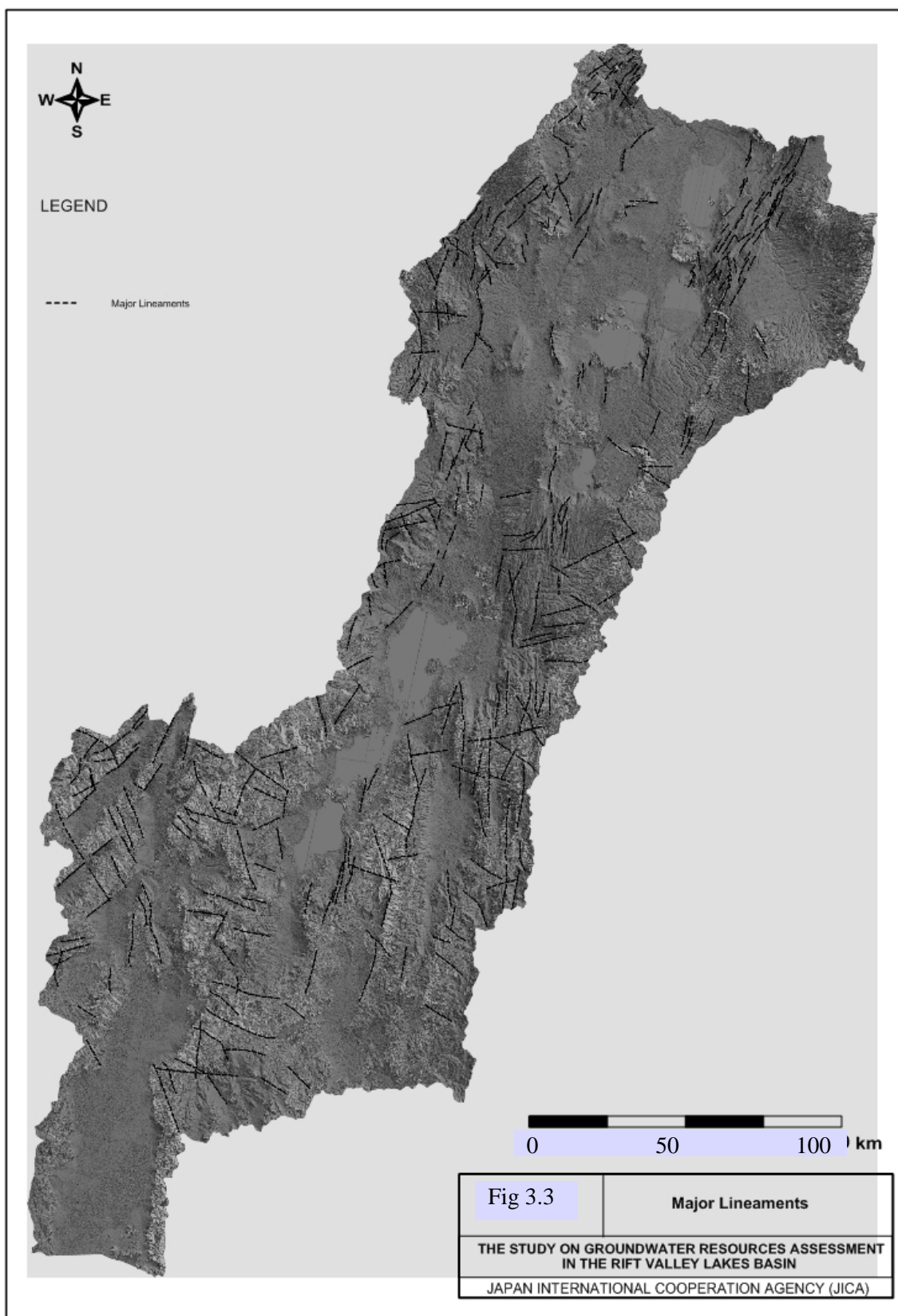Figure 3.2: Shaded Relief Model (Aster DEM)

Figure 3.3: Major Lineaments

The shaded relief model presents general geomorphological conditions in the Study Area. The Rift Valley Lakes Basin could be divided into two areas. The northern portion of the area around the lakes of Ziway to Awasa is almost flat in the valley bed with several mounds of hills in the west. The hills are mostly in the shape of cone or semi-conical crests that leave the traces of past volcanic activity. The eastern terrain shows the stepwise crests bounding the eastern end of the valley. The lineaments of NNE – SSW direction are mostly abundant.

In contrast to the northern geomorphological conditions, the southern area, from Lake Abay to Chew Bahir, has relatively precipitous terrain. East of Lake Abay-Chamo is characterized by a continuous range of mountains in a N-S to NNE-SSW orientation, and the lineaments can be tracked up to Lake Awasa. ENE-WSW oriented liniaments are also abundant in the northern portion.

The geological structures are characterized by two major rifts, the Main Ethiopian Rift (MER) and the South-western Ethiopian Rift (SWR), both of which are encompassed in RVLB.   The MER extends from the southern Afar margin to the Lake Chamo area, whereas the SWR is located to the west and represents roughly N-S trending basins related to the Kenya Rift. The Gregory rift of Kenya links to the north with Chew Bahir rift. In accordance with Halcrow 2008, the character of the faults in the two rifts is explained as follows.

Main Ethiopian Rift (MER)

The MER constitutes an area characterized by active extensional tectonics, due to an E-W oriented direction of extension. Two main fault systems have been identified in the MER: a N300E – N400E trending fault system, which characterizes mainly the rift margins, and a N-S to N200E trending fault system, the Wonji Fault Belt (WFB), which shows a number of sigmoidal, overlapping, right-stepping en-echelon fault zones, obliquely cutting the rift floor.

The margins of the MER are characterized by a few widely spaced faults with very large vertical displacements, to the rift floor. The eastern margin is well developed and it is defined by a more or less continuous system of boundary faults, whereas the western border is marked by only a few major faults in the Mt. Guragie area. The MER attains a width of about 100 km in its centre, between Fonko and Lake Langano, but narrows southward in the Lake Abaya region, where it is bifurcated by the N-S striking Amaro horst. This separates the Ganjuli basin in the west from the Gelana depression in the east.

The rift floor is affected by dense fault swarms, exhibiting relatively small throws (<100m). The rift floor faults have steep scarps related to the Wonji Fault Belt (WFB), which commenced its formation around 1.6 Ma. These sub parallel faults caused widespread deformation affecting the rift floor. In the centre of the rift floor, these faults are orientated at 200° with respect to the main trend of the rift.

The faults of the WFB, affecting the rift floor, are closely spaced, commonly en-echelon and linear or curved in plan view over distances of up to a few tens of kms. They delineate many fault bounded blocks. Associated with these faults are open fissures with or without vertical displacement, splay patterns, aligned cinder cones and complex rhomb-shaped structures.

South-western Ethiopian Rift (SWR)

The Gofa Basin and Range and Chew Bahir rifts dominate the area west and south of the Chamo Graben (Ganjuli graben) and consist of NE-SW trending fault blocks of Tertiary lavas tilted to the NW. Displacement along enclosing high angle faults diminishes due north, along strike, and the Gofa basin and range loses its topographic feature near latitude 6°30' being replaced by a few NE-SW trending stream valleys. In the north, this NE-SW

orientation is completely replaced by the E-W oriented Gojeb Graben. In the south, the southern Chew Bahir rift is more or less symmetric with its conspicuous, N-S trending, slightly curvilinear, main fault to the eastern side. Vertical displacement changes along strike and a maximum of about 200 m was encountered on the western main border fault, South of Woyito horst. The main border faults display a noticeable change of direction, striking approximately NNW. In this region the NE-SW oriented border faults have been interrupted by NNW-SSE oriented fault systems.

3.2   Previous studies of hydrogeology

3.2.1   General

The following data, reports and studies are referred to in this study

Topographical Maps
Ethiopian Mapping Authority (EMA)
        Scale   1:250,000   Sheet "NC37-14"   AK'AK' BESEK'A
                            Sheet "NC37-15"   NAZRET
                            Sheet "NB37-2"   HOSA'INA
                            Sheet "NB37-3"   ASELA
                            Sheet "NB37-5"   SAWLA
                            Sheet "NB37-6"   DILA
                            Sheet "NB37-9"   JINKA
                            Sheet "NB37-10"   AGERE MARYAM
                            Sheet "NB37-13"   IST'IFANOS HAYK
                            Sheet "NB37-14"   YABELO

Geological Maps
Geological Map of Ethiopia 1:2,000,000 Scale (GSE, 1996)
Geological Map of AGERE MAYAM "NB37-10" 1:250,000 scale (GSE, 1997)
Geological Map of SOLOLO "NA37-2" 1:250,000 scale, (GES, 1997)
Geological Map of The Ethiopian Rift 1:500,000 scale (GSE, 1981)
Maps of the central part of the rift 1:750,000 scale (Di paola, 1972 and 1976)
Geological map of northern and central parts of the Amaro Horst and adjacent regions 1:500,000 scale (Levitte, D. 1974, unpublished)
Geological map of Lake Ziway area, 1:500,000 scale (Birhane et al., 1976 unpublished)
Seife M. Berhe, 1978, Nazreth geological map 1:250,000 scale, EIGS.
Geological map of northern Lake Abaya, 1:250,000 scale (Birhane et al., 1981)
Geological map of Omo River Valley Project Area (southern halef), 1: 250,000 scale (Davidson et al., 1973)
Geological map of Omo River Valley Project Aresa, 1:500,000 scale (Davidson, 1983)
Geological map of Oromiya Region, 1:1,000,000 scal (Geoder-Afred, 1999)
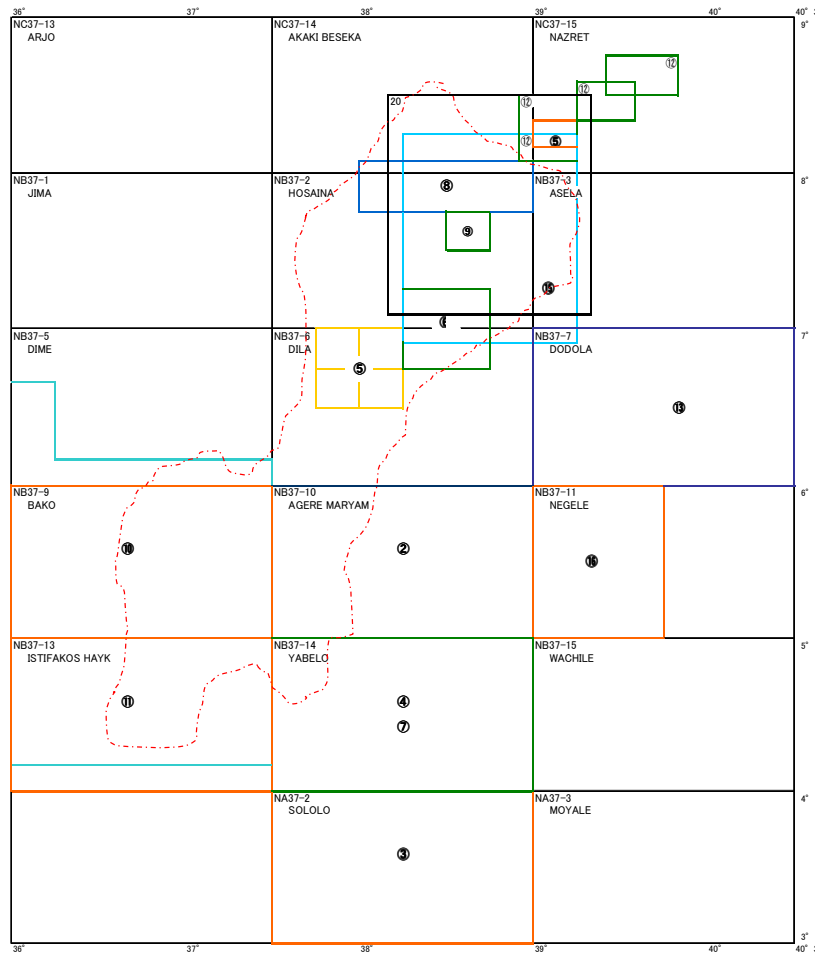Geological map of Lake Ziway-Asela Region 1:50,000 scale)Bekele et al., 1990)
Geological map of northern main Ethiopia Rift 1:200,000 scale (Tsigaye et al., 2005)
Geological and surface hydrothermal alteration maps of north-western Lake Abaya area, 1:50,000 scale (Tadiwos et al ., 2002)
Geological Map of Agere Mariam Map Sheet (NB 37-10) (W/Gabriel et al., 1997)

#	Code	Description	Scale
1	821-401-02	Compiled by A.DAVIDOSON, 1983, GSE THE OMO RIVER PROJECT Reconnaissance Geology and Geochemistry of Parts of Ilubabor, Kefa, Gemu Gofa, and Sidamo	scale = 1: 500,000
2	821-701-59	Compiled by WOLDEGABRIEL GENZEBU, NASIR HASSEN & TESFAYE YEMANE, 1994 GEOLOGY OF THE AGERE MARYAM AREA	scale = 1: 250,000
3	821-701-75	Compiled by Solomon Gerra and Amenti Abraham, 1999, GSE GEOLOGY OF THE SOLOLO AREA	scale = 1: 250,000
4	821-701-91	Compiled by Hailemeskel Awoke and Fekadu Hailu, 2007, GSE The Geology of Yabelo Map Sheet (NC37-14)	scale = 1: 250,000
5	860-051-28	Compiled by Abebe Ayele, Meseret teklemarian and Solomon Kebede, 2002, GSE Geothermal resource Exploration in Abaya and Tulu Moye Gedemisa geothermal Prospects, Main Ethiopian Rift	scale = 1: 50,000 & 1:20,000 (5area)
6	880-701-15	Tadesse Dessie, Zenaw Tessema,2003 Hydrogeology and Engineering Geology of Awassa Lake Cachement	scale = 1: 75,000 (Geo. & Eng. Map)
7	880-701-13	Yohannes Belete, Bekele Abaire, Bayesa Asfaw, Moges Tigabe, Degefe Shiferaw, Melese Belachew, Nigatu Adege(Dr), Alemay Hydrogeological, geophysical and engineering Geological Investigation of Yabelo Sheet (NB37-14)	scale = 1: 250,000 (Hydro. & Eng.)
8	– –	EWTEC, 2008 Butajira-Ziway Area Development Study Project, Hydrogical Map	Hydrical Map scale = 1: 150,000
9	860-451-17	elc electroconsult milano Itaria(1986) Ministry of mines and energy Geothermal exploration project ethiopian lakes district rift, exploitation of langano-aluto geothermal resources feasibility repo	Report (CD2)
10	880-401-02	Niri Sika, (1987) Hydrogeology and hydrochemistry of the Bako and Ist'Ifamos Hayk' area NB37-9 and NB37-13	
11	880-701-12	Yohannes Belete, Bayesa Asfaw, Muhedin Abdela, Dinku Belay, 2000, GSE Hydrogeological and Engineering Geological Investigation of Chew Bahir Sheet (NB37-13)	scale = 1: 250,000 (Hydro. & Eng.)
12	860-051-44	elc electroconsult, geptermica, (1987) Ministry of mines and energy geothermal reconnaissance study of selected sites of the ethiopian rift system geological report	scale = 1: 50,000
13	821-751-051	(No detail Info), 1997, GSE – Geology of the DODOLA AREA	scale = 1: 250,000
14	880-051-29	W. George Darling, Berhahu Gizaw and Musa K. Aruset, (1996) Lake groundwater relationships and fluid-rock interaction in the East African Rift Vallay	
15	880-051-16	Tesfaye Charnet, 1982 Hydrogeology of the Lakes Region, Ethiopia (Lakes Ziway, Langano, Abiyata, Shalla and Awassa)	
16	912-701-05	Tadesse Yihume, 2003 Chemical Th-U-total Pb isochronage of zircon and monazite from granitic rocks of the Negele area, southern Ethiopia	
17	860-051-09	Befekadu Oluma, Abiy Hunegnaw, Ketsela tadese and Mohammedberham Abdulkadir, 1986 Geothermal Exploration Project Lakes District	
18	860-051-15	Mohammedberham Abdulkadir, 1992 Interpretation of schulumberger Soundings and Head-on Profiling	
19	880-051-23	Continental Consultants,2002 Ethiopian Guidline Specification for Drinking Water Quality	
20	– –	N. Dainelli, M. Benvenuti, M. Sagri, 2001 (Department of Earth Sciences, University of Florence, Italy) Geological Map of the Ziway – Shala Lakes Basin	

Figure 3.4: Reference of Compiled Geological Map

The Study on Groundwater Resources Assessment
in the Rift valley Lakes Basin in Ethiopia, Final Report (Supporting Report)

JICA
KOKUSAI KOGYO CO., LTD.

Hydrogeological Map
Hydrogeological Map of Ethiopia 1:2,000,000 scale (GSE, 1988)
Hydrogeological Map of The Lakes Region 1:250,000 scale (GES, Compiled by Tesfaye Chernet, 1982)
Hydrogeology of Nazret 1:250,000 scale (GSE(Compiled by Getahun Kebede), 1985)
Hydrogeological Map of Butajira-Ziway Area 1:150,000 scale (EWTEC, 2008)

Publications:

Abebe A., Meseret T-M., and Solomon K., 2002 Geothermal Resources Exploration in Abaya and Tulu Moye-Gedemsa Geothermal Prospects, Main Ethiopian Rift, GSE. Addis Ababa, P12-39, 2-119.

Altaye, E, Befekadu Oluma, Abiy Hunegnaw, Ketsela Tadesse, Mohhamedberhan Abdulkadir (1986): A review of geological and geophysical exploration of Corbeti geothermal prospect, Ethiopia. Proceeding of 8th NZ Geothermal Workshop, p205-211.

Bigazzi, B., Bonadonna, F.P., Di Paula, G.M. and Giuliani, A., 1993. K-Ar and Ission Track Ages of the Last Volcano Tectionic Phase in the Ethiopian Rift Valley (Tulu Moye area). In, Geology and Mineral Resources of Samelia and Surrounding Regions, 1st Agron. Oltermore (Firenze), Vol, 113, P311-322

Birhane M., Molla B., Negusie M., Paulos T-G., and Tesfaye T-M., 1981. Geological Report on Northern L.Abaya Geothermal Region, Geothermal Exploration Project, EIGS, Addis Ababa
Davidson, D. C. Rex (1980): Age of volcanism and rifting in southwestern Ethiopia. Nature Vol. 283, p657-658 (hardcopy only)

Davidson, A.et. al., 1983. The Omo River Project, Reconnaissance Geology and Geochemistry of Parts of Ilubabor, Kefa, Gemu Kefa and Sidams, Ethiopia, EIGs

Di Oaika, G.M., Seife M. Berhe and Arno, V., 1993. The Kella Horst. Its Origin and Signigicalnce in Crustal Attenuation and Magimatic Processes in the 'Ethiopian Rift Valley In: Abbata, E., Sagri, M. and Sassi, F.P. (eds.) Geology and Mineral Resources of Somalia and Surrounding Regions. Instituto Agronoica per I'obtremare, Fireze, vol. 113,P 323-338

Di Paula, M., 1990. Geological, Geothermal Report on Central Part of the Main Ethiopian Rift Valley, GSE

Di Paora M., (1972): Geology of Corbetti Caldera Area. Bulletin of Volcanology Vol. 35, p497-506.

Ebinger, C.J., Yemane, T., W/Gabriel, G., Aronson,J.L, and Walter, R.C., 1992. Late Eocene-Recent Volcanism and Faulting in the Southern Main Ethiopian Rift, Jour. Of the Geol. Society of London, v.150, p99-108.

Ebinger, C.J. and Casey. M., 2001. Continental Break Up in Magmatic Probinces. An Ethiopian Example, Geology, V.29, P527-530, doi: 10.1130/0091-7613 (2001) 0292.0.co;2.

EIG-UND, 1973. Geology, Geochemistry and Hydrology of that Springs of the East African Rift System within Ethiopia, UN report, New York

Electro Consult, Geothermic Italiana, 1987. Geothermal Reconnaissance Study in the Selected Sites in the Ethiopian Rift System. EIGS lib No. 840-051-40-I Geological Report. ELC, Milano, Italy-Geothermal Italiana, Pisa, Italy.

Grove, A.T, F. Alayne Street, A. S. Goudie (1975) Former lake levels and climatic change in The Rift Valley of southern Ethiopia. The Geographical Journal, Vol. 141-2, p177-194

Katoh/Shigehiro, Shinji Nagaoka, Giday WoldeGabriel, Paul Renne, Mjorie G. Snow, Yonas Berene, Gen Suwa (2000): Chronostratigraphy and correlation of the Plio-Pliestcene tephra layers of the Konso Formation, southern Main Ethiopian Rift, Ethiopia. Quaternary Sciences Reviews Vol. 19, p1305-1317

Kazmin, V. and Seife M.Berhe, 1978. Geology and Development of the Nazreth Area, Northern Ethiopian Rift, EIGs.

Levitte, D., Colomba, J, and Mohr, P. 1974. Reconnaissance Geology of the Amaro Horst, Southern Ethiopia Rift

Le Tuldu/C, Jean-Jacques Tiercelin, Elisabeth Gibert, Yves Travi, Kiram-Eddine Lezzar, Jean-Paul Richert, Marc Massault, Francoise Gasse, Raymonde Bonnefille, Michiel Decobert, Bernard Gensous, Vincent Jeudy, Endale Tamrat, Mohammed Umer Mohammed, Koen Martens, Balemwal Atnafu, Tesfaye Chernet, David Williamson, Maurice Taieb (1999) : The Ziway-Shala Lake basin system, Main Ethiopian Rift : Influence of volcanism, tectonics and climatic forcing on basing formation and sedimentation. Palaeogeography, Palaeoclimatorogy, Palaeoecology Vol. 150, p135-177.

Mengesha Teferra, Tadiwos Cherenet and Workneh Haro, 1996 Explanatory Note for the Geol. Map of Ethiopia (2nd edi) Ball, No. 3, EIGS, Addis Ababa, Ethiopia.

Mohr, P.A., J. G. Mitchell, R. G. H. Raynolds (1980): Quaternary Volcanism and Faulting at O'A Caldera, Central Ethiopia Rift. Bulletin of Volcanology Vol. 43-1, p173-189.
Mohr, P.A., 1987. Patterns of Faulting in the Ethiopian Rift Valley. Tectonophysics, V.143, P 169-179, doi 10-1016/0040-1951 (87) 90086-2

Mohr, P.A., 1967. The Ethiopian Rift System. Bulletine of the Geophysical Observatory, Vol.71,P1-65, Addis Ababa.

Mohr, P.A., 1962. The Ethiopian Rift System. Bulls of the Geophysical Observatory, Addis Ababa, Vol.3, P33-62

Robert L. Laury, Claude C. Albritton Jr. (1999): Geology of Middle Stone Age archeological sites in the Main Ethiopian Rift Valley. Geological Society of America

Stephan Thiemann, Gerd Forch (2004): Water Resources assessment in the Birate River catchment – Precipitation Variability -. Lake Abaya Research Symposium 2004 Proceedings, p73-78.

Tadiwos Cherinet and Solomon Kebede, 1999. Geological and Surface Hydrothermal Alteration Mapping of NW DL. Abaya, at 1:50,000 scale, GSE, Geothermal Division, Internal report.

Tamiru A. Abiye (2008): Environmental resources and recent impacts in the Awassa collapsed caldera, Main Ethiopian Rift. Quaternary International Vol. 189, p152-162

Tesfaye Abebe, 1987. Geological and Petrochemical Study of Tulu Moye and Gedemsa Geothermal Project, Pisa, Italy.

Tesfaye Mamo, 2000. Report on the Geology and Surface Hydrothermal Alteration Around Tilu Moye Gedemsa Area for Siting Temperature Gradient Holes, GSE Geothermal Division, Internal Report.

W/Gabriel G., J.L. and Walter, R.c., 1990 Geology, Geochronology and Rift Basin Development in the Central Sector of the Main Ethiopian Rift: Geol. Society of America, Bull.,V.102, P439-458, doi: 10.1130 /0016-7606 (1990) 1022.3-coj2

W/Gabriel, G., Gesfay, Y., White, T., Asfaw, B.and Suwas G, 1991. Age of Volcanism and Fossils in the Buji=Soyoma Area, Amaro Horst, Southern Main Ethiopian Rift Journal of African Earth Sciences, V.13, P437-447, doi: 10.1016/0899-5362 (91) 90107-A.

W/Gabriel, G., Aronson, J.c., Walter, R.C. and Hart W.K., 1992. Geochronology and Distribution of Silicic Volcanic Rocks of Plio-Pleistocene Age from the Central Sector of the Main Ethiopian Rift Quaternary International, V.13-14, P69-76, doi 10-1016/1040-6182 (92) 90011-9

W/Gabriel, G., Nasir H., and Tesfaye Y., 1994. Geology of the Agere Mariam Area. Addis Ababa, Ethiopian Institute of Geological Surveys, Memoir No. 8.

W/Gabriel, G., Walter, R.C. and Hart, W.K., Mertzman, S.A. and Aronson, J.L., 1999. Temporal relations and Geochemical & Feature of Felsic Volcanism in the Central Sector of the Main Ethiopian Rift Acta vulcanologica, V.11, P53-67.

W/Gabriel G, Grant Heiken, Tim D. White, Berhane Asfaw, William K. Hart, Paul R. Renne (2000): Volcanism, tectonism, sedimentation, and the paleoanthoropological record in the Ethiopian Rift System. Geological Society of America Special paper 345, p83-99.

3.2.2   Summary of review

Most of the collected data, reports and studies are related to the various geological studies in the RVLB. Those reports are collected mainly from GSE, AAU and MoWE. In relation with the hydrogeological study of RVLB, there are two important studies that were reviewed from hydrogeological point of view. They were the following projects;

Halcrow 2008

The project of "Rift Valley Lakes Basin Integrated Resources Development Master Plan Study Project, June 2008, Halcrow Group Limited and Generation Integrated Rural Development Consultants, Ministry of Water Resources, The Federal Democratic Republic of Ethiopia" is refered to in this project as Halcrow 2008.

The Halcrow 2008 compiled studies both in geology and hydrogeological condition of the RVLB, and is most up to date study in the area. This report includes almost all references of the past documents including geological maps and hydrogeological consideration of the area. Therefore, this report can be considered as the overall reference of past reports.

The geological map of Halcrow 2008 made in combination of standard 1:250,000 scale geological mapping by the Geological Survey of Ethiopia and unpublished geological maps (mostly from AAU) and accompanying geological notes partially covering parts of the basin include:

Omo River Project Area: Under a bilateral assistance agreement between the Ethiopian and

Canadian Governments, regional geological mapping and geochemical mapping and geochemical exploration was carried out in the Omo River Valley region between 1972 and 1974 by the Ethio-Canadian team. This comprised of an area of approximately 81,000 km^2. The mapped area covers relatively a small part of the most southwestern corner, in the Chew Bahir area of the RVLB.

Agere Mariyam Map Sheet (NB 37-10) and Yabelo Map-sheet (NB 37-14): Geological mapping at the 1:250,000 scale conducted over the period between 1986 and 1989 (Agere Mariyam), 1999 and 2000 (Yabelo) by the Geological Survey of Ethiopia. The geological map at 1:250,000 scale has been published (W/Gabriel et al., 1997), whereas the accompanying geological report has remained unpublished (W/Gabriel et al., 1994).

Other Geological Maps: Geothermal Project exploration teams produced unpublished geological northern Lake Abaya area at 1:250,000 scale (Birhane et al., 1981) and Lake Ziway area 1:500,000 scale (Birhane et al., 1976) and 1:500,000 scale geological map of northern and central parts of the Amaro Horst and adjacent region (Levitte, 1974).

Also, the geothermal exploration team produced detailed (unpublished) 1:50,000 scale geological and surface hydrothermal alteration maps of the area northwest of Lake Abaya (Tadiwos et al., 2002) covering about 3000 km^2 area. More recently Tsegaye et al., (2005) published 1:200,000 scale geological map of Ziway area and an accompanying report.

ENGWIS

This project is initiated to develop a comprehensive data management system in the water sector for Ministry of Water & Energy (MoWE), GSE and Regional Water Bureau (RWB) funded by UNICEF. The project period is from June 2009 to March 2010.

The project focused on the establishment of centralized web-enabled information system and the training of the collection, compilation and utilization of the groundwater resources by the governmental and regional organizations.

This project does not include the reports but compiled the data collected from various sources related to the groundwater resources. The data set used in this project covers the whole of Ethiopia and includes updated data of RVLB area.

The data on RVLB was extracted from the database constructed by this project. Most of the compiled data is not fully transferred to computer files. However, the data set includes important parameter such as; well location, yield, water level, aquifer formation and its depth, water quality etc.

Other References

Extensive studies of the rift structures and volcanism in Ethiopia were conducted by French-Italian and former West German earth science teams in the late 1960s and early 1970s and produced very detailed descriptions of its petrology and structure.

Along with the scope of the project, one of the important issues in the geological section is to clarify the stratigraphical correlation of the volcanic activity and the continuity and distribution of the formations. Detailed references and compilation of the geological studies are described in the Chapter 3.

3.3 Characteristics of sub-basins

The rivers and streams distributed in the study area flow into the lakes in the middle of the valley. Therefore, the distribution of the lakes should be considered to classify the river networks in the area into the sub-basins. The main lakes (water surface of more than 100km^2) are: Ziway, Langano, Abijata, Shalla, Awassa, Abaya, Chomo and Chew Bahir. The lakes are divided into four lake basin groups of, Ziway-Langano-Abijata-Shalla basin, Awassa basin, Abaya-Chamo Basin and Chew Bahir basin based on its formation environment (basically Alluvium deposits) and their distribution. This classification seems to be reasonable as this is based on not only considering the inflow to the lake groups and its geological background but also have been standard of basin classification in the area. This Report also refers to this classification. The classification into sub-basins from the lake basin groups will be described as follows.

3.3.1 Classification of sub-basin

As aforementioned the major water basin will be divided into following four major groups:

1. Ziway-Shlla basin

2. Awassa basin

3. Abaya – Chamo basin

4. Chew Bahir basin

These basins are independent hydrological closed systems. However, it is too large scale classification for the purpose of this study, which is to grasp the hydrogeological relationship between basins and geological settings. Therefore the basin groups are divided into sub groups. The cross section along the lakes is shown in Figure 3.5.
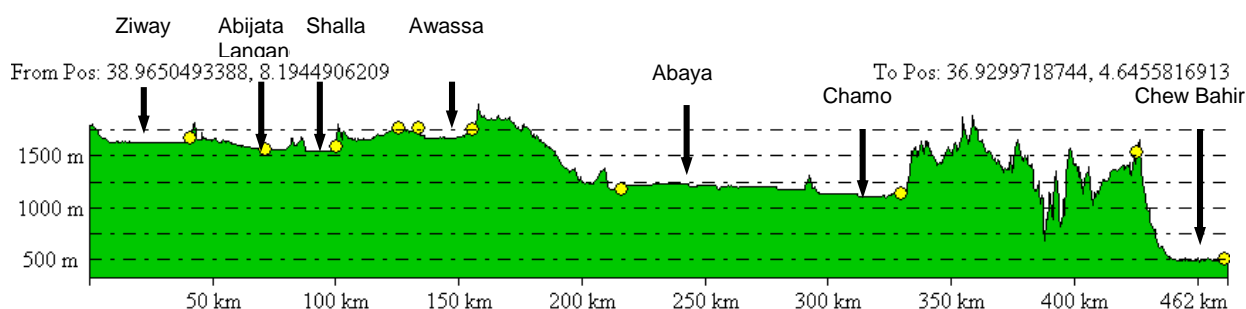
Figure 3.5: Cross Section of Major Lakes (with Lake Heights)

The major basins are classified into sub-basins in accordance with the river end of the respective rivers and its characteristics.

a.   Ziway-Shalla Basin

Respective sub-basins are divided by the rivers inflow of each lake. The Lake Ziway has mainly two inflow rivers and tributaries as sub-basins. These are Eastern Ziway sub-basin and Ziway-Abijata sub-basin. The river inflow at the western side of Lake Ziway is not clearly distinguished whether it flows into Lake Abijata or Lake Ziway. The tributaries

flowing into Lake Abijata and Lake Ziway from the west are defined as Ziway-Abijata sub-basin. Lake Langano has its own independent tributaries and rivers, and is classified as Langano sub-basin. Lake Shalla has western and eastern tributaries. They are considered as one basin as Lake Shalla sub-basin.

b.   Awassa Basin

Lake Awassa was considered as one independent sub-basin as Awassa sub-basin. This Lake is a completely closed system with its tributaries and rivers (if not considering groundwater outflow of the other lower lakes). It consists of a series of small streams flowing westerly from the eastern edge of the crest of Rift Valley, and they are directed into Lake Awassa pooled by the volcanic hills of Humo and Abaye in the east. The altitude of the Lake Awassa is higher than Lake Shalla and Abaya. Therefore, the interaction through the groundwater between Lake Awassa and other lakes can be assumed. Although a number of studies have been made in this area, the interaction and hydrology of Lake Awassa sub-basin is not clearly understood.

c.   Abaya-Chamo Basin

Lake Abaya is the largest lake in the Rift Valley Lakes Basin. The classification of the sub-basins is mainly focused on the major rivers and its tributaries flowing into this lake. Several major rivers flow into the two lakes. The major rivers and their tributaries correspond to the name of the sub-basin such as: Bilate river (Bikalate sub-basin), Gidabo river (Gidabo sub-basin), Amessa and Guraccha rivers (Amessa Guracha sub-basin), Kulfo and Gina rivers (Kulfo-Gina sub-basin). There are some arguments on the interaction between Lake Abaya and Lake Chamo, of which one supports the interconnection with Lake Chamo, and the other is independent two lakes. The major inflow of Lake Chamo is Sife and Chamo rivers, hence the sub-basin was classified as Chamo Sife.

d.   Chew Bahir Basin

The most southward basins in the study area were wrapped into Che Bahir basin. There are two major rivers namely, Segen, Weyto. Haru Shet river originates its flow at the east of Lake Chamo and Abaya, and flows west between the mountain range of Siyema and Yeterara Senselet and finally intersects with the Segen river. This area is defined as Segen sub-basin. Other small stream networks south of Lake Chamo are defined as Konso localised sub-basin, and the area of tributaries along the Weyto river is defined as Bezo Weyto sub-basin.

Table 3.2 shows the major basins and classification of sub-basins. The classification of sub-basins and their locations are presented in Figure 3.6.

Table 3.2: Major Basins and Classification of Sub-basins

| No	Large Scale Classification	No	Sub-basins	Total Area (km^2)
1	Ziway-Shalla	1	Western Ziway-Abijata	4398
		2	Eastern Ziway	3434
		3	Lake Shalla	3762
		4	Lake Langano	1807
2	Awassa	5	Lake Awassa	1201
3	Abaya-Chamo	6	Bilate	5419
		7	Amessa Guracha	1125
		8	Gidabo	3491
		9	Kulfo Gina	1302
		10	Sife Chamo	1436
		11	Galana	3856
4	Chew Bahir	12	Bezo Weyto	12143
		13	Konso Localized	1685
		14	Segen	5230
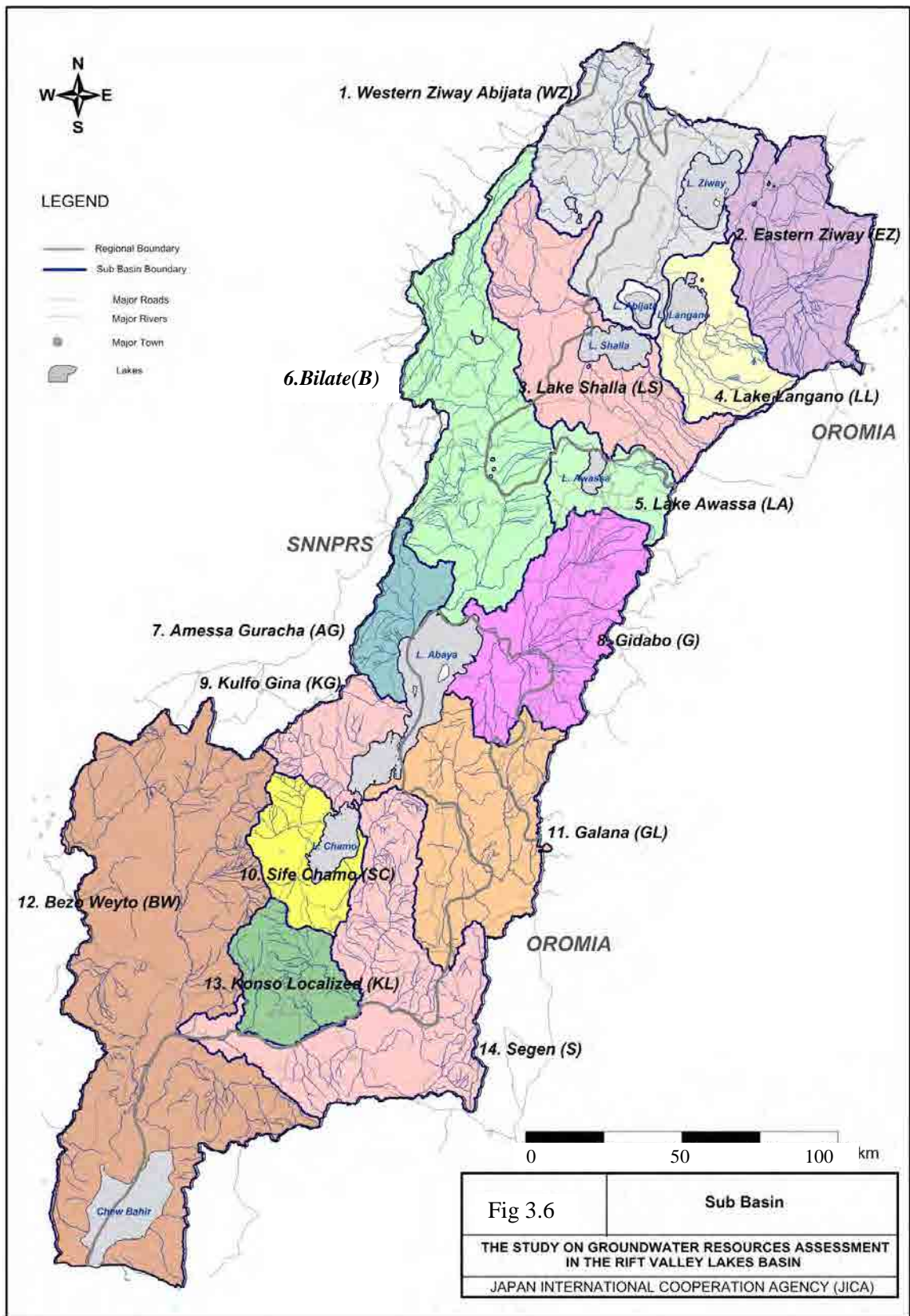
Figure 3.6: Sub-Basins

3.3.2 Topographic and hydrographic system of sub-basins

Characteristics of respective sub-basins in terms of topographic and hydrographic features are compiled into Table 3.3. As for the reference of the topographic features of sub-basins, it is presented in Figure 3.7 with a shaded relief model.

Table 3.3: Topographic and Hydrographic Nature of Sub-basins

No	Major	No	Sub-basins	Topography	Major Stream System	Area (km²)
1	Ziway-Shalla	1	Western Ziway-Abijata	Steep cliff and caldera walls at the west, gently slopes and low hilly terrain at East. Almost flat low land between East Butajira and Lake Ziway-Abiyata.	Meki river is major river in the area. Highly affected by the topographical profile which flows northerly in the west and easterly in the east. No major inflow is found near Lake Abijata	4398
		2	Eastern Ziway	Foot of Galema mountain range (altitude of 4000m) extends to cone shaped hollow. Passing fault cliff towards lower flat land of Lake Ziway. River gradient is relatively high.	Several ramiform stream networks are dominant and gather into the Ketar river. Flow direction is mainly WNW-ENE	3434
		3	Lake Shalla	Extends NW-SE direction. Steep cliffs are dominant at the margin of the valley. Flat low land around Lake Shalla. Several volcanic cones are observed.	Only minor non perennial rivers are found as inflow to the Lake. Small stream networks formed at NW-SE direction.	3762
		4	Lake Langano	At the foot of Kaka and Kubsa mountain range (4000m) with fault cliff of 100m, and reach at the flat of Lake Langano.	Only minor non perennial rivers are found as inflow to the Lake. Small stream networks formed at NW-SE direction.	1807
2	Awassa	5	Lake Awassa	Height difference of 600m between eastern cliff and Lake Awassa. The lake is surrounded by Humo mountain range at west.	Small stream network developed in the direction of EW. Large swamp of 100km² formed at west of the Lake	1201

No	Major	No	Sub Basins	Topography	Major Stream System	Area (km^2)
3	Abaya-Chamo	6	Bilate	Gentle slope along the Bilate river. Fault cliff and volcanic cones formed at the West.	Total length of the river exceeds 3km and it is the longest river system in the whole area. It inflows into Lake Abaya.	5419
		7	Amessa Guracha	Surrounded by a 2500m high mountain range, and forms wide flat land near Lake Abaya.	Gathering the small stream networks of all directions along the cone shaped slope of mountain range and join into the Amessa, Guracha rivers to Abaya.	1125
		8	Gidabo	300m high fault cliffs in the east. Mostly consists of steep hills but low flat land near Lake Abaya.	Major river system is Gidabo river. Collecting small streams over the direction of NS. Eastern direction near the Lake	3491
		9	Kulfo Gina	Occupied by high (3000m) mountain range and rarely found flat land.	The valley developed at NE-SW direction. The major river is Kuflfo river.	1302
		10	Sife Chamo	Mountain range developed surrounding Lake Chamo	Major rivers are flowing from southern and western hills toward Lake Chamo.	1436
		11	Galana	Tectonic line developed in NS direction. Wide valley exists between Furfursa、Haro mountain range.	Rivers flow in between Furfursa、Haro mountain range and join Galena river with the direction of NS to NW.	3856
4	Chew Bahir	12	Bezo Weyto	Tectonic line developed in NS direction. Predominant of fault cliff at east and west of the area.	Major river is Weyto river, and it is more than 200km in length. Flows toward the south	12143
		13	Konso Localized	Massive mountain range developed. Hilly terrain.	Short stream network developed and join Segen river.	1685
		14	Segen	Mountain range along the tectonic line is abundant. Steep valleys exist along the range.	Segen river is the major river which flows in an EW direction.	5230

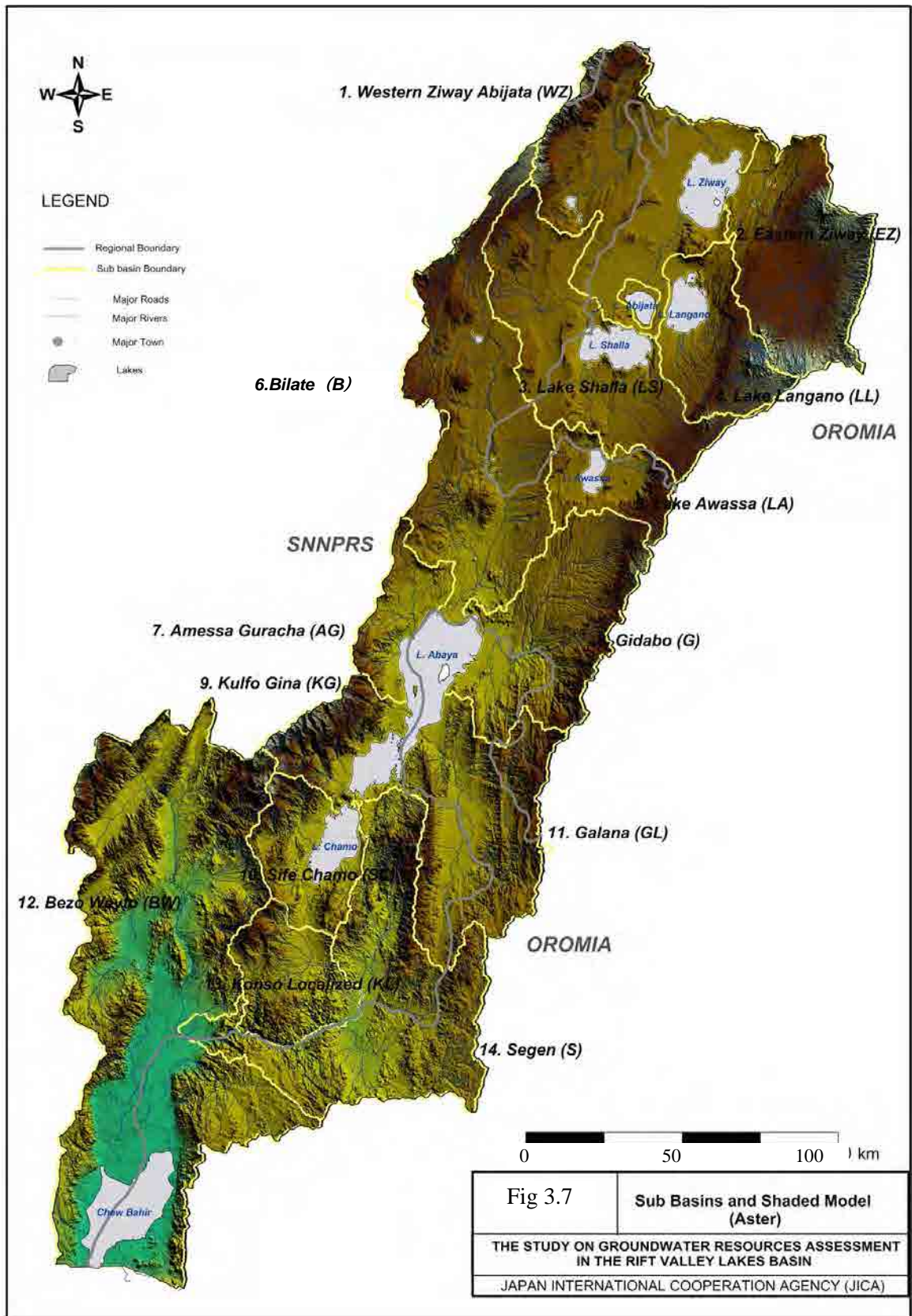| Fig 3.7	Sub Basins and Shaded Model (Aster)
	THE STUDY ON GROUNDWATER RESOURCES ASSESSMENT IN THE RIFT VALLEY LAKES BASIN
	JAPAN INTERNATIONAL COOPERATION AGENCY (JICA)

Figure 3.7: Sub-basins and Shaded Model (Aster)

3.4   Hydrogeological data collection and data analysis

The major activities were to understand the hydrological feature of the Study area, based on the database compiled by Halcrow 2008, ENGWIS, and data collected from regional governments of Oromia and SNNPRS. Further well inventory data were collected from Oromia regional governments. However, several problems were observed in the database

1) Duplication of same water points. The duplicated data have different values.

2) Insufficient description of data, which has only coordination and well No. information.

3) Insufficient data of hydrological parameters.

4) The unit of each parameter is not always correct.

5) Insufficient drilling logs and/or aquifer descriptions.

Accordingly, all data sets were examined one by one at the preparation stage of Progress Report 2, and the problematic water point information was screened out. The Study team dispatched an engineer for the collection of more detailed information to the regions of Oromia and SNNPRS. The data was collected through Woreda Water Offices, NGOs and well contractors.

At the collection of the additional data, effort was made to obtain the reports including the following information;

1) Coordination of water sources (some of the points were visited for data measurements)

2) Geology of the aquifers

3) Aquifer thickness and/or screen position of the casing

4) Description of hydrological parameters (at least the description of Q = discharge rate)

However, most of the reports and information did not satisfy the above mentioned. The coordination data was also collected accompanied by the Woreda engineer to measure GPS coordination. The data of Grant Aid Program executed in SNNPRS by JICA was also obtained from the SNNPRS Water Office. The spring source information is extracted from the database of Halcrow and ENGWIS. Further screening was undertaken for the reliable database. The final total number of wells is 324 (including 7 new JICA Test wells), and springs, 445. The data sources provided in this report are shown in Table 3.4: Total Data Number Used.

Table 3.4: Total Data Number Used

No	Data Source	Total Number of data (as of June 2011)			
		BH(PR1)	BH(PR2)	BH(PR2)	Spring
1	2010 Data (Halcrow Report、ENGWIS、Regional Water Bureau)	2,406	239	221	445
2	2011 Data（Regional Water Bureau, Woreda Water Office, NGOs, Contractors of well drilling）	-	103	103	-
	Total	2,406	342	324	445

3.4.1   Existing well data

The total number of data sets collected was less than that of Progress Report 1. However, more accurate and detailed analysis can be made from newly collected data which includes useful hydrological parameters. Figure 3.8 indicates the distribution of existing wells in the study area from the new version of data sets. It was identified that the wells are mostly distributed in the sub-basins of Western Ziway-Abijata, Bilate, Gidabo, and Galena. Limited data is available in other sub-basins (especially in Oromia Region). Where data is extremely lacking in Oromia Region, it shall be examined whether they have compiled data of wells. Further collection of the data has been made in Oromia Region, and it was concluded that the well inventory was extremely limited. This is largely due to missing of huge amount of reports and data sets caused by the frequent change of the responsibility area of regional water office due to uncertainty of border line between Oromia and SNNPR set by the government. However, total number of the data is small, but useful information on hydrological parameters is much more than that of ENGWIS and Halcrow, 2008 database.

The collected parameters of hydrology and aquifer information are summarized in Table 3.5.

Table 3.5: Total Number of Hydrological Data in the New Database

Parameter	Total Number of data sets	
	ITR(June, 2011)	PR2(2010)
Discharge (Ql/s)	319	650
Transmissibility	41	49
Aquifer	303	316

3.4.2   Springs

The total number of spring data is 445 points. Most of the data without discharge rate was screened out from the database. Also, the data was limited to inside of the study area. Total number of data at PR1 was 2,207 points, and it became 445 points. The data of spring points are plotted on the Figure 3.9. This figure also shows the lack of data in the Oromia Region.
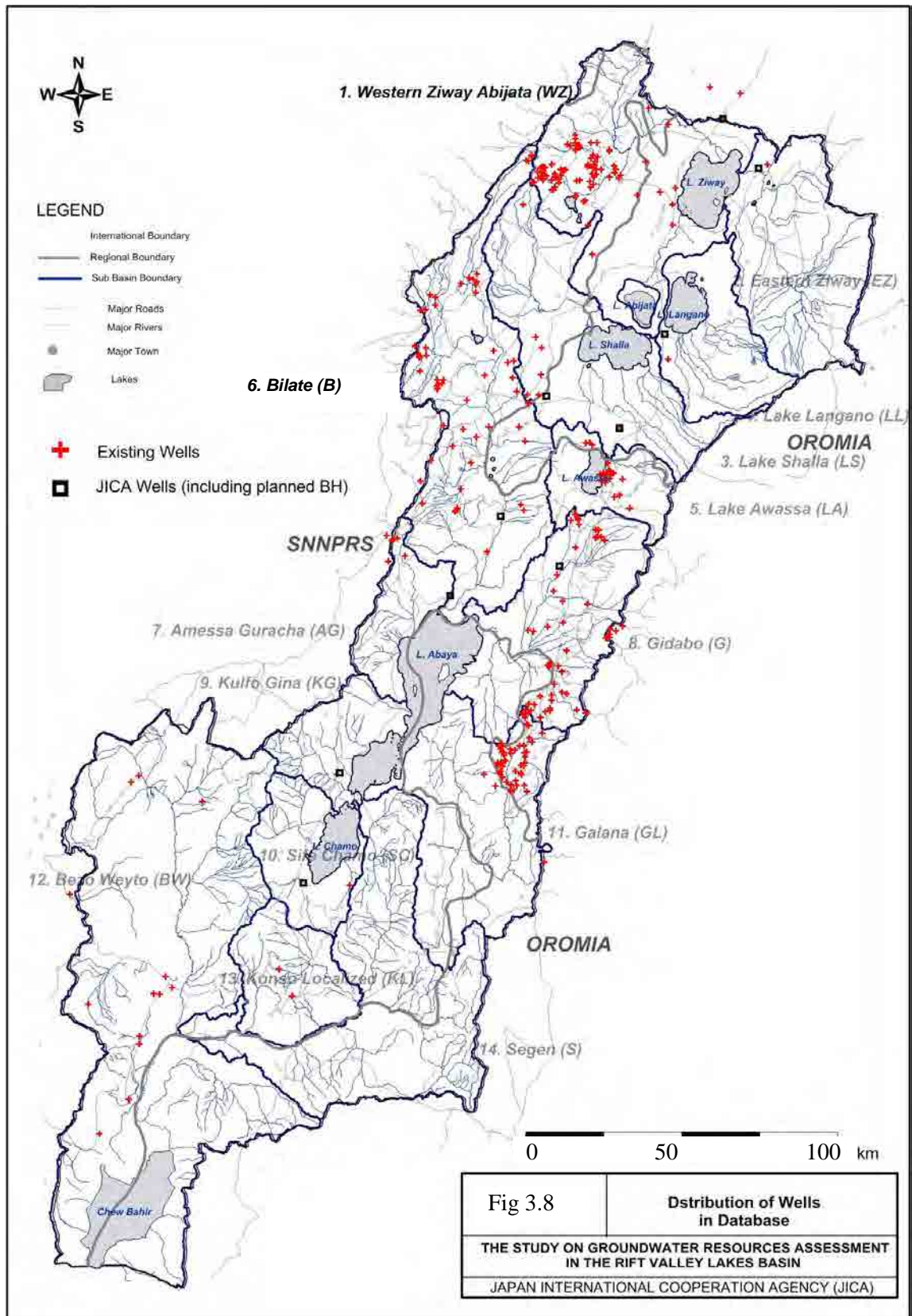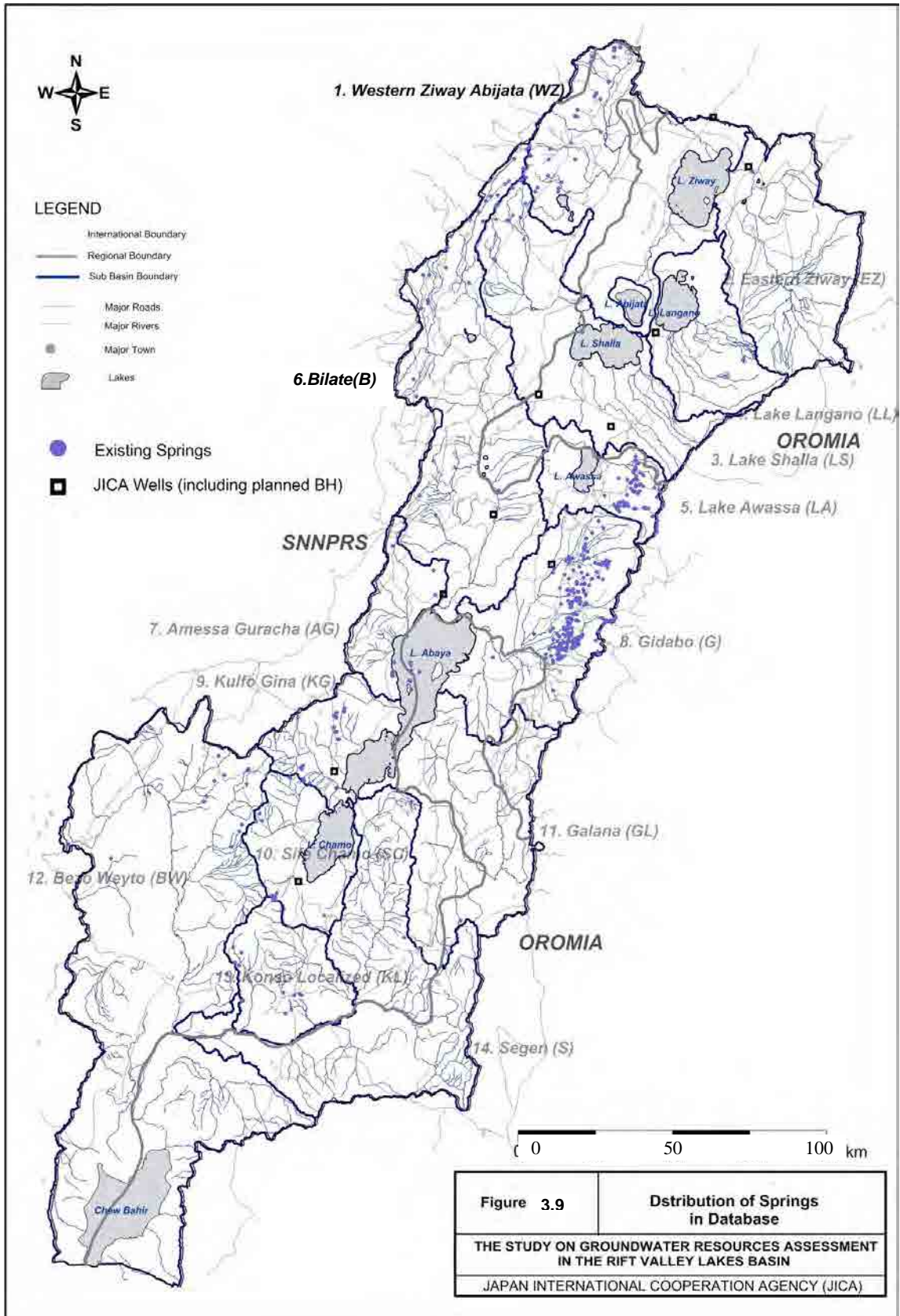
Figure 3.8: Distribution of Wells in Database

Figure 3.9: Distribution of Springs in Database

3.5   Potential of surface water

The study is mainly focused on the groundwater as a potential drinking water, and the surface water such as rivers and lakes was not considered as a potential water source. It is due to the river water and lake water in the study area having poor water quality, not meeting hygienic standards and not being permanent resources due to seasonal fluctuations. However, the review will be made as to know the nature of the river water and lake water from the view point of drinking water, reference with the available reports and information.

3.5.1   River water

Most rivers in the study area are categorized as non-perennial rivers. Even though some large rivers can be classified as perennial rivers, the amount of discharge in the dry season is quite limited. Therefore, stable provision of water volume and supply as drinking water from the river is out of consideration. Furthermore, most of the perennial rivers are randomly used by the surrounding community without any rules with activities such as washing, bathing, irrigation, and cattle feeding, therefore the water quality of these rivers in the dry season will not be considered as potable water.

Table 3.6 shows the low flows and high flows (m^3/s, mean figure of a month) of major rivers. Most of the flow rates are less than $2m^3$/s in the dry season, except Katar, Bilate, Kuflo and Weyto rivers. The flow rate of these rivers also decreases in the dry season. Even if an intake structure is constructed, a stable supply of drinking water throughout the year is not possible.

Table 3.6: Mean Monthly Flow of the Major Rivers (Dry and Wet Season)

River Name	Measuring Location	Low Flows(m^3/s)		High Flows(m^3/s)	
		Month	Mean	Month	Mean
Ziway-Abiyata-Langano Sub-catchment					
Katar	Abura	January	2.152	August	51.812
Meki	MekiVillage	December	0.781	August	30.661
Bulbula	AdamiTulu	June	1.246	October	16.735
Bulbula	Bulbula	May	1.095	September	9.815
Horakello	Langano	April	0.292	October	4.035
Debada	Kuyera	January	0.113	September	3.660
Awasa Sub-catchment					
Wesha	WendoGenet	January	0.480	October	0.866
TikurWiha	DatoVillage	March	1.640	October	5.327
Abaya-Chamo Sub-catchment					
Bilate	Bilaten	January	2.699	September	43.455
Kola	AletaWondo	February	0.555	August	5.696
Gibado	Tore	March	1.110	May	7.932
Gelana	Getem	February	1.033	October	14.037
Hamassa	Wajifo	January	0.503	August	9.057
Hare	ArbaMinch	February	0.796	May	4.085
Kulfo	ArbaMinch	January	1.441	September	7.815
Kulfo	Outlet	February	3.433	May	7.695
Weyto	WeytoBridge	February	7.881	May	23.170

Rift Valley Lakes Basin Integrated Resources Development Master Plan Study Project Phase 1 Finnal report (June 2008, Ministry of Water Resources, Halcrow, GIRD Consultants)

The Study on Groundwater Resources Assessment
in the Rift valley Lakes Basin in Ethiopia, Final Report (Supporting Report)

JICA
KOKUSAI KOGYO CO., LTD.

The water quality analysis results are shown in Table 3.7 and the Ethiopian standard of drinking water of the parameters of major concern are shown in Table 3.8. The river water in the dry season shows some concentration of toxic parameters such as fluoride, but it reduces in the wet season to drinkable levels. Although, the turbidity of the river water is very high, it will not affect human health. It is categorized into "Parameters that may give rise to complaints from consumers".

Table 3.7: Water Quality of Major Rivers (Major parameters only)

Parameters	Katar		Meki		Bulbula		TikurWiha		Bilate		Gidabo	Gelana	Kulfo		Sile		Weyto	
	Apr	Aug	Apr	Aug	Apr	Aug	Apr	Aug	Apr	Aug	Apr	Aug	Apr	Aug	Apr	Aug	Apr	Aug
pH	7.84	7.29	7.94	7.25	7.8	7.9	7.21	6.91	8.69	8.28	7.45	7.86	8.15	7.94	8.0	7.9	8.04	8.03
TDS(mg/l)	94	39	142	43	231	211	175	109	1014	64	39	67	52	60	69	74	98	91
DO(mg/l)	197	83.3	294	90.4	6.2	6.8	2.4	3.2	4.7	6.8	6.0	5.8	6.0	6.7	5.6	6.7	4.1	6.8
EC(SS/cm)	4.9	6.6	5.6	6.4	482	442	368	229	2120	135	83	140	110	128	145	156	206	193
TSS(mg/l)	94	312	530	3,600	96	122	196	68	168	1390	501	348	649	1480	450	542	1474	1036
TurbidityNTU	40	255	470	-	35	83	104	36	109	1242	256	306	321	1353	148	388	546	720
Na(mg/l)	16	5.2	29	15	54	60	57.5	35.0	450.0	12.0	6.6	7.0	5.2	6.0	7.9	7.7	11.6	13
K(mg/l)	5.1	3.5	10.1	5.9	12.3	10.6	13.5	6.0	21.5	8.1	2.9	1.9	1.2	1.3	1.5	1.5	3.1	2.0
Ca(mg/l)	15.2	8.0	25.6	4.8	25.6	20.8	8.8	9.6	16.8	15.2	4.8	14.4	14.4	13.6	14.4	15.2	19.2	19.2
Mg(mg/l)	4.86	1.944	6.804	0.486	8.75	6.8	4.86	2.92	2.43	2.43	1.94	4.37	1.94	4.86	5.35	4.86	6.8	5.83
HCO3(mg/l)	82	12.2	108	29.28	202	190	124	75.6	568	58.56	30	61	46	48.8	56	68.32	68	78.1
Cl(mg/l)	1.5	2.5	5.5	2.0	14	12.5	13.0	13.5	65.5	4.5	2.0	6.0	1.3	2.0	2.0	7.5	5.5	8.5
F(mg/l)	0.5	0.28	1.34	0.22	1.49	1.72	1.7	1.25	16.0	0.97	0.35	0.91	Trace	0.22	0.79	0.48	0.53	0.65
SO4(mg/l)	1.27	3.04	18.62	2.4	6.14	0.4	40.73	2.2	44.65	0.18	14.18	0.6	3.6	5.1	0.85	0.62	2.33	0.09
SAR	0.92	0.43	1.3	1.74	2.47	2.93	2.7	2.11	59.2	0.87	0.32	0.29	0.18	0.25	0.30	0.30		

Sampled in 2007, referred to Rift Valley Lakes Basin Integrated Resources Development Master Plan Study Project (June 2008, MOWR, Halcrow, GIRD Consultants)

Table 3.8: Guidelines of Major Substances and Parameters (Ethiopia 2002, WHO)

Parameter	Ethiopian Guideline	WHO Guideline
pH	6.5-8.5	6.5-8.5
Fluoride(mg/l)	3.0	0.6-1.57
Nitrate(mg/l)	50	45
Chloride(mg/l)	533	250
Iron(mg/l)	0.4	0.3
TDS(mg/l)	1776	1000

As aforementioned, the rivers in the study area do not have capacity to provide the stable potable water supply, and the water quality is not satisfactory for drinking. The potential of river water as a drinking water source is low.

3.5.2 Lake water

As the area is so called "the Rift Valley Lakes Basin", plenty of lakes exist in all sizes in the study area. The lakes are chiefly distributed in the center low profile of the valley and flat lands created by the rift. Dozens of lakes can be observed including small caldera lakes. In this section, the lake water will be examined as a potable water source. The lakes considered in this section are: Ziway, Langano, Abijata, Shalla, Abaya, and Chamo. Chew Bahir is not considered as it is a salt lake, and it has poor water quality and quantity (volume).

The major specification of the respective lakes is tabulated in Table 3.9. The largest lake in the study area is Lake Abaya, and it has the surface water of 1,160km^2, but the mean water

The Study on Groundwater Resources Assessment
in the Rift valley Lakes Basin in Ethiopia, Final Report (Supporting Report)

JICA
KOKUSAI KOGYO CO., LTD.

level is only 7m which stores 8.2km^3 of water. On the other hand, Lake Shalla has only 409km^2 surface area (which is one third of Lake Abaya) but it has a maximum depth of 266m, and average depth falls to 87m which reserves 36.7km^3 (4 times more than Lake Abaya).

Table 3.9: Specification of the Major Lakes

Lake	Altitude	Surface Area	Max depth	Avr depth	Volume
	m.a.s.l	km2	m	m	km3
Ziway	1636	440	8.95	2.5	1.1
Langano	1582	230	47.9	17	5.3
Abijata	1578	205	14.2	7.6	1.61
Shalla	1558	409	266	87	36.7
Awassa	1697	129	22	11	1.3
Abaya	1285	1160	13	7	8.2
Chamo	1235	551	13	6	3.3

Water Balance and Level Regime of Ethiopian Lakes as Integral Indicators of Climate Change (2008, A.M. Mikhailovich D, B.A. Getahum, the 12th World Lake Conference)

The water level of the major lakes has been recorded since the early 1970s. The variations by year and by lake are obvious, however, the water level change of the lakes is not large in the longterm. The water balance of the lakes, recharge and outflow (evaporation, groundwater outflow) seems to be well balanced. Therefore, securing a sufficient volume of drinking water seems to be possible.

However, the problem is not the quantity of water but the quality. The major substances and parameter values of these lakes are indicated in Table 3.10. The shaded cells are the values that exceed the drinking standard of Ethiopia. Most of the lakes have problems in the substances and parameters that may give rise to complaints from consumers. Furthermore, the value of Fluoride exceeds the limit of both Ethiopian and WHO standards. Only Lake Ziway exceeds WHO standards but lower figure for Ethiopian standards. The overall review of the water quality of the major lakes is poor. Lakes Abijata and Shalla have an extremely high fluoride content of more than 100mg/l throughout the year. The water is rather harmful to the human health.

Table 3.10: Water Quality of Major Lakes

Parameters	ZiwayLake		LakeAbiyata		LakeShala		LakeLangano		LakeAwasa		Abaya		Chamo	
	Apr	Aug	Apr	Aug	Apr	Aug	Apr	Aug	Apr	Aug	Apr	Aug	Apr	Aug
pH	8.7	8.0	10.1	10.0	9.8	9.8	8.9	9.2	9.0	9.0	9.1	9.1	9.6	9.4
TDS(mg/l)	220.0	214.0	41.5	41600.0	23160.0	21300.0	923.0	959.0	424.0	408.0	628.0	540.0	1004.0	899.0
DO(mg/l)	460.0	445.0	2.9	2.3	2.8	2.7	1932.0	1941.0	6.7	6.7	6.1	6.8	6.3	6.8
EC(SS/cm)	6.0	6.7	83.6	84250.0	48150.0	44000.0	6.7	6.8	886.0	848.0	1319.0	1116.0	2104.0	1827.0
TurbidityNTU	46.0	54.0	22.0	26.0	22.0	26.0	77.0	97.0	13.0	16.0	112.0	89.0	59.0	66.0
Na(mg/l)	63.5	59.0	12940.0	13100.0	6000.0	6950.0	405.0	375.0	162.0	168.0	246.0	222.0	430.0	425.0
K(mg/l)	11.9	11.2	6284.0	6300.0	240.0	244.0	23.5	23.0	26.0	30.0	19.0	16.0	20.5	20.0
Ca(mg/l)	22.4	20.8	3.2	4.0	0.0	6.4	4.8	4.8	11.2	10.4	15.2	14.4	6.4	8.0
Mg(mg/l)	7.3	6.3	0.0	0.0	3.9	0.0	1.5	0.5	4.9	5.4	1.9	2.9	7.8	7.8
HCO3(mg/l)	166.0	185.0	6286.0	6344.0	4652.0	244.0	426.0	505.0	194.0	310.0	354.0	395.0	566.0	568.0
Cl(mg/l)	12.5	12.0	10778.0	10900.0	3250.0	6300.0	182.0	200.0	27.0	51.0	63.5	107.5	130.0	300.0
F(mg/l)	1.5	1.6	370.0	370.0	156.0	220.0	7.9	10.2	7.7	9.6	8.2	8.0	9.3	8.9
SO4(mg/l)	1.4	25.4	17.3	15.8	5.2	12.6	2.1	1.2	0.1	4.8	3.4	9.7	1.2	5.2
SAR	3.0		653.0	267.0			41.5		10.2		15.7	27.0		

▨ Figures exceeds the Ethiopian Standard

Sampled in 2007, referred to Rift Valley Lakes Basin Integrated Resources Development Master Plan Study Project (June 2008, MOWR, Halcrow, GIRD Consultants)

The review indicates that the total volume of the lakes in the study area has huge potential to

use water resource in terms of its volume, but the consideration of the water quality shows inadequate for the domestic drinking water. On the other hand, this is historical proof of the use of drinking water in the communities surrounding the lakes. They mainly depend upon wells and springs for their drinking water, even there may be some intervention or instructions given by the central and local government.

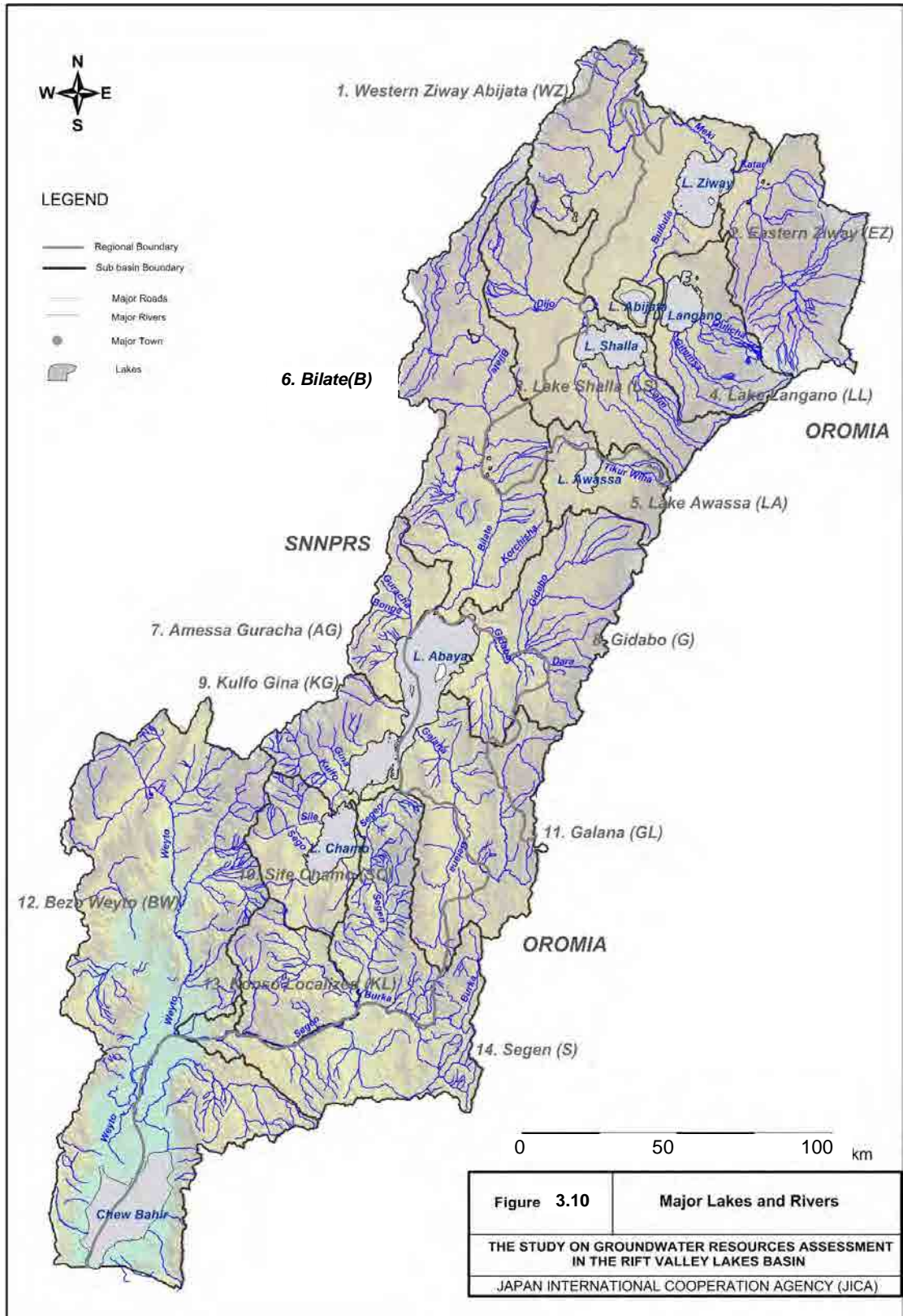The distribution of lakes and rivers in the area is shown in Figure 3.10.

Figure 3.10: Major Lakes and Rivers

3.6 Potential of groundwater

The review of surface water potential as a potable water source seems to be not satisfactory. This result shows the potential drinking water source may be limited to the groundwater resources through wells and springs. The advantage of the groundwater usage as a potential potable water source is summarized as follows;

1) Basically the water is clean in terms of water quality, and the quality is not largely affected by seasonal fluctuations.

2) The amount of water is steady throughout the year, and necessary volume of water can be extracted by type of water supply facility

3) Knowing that good aquifers exist below allows for flexibility in the point of source extraction. Therefore, the water supply facility can be provided within the vicinity of the community.

From the past, more than ten thousands wells and springs have been used as potable water sources in the Study area. It should be noted that not all of the point sources have the above mentioned characteristics of a potable water source. Hand dug wells and shallow wells which target the shallow aquifer in the Alluvium can be easily affected not only by the surface pollution such as cattle disposal and fertilizer, but also seasonal fluctuation of the water level. This means that these will not provide a stable water supply. Therefore, the identification of a good aquifer which satisfies the above mentioned criteria shall be put in first priority. The investigation of groundwater potential shall be clarified by the distribution of good aquifers, as well as its quality and quantity as an aquifer unit.

3.6.1 Classification and characteristics of aquifer units

The verification of aquifer will be made with reference to the result of geological field reconnaissance, JICA test wells and existing well data.

a. Verification of Existing Well Data

Aquifer characteristics will be examined by utilizing existing well inventories (including completed JICA test wells). Existing well inventories includes aquifer geology, aquifer thickness and the depth (aquifer position of some wells are represented by screen position). The variation of geology of the aquifer is presented in Table 3.11.

Table 3.11: The Composition Data by Geological Character of Aquifer

No	Aquifer Geology	Other reference of description	Data No	%
1	Alluvium	-	10	3.2
2	Clay	Sandy clay	4	1.3
3	Sand	Coarse sand, lacustrine	57	18.1
4	Gravel	Sandy gravel	38	12.1
5	Sand and Gravel	Sand gravel clay	-	-
6	Basalt	Fractured basalt, weathered basalt, scoracious basalt	86	27.3
7	Ignimbrite	Fractured ignimbrite, coria/ignimbrite, weathered ignimbrite	38	12.1
8	Pumice	Pumice sand, sand/pumice	23	7.3
9	Pyrolastics	-	4	1.3

10	Scoria	Scoria & sandy gravel	13	4.1
11	Tuff	Pumicious tuff, sandy tuff weathered tuff,	33	10.5
12	Welded tuff	-	2	0.6
13	Other volcanics	Trachyte, Rhyolite, volcanic sediments	7	2.2

The table above indicates that about 70% of aquifers in the area composed of volcanic rocks and its member.
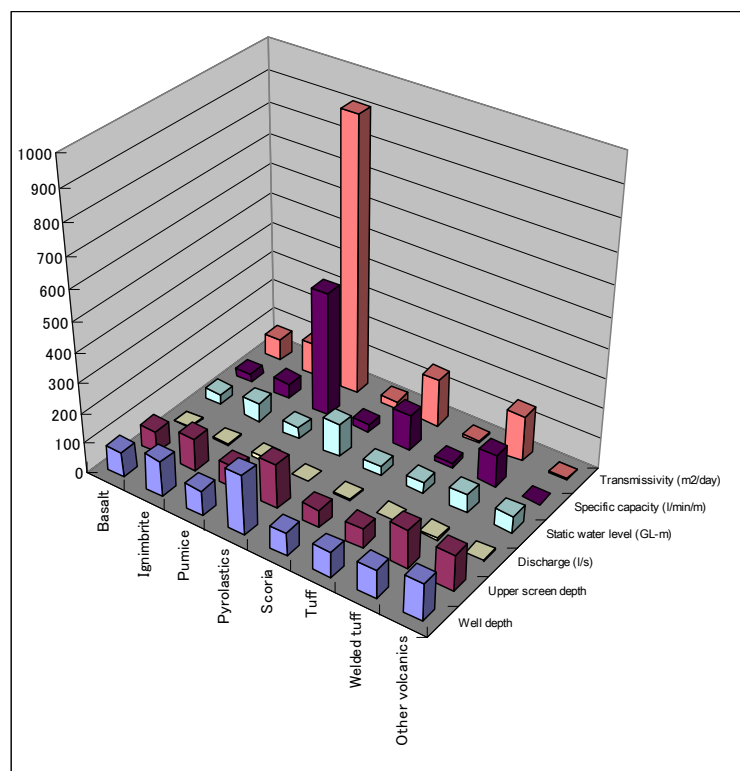

Figure 3.11: Comparison of major parameters by Volcanic Aquifer

Potential good aquifers are gravel, pumice and scoria formations as indicated in the above tables and figures. The average well depth is about 50 mbsl (meters below surface level), and more than 80 mbsl for most volcanic aquifers.

It should be noted that identification of the geology of respective aquifers depends on the drilling geologist's capacity of rock identification. Down the Hole Drilling method (DTH) is common in Ethiopia and the logging engineer (geologist) shall determine the geology from small rock chip samples. If the contractor does not have enough manpower to provide the skilled geologist, then the rock will be identified as sand, gravel etc., by merely evaluating the shape and size of the rock chips. Therefore, it is a quite difficult exercise to verify the accuracy of geological descriptions (whether they be alluvium deposits or volcanic rock chip samples). Some descriptions might actually be volcanic rock samples instead of just sand and gravel.

b.   Geological Correlation among JICA test wells, existing wells, and results of geological survey

The comparison will be made between survey result of geological field reconnaissance, core logging of JICA test well and the existing well inventory. The stratigraphy of the study area established by the detailed geological reconnaissance is presented in Table 3.12. The table

The Study on Groundwater Resources Assessment
in the Rift valley Lakes Basin in Ethiopia, Final Report (Supporting Report)

JICA
KOKUSAI KOGYO CO., LTD.

was compiled from the geological field survey emphasizing the volcanic geological point of view, and indicating the continuity and distribution of those volcanic formations.

Table 3.12: Stratigraphy of Rift Valley Lakes Basin

Period/Epoch				Stratigraphy	Name of strata	Name of Formation	Major Lithology	Distribution
Cenozoic	Quaternary	Holocene		Al	Alluvium,	Alluvium	Fine sand - mud	distributed in entire RVLB
				Q	Unclassified Fluvial Deposits	Quaternary sediments	Sandy gravel-mud	distributed in entire RVLB
				lac 2	Bulbula Lacustrine Deposits	Bulbula lacustrine deposits, Shalo lacustrine deposits	Lake deposits such as gravel, sand and mud	locally distributed in northern part of RVLB and surrounding Lake Awassa area
				Pm volcan	Corbetti Pumice Flow & Fall Deposits/ Corbetti Rhyolitic Volcanics	Mt. Aluto volcanics, Alge volcanics, Mt. Ambericho volcanics, Corbetti volcanics, Dugna Fango volcanics	Rhyolite lava flows, pumice falls, pumice flow deposits and Obsidian lava flows	locally distributed from Ziway to Abaya- Arba Minch area
				rb	Butajira Recent Basalt	Deneba Recent Basalt, Awara Recent Basalt, Butajira Recent Basalt, Awasa Recent Basalt, Abaya Recent Basalts	Basalt lavas and reddish brown basaltic scoria	zonally distributed on the floor of entire RVLB excluding southern part
				lac 1	Meki Lacustrine Deposits	Meki lacustrine deposits, Wondotika lacustrine deposits	Lake deposits such as poorly-sorted gravel, sand, pumice, tuff, and volcanic sand	locally distributed surrounding Lake Ziway and Lake Awassa area
		Pleistocene		Y	Langano Poorly Welded Pumiceous Pyroclastics	Asela poorly welded pumiceous pyroclastics, Langano poorly welded pumiceous pyroclastics, Dugba poorly welded pumiceous pyroclastics, Shashemene poorly welded pumiceous pyroclastics	Yellowish white rhyolitic pumice tuff	continuously distributed from Ziway to Awassa area
				ob	Kulmusa Highly Welded Tuff	Kulmusa highly Welded-Tuff, Kuyera highly Welded-Tuff, Koshe highly Welded-Tuff, Mt. Kuwe highly Welded-Tuff, Samero highly Welded-Tuff	Rhyolitic to andestic welded tuff	continuously distributed from Ziway to Dila area
				W	Ketar River Acidic Volcanic Sedimentary Rocks	Ketar river acidic volcanic sedimentary rocks, Lake Shala acidic volcanic sedimentary rocks, Amecho acidic volcanic sedimentary rocks, Yiega Alem acidic volcanic sedimentary rocks	Rhyolitic tuffs and pumice tuffs	continuously distributed from Ziway to Dila area
				G	Gonde Strongly Green Welded Tuff	Gonde Strongly Green Welded-Tuff, Bilate river Strongly Green Welded-Tuff, Hantate Strongly Green Welded-Tuff	Rhyolitic to andestic welded tuff	continuously distributed from Ziway to Dila area
				tb	Adami Tulu Basaltic Pyroclastics	Adami Tulu basaltic pyroclastics, Shala Senbete basaltic pyroclastics, Abaye ridge basaltic pyroclastics, Donga basaltic pyroclastics	Basaltic tuff breccias and lapilli tuffs	locally distributed in entire RVLB
				ba	Ogolche Pleistocene Basalt	Ogolche Basalt, Lake Chitu Basalt, Deneba Basalt, Yubo Basalt, Kebado Basalt, (Post-rift Volcanics)	Massive basalt lavas	locally distributed in entire RVLB
				lak	Lekansho Lacustrine Deposits	Lekansho Lake deposits	Lake deposits such as sand stone and alternate layer	locally distributed in Ziway and surrounding area
	Tertiary	Plio-Pleistocene		rh	Gademotta Rhyolite	Gademotta rhyolite, Aje rhyolite, Wendo Genet Rhyolite, Hobicha rhyolite, Gocho Rhyolite	Rhyolite lava flows and rhyolitic tuffs	continuously distributed in entire RVLB
				N2b	N2b Basal	Bofa Basalt, Lepis Basalt	Basalt lavas and basaltic pyroclastics	distributed only in the south of Lake Ziway
				NQs	NQs Rhyolite	NQs	Rhyolitic tuffs	locally distributed in Butajira area
		Pliocene		rht/N1_2n	N1_2n Rhyolitic Volcanics/Rhyolitic Tuff	Munesa rhyolite, Hangasu Rhyolite, Wijigra Rhyolite, N1_2n	Plagiocrase rhyolite tuff	locally distributed in entire RVLB
				N1n	N1n Basalt	N1n	Anchar Basalt	locally distributed in Butajira area
				N1ar	N1ar Rhyolite	N1ar	Rhyolite	locally distributed in Butajira area
		Miocene		Ngs	Sharenga Rhyolite	Sharenga Rhyolite	Rhyolite piles and necks	distributed only in Abaya- Alba Minch and surrounding area
				Ngu	Upper Basalt	Upper Basalt	Porous basalt lavas	continuously distributed in the south of Dila
				Ngb	Beyana Tuff	Beyana Tuff	Lapilli tuff with minor laminated tuff	continuously distributed in the south of Dila
				Ngm	Middle Basalt	Middle Basalt	Porphyritic basalt lavas	continuously distributed in the south of Dila
		Eocene-Origocene		Pgs	Shole Welded Tuff	Shole Ignimbrite	Densely-welded rhyolitic welded tuff	continuously distributed in the south of Dila
				Pgl	Lower Basalt	Lower Basalt	Porphyritic basalt lavas	continuously distributed in the south of Dila
Mesozoic				Mes	Adigrat Sandstone, Antaro Limestone	Adigrat Sandstone, Antaro Limestone	Sandstone, Shale and Limestone	locally distributed in Kella, northern part of Butajira
Pre-Cambrian				Pre	Biotite Gneiss, Pegmatite	Biotite Gneiss, Granite, Biotite Metagranite	Biotite Gneiss, Granite, Biotite Metagranite	distributed in Kella, northern part of ButajiraButajira and HagereSelam-Yabelo area

References: (1) Laury and Albritton 1975, (2) Mohr et al. 1980, (3) EIGS-GLE 1985, (4) Woldegabriel et al. 1990, (5) GSE 1994, (6) GSE 2002, (7) EWTEC 2008

There limited stratigraphy data that can be referred to as aquifer information because the past stratigraphical analysis is mainly focused on lithofacies. In this section, the aquifer unit will be compared to the respective lithofacies followed by identification of the hydrogeological characteristics of aquifer units. Definitely there are several events of volcanic activity from Tertiary to Quaternary epoch, and several cycles of volcanic rocks, such as basalt, tuff and welded tuff have been formed. The existing aquifer geology is described only by rock name. Therefore, the accuracy of the correlation between lithofacies and the rock names in the well inventory is not high. This correlation works shall be made in connection with the well logs of JICA test drilling and the geological cross section from the geological field reconnaissance.

b.1   Relation between geological cross section and existing well inventory

To analyze the relation of lithofacies of stratigraphy and the aquifer, geological cross sections established from the detailed geological field reconnaissance in the Bilate sub-basin was simultaneously used for the comparison. Existing aquifer information was projected on the geological cross section. It seems to be the aquifer units of basalt is correlated with the Plio-Pleistocene rhyolite lava flows and rhyolitic tuff (rh) and basalt lavas and basaltic pyroclastics. The upper formation of major aquifer of Pleistocene welded tuff and tuff breccia is potential aquifer. Pumice tuff formation is also a potential aquifer if aquiclude underlay this layer.

Table 3.13: Lithofacies and Aquifer Geology

Period/Epoch			Stratigraphy	Name of Formation	Aquifer Geology	Distribution
Cenozoic	Quaternary	Holocene	Al	Alluvium	**Alluvium**	distributed in entire RVLB
			Lac	Bulbula lacustrine deposits, Shalo lacustrine deposits	**Clay Sand Gravel**	locally distributed in northern part of RVLB and surrounding Lake Awassa area
			Pm / volcan	Mt. Aluto volcanics, Alge volcanics, Mt. Ambericho volcanics, Corbetti volcanics, Dugna Fango volcanics		locally distributed from Ziway to Abaya- Arba Minch area
			br	Deneba Recent Basalt, Awara Recent Basalt, Butajira Recent Basalt, Awasa Recent Basalt, Abaya Recent Basalts		zonally distributed on the floor of entire RVLB excluding southern part
			Lac	Meki lacustrine deposits, Wondotika lacustrine deposits		locally distributed surrounding Lake Ziway and Lake Awassa area
		Pleistcene	Y	Asela poorly welded pumiceous pyroclastics, Langano poorly welded pumiceous pyroclastics, Dugba poorly welded pumiceous pyroclastics, Shashemene poorly welded pumiceous pyroclastics	**Tuff**	continuously distributed from Ziway to Awassa area
			ob	Kulmusa highly Welded-Tuff, Kuyera highly Welded-Tuff, Koshe highly Welded-Tuff, Mt. Kuwe highly Welded-Tuff, Samero highly Welded-Tuff	**Ignimbrite Welded Tuff**	continuously distributed from Ziway to Dila area
			W	Ketar river acidic volcano- sedimentary rocks, Lake Shala acidic volcano- sedimentary rocks, Amecho acidic volcano- sedimentary rocks, Yiega Alem acidic volcano- sedimentary rocks	**Tuff**	continuously distributed from Ziway to Dila area
			G	Gonde Strongly Green Welded-Tuff, Bilate river Strongly Green Welded-Tuff, Hantate Strongly Green Welded-Tuff	**Pyroclastics Welded Tuff**	continuously distributed from Ziway to Dila area
			tb	Ogolche Basalt, Shala Senbete basaltic pyroclastics, Abaye ridge basaltic pyroclastics, Donga basaltic pyroclastics	**Scoria**	locally distributed in entire RVLB
			ba	Lepis Basalt, Deneba Basalt, Yubo Basalt, Kebado Basalt	**Basalt**	locally distributed in entire RVLB
			Lak	Lekansho Lake deposits		locally distributed in Ziway and surrounding area
	Tertiary	Prio-Pleistcene	rh	Gademotta rhyolite, Aje rhyolite, Wendo Genet Rhyolite, Hobicha rhyolite, Gecho Rhyolite	**Pumice Basalt**	continuously distributed in entire RVLB
			Bof	Bofa Basalt	**Basalt**	distributed only in the south of Lake Ziway
			rht	Hangasu Rhyolite, Wijigra Rhyolite		locally distributed in Ziway and Awassa area
		Priocene	Munesa	Munesa rhyolite		distributed at the shouder of RVLB in the east of Lake Langano
		Miocene	Nas	Sharenga Rhyolite		distributed only in Abaya- Alba Minch and surrounding area
			Nau	Upper Basalt	**Basalt?**	continuously distributed in the south of Dila
			Nab	Beyana Tuff		continuously distributed in the south of Dila
			Ngm	Middle Basalt	**Basalt?**	continuousely distributed in the south of Dila
		Eocene-Origocene	Pgs	Shole Ignimbrite		continuousely distributed in the south of Dila
			Pgl	Lower Basalt	**Basalt?**	continuousely distributed in the south of Dila
Mesozoic			Mes	Adigrat Sandstone, Antaro Limestone		locally distributed in Kella, northern part of Butajira
Pre-Cambrian			Pre	Biotite Gneiss, Granite, Biotite Metagranite		distributed in Kella, northern part of ButajiraButajira and HagereSelam-Yabero area

References: (1) Laury and Albritton 1975, (2) Mohr et al. 1980, (3) EIGS-GLE 1985, (4) Woldegabriel et al. 1990, (5) GSE 1994, (6) GSE 2002

b.2   Relation between JICA Test Well and Existing well inventory

The stratigraphical analysis has been completed on a total 8 wells of 10 JICA wells presented in Table 3.14. Some wells do not have hydrogeological parameters while the pumping tests have not yet been completed. The aquifer can be divided into 2 major units, which are: Pleistocene rhyolites – andesitic welded tuff (G), and basaltic tuff breccia – volcanic breccia (tb). In accordance with this comparison, the description of each formation is quite different. Welded tuff formation is described as sand, gravel and pumice, and tuff breccia is defined as rhyolite and ignimbrite without any description of the nature of the aquifer. Therefore, the ryolite, ignimbrite in the existing well classification is referred to as (tb). The remaining two wells were located in Arba Minch and its surrounding area and south part of Arba Minch, and the aquifer of wells consists of Basalt layer probably.

The Study on Groundwater Resources Assessment
in the Rift valley Lakes Basin in Ethiopia, Final Report (Supporting Report)

JICA
KOKUSAI KOGYO CO., LTD.

Table 3.14: Comparison between JICA Wells and Existing Wells

No	BasinName	Code	Locality	Eastings	Northings	Level	Type	Depth (m)	Upper Screen (GL-m)	Depth (m)	Aqufer	Q l/s	SWL GL-m	DWL GL0m	TDD	Sc (L/min/m)	T (m2/day)	S
JICA BH4	Gidabo	RVS BH4	Yirga Alem	424916	745491	1632	BH	244	82.00	1550	Tuff Breccia (tb)	6	7.7	44.9	37.2	9.60	27	2.90E-07
	Gidabo	SW102		424178	742349	1621	BH	141	72.00	1549	Gravel, w/fr/Rhyolite	6.5	0.5	9.12	8.62			
	Gidabo	SW101		422684	736474	1689	BH	134	95.00	1594	Ignimbrite & Sand	5	62		28.55	10.5	13.17	5.6
	Gidabo	SW112		431035	752301	1742	BH	120	72.00	1670	Volcanic Sand	6.6	9.75	69.85		5.66	2.71	4.29
BH5	Bilate	RVS BH5	Dimutu	404261	765667	1485	BH	250	28.00	1457	Basalt (Pleistocene)	100	Artesian	-	-	-	-	-
	Bilate	RVS BH1	Walayta	383591	734651	1237	BH	150	96.00	1141.00	Welded tuff (rh)	12	47.35	53.20	5.85	139.2	377	4.80E-08
	Bilate		Siaro1	410305	767729	1663	BH	221.7	130.00	1533	Gravel, sand	5	146.1				24.1	2.70E-05
	Bilate		Siaro2	411579	765908	1708	BH	300	162.00	1546		14	146.6					
	Bilate	Chericho	Chericho	397591	750809	1330	BH	111	15.40	1315	Basalt gravel, sand	5.6	5.65		1.93	12.90	211.7	
BH2	EasternZiway	RVS BH2	Meki	486788	907743	1688	BH	147	105.00	1583	Tuff Breccia (tb)	8.5	90.6	93.43	2.83	1731.00	914.4	2.03E-03
	EasternZiway		Alem Tena	493472	917127	1660	BH	102	58.90	1601	Highly weathered Ignimbri	7.2	57.4	57.52	0.12		60.4	0.987
BH10	EasternZiway	RVS BH10	Yabelo BW	500339	889953	1674	BH	200	94.00	1580	Welded tuff (G)	19	25.32	34.05	8.73	148.80	521	5.80E-11
	WesternZiwayAbijata	SW176		437406	858687	1822	BH	243	204.50	1618	sand + gravel	4.7	152.8	190	37.2			207
BH9	LakeLangano	RVS BH9	Konso	464826	829769	1635	BH	200	86.00	1549	Welded tuff (G)	16	43.41	52.37	8.96	114.00	261	3.00E-05
	WesternZiwayAbijata	SW189		439050	889444	1835	SW	31	21.45	1814	Pumice	2	10					20
BH3	LakeShalla	RVS BH3	Sheshemene	447623	795610	1801	BH	247	190.00	1611	Tuff Breccia (tb)	1	171	179.7	8.7	43.80	12.5	1.10E-02
	Lake Shalla	RVS BH6	Kenche	420114	807271	1869	BH	356	266.00	1603	Welded tuff (G)	4.6	247.6	253.2	5.6	51.60	88	2.00E-03
	LakeAwassa	SW162		436398	790447	1714	BH	66	45.00	1669	Sand	5.9	40.6					
	LakeAwassa	SW160		437444	789560	1720	BH	45.4	31.22	1689	Tuff	5.5	34					
BH7	Kulfo Gina	RVS BH7	Arba Minchi	341700	670517	1198	BH	200	86.00	1112	Basalt (Pgl)	16	4.89	53.8	48.91	20.4	41	1.70E-04
BH8	Sife Chamo	RVS BH8	Chamo South	327946	630717	1157	BH	152	50.00	1107	Basalt (Pgl)	26	15.3	17.89	2.59	-	1015	4.80E-02

▨ JICA borehole   ☐ Existing well inventory

c.   Classification of Aquifer

As aforementioned, it is difficult to review the aquifer potential by the stratigraphical classification. However, major aquifer unit can be classified as follows;

1.   Quaternary sediments and lacustrine

2.   Pleistocene tuff, welded tuff and basaltic rock members

3.   Tertiary tuff and basalt

Fractured basalt and ignimbrite are common in the description of existing well inventory. It is estimated that most of the volcanic rocks such as rhyolite and basalt are fragmented due to the event of rift activity. The major aquifer is the fracture zone of these volcanic rocks. Pumice and scoria tuffacious formation can be also potential aquifer with existence of impermeable layer at the lower level even these formations have high permeability.

d.   Classification and characteristics of aquifer

At this time, the correlation between lithofacies in the stratigraphy and aquifer unit is not yet clear. Therefore, review of aquifer potential by the aquifer unit has a limited accuracy. However, aquifer units can be subdivided into the following three lithofacies;

1) Alluvium and lacustrine deposits

2) Pleistocene tuff, tuff breccia and basaltic rock units

3) Plio-Pleistocene tuff and basalt

In the description of aquifer in the existing wells, basalt and igninbrites are common. It can be assumed that fracture and fissures are well developed in the volcanic rocks (such as

rhyolite, basalt) by the tectonic movement. Moreover, in between those rock units, tuff with pumice and scoria is abundant. These tuffacious units have good permeability, however the unit itself cannot be a good aquifer if an aquiclude exists below this formation. The relation between lithofacies and its potential as an aquifer is presented in Table 3.16 in reference with the aquifer classification of Hydrogeological Map of Ethiopia (2002, GSE) (see to Table 3.15).

Table 3.15: 1:2,000,000 Hydrogeological Map - Aquifer Classification and Definitions

No.	Description	Lithology	Productivity Classes	
1	Extensive aquifers with intergranular permeability	Unconsolidated sediments, alluvium, elluvium, colluvium, lacustrine sediments, poorly cemented sandstone	A	High
			B	Moderate
			C	Low
2	Extensive aquifers with fracture and/or karstic permeability	Consolidated sediments and metamorphosed carbonate: Limestone, sandstone, shale, marl, evaporite marble	Not distributed in the Study area	
3	Extensive aquifers with fracture permeability	Volcanic rocks, basalts, rhyolites, trachytes , ignimbrites	A	High
			B	Moderate
			C	Low
4	Localized aquifers with fracture and intergranular permeability	Non carbonate metamorphic rocks, granitic intrusives, dolerites	C	Low
			D	Poor
5	Main geothermal areas	Common occurrence of thermal groundwater in fractured volcanic rocks and subordinate unconsolidated sediments	Not distributed in the Study area	

The Study on Groundwater Resources Assessment
in the Rift valley Lakes Basin in Ethiopia, Final Report (Supporting Report)

JICA
KOKUSAI KOGYO CO., LTD.

Table 3.16: Aquifer Classification of RVLB

Period/Epoch	Stratigraphy	Name of strata	Major Lithology	Aquifer Code	Nature of Aquifer	Remarks
Cenozoic — Quaternary — Holocene	Al / Q	Alluvium, unclassified fluvial deposits	Fine sand - mud	1B	Aquifers with intergranular permeability	Good permeability at the sand layer and aquiclude at clay
	lac 2	Bulbula Lacustrine Deposits	Lake deposits such as gravel, sand and mud	1C	Aquifers with intergranular permeability	Permeability is high at sand and gravel. Clayey layer may become aquictard
	Pm volcan	Corbetti Pumice Flow & Fall Deposits/ Corbetti Rhyolitic	Rhyolite lava flows, pumice falls, pumice flow deposits and Obsidian lava flows	3C	Aquifers with fracture permeability	It may be good aquifer if the lower layer become aquitard
	rb	Butajira Recent Basalt	Basalt lavas and reddish brown basaltic scoria	3C	Aquifers with fracture permeability	Low permeability at the massive basalt. It may be good aquifer if the lower layer become aquitard
	lac 1	Meki Lacustrine Deposits	Lake deposits such as poorly-sorted gravel, sand, pumice, tuff, and volcanic sand	1B	Aquifers with intergranular permeability	It may be good aquifer if the lower layer become aquitard
	Y	Langano Poorly Welded Pumiceous Pyroclastics	Yellowish white rhyolitic pumice tuff	1B	Aquifers with intergranular permeability	Partialy good aquifer at the existance of lower aquitard
	ob	Kulmusa Highly Welded Tuff	Rhyolitic to andestic welded tuff	3B	Aquifers with fracture permeability	The lower aquitard is essential, however it has good potential aquifer
	W	Ketar River Acidic Volcanic Sedimentary Rocks	Rhyolitic tuffs and pumice tuffs	1B	Aquifers with intergranular permeability	The permeability is high knowing that the massive aquited existance at lower layer
Pleistocene	G	Gonde Strongly Green Welded Tuff	Rhyolitic to andestic welded tuff	3A	Aquifers with fracture permeability	The fractures and fissures are well developped and form good aquifer in the area
	tb	Adami Tulu Basaltic Pyroclastics	Basaltic tuff breccias and lapilli tuffs	3A	Aquifers with fracture permeability	The fractures and fissures are well developped and form good aquifer in the area
	ba	Ogolche Pleistocene Basalt	Massive basalt lavas	3B	Aquifers with fracture permeability	Even massive basalt, fracture and fissures are partially developped. The fissure zones are recognized as good aquifer
	lak e	Lekansho Lacustrine Deposits	Lake deposits such as gravel, sand and mud	1C	Aquifers with intergranular permeability	Semi consolidated formation. Partialy good aquifer has been formed
Tertiary — Plio-Pleistocene	rh	Gademotta Rhyolite	Rhyolite lava flows and rhyolitic tuffs	3A-3C	Aquifers with fracture permeability	The layer is defined as the upper portion of hydrogeological basement. Fracture basalt, ehyolite and permeable pumice layer has capacity of good aquifer
	N2b	N2b Basal	Basalt lavas and basaltic pyroclastics	3A		
	NQs	NQ s Rhyolite	Rhyolitic tuffs			
Pliocene	rht/N1_2n	N1_2n Rhyolite	Plagiocrase rhyolite tuff	3C	Localized aquifers with fracture and intergranular permeability	
	N1n	N1n Basalt	Anchar Basalt	3B	Localized aquifers with fracture and intergranular permeability	
	N1ar	N1ar Rhyolite	Rhyolite			
Miocene	Ngs	Sharenga Rhyolite	Rhyolite piles and necks			
	Ngu	Upper Basalt	Porous basalt lavas	3C	Localized aquifers with fracture and intergranular permeability	The basic nature of these formations are not cleary understood. Alternation of basalt and rhyolitic tuff. The possible aquifer may be localy developped fracture rich rocks and tuff
	Ngb	Beyana Tuff	Lapilli tuff with minor laminated tuff			
	Ngm	Middle Basalt	Porphyritic basalt lavas			
Eocene-Oligocene	Pgs	Shole Welded Tuff	Densely-welded rhyolitic welded tuff	3C	Localized aquifers with fracture and intergranular permeability	
	Pgl	Lower Basalt	Porphyritic basalt lavas			
Mesozoic	Mes	Adigrat Sandstone, Antaro Limestone	Sandstone, Shale and Limestone	4D	Localized aquifers with fracture and intergranular permeability	
Pre-Cambrian	Pre	Biotite Gneiss, Pegmatite	Biotite Gneiss, Granite, Biotite Metagranite			

References: (1) Laury and Albritton 1975, (2) Mohr et al. 1980, (3) EIGS-GLE 1985, (4) Woldegabriel et al. 1990, (5) GSE 1994, (6) GSE 2002, (7) EWTEC 2008

3.6.2   Evaluation of aquifer potential

The review of surface water potential as a potable water source seems to be not satisfactory. This result shows the potential drinking water source may be limited to the groundwater resources through wells and springs. The advantage of the groundwater usage as a potential potable water source is summarized as follows;

4) Basically the water is clean in terms of water quality, and the quality is not largely affected by seasonal fluctuations.

5) The amount of water is steady throughout the year, and necessary volume of water can be extracted by type of water supply facility

6) Knowing that good aquifers exist below allows for flexibility in the point of source extraction. Therefore, the water supply facility can be provided within the vicinity of the community.

From the past, more than ten thousand wells and springs have been used as potable water sources in the Study area. It should be noted that not all of the point sources have the above mentioned characteristics of a potable water source. Hand dug wells and shallow wells which target the shallow aquifer in the Alluvium can be easily affected not only by the surface pollution such as cattle disposal and fertilizer, but also seasonal fluctuation of the water level. This means that these will not provide a stable water supply. Therefore, the identification of a good aquifer which satisfies the above mentioned criteria shall be put in first priority. The investigation of groundwater potential shall be clarified by the distribution of good aquifers, as well as its quality and quantity as an aquifer unit.

The aquifers determined in the Study were compared to the description of aquifers in the existing well inventory. The distribution and classification is presented in Table 3.17. Description of existing well inventory is not accurate to correlate respective lithological description of aquifer. Therefore, the typical key composition (such as pumice, scoria, ignimbrite) of each description was referred to as the major aquifer units. Ignimbrite is most common lithology in the existing wells and corresponds to the Pleistocene rhyolite – andesitic welded tuff (from the comparison between JICA wells and existing wells). The major aquifer of Pleistocene basaltic tuff breccia – volcanic breccia can be referred to as scoricious tuff.

Most common groundwater source is extracted from Pleistocene tuff, tuff breccia and basaltic rock units (81% of total borehole water source). The members of this aquifer are, pumice tuff, welded tuff, tuff breccia and basalts (from upper formation). This aquifer is distributed from east of Lake Abaya to north of Lake Ziway.

Aquifer of Quaternary Sediments and lacustrine mainly consist of sand, gravel and silts. It is distributed throughout the entire study area (lacustrine is distributed chiefly in the area north of Lake Awassa). The Study referred to the water source mainly from boreholes and springs. However, most of hand dug wells are utilizing this shallow aquifer.

Tertiary rhyolitic rocks are supposed to be in a hydrogeological basement of the entire area. The older formations are commonly distributed in the southern part of the Study area. This old formation (Precambrian – Tertiary) has some potential as aquifer but is only distributed in a limited area, and utilized only 6% of total existing bore holes.

Table 3.17: Major Aquifer and Correlation with Existing Bore Hole

	Aquifer	Symbol	Major Lithology	Well No*	scription of Existing We	Distriution
1	Quaternary Sediments and Lacustrine	Al/Q	Alluvium	25	sand, gravel, alluvium, clay	distributed in entire RVLB
		Lac1	Lake deposits such as gravel, sand and mud	4	clay, sand, lacustrine	locally distributed in northern part of RVLB and surrounding Lake Awassa area
2	Pleistocene Tuff, Welded Tuff, Basalt	W	Rhyolitic tuffs and pumice tuffs	56	tuff, pumice tuff, pumice, sandy tuff	continuously distributed from Ziway to Dila area
		G	Rhyolitic to andestic welded tuff	35	ignimbrite, welded tuff	continuously distributed from Ziway to Dila area
		tb	Basaltic tuff breccias and lapilli tuffs	30	tuff breccia, scoricous basalt, scoria	locally distributed in entire RVLB
		ba	Massive basalt lavas	71	basalt, fractured basalt	locally distributed in entire RVLB
3	Tertiary Tuff and Basalt	rh, N2b	Rhyolite lava flows and rhyolitic tuffs	11	rholite, rholitic tuff, pyroclastics, trachyte	distributed in entire RVLB
		N1n, N1ar	Rhyolitic tuffs, basalt	4	fractured basalt, basalt	continuousely distributed in the south of Dila

* Some existing wells described Sand, Gravel, clay are not considered if not evidence to correlate the Aquifer

It is concluded that satisfactory water source shall be Pleistocene tuff, welded tuff, basaltic rock units which are largely distributed at the northern part of the Study area. This aquifer satisfies the requirement of quality, quantity and location of extraction. The extraordinary event of rift valley formation and followed by the creation of faults made enough fissures and pore zones in these volcanic rocks as the storage of huge amounts of groundwater.

a.   Evaluation of aquifer potential

Three (3) aquifers were identified by the study of existing well inventory, new borehole data and the geological survey. The aquifers are classified into the following criteria in reference with the aquifer classification of Ethiopian Hydrogeological map.

Aquifer 1 [Alluvium and lacustrine deposits] = 1B – 1C

Aquifer 2 [Pleistocene tuff, tuff breccia and basaltic rock units] = 3B – 3A (tuff = 1B)

Aquifer 3 [Plio-Pleistocene tuff and basalt] = 3C－3A

The quantitative review of the aquifers is made to grasp its potential as water source. Discharge (Q, l/sec), Specific Capacity (l/min/m) and Transmissivity (m^2/day) are shown by each layer of 3 aquifers. Aquifer 2 gave highest score in discharge, specific capacity and transmissivity. Basaltic tuff breccia – volcanic breccia scored mean discharge of 6.3 l/min, mean specific capacity of 134 l/min/m and mean transmissivity of 242 m^2/day. Note that some minimum figures fall below 1 as the Aquifer 2 classified as extensive aquifer with fracture permeability. However, at least 3-7 l/sec discharge (with maximum of more than 50 l/sec) can be expected if the bore hole hits the good fissure zone.

Aquifer 1 is also a good aquifer according to its nature of formation (sand, gravel). Most of this aquifer is shallow and unconfined. It should be noted that this aquifer is easily affected by surface pollution as well as seasonally affected by the water table.

Aquifer 3 is mainly distributed at the northern portion of entire study area. This aquifer is also stored in fissure in the volcanic rock. The distribution of this rock unit is said to be very

limited. The aquifer mainly occupies at the northern part of the study area, and it may become potential aquifer in those remote areas in the north.

In conclusion, the most potential aquifer in the area is Aquifer 2 in the entire study area

Table 3.18: Aquifer Parameters

	Aquifer	Symbol	Major Lithology	Q(l/sec)			Specific Capacity (l/min/m)			Transmissivity (m2/day)		
				AVE	MAX	MIN	AVE	MAX	MIN	AVE	MAX	MIN
1	Quaternary Sediments and Lacustrine	Al/Q	Alluvium	2.8	6.5	0.2	31.9	72.6	3.9	75.3	92.6	43.0
		Lac1	Lake deposits such as gravel, sand and mud	4.6	7.3	1.5	20.8	40.9	0.6	69.0	137.0	1.0
2	Pleistocene Tuff, Welded Tuff, Basalt	W	Rhyolitic tuffs and pumice tuffs	5.5	47.0	0.2	42.4	106.6	1.0	42.5	84.8	0.2
		G	Rhyolitic to andestic welded tuff	4.6	18.5	0.2	31.2	91.2	0.3	65.3	173.9	0.0
		tb	Basaltic tuff breccias and lapilli tuffs	6.3	22.0	0.1	134.6	414.6	2.5	242.0	914.4	12.5
		ba	Massive basalt lavas	2.9	7.7	0.2	19.3	55.1	2.9	77.7	211.7	2.7
3	Tertiary Tuff and Basalt	rh, N2b	Rhyolite lava flows and rhyolitic tuffs	4.9	19.6	0.6	11.6	25.6	3.8	9.3	24.8	0.1
		N1n, N1ar	Rhyolitic tuffs, basalt	3.9	6.0	2.0	13.5	13.5	13.5	12.6	12.6	12.6

Figure 3.12 shows the discharge of the well and springs. In general, high production water sources can be found at the area between slope along the rift ridge and flat lowland. High groundwater gradient can be expected at the escarpment. High discharge cannot be expected at the escarpment both located at the eastern and western ridge of the valley.

The Study on Groundwater Resources Assessment
in the Rift valley Lakes Basin in Ethiopia, Final Report (Supporting Report)

JICA
KOKUSAI KOGYO CO., LTD.
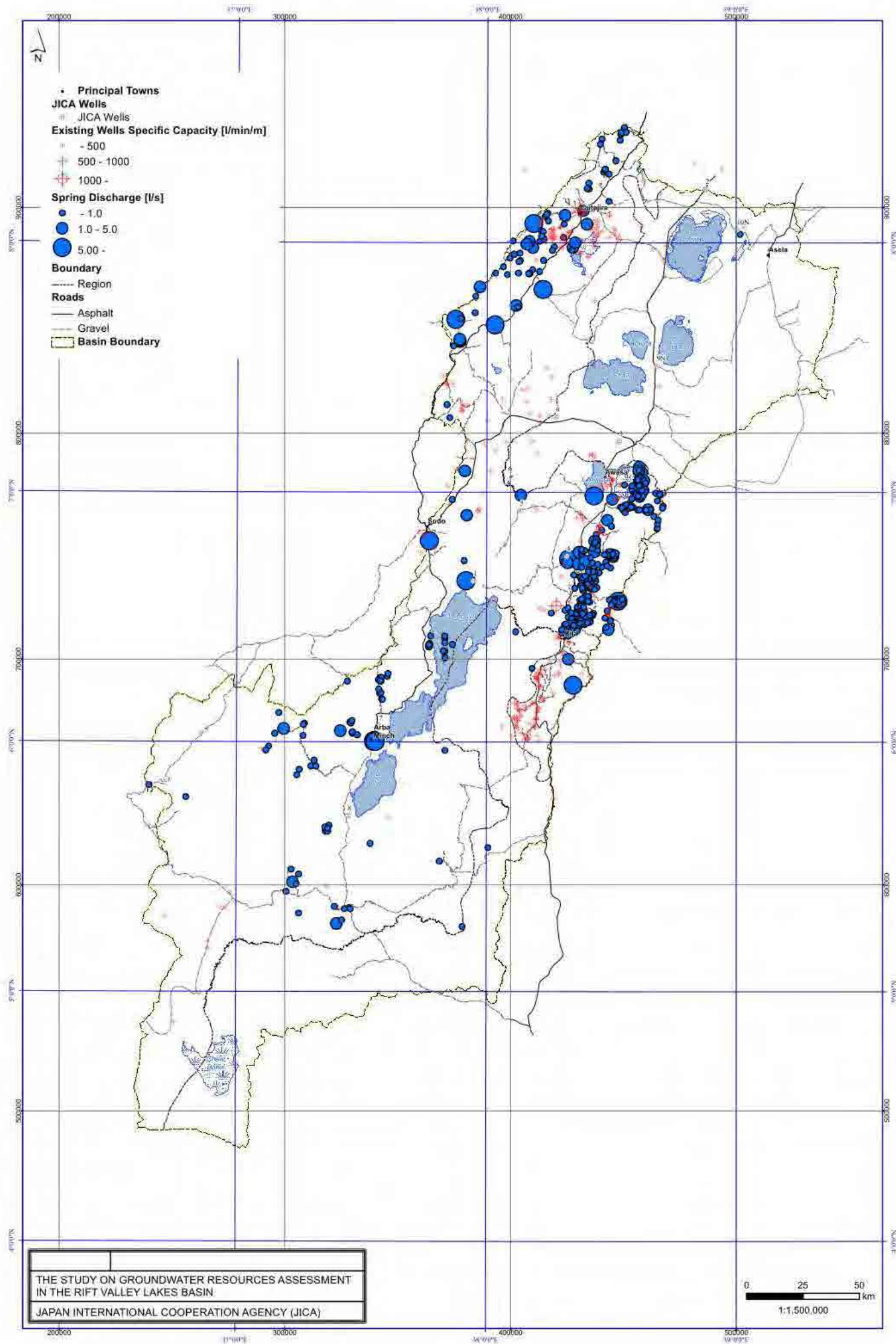
Figure 3.12: Discharge of Water Sources

3.7   Creation of hydrogeological maps and profiles

3.7.1   Hydrogeological maps

The hydrogeological map is established based on the hydrogeological features and characteristics of strata in reference with existing well inventory and survey results. The map is shown in Figure 3.13. The hydrogeological characteristics will be described based on the hydrogeological map.

The hydrogeological feature of Rift Valley Lakes Basin can be divided into two major areas, that is;

> 1) Northern Pleistocene volcanic zone from Ziway to Dila

> 2) Older volcanic zone and basement rocks at the southern region of Lake Abaya

Both areas have the feature of alternation of volcanic rocks (such as tuff, tuff breccia, pyroclastics, welded tuff and basaltic or rhyolitic lava) by several volcanic activities. However, the hydrological conditions are quite different. The major difference will be described below with some additional information of Quaternary sediments.

a.   Unconsolidated Quaternary Sediments Surrounding Rift Valley Lakes

Lacustrine deposits (lac2, lac1) are represented by sand, gravel, mud layers which are distributed in the areas surrounding Lake Ziway to Lake Awassa, Lake Abaya, Lake Chomo and Chew Bahia (with some salt lakes). Quaternary sediments (Al, Q = sand, mud and gravel) are distributed around the lakes and rivers. In general, lacustrine deposits are relatively more consolidated than Quaternary sediments. The lacustrine deposit may have lower production capacity than Quaternary deposits as it includes some impermeable clay layers. However, the mean discharge rate of lacustine is higher than Quaternary deposits (see the Table 3.18). In general these deposits occupy a lower profile of the rift valley and mainly stores shallow aquifer. The aquifer is mainly used for the hand dug well and ring wells with depths up to 8 -12 m. However, shallow wells at north western flat of Lake Ziway – Shalla, and lake itself produces high fluoride water (above Ethiopian drinking water standard). The circumstance of the aquifer in this category is also highly affected by the surface water condition such as rainfall and heat. Therefore this aquifer does not satisfy the domestic standards for portable water sources.

The high groundwater potential areas in this type of deposits are distributes at relatively highland area of north eastern to eastern of Lake Ziway and low land of western Lake Ziway, in particular, alluvial and Lacustrine deposits were recognized widely and thickly in western area of Lake Ziway with high groundwater potential, and the areas of flat along the Bilate river and northern Lake Abaya also have high groundwater potential.

b.   Hydrogeological Condition of Northern Pleistocene Volcanic Zone

The main aquifer in this area is Aquifer 2 [Pleistocene tuff, tuff breccia and basaltic rock units] which printed as light blue color in the Hydrogeological map (draft). Late volcanic activities of late Pleistocene – early Holocene produced a lot of members of volcanic rocks. These members are basaltic pyroclastics with scoria (rb), pumice tuff (Pm), tuff, volcanic breccia, Basalt (volcan) of which (rb) and (Pm) has extensive permeability with high porosity.

The condition to be an aquifer is the existence of impermeable layer below this formation. The rock units in this category are abundant at Ziway area. Most of the member are not aquifer with some exception of very local storage of water.

Early Pleistocene volcanic deposits, rhyolitic tuff – tuff (W), rhyolite – andesitic welded tuff (G), basaltic tuff breccia – volcanic breccia (tb), basalt (ba), are the most promising potential aquifer in the entire Study area. Lake deposits will be an aquiclude consist of well consolidated conglomerate and mud stone. Therefore, the upper formations, if the certain condition allows storing the water, can become good aquifer. The condition is the degree of developing fissures and cracks by the mass movement of the crust during the formation of rift. The upper tuff (W) is also potential aquifer knowing that aquiclude exists at lower formation. About 80% of the bore hole (drilling hole) extracts the water from this early Pleistocene volcanics.

Hydrogeological map seems to be covered with the rhyolitic tuff – tuff (W) layer, but it should be noted that the other volcanic member exists underneath. The topographical features of high yielding aquifers are distributed in the emerging point of escarpment and flat of the valley. The fissure developed in the volcanic rocks at the escarpment by the rift activity and the permeability became higher. The emerging point provides favorable water pool between fissure rich rock units and those without fissures.

This aquifer has developed parallel to the original valley shape. Direction of water flow is also parallel to the valley which means it has a steep flow down below the escarpment and runs into the middle of the valley. The final destination of the groundwater is not lakes but the subsurface groundwater valley existing between Lake Abaya and Lake Awassa.

High potential area for water extraction are northern Lake Abaya where chiefly occupied by this type of volcanic rocks in general. Specific areas are at the intersection of eastern escarpment to central plane the valley of eastern Lake Ziway to eastern Bilate River, and at the intersection of western escarpment to central plane of rift valley of Awassa to Dila.

c.   Hydrogeological Condition of Southern Tertiary Volcanic and Basement

The light brown and khaki colored portion on hydrological map is this formation. Major lithology of this rock unit is alteration of Tertiary basalt and rhyolite and its members. Mesozoic sandstone, limestone (Mes) and Precambrian biotite gneiss, granite (Pre) are also observed in limited area. These formations considered to be the hydrological basement rocks in the entire basin. However, very limited but some formations contain a local aquifer. Plio Pleistocene fissure rich rhyolite lava and tuff (rh) are potential storage for groundwater. Basalt lava and basaltic pyroclastics (N2b) are also considered as potential aquifers. There are some other potential aquifers such as tuff and basalt (N1n) and rhyolite and basaltic lava (N1ar), but the continuity of these layers is very limited and not well understood. The potential of the aquifer is limited in the means of its production. The well information in this area is very limited, therefore the qualitative feature and the flow direction of aquifer is not known.

In general, the groundwater potential of extracting water is relatively low in these geologic formations. However, the lack of drilling data at this area prevents further analysis for the groundwater distribution and its nature. It shall be noted that further investigation required by adding more drilling and its inventory.
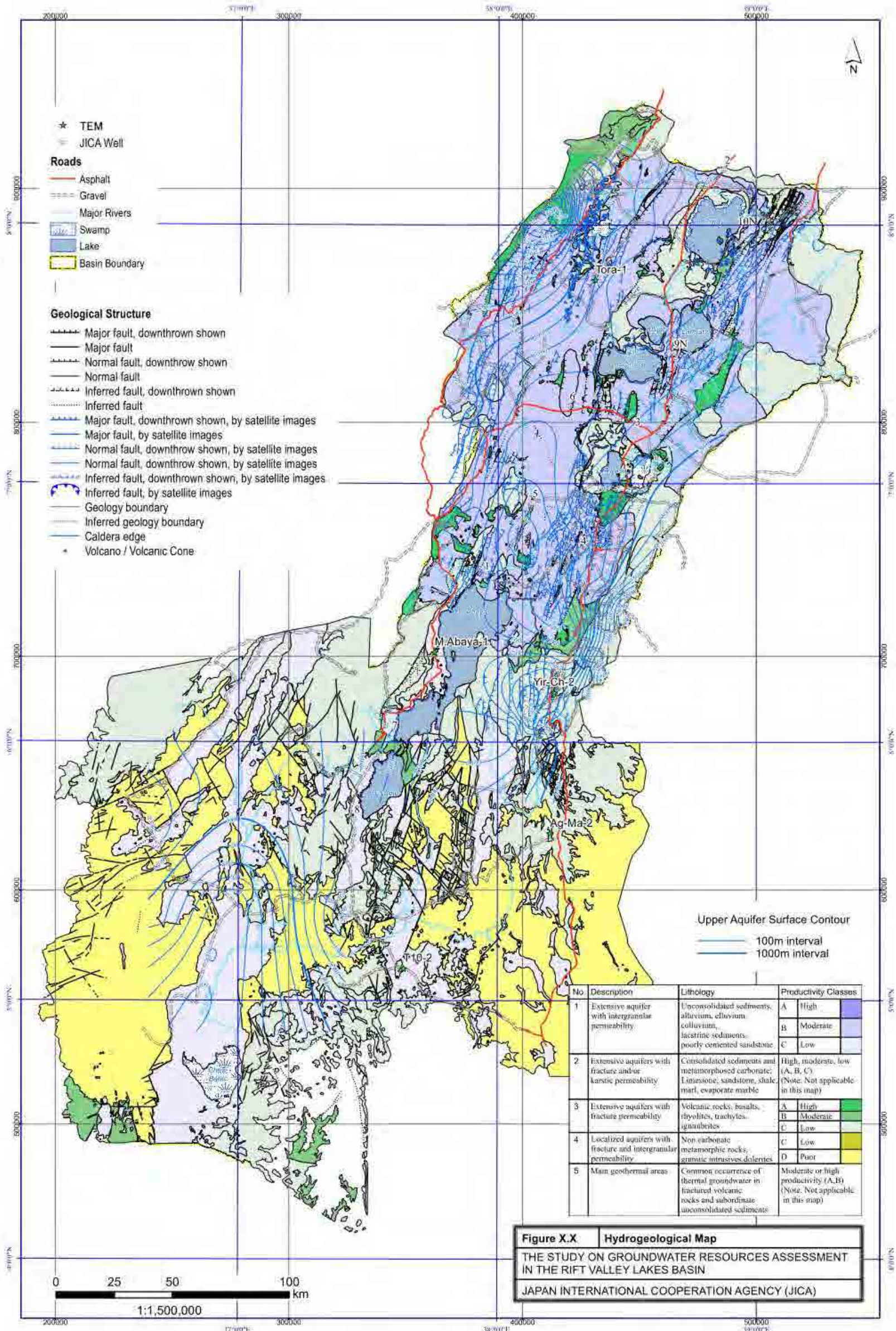
The Study on Groundwater Resources Assessment
in the Rift valley Lakes Basin in Ethiopia, Final Report (Supporting Report)

JICA
KOKUSAI KOGYO CO., LTD.

Figure 3.13: Hydrogeological Map

The Study on Groundwater Resources Assessment
in the Rift valley Lakes Basin in Ethiopia, Final Report (Supporting Report)

JICA
KOKUSAI KOGYO CO., LTD.

3.7.2 Hydrogeological profiles

The major aquifer in the entire study area is early Pleistocene volcanic formations. The upper surface and lower surface of the aquifer has been tracked and its cross sectional trend is shown in Figure 3.14. It was pointed out at the Hydrogeological map section, the groundwater gradient is high at the escarpment of the rift valley and forms a concave concentration point at the rift center. It should be noted that this concave shape is not affected by uplifting in the valley, mostly made up with recent volcanic cones and hills. The maximum thickness of the aquifer is almost 100m, but it shall be more realistic to consider it as a thick and wide fissure developed zone. Even it belong to the same aquifer, the capacity of aquifer may differ horizontally or vertically. However, consideration of the 3D distribution of the aquifer for the exploration of the target water source will be useful to exploit the good quantity and quality groundwater with good accuracy, by avoiding the fluoride concentration zone.
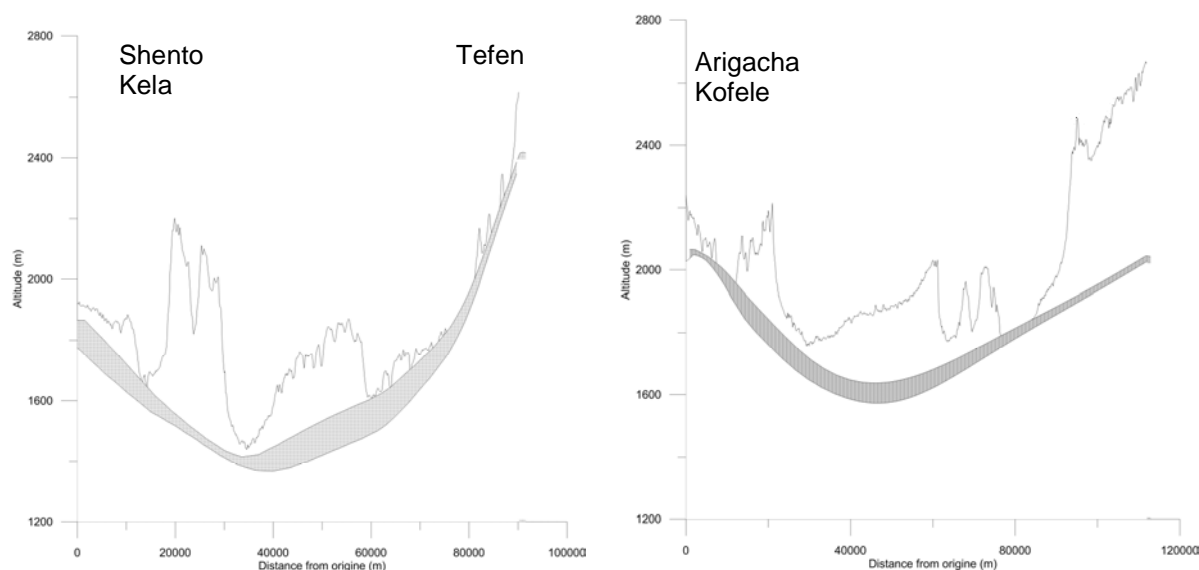
Figure 3.14: Cross Sectional Distribution of Aquifer (Hach=Aquifer, Ratio V:H 1:100)

3.7.3 Examination of groundwater flow

The important parameter for the consideration of the groundwater flow is static water level of existing borehole. Therefore, the density of the borehole position and its distribution largely affects the result. Initially the study focused on the database provided by ENGWIS and HALCROW to extract whole static water data of entire borehole. Alteration of tuff, tuff breccia, welded tuff and basaltic rocks are widely distributed by the repeated volcanic activity. Furthermore, the formations of volcanics are segmented by the active mass movement of the rift. The lakes are distributed at the bottom of the valley and accumulation of Alluvium at the floor of the valley is active. This complex distribution of the several formations made both confined and unconfined aquifer randomly. The existing well inventory provided by above database does not include the description of confined and unconfined layer.

The groundwater contour from the original database (SWL) is indicated in the. There are several ups and downs, such as cones and concaves, randomly observed. Therefore, the upper and lower surface of the aquifer is defined as simulated water level contour to avoid the affect

of unconfined state of groundwater. The groundwater flow was considered on the basis of this simulated water level contour.

Figure 3.15 shows the contour of upper surface of aquifer. However, the lack of bore hole at sub basins of Galana, Segen-Amessa Guracha, Kulfo Gina and Eastern Ziway、Lake Langano. There is no indication of groundwater flow in these areas.
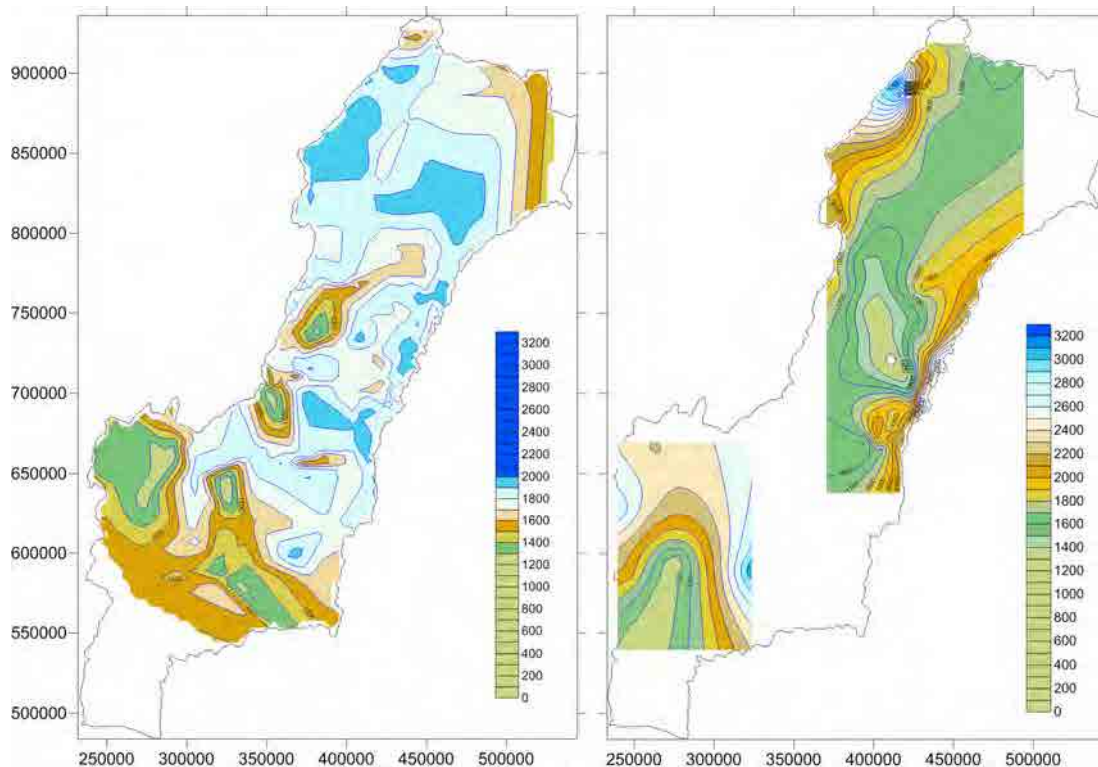

Figure 3.15: Groundwater Level Contour

The contouring of upper (or lower) surface of the aquifer indirectly suggests the distribution of available groundwater level.

The Figure shows the groundwater gradient is high at the escarpment of sub basins of Western Ziway, Bilate, Awassa, Gidabo and Galena. The groundwater rapidly flows down and becomes gentle at the valley floor. The gradient is almost parallel to the original shape of the valley (not considering undulation of volcanic cones and hills). The end point is not necessarily the lakes but seems to be gathered into the depression of groundwater between Lake Abaya and Lake Awassa. At the far north of the study area, groundwater runs down along the Weto River and ends its flow into Chew Bahir.

3.8 Groundwater quality

3.8.1 Parameters and methodology of water quality analysis

The total number of samples is 100, of which 90 samples are taken from existing wells and springs, and 10 samples from the test wells. The samples are to be collected and analyzed through a sub-contractor.

a.   Site Analysis

The 12 parameters for on-site water quality measurements are conducted. Three analysis experts measured each item promptly after having gathered water with a water level sampler from the existing well. The analysis items of water quality are: basics items (temperature, electric conductivity, pH, ORP), items which may affect human health (Fe, Mn, F, NO_3, As, NH_4), and bacteria (Coliform, general bacteria). It was intended to grasp the summary of the quality of the water before the laboratory analysis will be completed. Water quality parameters, and analysis methods and the Ethiopian drinking water standard corresponding to measurement item are shown in the following table.

Table 3.19: Parameters of Water Quality Analysis for Site Analysis

NO	Parameters	Methodology	Ethiopian Drinking Water standard*
1	Temperature	thermometer	N.A.
2	Electrical Conductivity（EC）	Conductivity meter	N.A.
3	pH	pH meter	N.A.
4	Oxidation reduction potential （ORP）	ORP meter	N.A.
5	Iron（Fe）	Pa	0.4 mg/l
6	Manganese（Mn）	Pack test	0.8 mg/l
7	Fluoride（F）	Pack test	3.0 mg/l
8	Sulfite（NO_3）	Pack test	6.0 mg/l
9	Arsenic（As）	Pack test	0.01 mg/l
10	Ammonia（NH_4）	Pack test	2 mg/l
11	Coli form	litmus paper	0/100ml
12	General Bacteria	litmus paper	0/100ml

*Specification for Ethiopian Drinking Water Quality Guidelines (September 2002, Ministry of Water Resources, the Federal Democratic Republic of Ethiopia)

b.   Laboratory Analysis

The parameters for the water quality analysis were selected for examination of whether the groundwater quality (including spring water) could be classified by sub-basins or by geology (of aquifer). Elements harmful to the human body were also selected, however parameters were emphasized that specify the origin of water, such as Ca, Cl, Mg, Na, K, HCO_2, SO_4, NO_3 which are more useful for making Trilinear and Hexa Diagrams.

Table 3.20: Laboratory Water Quality Analysis and its Reasons

NO	Parameter	Guide line* (mg/l)	Reasons of Analysis
1	Taste	Non-Objectionable	May give rise to complaints from consumers
2	Odor	Non-Objectionable	May give rise to complaints from consumers
3	Turbidity	7	May give rise to complaints from consumers
4	Total Dissolved Solids (TDS)	1776	May give rise to complaints from consumers
5	Suspended Solid (SS)	NA	May give rise to complaints from consumers
6	pH	6.5 – 8.5	May give rise to complaints from consumers
7	Electric Conductivity (EC)	NA	May give rise to complaints from consumers
8	Total Hardness (CaCO$_3$)	NA	May give rise to complaints from consumers
9	Calcium (Ca)	NA	Characteristics of ion composition
10	Magnesium (Mg)	NA	Characteristics of ion composition
11	Potassium (K)	NA	Characteristics of ion composition
12	Sodium (Na)	358	May give rise to complaints from consumers・Characteristics of ion composition
13	Iron (Fe)	0.4	Health effect to human body
14	Manganese (Mn)	0.8	Health effect to human body
15	Chloride (Cl)	533	Health effect to human body・Characteristics of ion composition
16	Sulfate (SO$_4$)	483	Characteristics of ion composition
17	Nitrate (NO$_3$)	50	Health effect to human body・Characteristics of ion composition
18	Nitrite (NO$_2$)	6.0	Health effect to human body・Characteristics of ion composition
19	Alcalinity (CO$_3^{2-}$, HCO$_3^-$)	NA	Characteristics of ion composition
20	Fluoride (F)	3.0	Health effect to human body
21	Total Phosphorus (TP)	NA	Reference
22	Ammonia (NH$_3^+$＋NH$_4^+$)	2	May give rise to complaints from consumers

*Specification for Ethiopian Drinking Water Quality Guidelines (September 2002, Ministry of Water Resources, the Federal Democratic Republic of Ethiopia)

However, the result does not include the water quality analysis of JICA test wells of RVS-BH-4 – 10.

c.   Isotopic Analysis

The ratio of stable isotopes in water will be analyzed to estimate the origin of the sampled groundwater. The results can be used, for example, to understand the relation between groundwater recharge mechanisms and high fluoride concentrations in an area.

Stable isotopes of hydrogen (D) and Oxygen (^{18}O) will be analyzed and the results will be plotted on a diagram presented below. The diagram will help discern chemical proximity of waters within each of different groundwater basins by knowing their origins.

3.8.2   Selection of sampling points

In order to grasp the difference of water quality by aquifer and by water basins in the LVLB, the sampling sites are selected by the following procedure.

1. Divide the water basin into 14 characteristic basins

2. From the respective 14 sub-basins, 6 or 7 samples were taken from the different geological (aquifer) conditions and type of source.

3. If the site is not possible to sample, the sample site will be shifted to the same aquifer upon consultation with a Regional Water Engineer

The plan of sampling point map is presented in and the list of sampling points is tabulated in Table 3.21.
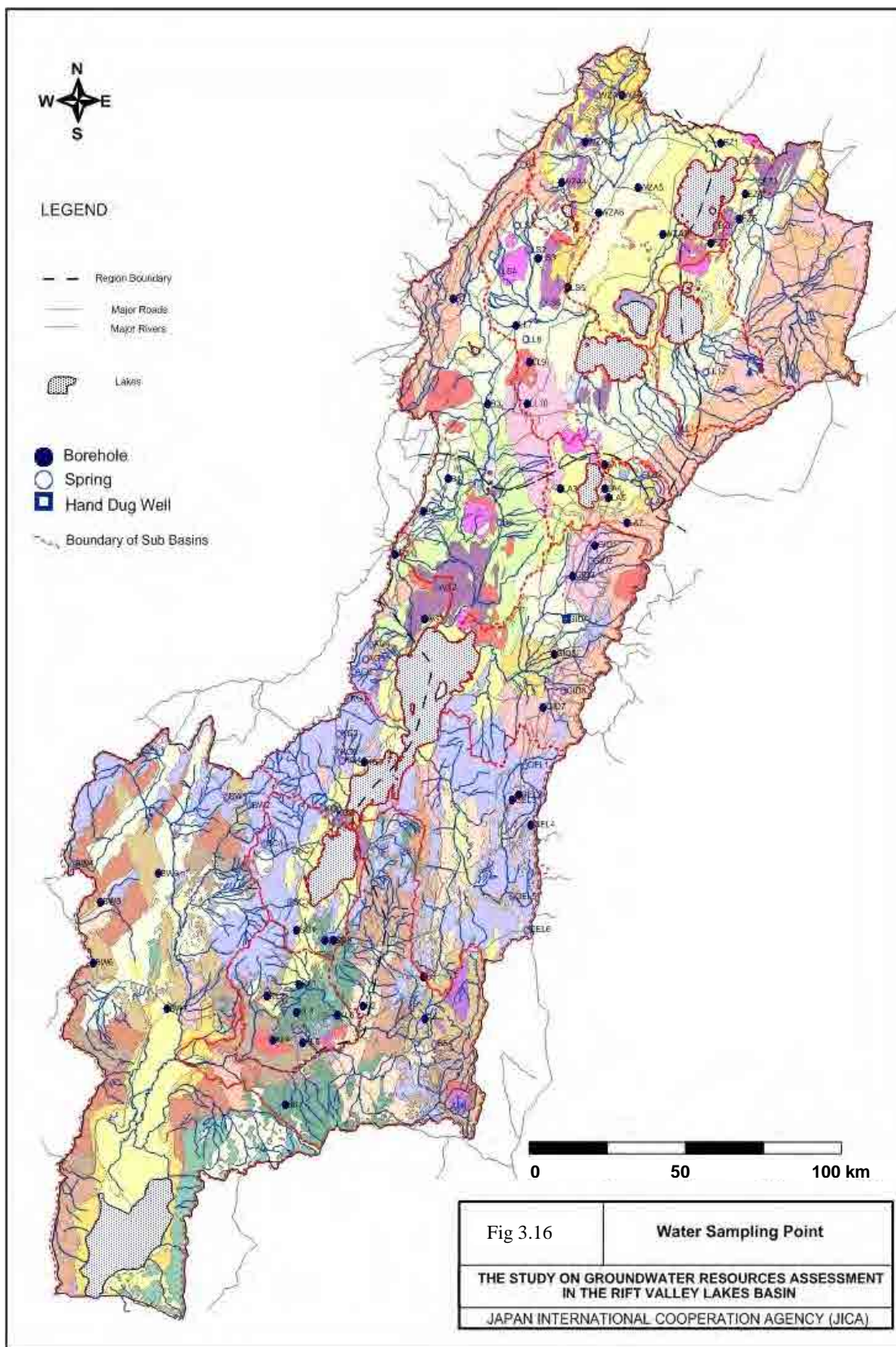
Figure 3.16: Sampling Point for Water Quality Analysis

Table 3.21: Geology and Sub-basin of Water Quality Analysis Sampling Point

Bno	BasinName	Samp_P_ID	Geology	SourceType	Eastings	Northings	Remarks
1	Western Ziway-Abjata	WZA1	Qwbh	spring	440353.00	918436.00	
		WZA2	N1_2n	Borehole	449814.00	918599.00	
		WZA3	Qwbh	Borehole	436107.39	901949.82	
		WZA4	Qdi	Borehole	426750.58	887592.79	
		WZA5	Qdi	Borehole	455903.00	885591.00	
		WZA6	Qdi	Borehole	440921.00	876752.00	
		WZA7	Ql	Borehole	465363.00	869206.00	
2	Eastern Ziway	EZ1	Ql	Borehole	487538.00	901548.00	
		EZ2	Ql	spring	495889.00	895142.00	
		EZ3	Ql	spring	502396.00	887587.00	
		EZ4	Ql	Borehole	496746.00	883403.00	
		EZ5	Qwbh	Borehole	494507.00	874562.00	
		EZ6	Ql	spring	485555.00	872111.00	
		EZ7	Ql	Borehole	483552.00	866076.00	
3	Lake Shalla	LS1	Qdi	spring	410040.00	872237.00	
		LS2	Qwpu	spring	414532.00	863503.00	
		LS3	Qdi	Borehole	418241.00	860616.00	
		LS4	Qwpu	spring	403414.00	855821.00	
		LS5	N1_2n	Borehole	429417.53	850002.26	
		LS6	Qwbh	spring	420168.00	844740.00	
4	Lake Langono	LL10	Qdp	Borehole	413811.47	808766.15	
		LL11	Qdi	spring	471440.00	799751.00	
		LL12	Qdi	spring	481628.00	820252.00	
		LL7	Qdi	Borehole	409686.00	836778.00	
		LL8	Qdi	spring	413167.00	831630.00	
		LL9	Qws	Borehole	414848.79	823508.22	
5	Lake Awasa	LA1	Qws	Borehole	443247.00	787145.00	
		LA2	Qdi	spring	458768.00	783746.00	
		LA3	Ql	Borehole	426416.00	778488.00	
		LA4	Ql	Borehole	443296.00	778694.00	
		LA5	Qws	Borehole	444891.00	775368.00	
		LA6	N1_2n	spring	459970.00	773976.00	
		LA7	NQs	Borehole	451604.00	766446.00	
6	Bilate	B1	NQs	spring	412472.00	893811.00	
		B2	NQs	Borehole	385835.00	846152.00	
		B3	Qdi	Borehole	399055.00	808866.00	
		B4	Qdi	Borehole	383940.00	782096.00	
		B5	Qdi	Borehole	374310.00	770488.00	
		B6	Qvs	spring	403650.00	766500.00	
7	Amessa Guracha	AG1	NQs	Borehole	363549.00	755433.00	
		AG2	Qwbp	spring	379661.00	743494.00	
		AG3	Qwbp	Borehole	374898.00	732412.00	
		AG4		spring	354515.00	723336.00	
		AG5	Pv	spring	352367.00	718157.00	
		AG6	Pv	spring	347611.00	713476.00	
8	Gidabo	GID1	Qdp	Borehole	439758.00	758653.00	
		GID2	Qdp	spring	438017.00	753002.00	
		GID3	Qdp	Borehole	431299.00	747854.00	
		GID4	Qdi	hand dug well	428801.00	732211.00	
		GID5	Qa	Borehole	424000.00	720000.00	
		GID6	PNv	spring	427915.00	706700.00	
		GID7	PNv	Borehole	420150.00	701089.00	
9	Kulfo Gina	KG1	Pv	spring	345897.00	704036.00	
		KG2	Pv	spring	342307.00	691646.00	
		KG3	PNv	spring	342008.00	684900.00	
		KG4	Pv	spring	343470.00	682077.00	
		KG5	Qa	Borehole	351823.00	681377.00	
		KG6	Pv	spring	335938.00	664942.00	
		KG7	Qwbp	spring	340514.00	663331.00	
10	Sife Chamo	SC1	Pv	spring	313955.00	652539.00	
		SC2	Qa	spring	325813.00	650053.00	
		SC3	Pv	spring	323955.00	631606.00	
		SC4	Qa	Borehole	326268.00	621806.00	
		SC5	NMt	Borehole	337177.93	618029.40	
		SC6	NMt	Borehole	340044.00	618188.00	
11	Gelana	GEL1	Pv	spring	413097.00	680370.00	
		GEL2	PNv	Borehole	410584.00	669815.00	
		GEL3	PNv	Borehole	408331.00	668006.00	
		GEL4	PNv	Borehole	415473.00	659170.00	
		GEL5	Pcgn4	spring	408449.00	633710.00	
		GEL6	Pv	spring	413840.00	621971.00	
12	Bezo Weyto	BW1	Pcgn4	spring	299599.00	669160.00	
		BW2	Pv	spring	308307.00	666051.00	
		BW3	Pcgn4	Borehole	273518.78	641784.04	
		BW4	Pcgn3	spring	241142.00	645216.00	
		BW5	NQs	Borehole	251506.68	631850.39	
		BW6	Pcgn4	Borehole	248647.00	610123.00	
		BW7	QHr	Borehole	276954.74	593722.42	
13	Konso Localized	KL1	Qa	Borehole	327166.32	602575.18	
		KL2	Pcgn1	Borehole	314963.82	598184.77	
		KL3	NMt	Borehole	326032.44	592626.67	
		KL4	Pcgt4	Borehole	317138.94	582698.21	
		KL5	Pcgn1	Borehole	328439.00	581952.00	
		KL6	NMt	Borehole	341546.24	591483.08	
14	Segen	S1	NMt	spring	366914.00	649685.00	
		S2	Qe	Borehole	351527.97	594777.38	
		S3	Qe	Borehole	374494.00	605132.00	
		S4	Pv	Borehole	374737.00	590400.00	
		S5	Pcgn4	spring	378773.00	581400.00	
		S6	NMt	Borehole	321726.00	559650.00	

3.8.3   Results of water quality analysis

The result of water quality analysis (including site analysis, laboratory analysis and isotopic analysis) are filed in the Data book of this report. The review will be made with respective values of parameters in reference with the Specification for Ethiopian Drinking Water Quality Guidelines (2002) which is also presented in the Data book.

The site measurements give a general idea of the water quality, which shows some high fluoride contents compared to the standard value (3.0mg/l). Four samples out of seven indicate a fluoride value of 3.0mg/l in Awassa sub-basin. Some samples from the northern area of Awassa sub-basin (between Lake Ziway and Awassa) also show higher values of fluoride content. The aquifers in this area are mainly lacustrine, welded tuff, tuff and pyroclastics. On the other hand, the southern area of Lake Abaya has relatively small fluoride concentration, except the samples from lacustrine. Despite the fact that no bacteria have been detected in the laboratory analysis, most of the site samples show the existence of coliform and general bacteria. Probably it is affected by artificial reasons such as careless treatment of litmus paper, and/or humans saliva etc.

There are few results showing values high above the Standard, but some of them certainly exceed the limit of guideline values in the laboratory analysis results. High values of fluoride, iron, nitrate are harmful to human health, and turbidity, total dissolved solids, ammonia, hardness and sulfates may give rise to complaints from consumers. The fluoride content of groundwater originated from the lacustrine aquifer in the East Ziway sub-basin (7.4mg/l) and the spring from volcanic rocks in Awassa sub-basin (10.33mg/l) display high values. Iron content mostly falls under the guideline value of 0.5mg/l, but some values exceed the limit with the maximum of 0.8mg/l. However, most high values of iron are found in basement rock areas (58.8mg/l). This iron concentration may be a result of hydrothermal activity in the area. Some samples show relatively high turbidity, total dissolved solids, ammonia, hardness and sulfate which may give rise to complaints from consumers. However, these sources are presently used as drinking water for more than 30 years. With some exceptions, the water quality analysis in this Study suggests the water is generally acceptable for drinking water.

The discussion on the origin of water, in relation with the ion balance will be described in the next chapter.

3.8.4   Evaluation of water quality

The characteristics of the water quality in terms of each sub-basin and geology of aquifer will be discussed based on the projection onto the trilinear diagram, hexa diagram and isotopic diagram.

a.　　　　　Evaluation by the Trilinear Diagram

The characteristics of water quality by sub-basin and geology will be examined. The ion ratio of major cations represented by calcium, magnesium, sodium and anions such as sulfate, chloride and bicarbonate are plotted on the diagram shown in Figure 3.17. The projection of such ion balance to the diagram (trilinear diagram, piper diagram) represents the nature of the water as indicated as follows;
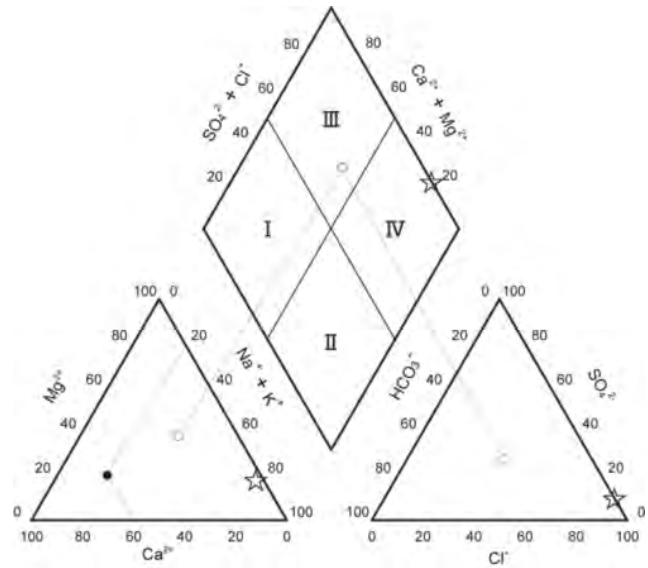

Figure 3.17: Trilinear Diagram

I $Ca(HCO_3)_2$ Type (Carbonate hardness): Shallow groundwater, River water

II $NaHCO_3$ Type (Carbonate alkali): Deep groundwater

III $CaSO_4$ $CaCl_2$ Type (Non-carbonate hardness):

IV $NaSO_4$ $NaCl$ (Non-carbonate alkali):Seawater, fossil saline water, hot spring

a.1　　　　　Characteristics of groundwater by sub-basins

The pattern of water quality on trilinear diagram by sub-basins is shown in Figure 3.18. Low in chloride ions, the pattern is classified into $NaHCO_3$ type and $Ca(HCO_3)_2$ type, in general. Chew-Bahir sub-basin and Abaya-Chamo sub-basin are classified as $Ca(HCO_3)_2$ type. The major pattern of groundwater quality in the Study area is $Ca(HCO_3)_2$ type, which suggests the origin of water comes from shallow groundwater and river water. The existing studies on the chemical composition of groundwater suggests that the $Ca(HCO_3)_2$ type groundwater is mainly occurring in circulating groundwater. In contrast, Awassa sub-basin tends to have a pattern of $NaHCO_3$ type where the water is originated in deep groundwater mainly occurring in stagnant groundwater environments. Ziway-Shalla sub-basin has both patterns of $NaHCO_3$ and $Ca(HCO_3)_2$ type. Overall groundwater pattern indicates the groundwater environment is circulating in the south, while the northern part has stagnant conditions by sub-basin.
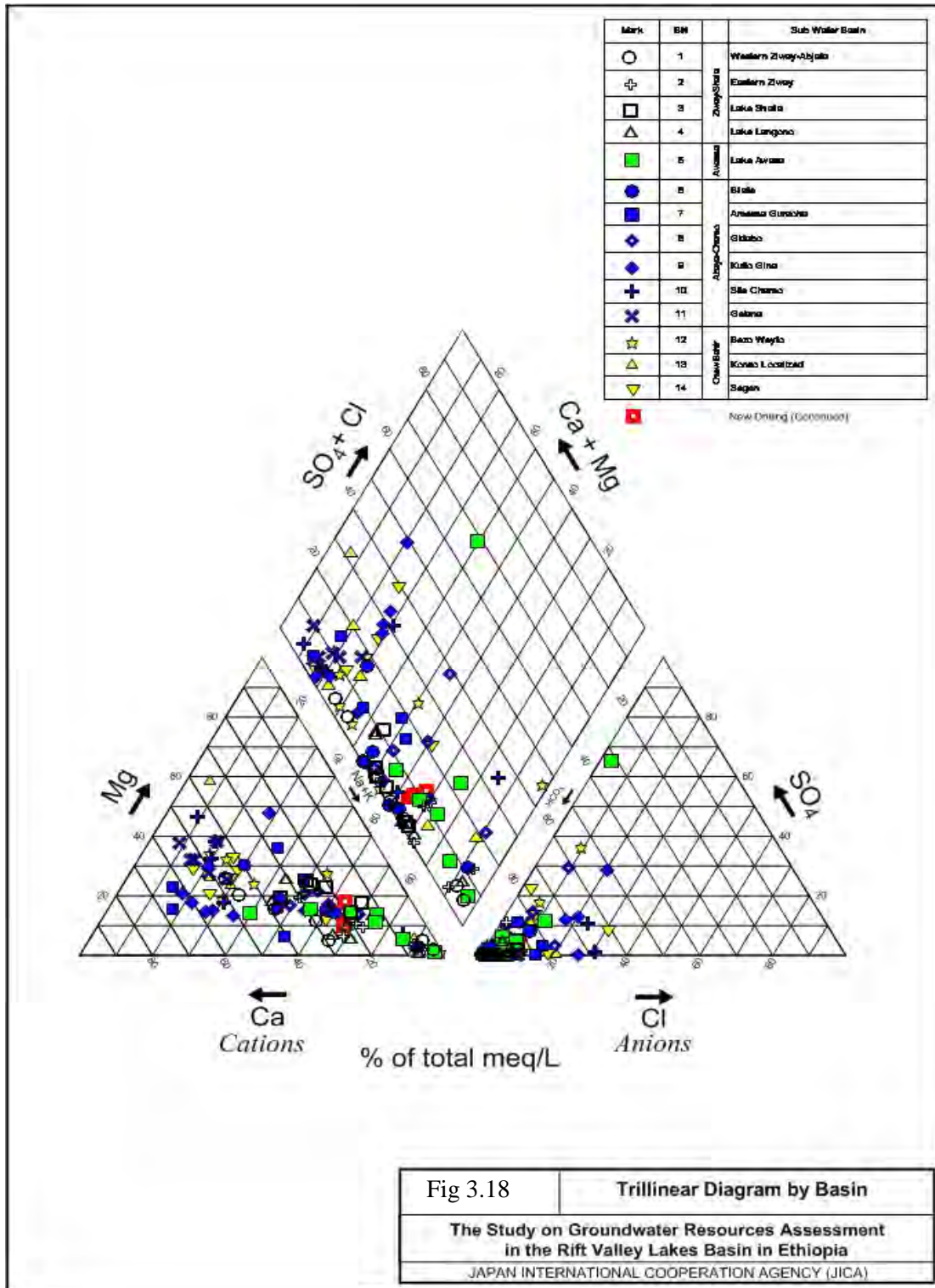
Figure 3.18: Trilinear Diagram by Basin

a.2   Characteristics of groundwater by geology of aquifer

The pattern of water quality on trilinear diagram by geology of aquifer is shown in Figure 4.11. Groundwater in sandstone, limestone, basalt, pyroclastics, granite and gneiss (2A-2C in the Figure) are categorized as $Ca(HCO_3)_2$ type, and groundwater in tuff, tuff breccia, lacustrine and alluvium is classified into $NaHCO_3$ type and $NaHCO_3 + Ca(HCO_3)_2$ type. This pattern suggests the fissure and fracture groundwater exists under the circulation environment, and the layered water has nature of stagnant environment. It suggests that the groundwater exists in the alluvium and lacustrine in the central lower part of the Rift Valley is in a stagnant condition, and the fissure groundwater in the volcanic and gneiss is circulatory by nature.
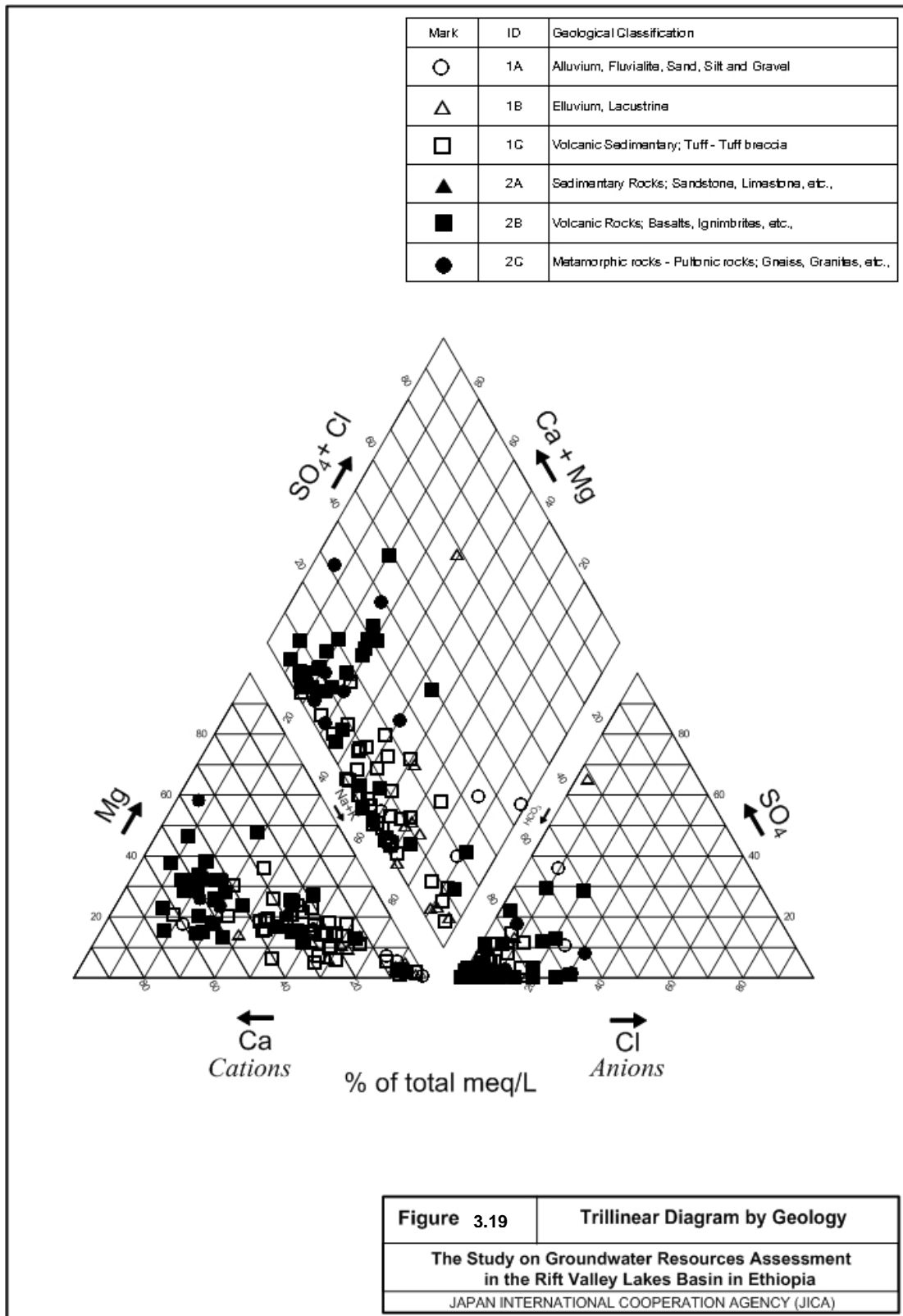
Figure 3.19: Trilinear Diagram by Geology

b.   Evaluation by the Hexa Diagram

As in the evaluation by trilinear diagram, hexa diagram indicates the type of water by the composition of the chemicals. Figure 3.20 shows the classification of the type by its shape into the projection in the diagram. Hexa diagrams of all water samples are presented in the Databook. This type classification result indicates similarity with the result of trilinear diagram. The result shows that the analyzed water can be classified into Ca-HCO$_3$ type, Na-HCO$_3$ type and its combination type.

b.1   Na-HCO$_3$ type

Basically, the environment of the groundwater in this type is stagnant. The deep groundwater is said to be classified as this pattern. The Na-HCO$_3$ type groundwater is abundant at the northern area of the study area.
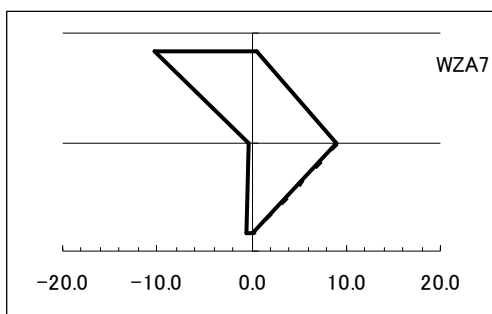
Na-HCO$_3$ type (Western Ziway)-

b.2   Ca-HCO$_3$ type, Combination type

Majorities of the groundwater are classified in this type which has the nature of circulation environment of groundwater.
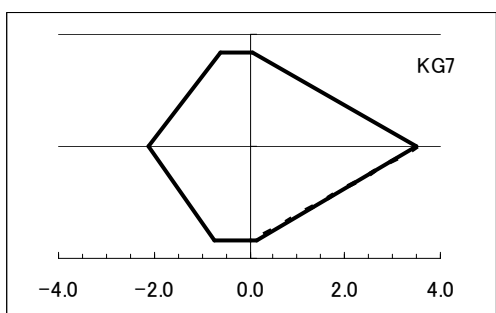
Ca-HCO$_3$ type (Kulfo Gina)
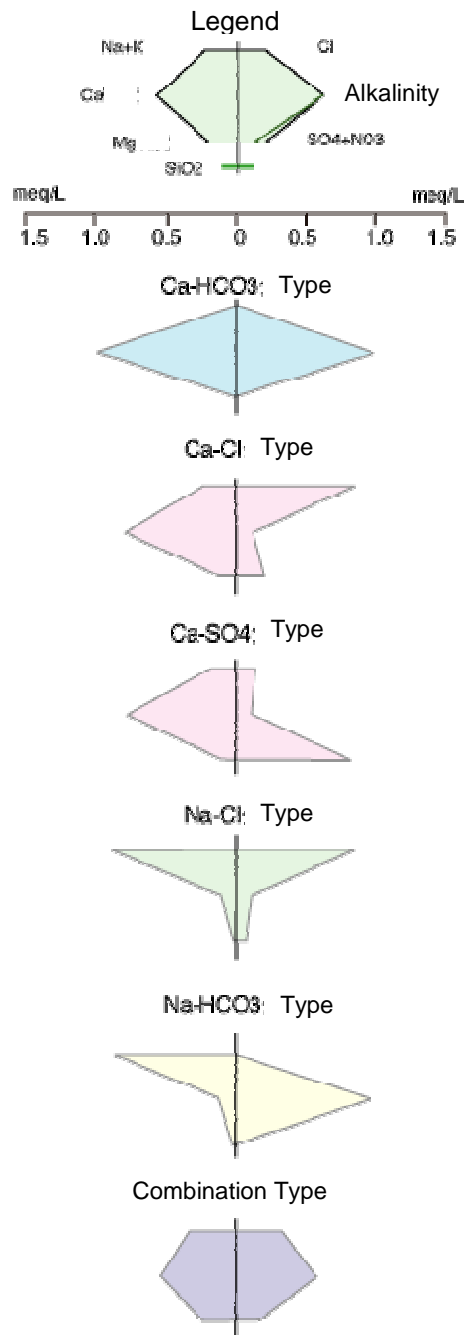
Figure 3.20: Type of Hexa Diagram
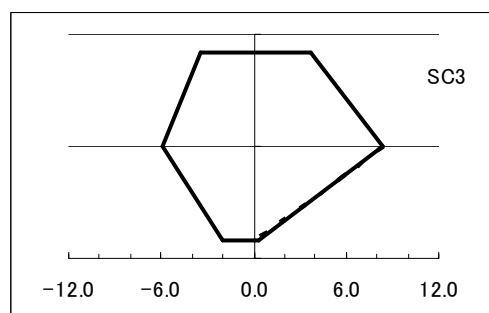
Shape of Combination type (Sife Chamo)

3.8.5   Isotopic analysis

Craig (1961) conducted the hydrogen and oxygen isotope analysis of river water, lake water, rain water, and snow all over the world, and came up with the relation of the isotope can be represented by the following formula;

$$\delta D = 8 \delta^{18}O + 10$$

The line represented by this equation is called meteoric line, and the formula is widely used for estimation the origin of water (represented by groundwater) and evaporation environment. In principal, the correlation of hydrogen and oxygen isotope indicates proximity to the line represented by the above formula, the origin of the groundwater can be estimated as rainfall.

If the water is affected by a high evaporation environment (such as lake water), it can be represented by the following formula;

$$\delta D = 5 \delta^{18}O + \alpha$$

The saline water in oil fields and hydrothermal water indicates a different isotope ratio compared to meteoric line. Application of this nature of isotopic character, the origin of the groundwater can be assumed.

a.1   Evaluation of isotopic analysis result

The isotopic analysis results in the Rift Valley Lakes Basin by sub-basins and geology of aquifer are compiled in Figure 3.21 and Figure 3.22. Regression line of the plotted isotope value is represented by the following formula.

$$\delta D = 7.12 \delta^{18}O + 12.3$$

This line is near to the meteoric line presented by Craig, 1961. Majority of $\delta^{18}O$ values are in the negative territory. Contrary, the values of δD are in the ranges from -10 to 10, and the plot of the value concentrated below SMOW (0, 0 = sea water value). However, in principle, the values are proximity of meteoric line which indicated that the majority of groundwater in the Study area is originated from rainfall. Probably, the low value of δ presents the altitude effect of the origin, which most of the rainwater is infiltrated in the west-eastern high altitude ridge of the margin of the Rift Valley. However, some data shows high and low value of δ, and those data plotted at different areas against the meteoric line, and it could be represented by the formula of $\delta D = 5 \delta^{18}O + \alpha$ ($\alpha = 2$-20). This line is also presented in the figure as a dotted line.

The values close to the trend of $\delta D = 5 \delta^{18}O + \alpha$ are mainly from the sub-basins of Ziway-Shalla and Chew Bahir. The geology of aquifer of the area is mainly composed of alluvium, lacustrine, limestone and pyroclastics. It can be assumed that the water affected by the hydrothermal activity and salty lake water may have different values than others.

For the evaluation of isotopic data, it is essential to consider the altitude effect (higher the altitude, lower the δ) and temperature effect (higher the temperature, lower the δ). By using these effects in the area, a more detailed evaluation can be made. The lakes shall also be considered for the isotopic analysis so that the relation of groundwater can be discussed. However, little isotopic study has been made in the area. It is recommended that a more detailed isotopic study shall be made by governmental and educational authorities.
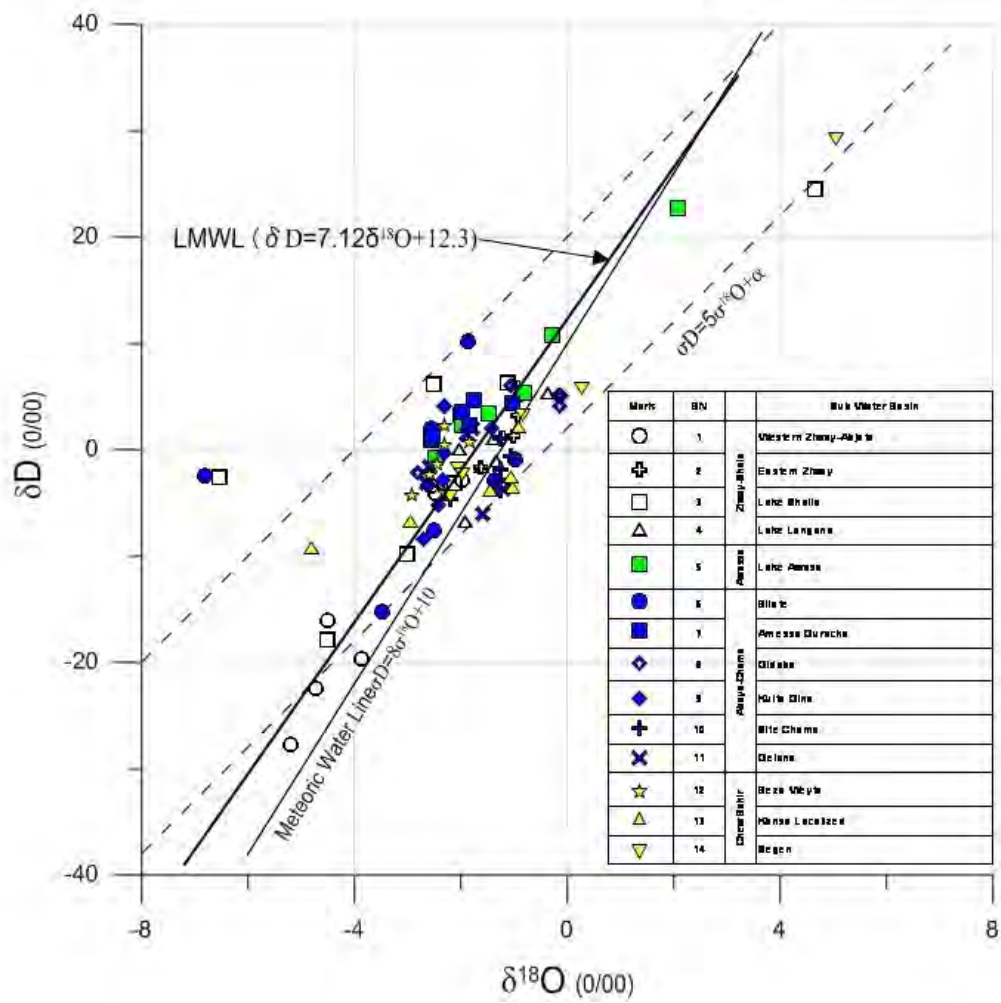
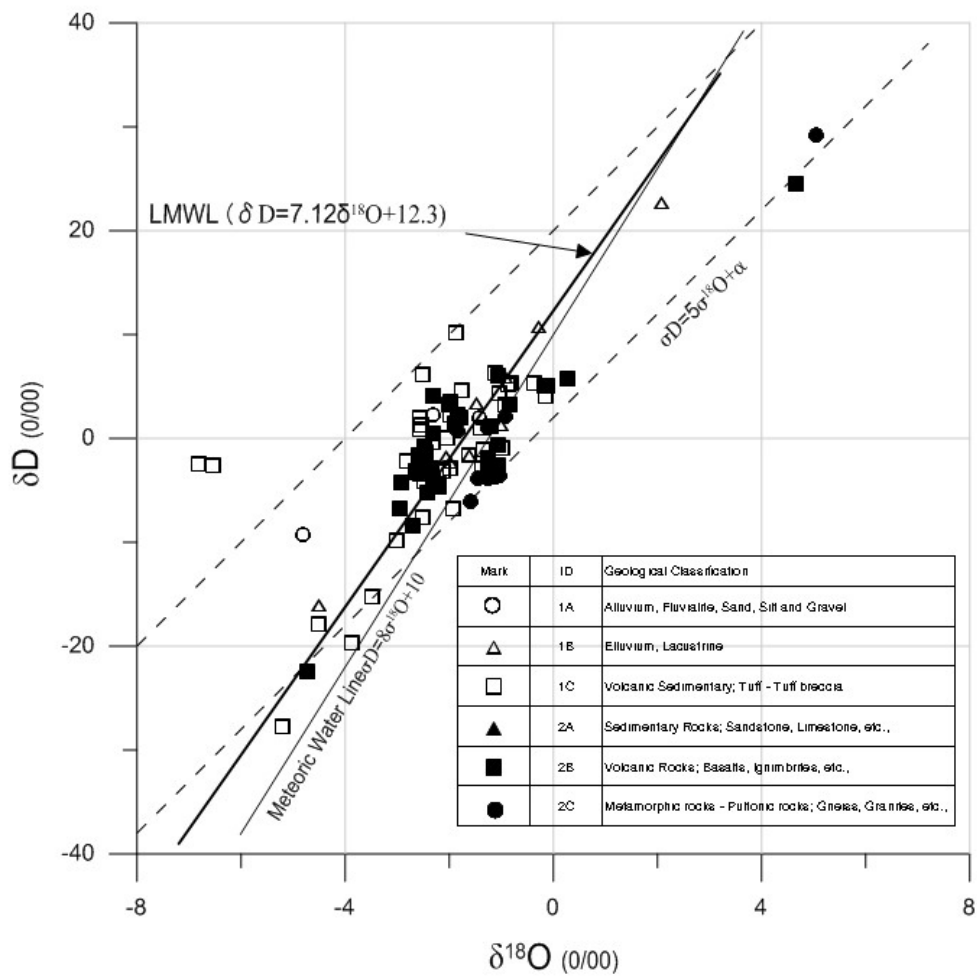Figure 3.21: Distribution of Hydrogen and Oxygen Isotope Ratio (by sub-basin)

Figure 3.22: Distribution of Hydrogen and Oxygen Isotope Ratio (by aquifer geology)

3.8.6   Distribution and trend of fluoride

The tendency fluoride value by the surface distribution and by the difference of depth was examined using the database in the Study area. Figure 3.25 shows the concentration of fluoride in the Study area. High fluoride concentration (more than 3 mg/l in reference with Ethiopian drinking water quality guidelines, 2002) distributes at north-western portion from Lake Ziway to Lake Shalla, especially at the inflection point at the slope and plane area. High concentration also can be observed in the northeastern area of the Bilate River, and surrounding area of Lake Awassa. Figure 3.23 presents the fluoride value by depth of water source (borehole and hand dug well). Figure 3.24 shows all fluoride data collected in this Study by the depth of bore hole. The characteristic of fluoride concentration is summarized as follows in regard to the data shown in these figures.

1.   The concentration is high at the vicinity of recent volcanic cones surrounded Bitajila
2.   High concentration zone can be observed at the area surrounding Lake Awassa
3.   It is not quite clear, but the fluoride value decreases by the depth of water source

It is more realistic to consider high concentration is related to the recent volcanic activity occurs at the shallower sub surface rather than it was brought from the deep ground. However, further study is required to justify the origin of fluoride concentration.

The researchers are actively analyzing the reason and origin of the fluoride content in this area, and are divided into two scenarios. One is the fluoride concentration occurs from the obsidian of recent volcanic activity, and the other is provided by the hydrothermal activity of the area. The Study is not intended to clarify the origin of fluoride concentration. However, it may be more realistic to consider the fluoride concentration is related to recent shallow volcanic activity.
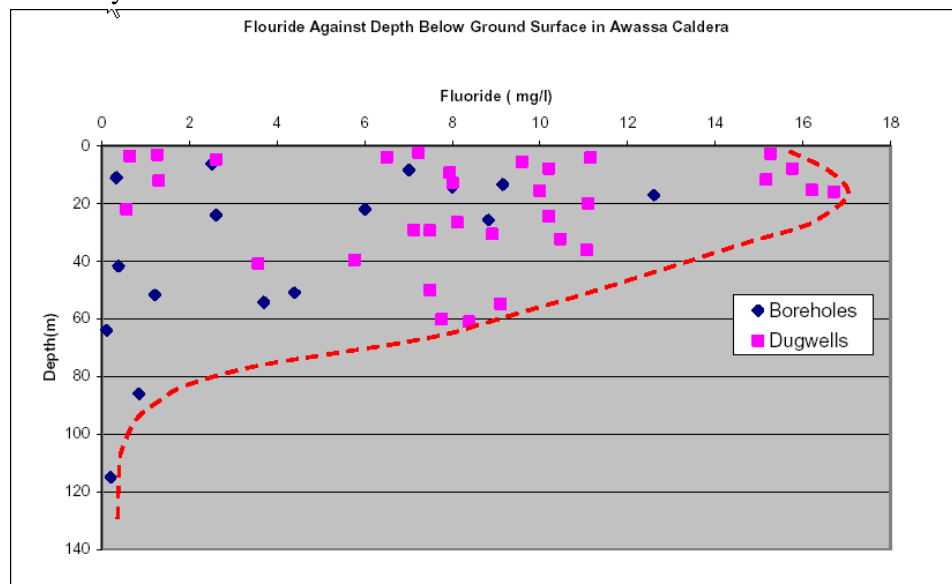
National Fluoride Mitigation Project (NFMP) Short Course on Integrated Fluorosis Mitigation Approaches: Fluoride Distribution Mapping、October 5- 15, 2009Zenaw Tessema
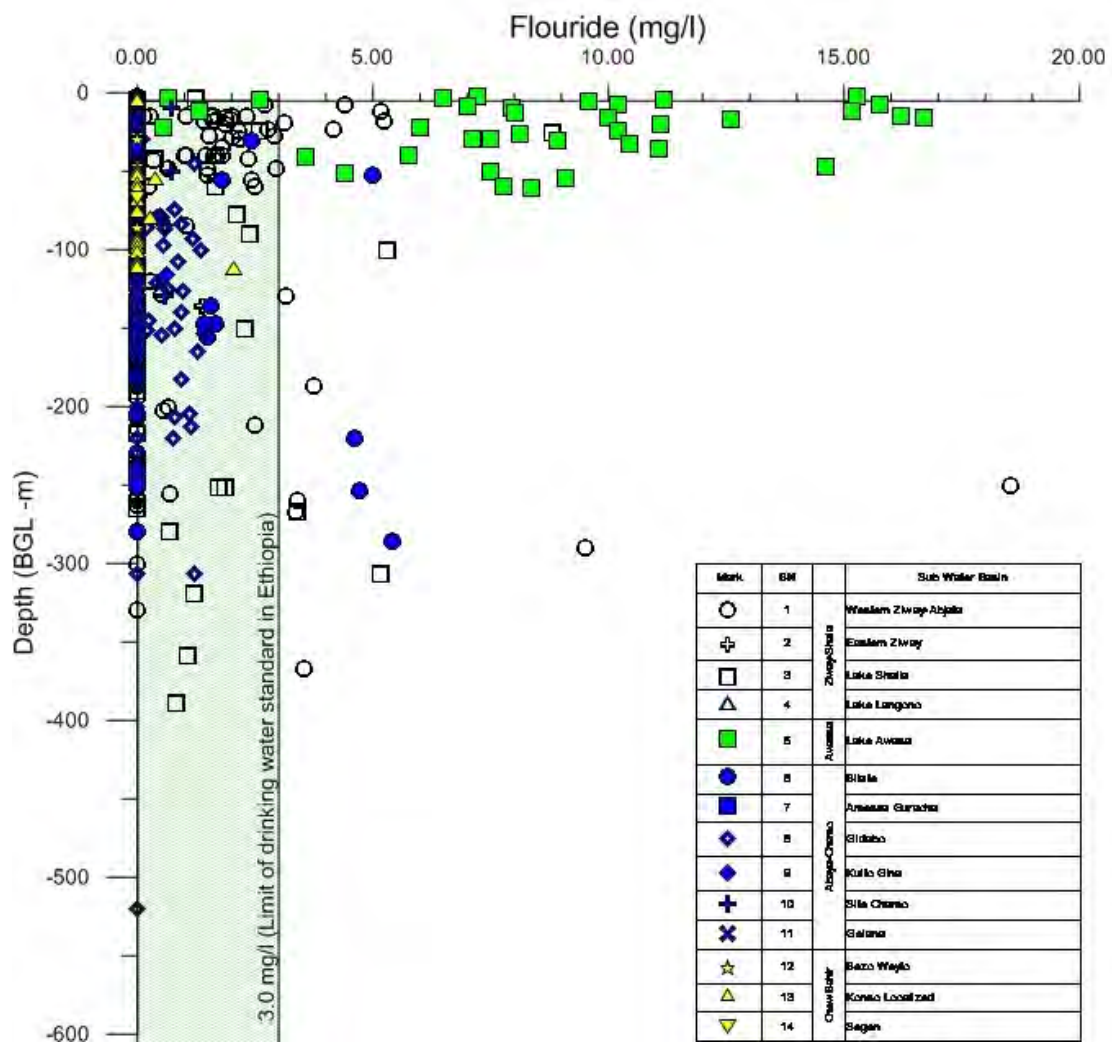
Figure 3.23: Well Depth and Fluoride Value at Awassa Area

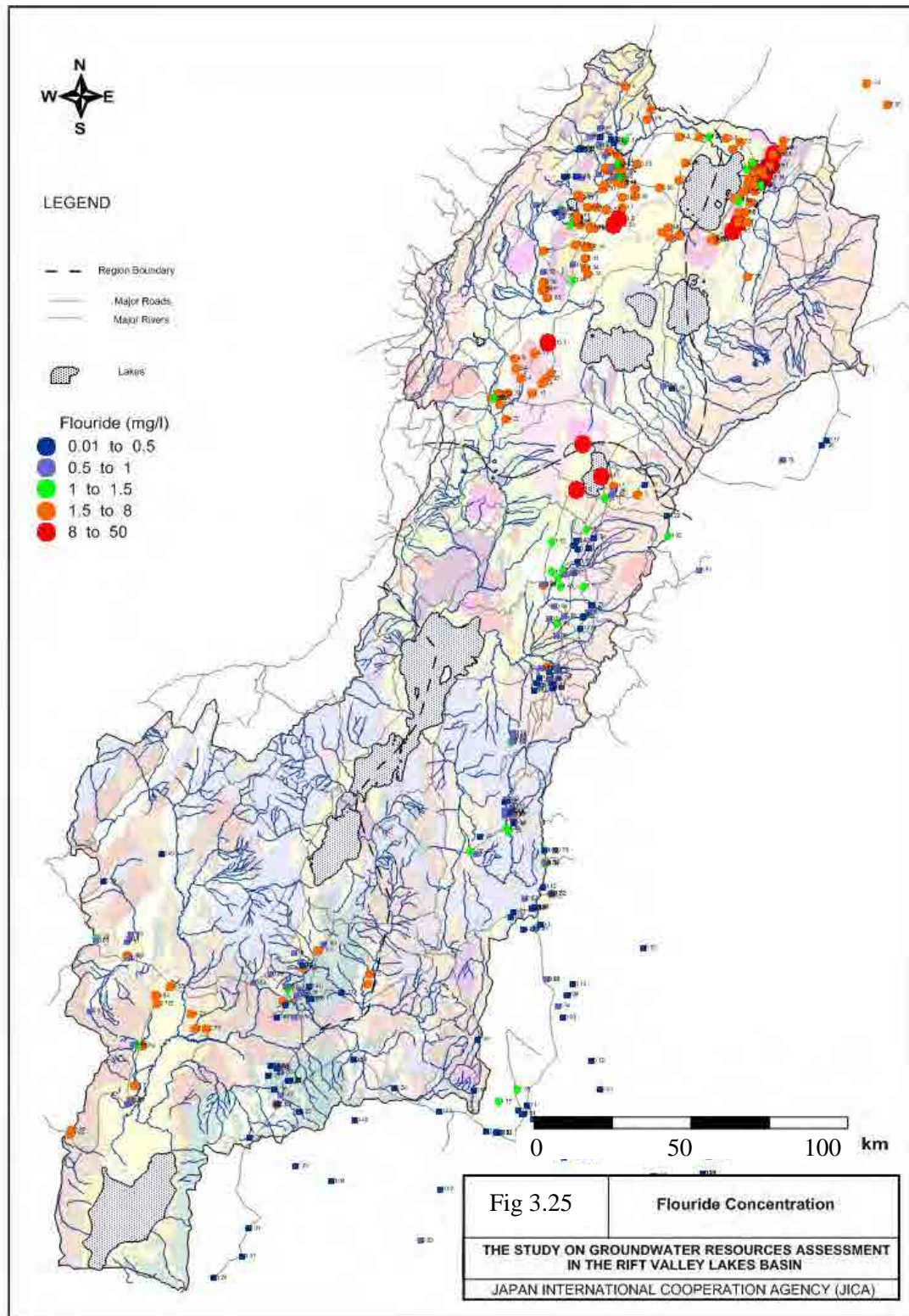Figure 3.24: Well Depth and Fluoride Value of the Study Area

Figure 3.25: Fluoride Concentration

Chapter 4

Geophysical Survey

# 4   Geophysical Survey

4.1   Electrical sounding method

4.1.1   Principle and method of survey

An artificial current is run through electrodes into the ground to measure the distribution of the potential field. The result then provides the basis for analyzing resistivity structure below the ground. In other words, electrical survey is to analyze the conditions of groundwater and the geological structures by researching the resistivity of the rocks and the geology in the ground through the use of the diversity of electrical characteristics of rocks, or the phenomena occurred by that fact. In this survey the Study Team used the vertical electrical sounding and horizontal profiling methods.

a.   Horizontal electric profiling method

The horizontal electric profiling is to identify apparent resistivity anomalies (fractured zones of rock and/or points that differ from the surrounding geological structure). Wenner's electrode configuration is used for the horizontal profiling. Maintaining an electrode interval shown in Figure 4.1, Wenner's array is used to measure apparent resistivity by moving the electrode profile along a measuring line while maintaining a constant electrode interval. In the survey, electrode spacing was 50m, 100m, and 200m. The survey profiles were chosen perpendicularly to the trend of major lineaments, and the survey point spacing was set at 25m.

Entering the measurement data in the field book, and plotting it as the apparent resistivity curve (apparent resistivity (ρ_a)—electrode interval (a) on logarithmic graph paper, the Study Team identified the abnormal points in the plotted graphs and selected them as the measuring points for the vertical electrical sounding.
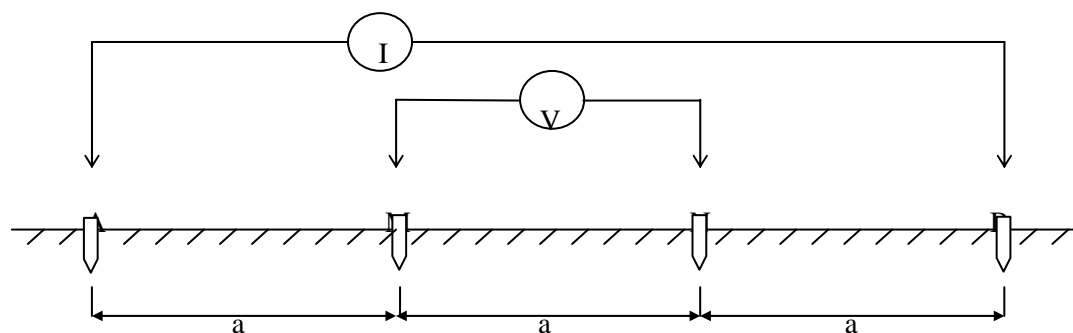
$\rho_a=2\pi a \times (V/I)$、 $\rho_a=$ apparent resistivity(ohm-m)
I: current between of A and B (Ampere), V: potential between of M and N(Voltage)
AB: current electrodes, MN: potential electrodes, a: inter-electrode spacing

Figure 4.1: Wenner Electrode Configuration

b.   Vertical electrical sounding method

Vertical electrical sounding (VES) is a method to investigate layered structure. Schlumberger electrode configuration was applied to estimate layered resistivity structure

(see to Figure 4.2).

$$\rho_a = \pi/4 \times ((AB^2 - MN^2)/MN) \times (V/I), \quad \rho_a = \text{apparent resistivity (ohm-m)}$$

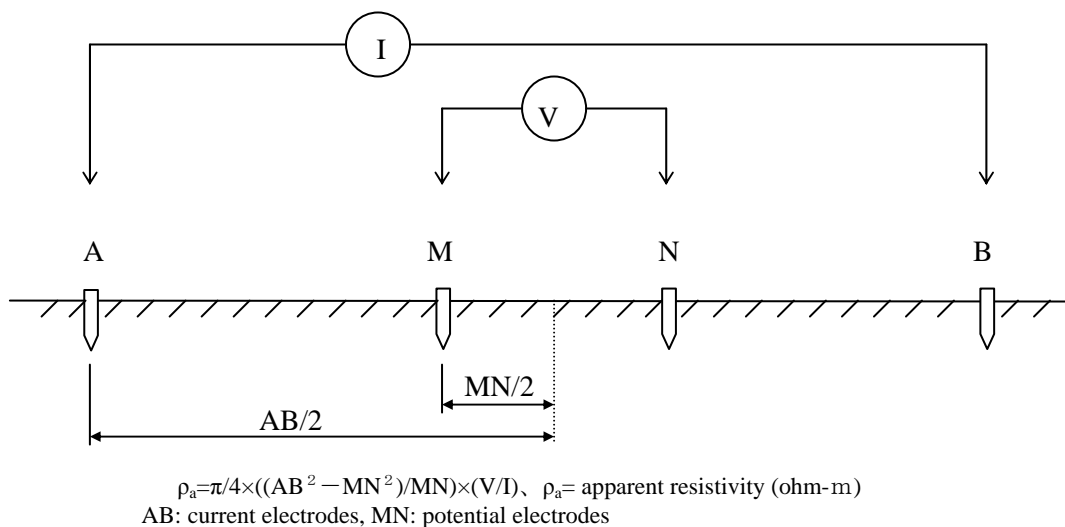AB: current electrodes, MN: potential electrodes

Figure 4.2: Schlumberger Electrode Configuration

The center of the symmetrically-arranged electrode configuration is fixed in place, while the positions of the current and potential electrodes are varied to measure changes in apparent resistivity (ρ_a) with depth. The ρ_a-a curve derived therefore is used to obtain the thicknesses of the layers and their resistivity. In other words, current is energized through outer electrodes A and B that are installed on the measurement profile, while electrodes M and N on the inside are used to measure differences in electrical potential. The equipment used for this measurement is the same as that for horizontal electrical profiling. The measurement data are recorded in a log book and plotted on the $\rho_a - a$ apparent resistivity curve on double-logarithm graph paper (VES curve; Vertical Electric Sounding curve). The electrode spacing's used in the Schlumberger configurations are shown in Table 4.1.

Table 4.1: Schlumberger Electrode Spacing

(AB/2)	1.5	2.1	3	4	6	9	13
(MN/2)	0.5	0.5	0.5	0.5	0.5	0.5	0.5
(AB/2)	20	25	30	35	40	50	60
(MN/2)	0.5	0.5/10	0.5/10	10	10	10	10
(AB/2)	80	100	130	160	200	250	300
(MN/2)	10	10	10	10	10/45	10/45	45
(AB/2)	350	400	500	600	700	-	-
(MN/2)	45	45	45	45	45	-	-

c.   Measurement instrument

The STING R1 Earth Resistivity Meter made by Advanced Geosciences Inc, USA was used for this survey. The appearance of this electrical prospecting instrument and its specifications are as shown in Figure 4.3 and Table 4.2.

Figure 4.3: Electric Prospecting Instruments

Table 4.2: Specifications of Electric Prospecting Instrument

Instrument	Specification
STING R1	Output current : 1～500mA

d.   Field measurement

d.1   Measurement method

Geophysical investigations were carried out at 10 planned well drilling sites with the vertical Electrical sounding and horizontal profiling methods. Points indicating abnormal/anomalous values were identified by the horizontal method. Then these points were surveyed by the vertical sounding method to clarify the depth of estimated layers and fissures that may contain groundwater.

d.2   Measurement situations

The traverse lines for the horizontal prospecting were set in the directions that cross major lineaments exactly at right angles. Additional traverse lines were also set in valley bottoms and lowlands with hydrogeological features of interest that have developed no lineaments. In some areas survey lines had to be laid out by cutting through bushes.

At places where the surface soil was very dry and indicated high ground resistance, the terrain hardly allowed electrical current to pass through. Therefore in such cases, some of the current electrodes were relocated, or additional current electrodes were fixed, or the topsoil was watered to lower the ground resistance before the measurement was commenced.

In measurements that used a conducting current of 50mA or less, measurement values had no repeatability. Thus, measurement values with 50mA or higher current conducted were adopted. Most of the data obtained were in good condition. The Easting and Northing of the measurement points were identified with the help of a hand held GPS. A site map was prepared for each area (refer to Figure 4.5 to Figure 4.14), and some photos of the measurement points were taken (refer to Data book).

e.   Data analysis method

A "Resix-Plus" interpretation software was used to analyze the data. In order to determine the subsurface resistivity structure from the field data, an analysis technique called Layered

Earth Inversion was used. The resistivity model was refined by considering the groundwater level from existing wells, the analytical results from neighboring points, topography, geology, and so on.

Layered earth structure inversion provides the number of layers, resistivity value of each layer and thickness value of each layer as initial values and analyzes a horizontal multilayer structure that is most suitable to measurement results based on these initial values (see to Figure 4.4). Figure 4.4 is the analytic example of the Electric survey site No-2 (RVS BH No-2 Berta/Meki) in Oromiya Region. The graph on the left shows the match between the field curve and the theoretical curve computed for the interpreted resistivity structure. The right figure shows the interpreted subsurface resistivity structure.
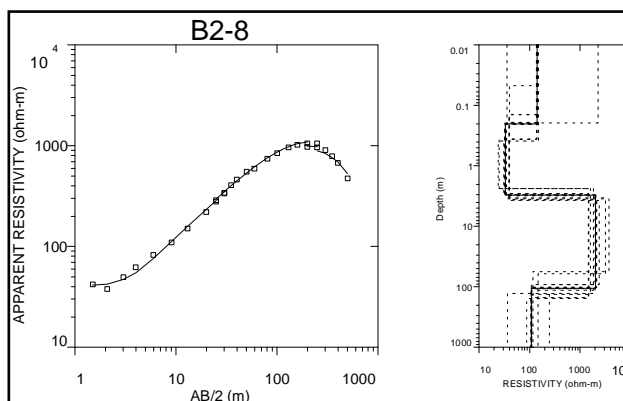

Figure 4.4: Layer Configuration Inversion

4.1.2   Selection of measurement points

a.   Quantity of survey

Target survey areas cover 10 planned well drilling sites in the Region of Oromia and SNNPRS. Table 4.3 shows the geophysical survey quantity at each site (for details, refer to Data book for the Geophysical survey data).

Table 4.3: Quantity of Geophysical Survey

Region	Well drilling site No.	Site area	Total number	
			Vertical Electrical Sounding	Horizontal electrical sounding
Oromia	2	Berta/Meki	10	1line, 500m
	3	Oyne-Umbure -Chefo	10	1line, 500m
	10	Brindar	10	3lines, 1500m
SNNPRS	1	Abaya Chokare	10	2lines, 775m
	4	Chancho	10	1line, 500m
	5	Fango Damot	10	1line, 500m
	6	Lajo/Yaye	10	1line, 500m
	7	Arbaminch	10	2lines, 1000m
	8	Walesa	10	1line, 500m

| | 9 | Beresa | 10 | 2lines, 1000m |
| Total | 10 | 10 | 100 | 15lines, 7275m |

b.   **Field reconnaissance survey and selection of survey points**

All the prospecting sites were visited by the hydrogeologist in charge, and confirmation such as road conditions and accessibility to the position of the electric exploration and the investigation area was done. As a preliminary survey, when geophysical survey started, explanation of the project was given to the neighboring villagers of the well drilling site, and the cooperation of the inhabitants in laying out horizontal and vertical prospecting lines was sought. Information about existing wells and the current water supply situation is also obtained from the local community.

4.1.3   Results of survey and analysis

a.   **Results of survey**

The results of the geophysical survey are presented in figures and tables. The location map showing the distribution of VES points and horizontal profiling lines are presented in Figure 4.5 to Figure 4.14. Data book shows the raw VES data together with the interpreted layer parameters, whereas the apparent resistivity profiling data are given in Data book. The interpreted layered resistivity structure for each VES is presented in Table 4.4, and resistivity cross section made from the interpreted layer parameters are given in Data book. Field photographs of the geophysical survey are also shown in Data book.

Based on the analysis of results at each planned well drilling sites, the Study Team selected drilling points that indicated existence of low resistivity layers as being favorable layer for groundwater storage and movement. It seems that these low resistivity layers are chiefly made of weathered layers or sediments while the high resistivity beds beneath these layers seem to consist of the bedrock.

Table 4.4: Results of Geophysical Survey

BH.No.	Area	No.	Coordinates (UTM)	Elevation (m)	Parameter	Layers					
						L1	L2	L3	L4	L5	L6
1	Berta/Meki	1	37N 734542 383212	1226	Resistivity(Ohm-m)	11	16	494	59		
					Thickness(m)	0.6	11.0	25	-		
					Depth(m)	0.6	11.6	36.6	-		
		2	37N 734744 383449	1234	Resistivity(Ohm-m)	168	15	756	11		
					Thickness(m)	0.4	9.0	38	-		
					Depth(m)	0.4	9.4	47.4	-		
		3	37N 734852 383283	1229	Resistivity(Ohm-m)	390	14	196	72		
					Thickness(m)	0.2	6.1	41	-		
					Depth(m)	0.2	6.3	47.3	-		
		4	37N 734903 383187	1223	Resistivity(Ohm-m)	34	17	291	48		
					Thickness(m)	6.9	5.6	31	-		
					Depth(m)	6.9	12.5	43.5	-		
		5	37N 734684 383111	1221	Resistivity(Ohm-m)	23	11	598	25		
					Thickness(m)	3.8	4.1	37	-		
					Depth(m)	3.8	7.9	44.9	-		
		6	37N 734695 383584	1241	Resistivity(Ohm-m)	62	10	1330	17		
					Thickness(m)	0.5	8.0	53	-		
					Depth(m)	0.5	8.5	61.5	-		
		7	37N 734899 383672	1237	Resistivity(Ohm-m)	12	28	239	96		
					Thickness(m)	0.2	11.0	66	-		
					Depth(m)	0.2	11.2	77.2	-		

		8	37N	734844 383569	1226	Resistivity(Ohm-m) Thickness(m) Depth(m)	21 1.1 1.1	9.8 6.7 7.8	1195 30 37.8	7.1 - -	
		9	37N	734938 383521	1231	Resistivity(Ohm-m) Thickness(m) Depth(m)	561 0.2 0.2	19 11.0 11.2	733 33 44.2	61 - -	
		10	37N	735059 383453	1236	Resistivity(Ohm-m) Thickness(m) Depth(m)	1377 0.3 0.3	16 13.0 13.3	410 41 54.3	64 - -	
2 Awara Godaha		1	37P	908215 486440	1703	Resistivity(Ohm-m) Thickness(m) Depth(m)	141 0.6 0.6	51 6.9 7.5	4269 59 66.5	46 - -	
		2	37P	908100 486650	1703	Resistivity(Ohm-m) Thickness(m) Depth(m)	90 0.2 0.2	82 6.3 6.5	1437 150 156.5	59 - -	
		3	37P	907905 486546	1703	Resistivity(Ohm-m) Thickness(m) Depth(m)	331 0.3 0.3	49 4.6 4.9	1714 130 134.9	63 - -	
		4	37P	907710 486440	1703	Resistivity(Ohm-m) Thickness(m) Depth(m)	23 0.6 0.6	20 1.7 2.3	6139 41 43.3	9.7 - -	
		5	37P	907830 486230	1703	Resistivity(Ohm-m) Thickness(m) Depth(m)	67 0.4 0.4	42 4.0 4.4	1263 198 202.4	86 - -	
		6	37P	908030 486340	1703	Resistivity(Ohm-m) Thickness(m) Depth(m)	103 0.7 0.7	50 6.4 7.1	4239 62 69.1	184 - -	
		7	37P	907280 486860	1703	Resistivity(Ohm-m) Thickness(m) Depth(m)	161 0.3 0.3	62 3.7 4.0	999 198 202.0	161 - -	
		8	37P	907780 486760	1703	Resistivity(Ohm-m) Thickness(m) Depth(m)	142 0.2 0.2	33 2.9 3.1	2040 102 105.1	109 - -	
		9	37P	907580 486660	1703	Resistivity(Ohm-m) Thickness(m) Depth(m)	236 0.2 0.2	29 3.2 3.4	1733 139 142.4	44 - -	
		10	37P	907660 486980	1703	Resistivity(Ohm-m) Thickness(m) Depth(m)	64 0.1 0.1	36 3.2 3.3	1806 129 132.3	41 - -	
3 Oyne Umbure Chefo		1	37N	796402 448142	1812	Resistivity(Ohm-m) Thickness(m) Depth(m)	849 0.2 0.2	11916 1.7 1.9	181 26.0 27.9	776 94.0 121.9	603 - -
		2	37N	796293 448035	1809	Resistivity(Ohm-m) Thickness(m) Depth(m)	2535 0.5 0.5	14180 1.9 2.4	313 35.0 37.4	638 79.0 116.4	125 - -
		3	37N	796232 447888	1813	Resistivity(Ohm-m) Thickness(m) Depth(m)	2447 0.5 0.5	6513 2.3 2.8	272 27.0 29.8	347 55.0 84.8	309 - -
		4	37N	796100 447864	1817	Resistivity(Ohm-m) Thickness(m) Depth(m)	2077 0.6 0.6	7638 3.2 3.8	174 24.0 27.8	1002 81.0 108.8	247 - -
		5	37N	796079 448008	1814	Resistivity(Ohm-m) Thickness(m) Depth(m)	3053 0.4 0.4	7932 3.1 3.5	178 31.0 34.5	1004 66.0 100.5	80 - -
		6	37N	796116 448151	1808	Resistivity(Ohm-m) Thickness(m) Depth(m)	1665 0.8 0.8	6579 2.0 2.8	193 75.0 77.8	4225 41.0 118.8	118 - -
		7	37N	796145 448370	1818	Resistivity(Ohm-m) Thickness(m) Depth(m)	128 0.1 0.1	15885 0.8 0.9	127 21.0 21.9	705 107.0 128.9	71 - -
		8	37N	795926 448131	1821	Resistivity(Ohm-m) Thickness(m) Depth(m)	280 0.1 0.1	13537 1.2 1.3	124 25.0 26.3	839 98.0 124.3	45 - -
		9	37N	795960 448290	1819	Resistivity(Ohm-m) Thickness(m) Depth(m)	136 0.1 0.1	11164 0.9 1.0	90 9.7 10.7	597 152.0 162.7	87 - -
		10	37N	796001 448498	1817	Resistivity(Ohm-m) Thickness(m) Depth(m)	837 0.3 0.3	10164 1.3 1.6	139 45.0 46.6	908 99.0 145.6	76 - -
4 Chancho		1	37N	745299 424849	1639	Resistivity(Ohm-m) Thickness(m) Depth(m)	11 0.8 0.8	34 1.4 2.2	12 30.0 32.2	45 116.0 148.2	17 - -
		2	37N	745363 424658	1640	Resistivity(Ohm-m) Thickness(m) Depth(m)	23 2.0 2.0	19 17.0 19.0	62 16.0 35.0	10 36.0 71.0	46 - -
		3	37N	745429 424917	1638	Resistivity(Ohm-m) Thickness(m) Depth(m)	11 0.8 0.8	24 1.1 1.9	9.3 26.0 27.9	55 122.0 149.9	4.8 - -
		4	37N	745614 424971	1642	Resistivity(Ohm-m) Thickness(m) Depth(m)	20 0.5 0.5	57 0.8 1.3	10 26.0 27.3	49 91.0 118.3	15 - -
		5	37N	745625 424839	1642	Resistivity(Ohm-m) Thickness(m) Depth(m)	11 0.8 0.8	31 25.0 25.8	9.9 37.0 62.8	56 - -	

Area	No	Zone	X	Y	Elev	Parameter						
	6	37N	745472 424829		1642	Resistivity(Ohm-m)	22	41	16	43		
						Thickness(m)	1.4	8.6	44.0	-		
						Depth(m)	1.4	10.0	54.0	-		
	7	37N	745130 424754		1634	Resistivity(Ohm-m)	8.9	34	9.1	52	23	
						Thickness(m)	1.6	7.3	38.0	121.0	-	
						Depth(m)	1.6	8.9	46.9	167.9	-	
	8	37N	755005 424642		1637	Resistivity(Ohm-m)	7.6	16	10	76	10	
						Thickness(m)	6.2	37.0	19.0	126.0	-	
						Depth(m)	6.2	43.2	62.2	188.2	-	
	9	37N	745208 424589		1638	Resistivity(Ohm-m)	7.2	19	16	34	21	63
						Thickness(m)	0.5	0.6	13.0	41.0	77.0	-
						Depth(m)	0.5	1.1	14.1	55.1	132.1	-
	10	37N	745488 424417		1654	Resistivity(Ohm-m)	72	18	145	37		
						Thickness(m)	2.4	5.6	34	-		
						Depth(m)	2.4	8.0	42.0	-		
5 Fango Damot	1	37N	763713 403064		1477	Resistivity(Ohm-m)	27	78	15	51	20	
						Thickness(m)	1.4	10.0	6.8	155.0	-	
						Depth(m)	1.4	11.4	18.2	173.2	-	
	2	37N	763727 402963		1483	Resistivity(Ohm-m)	59	25	47	27	171	18
						Thickness(m)	0.8	1.0	18.0	16.0	38.0	-
						Depth(m)	0.8	1.8	19.8	35.8	73.8	-
	3	37N	763735 402743		1487	Resistivity(Ohm-m)	143	643	36	253	29	
						Thickness(m)	2.7	5.8	8.0	108.0	-	
						Depth(m)	2.7	8.5	16.5	124.5	-	
	4	37N	763758 402620		1490	Resistivity(Ohm-m)	72	13	224	51		
						Thickness(m)	0.4	3.4	65	-		
						Depth(m)	0.4	3.8	68.8	-		
	5	37N	763369 403131		1475	Resistivity(Ohm-m)	57	26	97	1.7		
						Thickness(m)	0.2	16.0	103	-		
						Depth(m)	0.2	16.2	119.2	-		
	6	37N	763373 402983		1484	Resistivity(Ohm-m)	550	40	141	9.1		
						Thickness(m)	0.3	7.2	82	-		
						Depth(m)	0.3	7.5	89.5	-		
	7	37N	763379 402779		1487	Resistivity(Ohm-m)	17	5.5	269	7.4		
						Thickness(m)	0.6	3.7	53	-		
						Depth(m)	0.6	4.3	57.3	-		
	8	37N	763379 402627		1494	Resistivity(Ohm-m)	40	7.2	1072	37		
						Thickness(m)	0.4	3.0	22	-		
						Depth(m)	0.4	3.4	25.4	-		
	9	37N	763189 402973		1481	Resistivity(Ohm-m)	52	39	262	22	261	1.9
						Thickness(m)	0.6	15.0	15.0	16.0	33.0	-
						Depth(m)	0.6	15.6	30.6	46.6	79.6	-
	10	37N	763103 402737		1481	Resistivity(Ohm-m)	87	12	141	21		
						Thickness(m)	0.5	2.2	93	-		
						Depth(m)	0.5	2.7	95.7	-		
6 Lajo	1	37N	807110 419595		1878	Resistivity(Ohm-m)	551	56	352	84		
						Thickness(m)	2.7	5.5	170.0	-		
						Depth(m)	2.7	8.2	178.2	-		
	2	37N	806969 419804		1878	Resistivity(Ohm-m)	165	25	326	127		
						Thickness(m)	1.3	1.9	115.0	-		
						Depth(m)	1.3	3.2	118.2	-		
	3	37N	807026 419973		1880	Resistivity(Ohm-m)	218	29	191	256	57	
						Thickness(m)	1.2	2.2	45.0	226.0	-	
						Depth(m)	1.2	3.4	48.4	274.4	-	
	4	37N	807098 420187		1880	Resistivity(Ohm-m)	143	26	318	337	131	
						Thickness(m)	1.4	2.7	52.0	66.0	-	
						Depth(m)	1.4	4.1	56.1	122.1	-	
	5	37N	807200 419900		1873	Resistivity(Ohm-m)	365	31	280	67		
						Thickness(m)	1.4	2.4	198.0	-		
						Depth(m)	1.4	3.8	201.8	-		
	6	37N	806900 420175		1889	Resistivity(Ohm-m)	259	44	624	198	69	
						Thickness(m)	0.8	2.6	11.0	286.0	-	
						Depth(m)	0.8	3.4	14.4	300.4	-	
	7	37N	807295 420185		1882	Resistivity(Ohm-m)	185	29	386	244	59	
						Thickness(m)	1.8	2.7	22.0	197.0	-	
						Depth(m)	1.8	4.5	26.5	223.5	-	
	8	37N	806775 419800		1877	Resistivity(Ohm-m)	393	33	410	256	48	
						Thickness(m)	1.2	2.4	18.0	243.0	-	
						Depth(m)	1.2	3.6	21.6	264.6	-	
	9	37N	806840 420000		1884	Resistivity(Ohm-m)	294	34	141	281	56	
						Thickness(m)	2.5	3.4	21.0	189.0	-	
						Depth(m)	2.5	5.9	26.9	215.9	-	
	10	37N	805176 418712		1901	Resistivity(Ohm-m)	599	21	361	104		
						Thickness(m)	3.7	3.5	91.0	-		
						Depth(m)	3.7	7.2	98.2	-		
7 Arba Minch	1	37N	670539 341465		1203	Resistivity(Ohm-m)	7.3	47	1.8	12	3.6	106
						Thickness(m)	1.1	5.0	4.0	85.0	117.0	-
						Depth(m)	1.1	6.1	10.1	95.1	212.1	-
	2	37N	670519 341711		1203	Resistivity(Ohm-m)	14	6.9	22	7.5	9.9	
						Thickness(m)	1.0	1.1	34.0	64.0	-	
						Depth(m)	1.0	2.1	36.1	100.1	-	
	3	37N	670498 342009		1203	Resistivity(Ohm-m)	11	20	11	15	5.1	92
						Thickness(m)	1.2	12.0	15.0	96.0	158.0	-
						Depth(m)	1.2	13.2	28.2	124.2	282.2	-

The Study on Groundwater Resources Assessment
in the Rift Valley Lakes Basin in Ethiopia, Final Report (Supporting Report)

JICA
KOKUSAI KOGYO CO., LTD.

No	Name	Pt	Zone	Coord	Elev	Parameter	1	2	3	4	5	6
		4	37N	670477 342306	1203	Resistivity(Ohm-m)	9.4	7.4	24	9		
						Thickness(m)	0.7	1.6	60.0	-		
						Depth(m)	0.7	2.3	62.3	-		
		5	37N	670150 341440	1203	Resistivity(Ohm-m)	13	36	7.5	38	4.9	17
						Thickness(m)	1.4	2.7	6.7	20.0	70.0	-
						Depth(m)	1.4	4.1	10.8	30.8	100.8	-
		6	37N	670110 341880	1203	Resistivity(Ohm-m)	6.3	88	4.6	27	11	
						Thickness(m)	1.3	18.0	18.0	63.0	-	
						Depth(m)	1.3	19.3	37.3	100.3	-	
		7	37N	670070 342270	1203	Resistivity(Ohm-m)	9.4	167	1.1	64	1.4	
						Thickness(m)	12.0	6.8	18.0	73.0	-	
						Depth(m)	12.0	18.8	36.8	109.8	-	
		8	37N	669760 341410	1203	Resistivity(Ohm-m)	8.9	152	16			
						Thickness(m)	0.6	19.0	-			
						Depth(m)	0.6	19.6	-			
		9	37N	669720 341850	1203	Resistivity(Ohm-m)	7.6	14	70	12		
						Thickness(m)	0.8	13.0	7.0	-		
						Depth(m)	0.8	13.8	20.8	-		
		10	37N	669680 342230	1203	Resistivity(Ohm-m)	14	8.7	60	17		
						Thickness(m)	3.0	2.1	13.0	-		
						Depth(m)	3.0	5.1	18.1	-		
8	Walesa	1	37N	630294 327372	1157	Resistivity(Ohm-m)	7.6	28	5.5	129		
						Thickness(m)	1.3	15.0	159.0	-		
						Depth(m)	1.3	16.3	175.3	-		
		2	37N	630500 327541	1160	Resistivity(Ohm-m)	14	47	3	11		
						Thickness(m)	3.2	5.6	37.0	-		
						Depth(m)	3.2	8.8	45.8	-		
		3	37N	630591 327620	1160	Resistivity(Ohm-m)	5.6	38	5.7	45		
						Thickness(m)	0.4	9.6	197.0	-		
						Depth(m)	0.4	10.0	207.0	-		
		4	37N	630664 327740	1155	Resistivity(Ohm-m)	20	14	4.6	5.9		
						Thickness(m)	0.8	9.7	105.0	-		
						Depth(m)	0.8	10.5	115.5	-		
		5	37N	630726 327884	1150	Resistivity(Ohm-m)	14	34	5.5	1.1	83	
						Thickness(m)	2.4	4.4	50.0	49.0	-	
						Depth(m)	2.4	6.8	56.8	105.8	-	
		6	37N	630169 327374	1154	Resistivity(Ohm-m)	13	231	13	1.3	136	
						Thickness(m)	1.4	0.9	111.0	87.0	-	
						Depth(m)	1.4	2.3	113.3	200.3	-	
		7	37N	630123 327654	1145	Resistivity(Ohm-m)	13	23	5.6	10		
						Thickness(m)	1.6	6.9	133.0	-		
						Depth(m)	1.6	8.5	141.5	-		
		8	37N	630050 328071	1144	Resistivity(Ohm-m)	5.1	15	3.7	7.8	23	
						Thickness(m)	0.6	6.1	43.0	157.0	-	
						Depth(m)	0.6	6.7	49.7	206.7	-	
		9	37N	630264 327750	1145	Resistivity(Ohm-m)	41	16	2.4	20	2	49
						Thickness(m)	2.0	15.0	21.0	37.0	99.0	-
						Depth(m)	2.0	17.0	38.0	75.0	174.0	-
		10	37N	630351 328010	1145	Resistivity(Ohm-m)	9.6	15	1.9	24	1.6	184
						Thickness(m)	1.1	14.0	16.0	27.0	67.0	-
						Depth(m)	1.1	15.1	31.1	58.1	125.1	-
9	Beresa	1	37N	596847 330444	1200	Resistivity(Ohm-m)	4.6	1.7	109	42		
						Thickness(m)	7.2	3.5	19.0	-		
						Depth(m)	7.2	10.7	29.7	-		
		2	37N	597037 330474	1196	Resistivity(Ohm-m)	8.8	21	45	33		
						Thickness(m)	3.1	14.0	39.0	-		
						Depth(m)	3.1	17.1	56.1	-		
		3	37N	597164 330545	1181	Resistivity(Ohm-m)	22	85	18	98	16	153
						Thickness(m)	0.9	1.8	9.3	21.0	64.0	-
						Depth(m)	0.9	2.7	12.0	33.0	97.0	-
		4	37N	597249 330600	1187	Resistivity(Ohm-m)	8.1	24	41	25		
						Thickness(m)	0.9	13.0	135.0	-		
						Depth(m)	0.9	13.9	148.9	-		
		5	37N	596949 330314	1202	Resistivity(Ohm-m)	34	4.1	32			
						Thickness(m)	0.3	10.2	-			
						Depth(m)	0.3	10.5	-			
		6	37N	596731 330662	1202	Resistivity(Ohm-m)	7.4	4	157	6.2		
						Thickness(m)	2.9	15.0	55.0	-		
						Depth(m)	2.9	17.9	72.9	-		
		7	37N	596853 330823	1200	Resistivity(Ohm-m)	94	8.2	73	26		
						Thickness(m)	0.4	23.0	46.0	-		
						Depth(m)	0.4	23.4	69.4	-		
		8	37N	596750 330892	1205	Resistivity(Ohm-m)	3.5	12	1.3	127	28	
						Thickness(m)	1.6	2.0	5.1	59.0	-	
						Depth(m)	1.6	3.6	8.7	67.7	-	
		9	37N	596923 330674	1199	Resistivity(Ohm-m)	5.9	25	3.6	133	27	
						Thickness(m)	2.4	2.0	4.8	23.0	-	
						Depth(m)	2.4	4.4	9.2	32.2	-	
		10	37N	597073 330723	1200	Resistivity(Ohm-m)	5.9	124	27			
						Thickness(m)	5.5	21.0	-			
						Depth(m)	5.5	26.5	-			

	No.	Zone	Coordinate	Elev.	Parameter						
10 Brindar	1	37N	566688 348801	890	Resistivity(Ohm-m)	2.8	86	2.5	68	5	14
					Thickness(m)	0.2	1.4	5.8	28.0	78.0	-
					Depth(m)	0.2	1.6	7.4	35.4	113.4	-
	2	37N	566601 349030	887	Resistivity(Ohm-m)	37	2.8	5.2	6.4		
					Thickness(m)	0.2	6.9	152.0	-		
					Depth(m)	0.2	7.1	159.1	-		
	3	37N	566526 349214	887	Resistivity(Ohm-m)	17	1.4	7.7	1.3	72	
					Thickness(m)	0.4	9.9	11.0	29.0	-	
					Depth(m)	0.4	10.3	21.3	50.3	-	
	4	37N	566443 349420	887	Resistivity(Ohm-m)	7.1	3	9.9	2.8	9.6	
					Thickness(m)	5.3	9.3	18.0	26.0	-	
					Depth(m)	5.3	14.6	32.6	58.6	-	
	5	37N	566343 349678	887	Resistivity(Ohm-m)	8.2	22	2.2	40		
					Thickness(m)	0.6	1.3	94.0	-		
					Depth(m)	0.6	1.9	95.9	-		
	6	37N	566764 348611	892	Resistivity(Ohm-m)	15	37	14	23		
					Thickness(m)	1.1	42.0	117.0	-		
					Depth(m)	1.1	43.1	160.1	-		
	7	37N	566285 349826	887	Resistivity(Ohm-m)	12	2.7	7.9	1.9	67	
					Thickness(m)	3.0	3.6	45.0	56.0	-	
					Depth(m)	3.0	6.6	51.6	107.6	-	
	8	37N	566249 349915	887	Resistivity(Ohm-m)	14	1.4	7.8	2.6	1010	
					Thickness(m)	3.1	3.5	20.0	100.0	-	
					Depth(m)	3.1	6.6	26.6	126.6	-	
	9	37N	566191 350055	887	Resistivity(Ohm-m)	3.9	1	11	2.2	45	
					Thickness(m)	5.1	6.1	19.0	126.0	-	
					Depth(m)	5.1	11.2	30.2	156.2	-	
	10	37N	566157 350148	887	Resistivity(Ohm-m)	8.9	17	6	2.4	82	
					Thickness(m)	0.4	4.1	36.0	95.0	-	
					Depth(m)	0.4	4.5	40.5	135.5	-	

b.   Relationship between survey results and geology

b.1   Apparent resistivity and geology

The apparent resistivities, ρa, acquired at each drilling site are shown in Table 4.5. Table 4.6 shows the correlation of the interpreted resistivity structure to the local and/or regional geology.

Table 4.5: Apparent Resistivity Ranges of Drilling Sites

Region	Well drilling site No.	Area site	Apparent Resistivity (ohm-m) (Min –Max, Average)
Oromia	2	Berta/Meki	25-1148, 46-1049
	3	Oyne Umbure	181-6656, 243-4818
	10	Brindar	3-41, 5-15
SNNPRS	1	Abaya Chokare	13-250, 23-144
	4	Chancho	10-103, 16-40
	5	Fango Damot	11-190, 28-113
	6	Lajo	46-589, 75-328
	7	Arbaminch	9-94, 13-32
	8	Walesa	3-55, 6-26
	9	Beresa	6-68, 10-39

Table 4.6: Resistivity Range and Lithology

Code.No.	Lithology	Resistivity range(ohm-m)
1	Unconsolidated sediments-fine grained (Clay,silt)-Saturated with water	<10
2	Unconsolidated sediments-coarse grained -Saturated with water	10-100
3	Highly weathered,decomposed,altered rock	<20
4	Highly to moderately weathered/fractured rock	40-200
5	Highly to moderately weathered/fractured rock, saturated with water	10-100
6	Moderately weathered to fresh pyroclastics	100-1,000
7	Dry pumiceous pyroclastics	>1,000-1,5000
8	Water saturated pyroclastics	10-100

b.2   Oromia Region

●BH-2 (Berta/Meki)
  The Meki area is covered with unconsolidated sediments (alluvium and lacustrine sediments) that consist of sand and clay. Below the sediments, the Dino Formation consisting of unwelded pyroclastic rocks, welded tuff and acidic volocanics and tuffs are probably found mostly intercalated with sediments. This is clearly apparent from the geologic log of the borehole drilled in the Study in the area.

●BH-3 (Oyne-Chefe-Umbure)
  The site is extensively covered with loose and coarse pumiceous pyroclastics belonging to the Dino Formation. Tuffs and welded tuff and acidic volocanics are expected to underlie the surficial cover intercalated with sediments.

●BH-10 (Brindar)
The surface of the site is covered with loose unconsolidated material composed mainly of basaltic gravels, sand and silt, which is probably of alluvial origin. Below the surficial layer, the entire area is probably underlain by the Teltele basalt, which is flood basalt of Miocene age lying unconformably on the crystalline basement rocks.

b.3   SNNPRS

●BH-1 (Abaya Chokare)
  This area lies in an intensively faulted zone which is part of the Wonji Fault Belt, where latest volcanism related to the axial extensional zone of the Ethiopian Rift is evident. At the site, the dominant geology consists of very coarse unwelded pumiceous pyroclastics exposed due to the severe erosion prevalent in the area. These rocks are probably underlain by the stratoid silicics of the Nazret Group. At adjacent high areas (ridges), however, outcrops recent basalt (e.g. the site of VES1-7).
  In the vicinity, numerous hot springs and fumaroles are found indicating intense geothermal activity.

●BH-4 (Chancho)
  The Chancho area is covered with acidic volcanics mainly unwelded pyroclastics, tuffs and welded tuff and acidic volocanics. These rocks are probably underlain by the stratoid silicics

of the Nazret Group. Alluvial cover exists in the flood plains of the small river crossing the area.

The area is located in a highly faulted region trending NE-SW, with the faults probably extending from south of Lake Awasa to northeast of Lake Abaya.

●BH-5 (Fango Damot)

The Fango Damot area lies in the foot hills of the Duguna Mountain close to the Bilate River. North of the site the exposed geology consists of unwelded pyroclastics probably of the Dino Formation. These rocks are probably underlain by the stratoid silicics of the Nazret Group. To the west, the Duguna Mountain is covered with rhyolitic and trachytic lava flows.

●BH-6 (Yaye/Alaba)

The site is extensively covered with loose and coarse pumiceous pyroclastics belonging to the Dino Formation. These rocks are probably underlain by the stratoid silicics of the Nazret Group.

●BH-7 (Arba Minch)

The site is located in the extensive plain southwest of Lake Abaya. Thick unconsolidated sediments of alluvial and lacustrine origin may be found. Often, gravelly clay alluvium covers the surface.

A major fault scarp bounds the plain and the Gemu highlands, the latter being extensively covered by volcanic rocks. Thus, the unconsolidated sediments may be underlain by the same volcanics.

●BH-8 (Walesa)

Thick unconsolidated sediments (alluvium, colluvium, lacustrine sediments) may be anticipated in the area owing to its flat topography and proximity to Lake Chamo and the steep scarp to the west. The Wazeka River floods the eastern part of the area, depositing coarser sediments of boulder, cobble and gravel size.

The escarpment bounding the Gidole highland and the adjacent lowlands is well defined in the area by a major fault trending NE-SW, which forms the western edge of the Lake Chamo Basin.

The Gidole Mountains to the west of the site are covered with thick volcanic rocks, consisting of sub-horizontal basaltic lava flows occurring between a basal residual sandstone and overlying salic lava flows. The Precambrian basement rocks unconformably underlie the volcanics.

●BH-9 (Beresa)

The Beresa site lies over an area mapped as volcanic lava flow, which is the continuation of the most widespread formation found in the Gemu and Gidole highlands. It unconformably overlies the Precambrian basement rocks. Locally, highly to moderately weathered and fractured basaltic rock is exposed at several places with little or no soil cover.

c.   VES curves

VES curves are classified into three types. Type A is the VES curve whose apparent resistivity values indicate "high to low to high" or "high to low to high to low to high" beneath the ground surface (concave type); type B is the VES curve whose apparent resistivity values lowers in the deep underground (convex type). ; type C is the VES curve whose apparent resistivity values are "low to high" from the ground surface (rising type).

Type A accounts for some 25% of the VES curves, and type B, 70% (see to Table 4.7). Type A and B indicates occurrences of groundwater. Thus, the possibility of groundwater existence seems to be high.

Table 4.7: Resistivity Structure and Type of VES

Layers	Measurement point	VES type		
		A(concave)	B(convex)	C(rising)
3	3	1	2	−
4	49	8	38	3
5	38	9	28	1
6	10	6	3	1
Total	100	24	71	5

d.   Resistivity structure

Resistivity structure consists of 3 to 6 layers. In general, 4 to 6 layer models account for about 90% of the structure (see to Table 4.7). Generally surface soil is dry and resistivity is high. As for the layers beneath the surface, the specific resistivity values are generally lower due to the weathering of layers or shallow groundwater. There are many cases that high resistivity is shown in the deep part. The layers further below this high resistivity zone tend to show lower resistivity again. The types with high possibilities of existence of groundwater are A and B type, accounting for 95% of all types. The test drilling point of each site selected from the resistivity structure and planned drilling depth and the geology estimated based on the resistivity structure of each site are shown in Table 4.8.

Table 4.8: Resistivity Structure and Geology at Each Well Drilling Site

Region	Well drilling site No	Area site	Layers	VES No. Drilling Depth(m)	Geology
Oromia	2	Berta/Meki	4	VES10 250	1st-2nd:topsoil 3rd:dry pyroclastic(tuffs,volcanic,ash) 4th:Highly weathered / fracture rocks or pyroclastic(water bearing aquifer)
	3	Oyne Umbure Chefo	5	VES8 250	1st-2nd:topsoil and/or pumiceous pyroclastic 3rd:weathered pyroclastic 4th:fresh and dry pyroclastic 5th:water bearing pyroclastic. weathered / fracture rock saturated water
	10	Brindar	4-6	VES8 150	1st-2nd:coarse sediments(gravel, sand) 3rd-5th:unconsolidated sediments, probably fine grained sediments or saturated with saline water 6th:volcanic rock(basalt)
SNNPRS	1	Abaya Chokare	4	VES6 150	1st-2nd:decompose tuff 3rd:dry coarse pumiceous pyroclastic 4th:highly weathered and/or fracture ignimbrite(water bearing aquifer)
	4	Chancho	4-6	VES3 250	1st-2nd:topsoil clayey 3rd:clay altered pyroclastic 4th:highly to moderately weathered pyroclastic 5th-6th:water bearing pyroclastic, weathered or fracture volcanic rock saturated with water

5	Fango Damot	4-6	VES3 250	1st-3rd:topsoil clayey, altered pyroclastic 4th:highly to moderately to weathered pyroclastic 5th-6th:weathered or fracture volcanic rock, water bearing pyroclastic
6	Lajo	4-5	VES7 400	1st-2nd:topsoil and/or decomposed pyroclastic 3rd-4th:pumiceous pyroclastic 4th-5th:water bearing highly to moderately weathered and/or fracture rock or pyroclastic
7	Arbaminch	3-6	VES6 250	1st-2nd:topsoil, gravel 3rd:sedimentary(relatively coarse sediment) 4th-5th:sediment(clayey, silty or saturated with relatively saline water 6th:bedrock or volcanic rock
8	Walesa	4-6	VES5 250	1st-2nd:topsoil 3rd:sedimentary(relatively coarse sediment) 4th:fine grained sediment(saturated with saline water) 5th-6th:bedrock or volcanic rock
9	Beresa	3-6	VES2 150	1st-2nd: decomposed, highly weathered 3rd-6th:highly weathered rock(aquifer)

e.   Hydrogeological interpretation of the survey results

e.1   Oromia Region

●BH-2 (Berta/Meki)

  The resistivity structure at the site is composed of three to four main resistivity layers. The two topmost low resistivity layers with thickness varying between 3 and 10m and resistivity less than 100 ohm-m are the response of the top soil and weathered/altered pyroclastics. The intermediate layer has a high resistivity response of 1,200-4,300 ohm-m, which is the response of dry pyroclastics.

  The last layer has a relatively low resistivity response of 10-100 ohm-m, probably attributed to water saturated pyroclastics or highly weathered and/or fractured volcanic rocks.

●BH-3 (Oyne-Chefe-Umbure)

  The interpretation results show that the area is underlain by four to five resistivity layers. Very high resistivity response characterizes the topmost 2-4m part with resistivity range of 1,000-6,000 ohm-m clearly indicating dry pumiceous pyroclastics. Below the topmost layers, a relatively low resistivity layer of 100-300 ohm-m is found which could be the response of highly to moderately weathered pyroclastics.

  The fourth layer is again characterized by high resistivity of 300-4,200 ohm-m, interpreted as the response of dry pyroclastics or fresh rocks, whereas the last/fifth layer has a low resistivity response of less than 100 ohm-m to about 300 ohm-m. This low resistivity layer is probably due to either water saturated pyroclastics or weathered/fractured rocks.

●BH-10 (Brindar)

The site is generally characterized by two to three main resistivity layers. The top part has a low resistivity response of less than 10 ohm-m, and probably represents either unconsolidated sediments (alluvium) and/or highly weathered/fractured rocks. This layer is anticipated to be

the water bearing formation in the area. Underlying it, a relatively high resistivity layer of 40-100 ohm-m is detected probably attributed to the bottom bedrock.

e.2   SNNPRS

●BH-1 (Abaya Chokare)
  The survey area is generally underlain by three main resistivity layers. The topmost part is characterized by low resistivity (<20 ohm-m) which is probably attributed to altered/decomposed tuff. The topmost layer is underlain by very high resistivity material (200-1,200 ohm-m) which may be the response of dry and coarse pumiceous pyroclastics.
  At the bottom, relatively low resistivity characterizes the subsurface varies between 10-100 ohm-m, which probably corresponds to highly weathered and/or fractured rock. This layer probably forms the water bearing layer in the area, with depth to the top of the aquifer being on average 50m.

●BH-4 (Chancho)
  Four to five resistivity layers have been found to underlie the area. The topmost two layers have low to very low resistivity response of 10-20 ohm-m attributed to clay or altered pyroclastics. Below these, a low to moderate resistivity material of 40-100 ohm-m is found which is interpreted as highly to moderately weathered pyroclastics. The bottom layer characterized by very low resistivity of 5-20 ohm-m may be due to either water bearing pyroclastics or saturated weathered/fractured rocks.

●BH-5 (Fango Damot)
  The interpretation results identified three to four main resistivity layers, of which the topmost layers having resistivity of 10-200 ohm-m and thickness of 2-16m are due to clay and weathered pyroclastics.
  The intermediate layer has moderate to high resistivity response of 100-1,000 ohm-m indicating variable degree of weathering. In contrast, the bottom layer detected has low resistivity in the range of 20-30 ohm-m, which is probably the response of either saturated weathered/fractured rocks or pyroclastics.

●BH-6 (Yaye/Alaba)
  The area is underlain by four main resistivity layers. The first layer has relatively high resistivity of 140-600 ohm-m related to sandy top soil of 1-4m thickness. Below the top soil, a low resistivity layer (20-60 ohm-m) is found attributed to weathered, decomposed pyroclastics.
The third layer is characterized by high resistivity of 200-600 ohm-m, and may be the response of moderately weathered to fresh pyroclastics, whereas the last layer having low resistivity of 50 to 130 ohm-m could indicate saturated rocks and/or pyroclastics.

●BH-7 (Arba Minch)
  The area lies on a large plain covered with thick unconsolidated sediments which is underlain by volcanic rocks at depth. The interpretation results clearly differentiated the subsurface materials. High resistivity layers of 90-100 ohm-m characterize the bottom bedrock, whereas above the bedrock unconsolidated sediments are identified as having variable composition owing to their variable resistivity responses with an average thickness of 130 to 150m.
  The nature of the sediments as characterized from their resistivity response is grouped in to three. Very low resistivity of less than 10 ohm-m probably indicates fine grained sediments

(clay, silt) or saturation with relatively saline water. Low resistivity in the range of 10-20 ohm-m probably suggest mixing of both fine grained and coarse grained sediments; and high resistivity response of 20 to 100 ohm-m indicate coarser material like sandy and/or gravelly layers. For example, coarse grained sediments are mapped at shallow depth below VES7-6 and VES7-8.

●BH-8 (Walesa)

The Walesa area is also expected to be underlain by thick sediments of alluvial and lacustrian origin. The resistivity survey conducted has identified the nature of sediments and the underlying bedrock. The bedrock is characterized by variable resistivity of 40-200 ohm-m indicating its variable nature.

The sediments also have variable resistivity response, with coarser material having resistivity of 10-40 ohm-m, and finer sediments being less than 10 ohm-m. Very low resistivity (<5 ohm-m) horizons within the sediments probably indicate saturation with poor quality/saline water. In general, the sediment thickness varies between 100 and 200m.

●BH-9 (Beresa)

The Beresa area is dominantly covered with basalts of varying degrees of weathering and/or fracturing. The resistivity interpretation results show that the area is underlain by three to four main layers.

The topmost two layers are characterized by low to very low resistivity of less than 20 ohm-m attributed to highly weathered, decomposed material. Below the top layers, a relatively high resistivity layer (40-160 ohm-m) is found which probably corresponds to highly to moderately weathered/fractured rock. The underlying bottom layer has a low resistivity response of 10-40 ohm-m, which may be the result of highly weathered/fractured rock saturated with water. At one particular location (VES9-3), the massive rock below the aquifer was detected at depth of about 100m.

The Study on Groundwater Resources Assessment
in the Rift Valley Lakes Basin in Ethiopia, Final Report (Supporting Report)

JICA
KOKUSAI KOGYO CO., LTD.
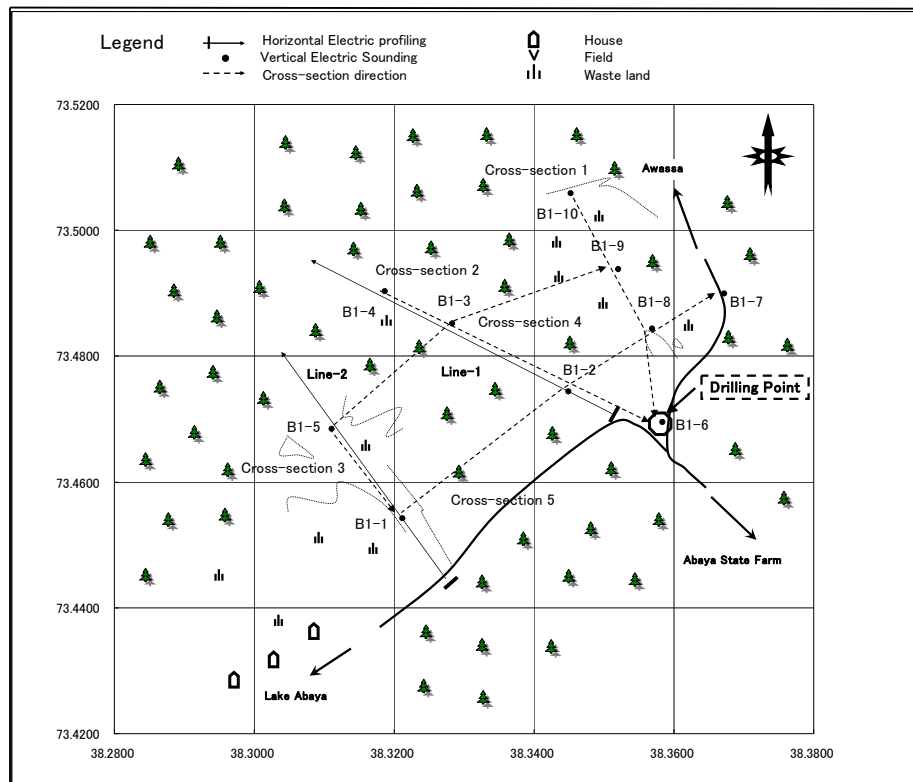
Figure 4.5: Location Map (Borehole No.1 : Abaya Chokare)
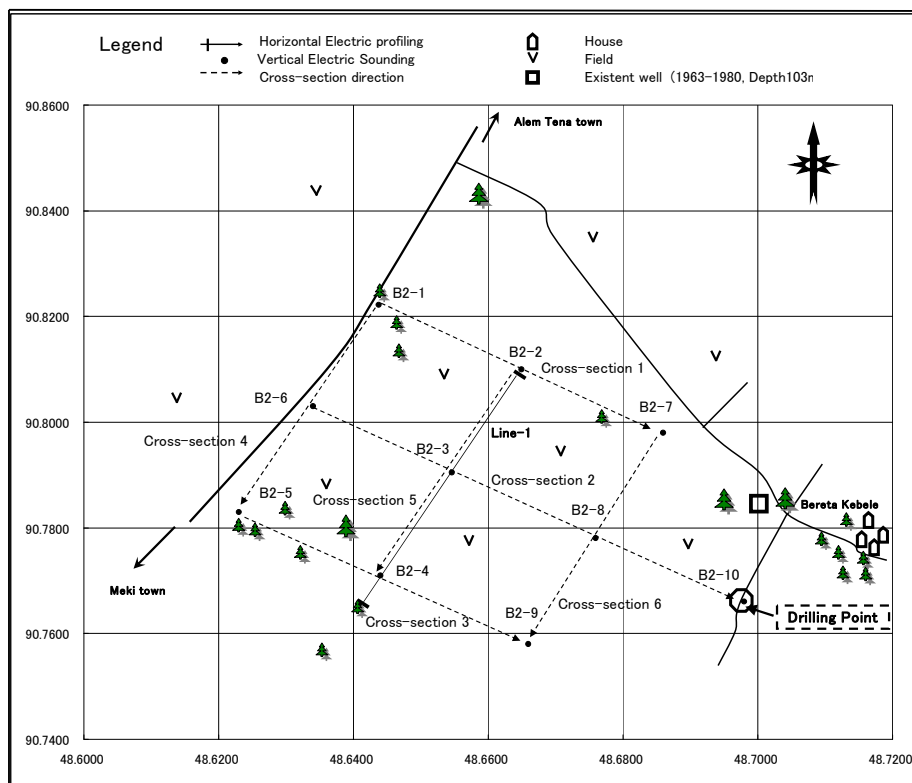
Figure 4.6: Location Map (Borehole No.2 : Awra Godana)
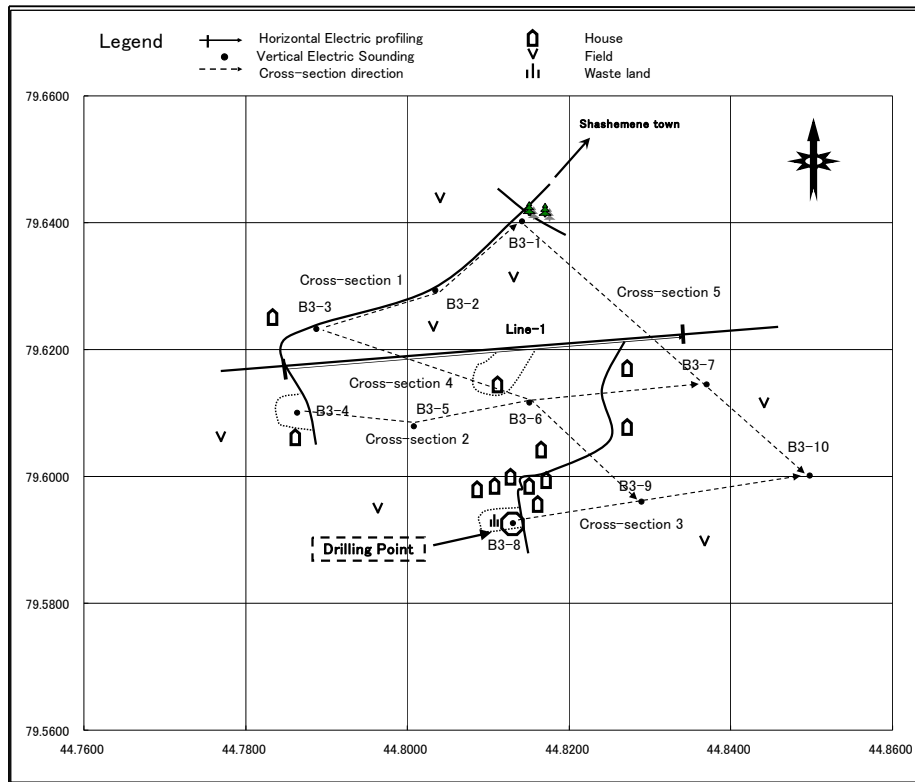
Figure 4.7: Location Map (Borehole No.3 : Oyne Umbure Chefo)
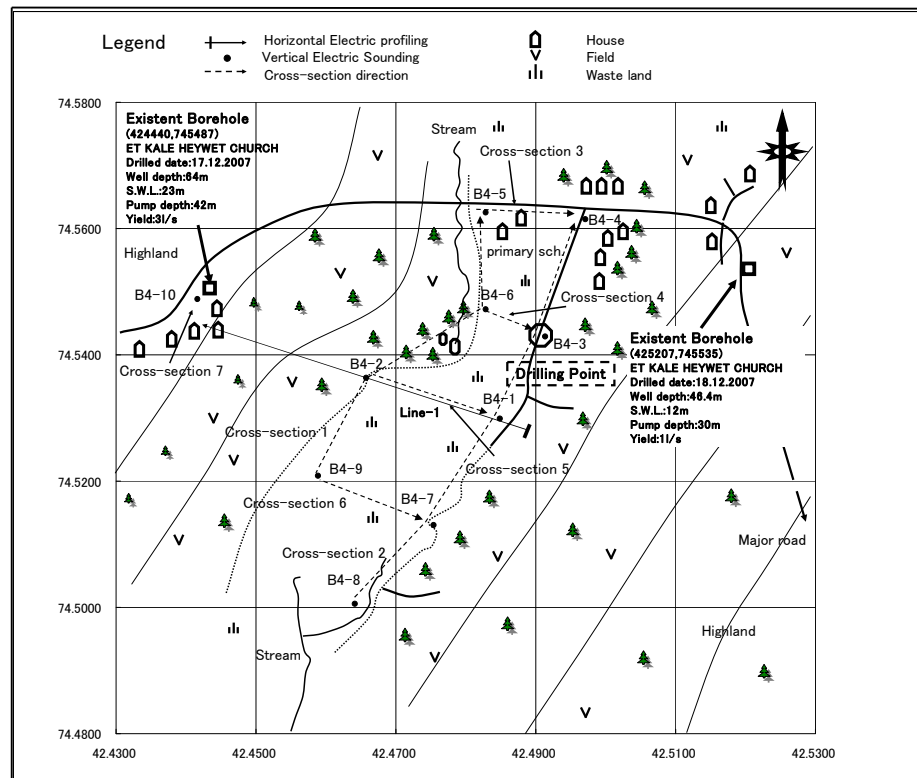
Figure 4.8: Location Map (Borehole No.4 : Chancho)
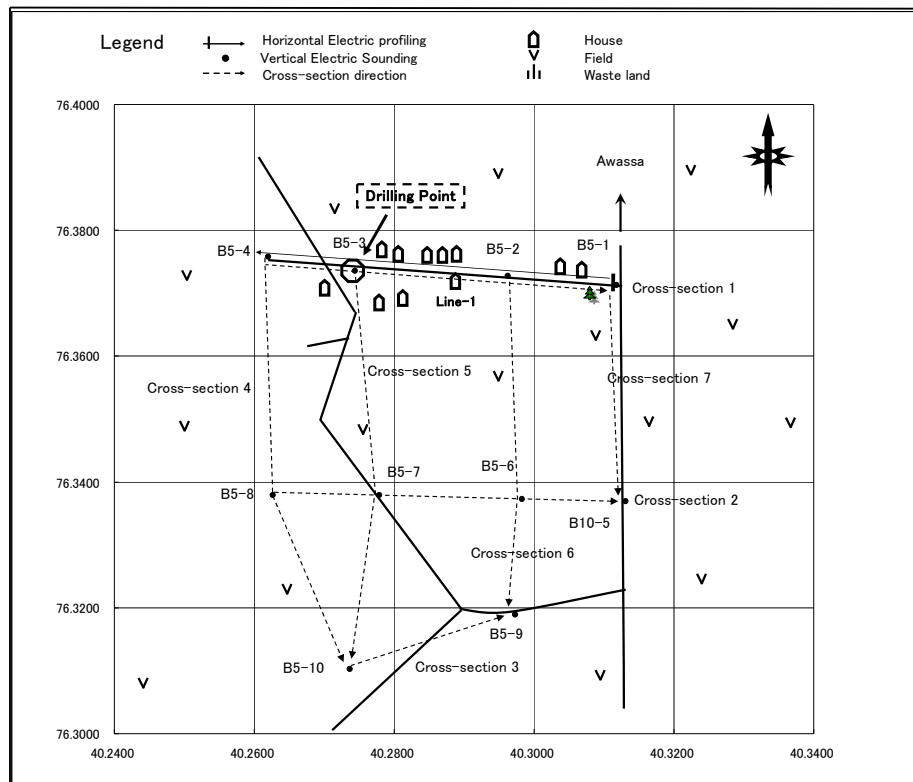
Figure 4.9: Location map   (Borehole No.5 : Fango Damot)
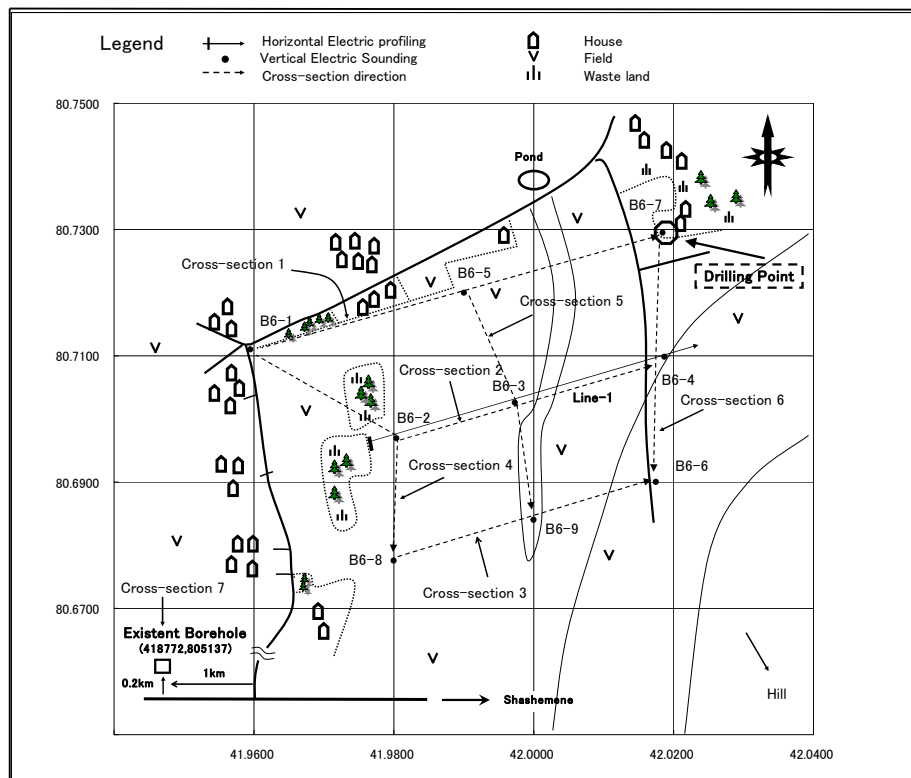
Figure 4.10: Location Map   (Borehole No.6 : Lajo)
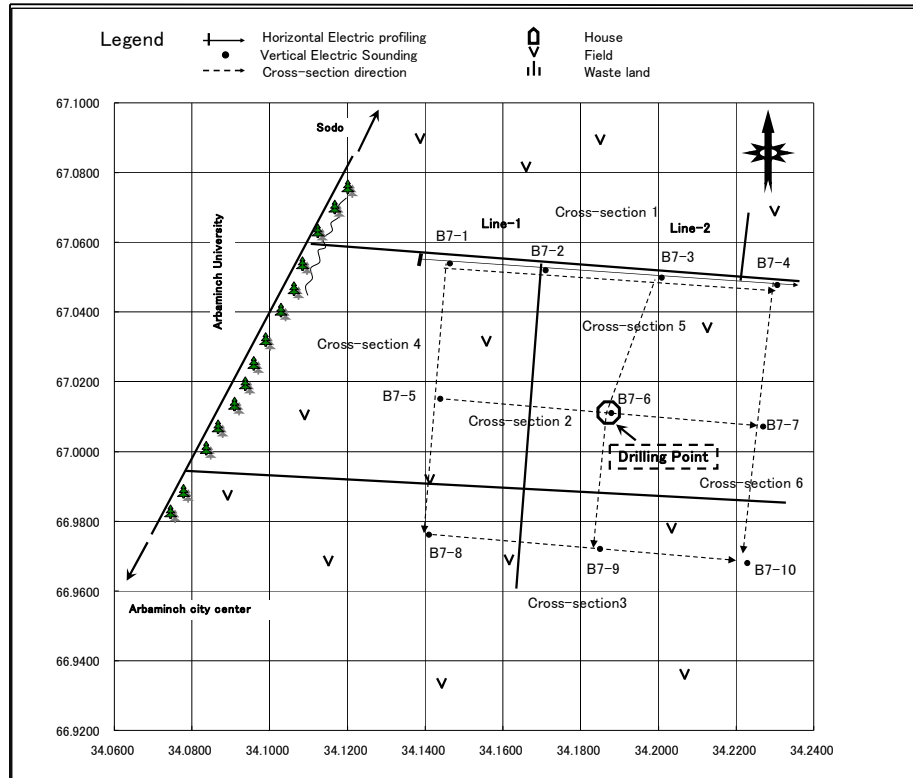
Figure 4.11: Location Map　(Borehole No.7 : Arbaminch)
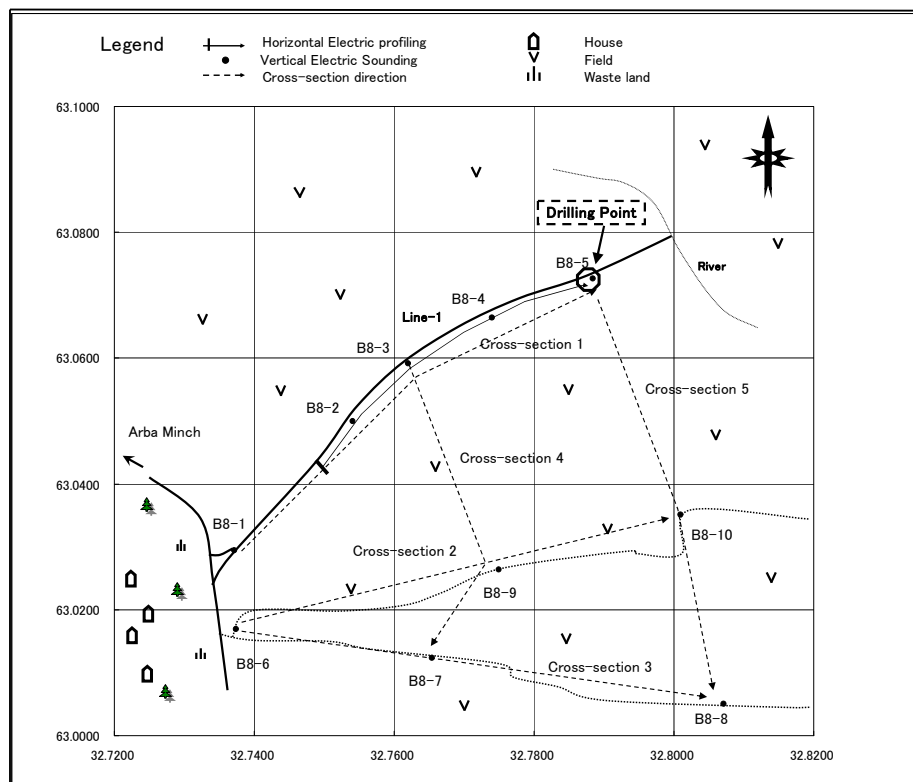
Figure 4.12: Location Map　(Borehole No.8 : Walesa)
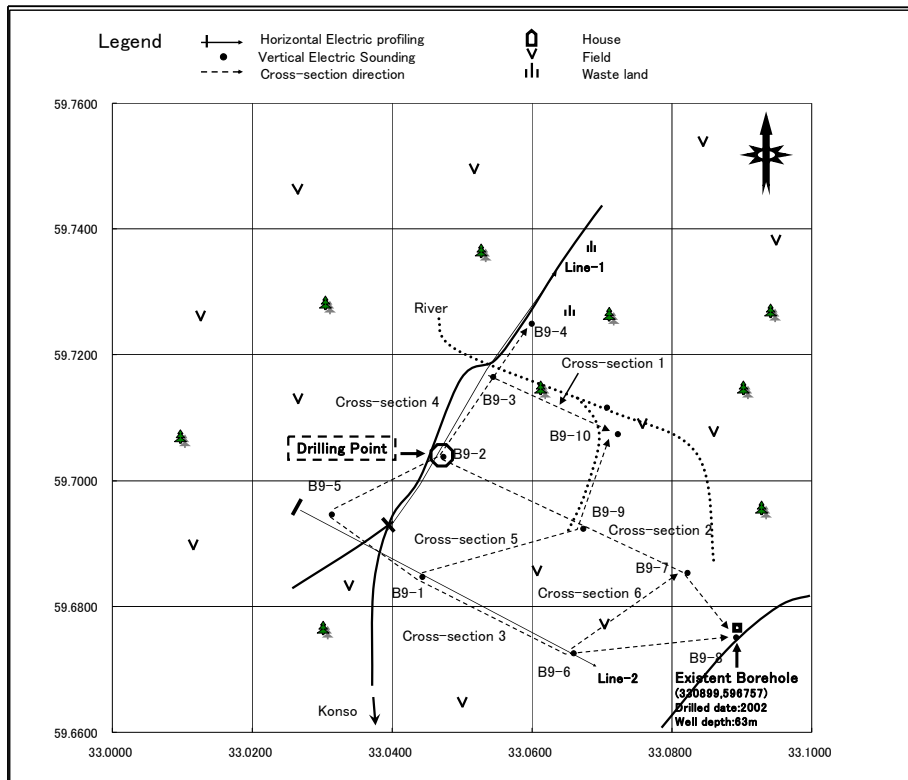
Figure 4.13: Location Map   (Borehole No.9 : Beresa)
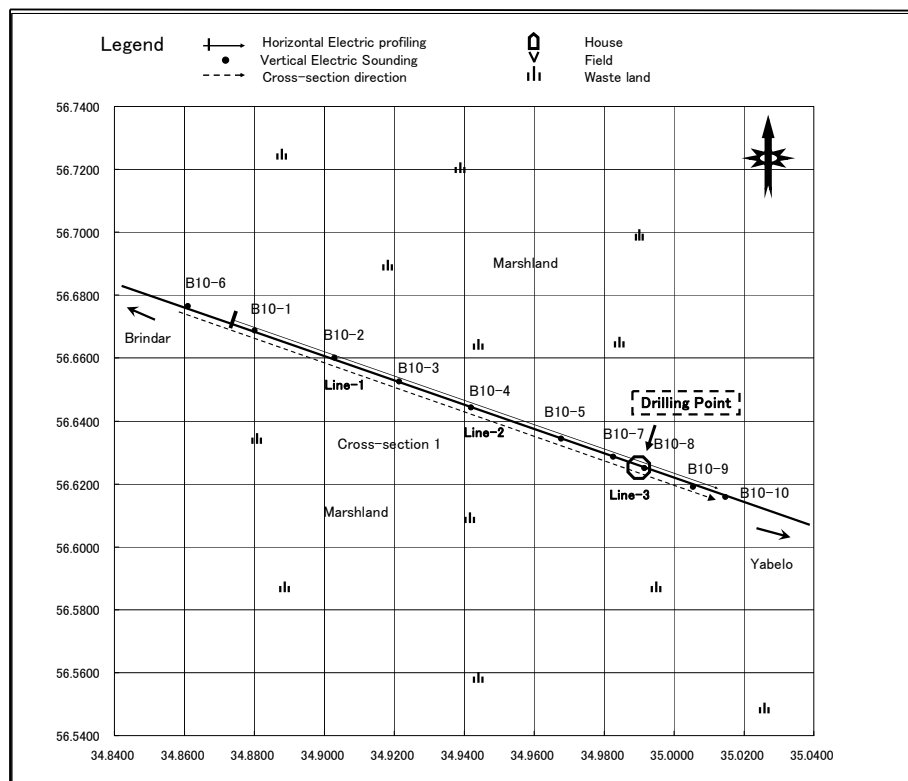
Figure 4.14: Location Map   (Borehole No.10 : Brindar)

The Study on Groundwater Resources Assessment
in the Rift Valley Lakes Basin in Ethiopia, Final Report (Supporting Report)

JICA
KOKUSAI KOGYO CO., LTD.

4.2 TEM electromagnetic survey

4.2.1 Principle and method of survey

The Transient-phenomenon (or Time-domain) Electromagnetic Exploration Method (TEM method) is used to investigate underground resistivity structures by artificially exciting a magnetic field by a transmitter and by measuring responses from the underground in a time domain. In this method, a cable is usually installed on the ground in a loop shape and a constant-voltage (DC) current is passed through this cable. Variation ratios with time of the magnetic field after this current is abruptly cut off are measured by a coiled magnetic-field sensor. The loop transmission source sends signals without directly coming into contact with the ground. This method is also suitable for studies in areas where direct-current electrical exploration is not feasible due to a high grounding resistance, such as deserts and areas where rock masses are exposed.

After the current is cut off, a secondary magnetic field is generated by an eddy current that is excited underground. As shown in Figure 4.15, an eddy current flows deep underground over time. This phenomenon is likened to the spreading of cigarette smoke and is sometimes called a "smoke ring". On the other hand, the output coil voltage after a current cutoff (changes in a magnetic field over time) is influenced by the resistivity structure of the underground. For example, the output voltage immediately after a current cutoff is high if the resistivity is high. However, the output voltage decays rapidly thereafter. Conversely, in a low resistive medium, the output voltage immediately after a current cutoff is low compared with the output voltage of a highly resistive medium, even though its decay ratio is low. The coil output voltage can be converted into an apparent resistivity value and information on deep areas can be related to time elapsed after a current is cut off.
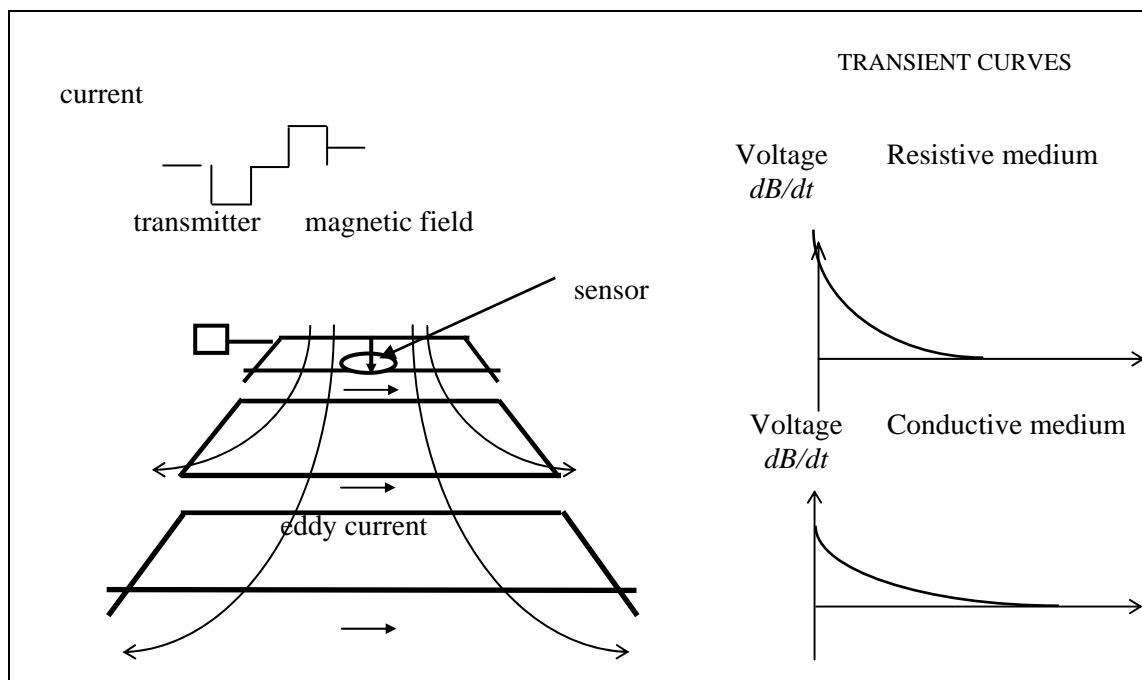
Figure 4.15: TEM survey Configuration and Transient Curves

This method has the following features:

1) An electrode does not have to be grounded to the ground surface and all that is required for the reception coil is to lay it on the ground horizontally. A significantly high work

efficiency can be achieved if grounding resistance is high, such as deserts and in areas where rock mass is exposed.

2) The measuring apparatus can be compact and light so that the method can also be used in deserts and mountains which are not easily accessible.

3) Transient phenomena of a magnetic field after the transmission current is cut off are measured and a primary magnetic field does not exist during measurement, thereby assuring measurement of very stable reception signals.

4) Only a magnetic field is measured and a static shift (a phenomenon of local resistivity in an anomalous body immediately below the surface affecting deep inside the underground), which present problems to techniques that require measurement of electric fields, can be prevented.

The measuring equipment consisting of a TEM system (Geonics Co., Canada) was borrowed from EWTEC. Table 4.9 shows the specifications of this system. It consists mainly of a receiver, a receiver coil, and a transmitter.

Protem57-MK2D is a TEM-type data collector/recorder which sets various measuring time ranges based on the target depth in order to record the rate of change in a magnetic field after the current is cut off. This device can use three types of measuring ranges: 85.29 to 6,980μs for H (after the current is cut off), 352 to 27,900 μ s for M, and 881 to 69,800 μ s for L. These measuring ranges are called standard frequencies and are controlled along with the transmitter. In addition, each measuring range has about 20 gates that are set at logarithmically-space time intervals. Table 4.10 shows an overview of the sampling times of each gate.

The transmitter (TEM57-MK2) can be operated either by battery power or with an electric generator and can transmit up to 25A.

The magnetic field sensor utilizes an induction magnetometer, or coil.

The Protem57-MK2D contains a built-in clock that is used to synchronize its time with the transmitter via connection with a reference cable.

After the signals received from the magnetic field sensor are amplified by an amplifier in the recording equipment, they are subjected to stacking. After stacking, the reception signals are sampled at the 20 gates (measuring times) and are recorded in the internal memory. After the field work is finished, the measurement data are forwarded to from the measuring equipment's memory to a computer.

Table 4.9: Specifications of the TEM Survey Equipment

Equipment		PROTEM 57
Receiver	Measured Quantity	Time rate of decay of induced magnetic field
	Repetition Rate(Hz)	285/237.5, 75/62.5, 30/25, 7.5/6.25 ,3/2.5
	Time Gates	20 geometrically spaced time gates
	Synchronization	(1)Reference cable, (2) Highly stabile quartz crystal
Transmitter	Current Wave Form	Bipolar rectangular current with 50% duty cycle
	Maximum Current	25A
	Output	110 and 120 VAC for 120V

	Voltage	210 and 230 VAC for 220V
Receiver Coil		Air-cored Coil Effective Area:100m2

Table 4.10: Sampling Gate Times

Gate No	EM57 time range		
	H	M	L
1	0.0859	0.352	0.881
2	0.104	0.427	1.06
3	0.129	0.525	1.31
4	0.159	0.647	1.61
5	0.198	0.802	2.00
6	0.248	1.00	2.50
7	0.312	1.25	3.14
8	0.393	1.58	3.95
9	0.497	1.99	4.99
10	0.629	2.52	6.31
11	0.797	3.19	7.99
12	1.01	4.05	10.13
13	1.28	5.14	12.86
14	1.63	6.54	16.35
15	2.07	8.32	20.80
16	2.64	10.59	26.47
17	3.37	13.49	33.72
18	4.29	17.19	42.99
19	5.47	21.90	54.74
20	6.97	27.92	69.77

Unit: milliseconds (ms)

Protem D Receiver   Transmitter/Electric generator

Figure 4.16: TEM Survey Instruments

a.   Field measurement

a.1   Positioning of measuring points

The measuring points were positioned using GPS (Global Positioning System). The rough location map of measuring points is shown in Figure 4.17.

The Study on Groundwater Resources Assessment
in the Rift Valley Lakes Basin in Ethiopia, Final Report (Supporting Report)

JICA
KOKUSAI KOGYO CO., LTD.
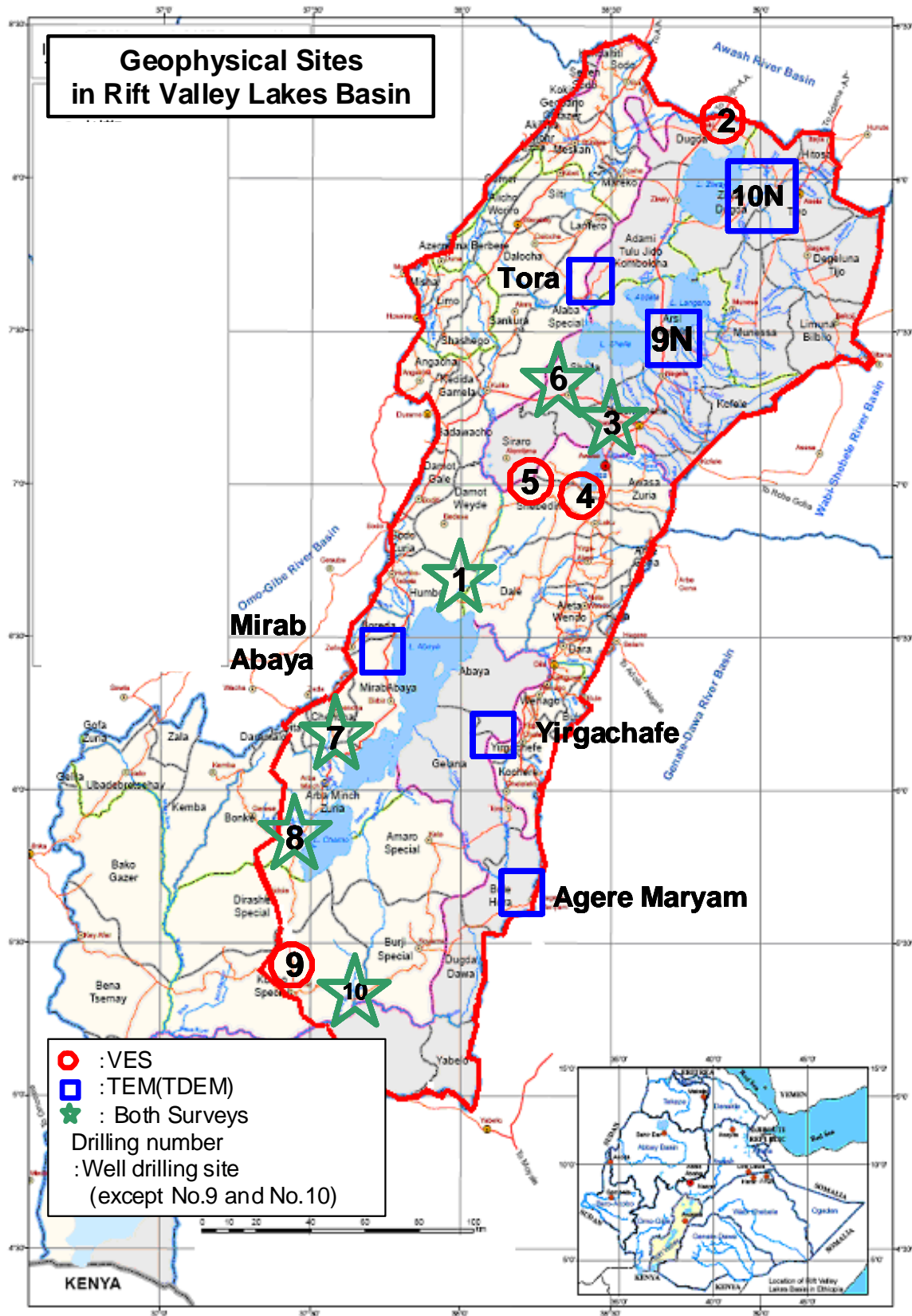
Figure 4.17: Location of the Measuring Points

a.2   Measuring method

The arrangement of TEM measurements was mainly based on the central loop method, although the outloop method was used at a BH6. As shown in Figure 4.18, the arrangement of central loop measurements consisted of a 100m x 100m transmission loop with an EM57 sensor set in the middle on the ground surface. However, in the outloop measurement system the EM57 sensor was installed at a point about 50m away from the center of the transmission loop. The measurements were taken in a time range of 85.29μs to 69.8ms after cutting off the transmission current. Specific resistance data were extracted from a shallow area down to a deep area of about 400m.

In the 4 corners of the transmission loop, direction and distance were determined with a simple positioning device (Compass Glass, magnification 10°×2.2) and a tape measure.
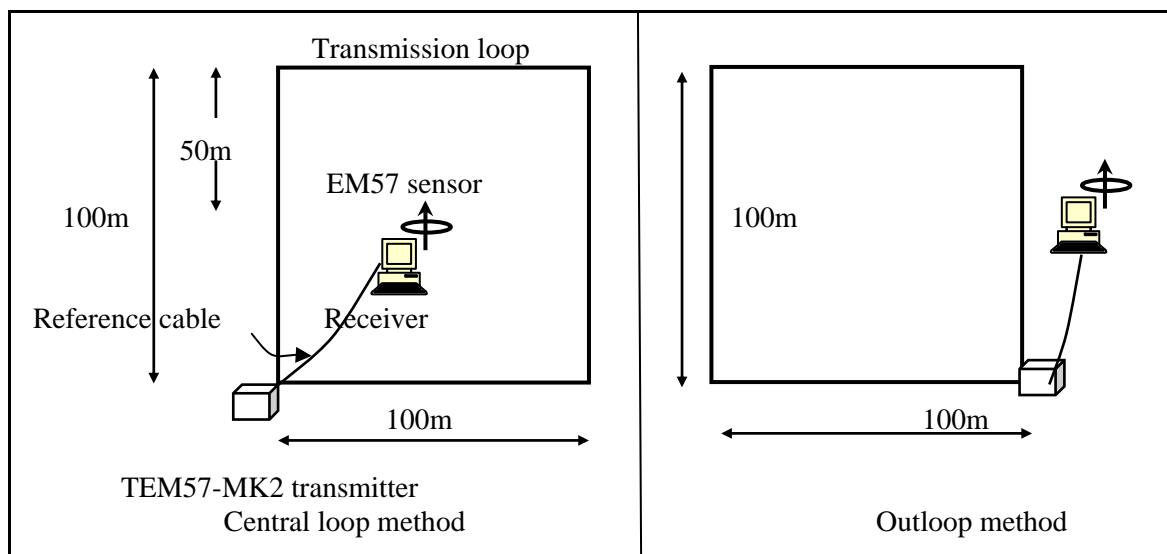
Figure 4.18: Configurations of the Transmitter Loop and Survey Station

The procedure for taking measurements with TEM is as follows:

1）The measuring points are determined using a simple positioning device and a tape measure.

2）The direction and length of the transmission loop are measured with the simple positioning device, and a 100m x 100m loop is set up.

3）The two ends of the transmission loop cable are used to connect the TEM57 with the MK2 transmitter.

4）Magnetic sensors are placed horizontally on measuring points set up inside the transmission loop.

5）The receiver is installed about 5m away from the magnetic sensor.

6）The transmitter and receiver are connected to each other via reference cable.

7）The transmission current is set between 9 and 17A, and measurements are taken in the H/M/L measuring ranges.

8）After finishing the measurements with the Protem57-MK2system, the measuring apparatus are removed and taken to the next transmission loop installation site.

a.3   State of measurements

High-tension power lines run through areas near the BH-3and BH-10N areas, and mixed in with the data at some of the measuring points was artificial noise that appears to have originated from these power lines. In addition, there was some variability of data in the Tora area and at some points in BH-6. Therefore, another survey was conducted at points BH-3, BH-10N, Tora, and BH6. Relatively good data could be obtained at the other measuring points.

b.   Data analysis method

The analysis software used here was "IX1D ver3" (Interpex Ltd., USA). In order to derive the underground resistance structure from the measurement data, the analysis involved the use of two methods: Smooth inversion (described below), and hierarchical inversion.

b.1   Smooth Inversion

In the actual analysis, the first method used was Smooth Inversion (see to Figure 4.19).

In Smooth Inversion, the layer thickness is automatically set so that it logarithmically increases with depth, and only the resistance values of each layer are analyzed by inversion. In addition, restraining conditions are set so that there are no abrupt changes in the resistance between layers.

In this method, analytical results are obtained without giving an initial value so that the same results can be obtained regardless of who the analyst is.

The results of Smooth Inversion analysis are used to create an image of the underground structure ("imaging") which is used to get a general idea of changes in relative resistivity.

Figure 4.19 shows an example of an analysis of the BH-10N-7 excavation site. The diagram on the left side is a theoretical curve of the resistivity structure, while the diagram on the right is an analytical diagram created from Smooth Inversion.
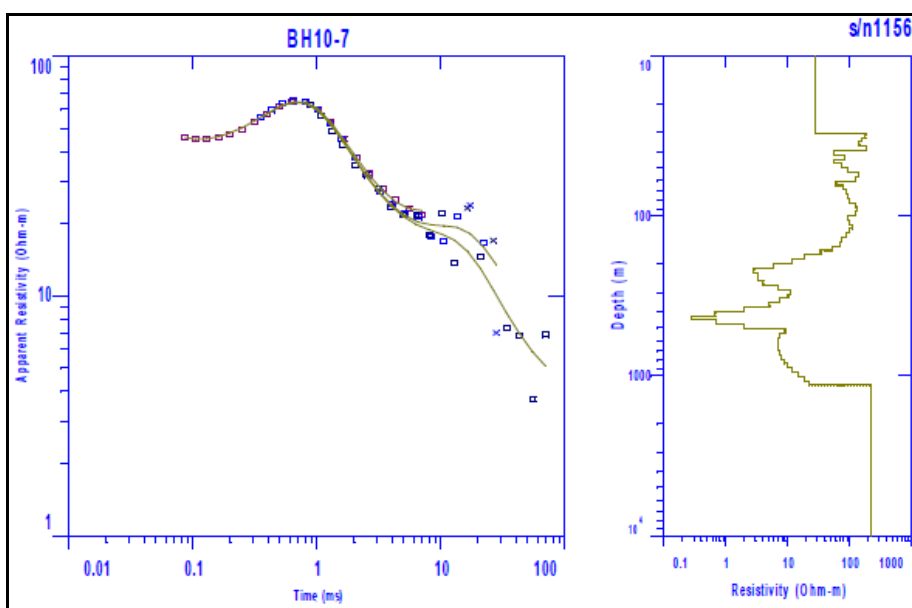
Figure 4.19: Example of Smooth Inversion Analysis of BH-10N

b.2   Layered structure Inversion

If there is an abrupt change in a geological boundary, Hierarchical Inversion is employed to derive accurate information about the depth of layer boundaries because it enables values for resistivity and thickness to be freely varied.

Initial values in hierarchical inversion include the number of layers, and relative resistivity and other values for each layer. Based on these initial values, the most optimal horizontal multi-layer structure is analyzed in the measurement results.

Figure 4.20 shows an example of analysis of BH-10N-7. The right-hand diagram depicts the result of the hierarchical structure analysis, with the red line indicating the layered structure inversion.
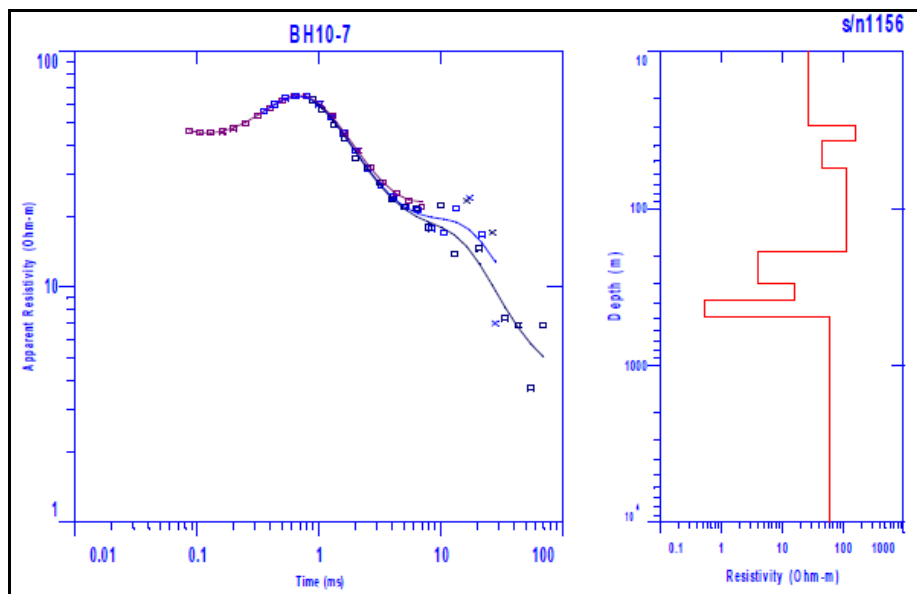
Figure 4.20: Example of Layered Structure Inversion Analysis of BH-10N

Figure 4.21 shows the procedure used for analyzing the data in the present study.

After checking such things as dimensions of loops, and values for receiver gain, electrical current, etc., the measured values for each gate were converted into values of apparent resistivity.

The voltages, V_0 (in unit of mV), which are measured by the PROTEM57(D) system are converted to magnetic field decay rate, dB/dt (nV/m^2), using the following formula (Geonics, 1992).

$$dB/dt=(V_0 \times 19200) \diagup (E \times 2^n)$$

where E is the receiver coil moment (m^2), and n is amplitude gain setting. Apparent resistivity $\rho_a\,(t)$ (ohm-m) as a function of time are then given by,

$$\rho_a(t) \quad (\mu \diagup 4\pi t_c) \times (2\mu M \diagup (5t_c dB/dt)^{2/3}$$

where m is magnetic permeability ($*4p*10^{-7}$ in unit of H/m), t_c is measurement time or the gate center time in s, and M is transmitter moment which is the product of loop area (m^2) and current (A).

The one-dimensional inverse processing is used to obtain one-dimensional resistivity structures that can be assumed to be layered models from a geological point of view. In this process we can estimate structural parameters (e.g., resistivity and thickness) of best fitting models with up to 7 layers using a least squares method called automatic ridge regression.

Data Collection
↓
Stacking Filtering
↓
Editing of Data
↓
Conversion to Apparent Resistivity

Occam's Inversion   Structure Inversion
↓   ↓
Imaging Section   Structure Section
↓   ↓
Geological Information   ←→   Existing Data
↓
Geology evaluation
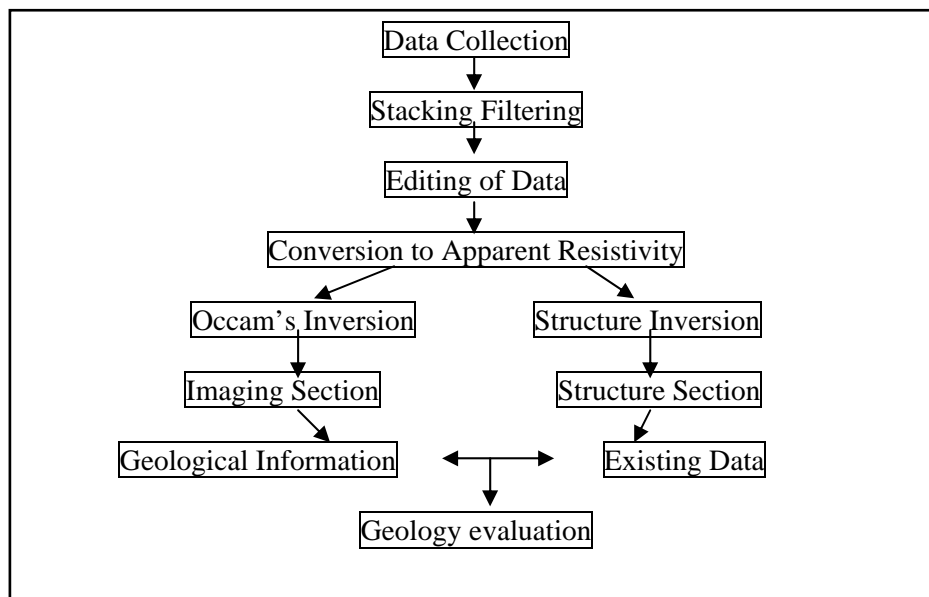
Figure 4.21: Flow of the Data Analysis

4.2.2   Selection of measurement points

a.   Reasons for selection and quantity of survey

The measurement points were selected for the purpose of creating the geological profiles and making a comparative corroboration with the electrical survey and drilling results that had been finished in the first year and electromagnetic survey. Still another purpose was to evaluate the groundwater potential of major aquifers by obtaining the resistivity structure of the new drilling points.

The study areas included 12 locations in two regions, i.e., Oromia Region and SNNPRS (refer to the Figure 4.17). The electromagnetic prospecting at 5 locations that were scheduled to be test drilling sites (BH-6、BH-7、BH-8、BH-9N、BH-10N), and 2 sites where drilling had been completed in the first year (BH-1 and BH-3). There were also 4 sites that were selected to learn more about the geological structure (the Tora, Mirab Abaya, Yirgachefe, and Agere Maryam areas), and one location (BH-10) where electric prospecting would be conducted.

Table 4.11 shows the number of electromagnetic surveys that were made. Further information is provided in the Record of Electromagnetic Survey Measurements of Annex.

Table 4.11: Quantity of Electromagnetic Survey Measurements

Name of area	Site	Kebele / Village	TEM	VES	Drilling completed
Oromia	BH-9N	Hadda Boso/Dole	10	-	-
	BH-10N	Ubo Bericca/Ogolcho	10	-	-
	BH-3	Meja Dema	4	○	○
	BH-10	Brindar	3	○	-
	Tora	Meded Gagebo/ Anshebeso Kuchi	3	-	-
	Yirgachefe	Budukisa/Worago	3	-	-
	Agere Maryam	Bule Kagna	3	-	-
SNNPRS	BH-1	Abaya Chokane	3	○	○
	BH-6	Yeye Alaba/Lajo	3	○	-
	BH-7	Waz/Arbaminch	3	○	-
	BH-8	Walesa	3	○	-
	Mirab Abaya	Fetle Doronje	3	-	-
Total	12	12	51	-	-

b.   Field reconnaissance survey and selected points

In the initial plan, drilling was scheduled for BH-9 and BH-10 in the southern part of the study area, but the two drilling sites were moved to the northern area due to hydrogeological considerations. After working with hydrogeologists and GSE members, candidate sites were reconnoitered. The newly selected sites were named BH-9N and BH-10N. In addition, to create cross-sectional maps of geology and hydrogeology, supplementary electromagnetic prospecting points were located between the two drilling sites. At the start of the exploration, local residents were given an explanation about the project. Residents confirmed existing wells, were asked about water supply conditions, and agreed to provide assistance with the physical prospecting.

4.2.3   Results of the survey and analysis

a.   Results of the survey

The results of the electromagnetic survey are shown in various annexes, including Data book (Field photos of electromagnetic prospecting), Data book (Locations of electromagnetic prospecting), Data book (Apparent resistivity curves and result of interpretation), and Data book (List of electromagnetic prospecting measurements).

b.   Comparison with VES, drilling data, and hydrogeological interpretation

As reported earlier, the analysis involved Smooth Inversion, which was used to derive the resistivity structure, and layered structure inversion comprised of 4 to 8 layers.

Longitudinal resistivity diagrams were created based on the results of each of the inversion analyses. The imaging longitudinal diagram of resistivity shows resistivity values with color bars on a logarithmic axis: high resistivity is shown with "warm" colors, while low resistivity is shown with "cool" colors.

b.1   Regarding differences between TEM and VES resistivity measurements

The Study on Groundwater Resources Assessment
in the Rift Valley Lakes Basin in Ethiopia, Final Report (Supporting Report)

JICA
KOKUSAI KOGYO CO., LTD.

The TEM electromagnetic survey method is especially effective in areas where groundwater is highly sensitive to low resistivity. However, it may not produce accurate readings in areas where the ground resistivity is as high as several thousand ohm-m. TEM surveys use the responses from magnetic fields induced underground to measure conductivity (the reciprocal value of ground resistivity). Electromagnetic surveys use varying wave frequencies at different depths of permeation to detect changes in the depth and direction of conductivity. The wave frequencies decrease along with survey depth. The depth ranges from several meters to several hundred meters. Analysis of electromagnetic readings was done using IX1D software version 3 by Interpex Limited of Colorado, USA. Typically, the readings taken are frequently analyzed to fit low resistances, so the analysis values are often lower than the readings taken in electrical surveys.

In contrast, VES surveys are especially effective in areas where groundwater is highly sensitive to high resistivity. The objective of a VES survey is to assess the characteristic electrical resistivity. Electrode probes are placed in the ground at increasing distances to measure the underground resistivity. The probe depth can be from quite shallow, up to 200 meters deep. As readings at depths below 200 meters often require the probes to be extended beyond their practical usability, alternate readings are sometimes also taken using the TEM electromagnetic method. The results of both methods are synthesized for analysis. Also, when two thin strata of differing types intermingle, they can be mistakenly read in electrical surveys as a single layer. And, even where an anisotropy in the ground does exist, it's possible that a VES electrical reading might miss it, leading to a mistaken assessment of the resistivity and thickness of geological formations. Analysis of electric readings was done using RESIX-P software, also by Interpex Limited of Colorado, USA. Resistivity readings are often shifted upward for analysis, thus they are often higher than electromagnetic readings.

It is also possible to see differences depending on the time of year the readings are taken. For electric surveys, it is thought that during the small rainy season, from March to May, the groundwater table slightly rises, and the surface of ground can easily become saturated. For electromagnetic surveys carried out in the dry months of November and December, it is thought that location of underground water is lower, and that changes in the volumetric water content (saturation multiplied by porosity) may cause discrepancies in readings. So, even in locations with consistent readings, there could be discrepancies in the readings, and different aquifer sizes could cause variations in the data.

In comparing the TEM and VES readings for this survey, some discrepancies were seen in the analysis of resistivity and depth measurements, but the resistivity structure can be said to approximately match the layer structure.

The following is a description of the characteristics of the resistivity structure of each site.

c.   Oromia Region State

c.1   BH-9N (Hadda Boso/Dole)

This is a flat area that is surrounded by 3 lakes: Langano, Abijata, and Shala. The elevation is about 1,640m, a high position that is several tens of meters higher than the surface of Lake Langano. There were 10 TEM-based measuring points, and they were spaced about 200m apart (refer to Data book). It should be noted that this area was slated for the drilling of an observation well which would be drilling depth of 200m.

From the results of TEM-based analysis, 3 Cross sections of resistivity were created based on the Smooth Inversion and layered structure analyses. The following is a description of the characteristics of each measuring line.
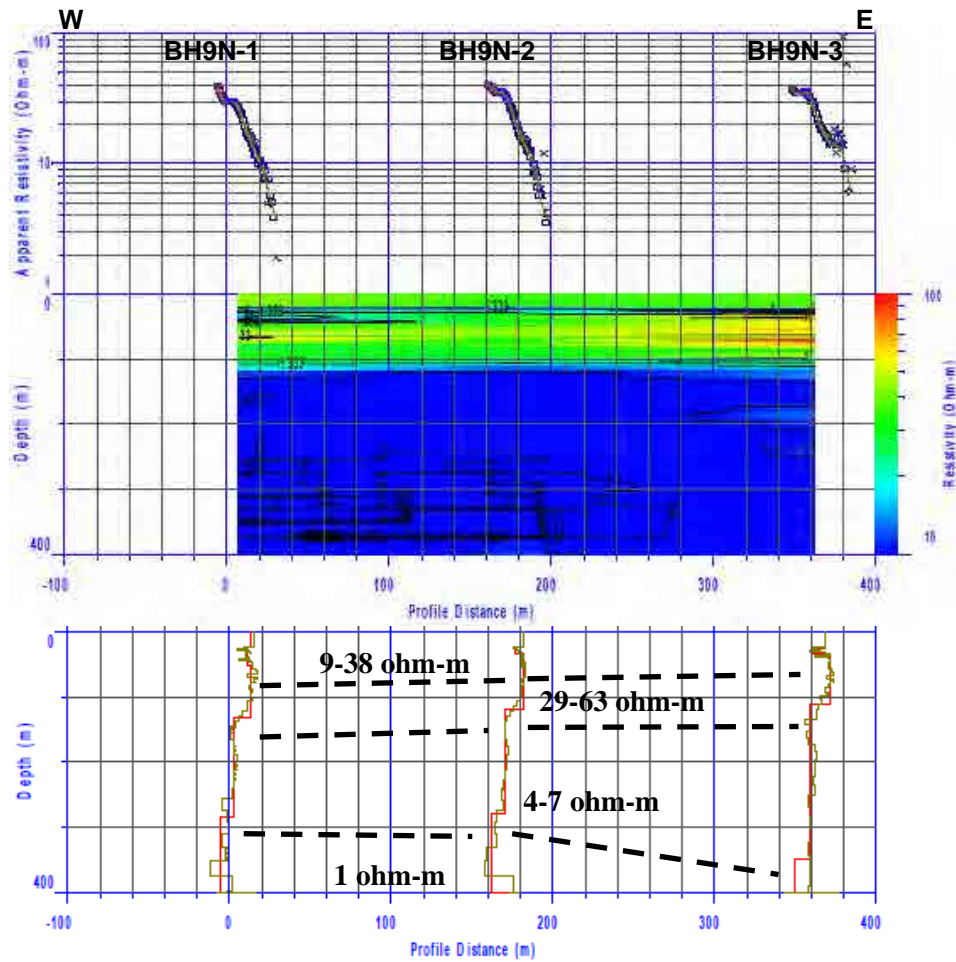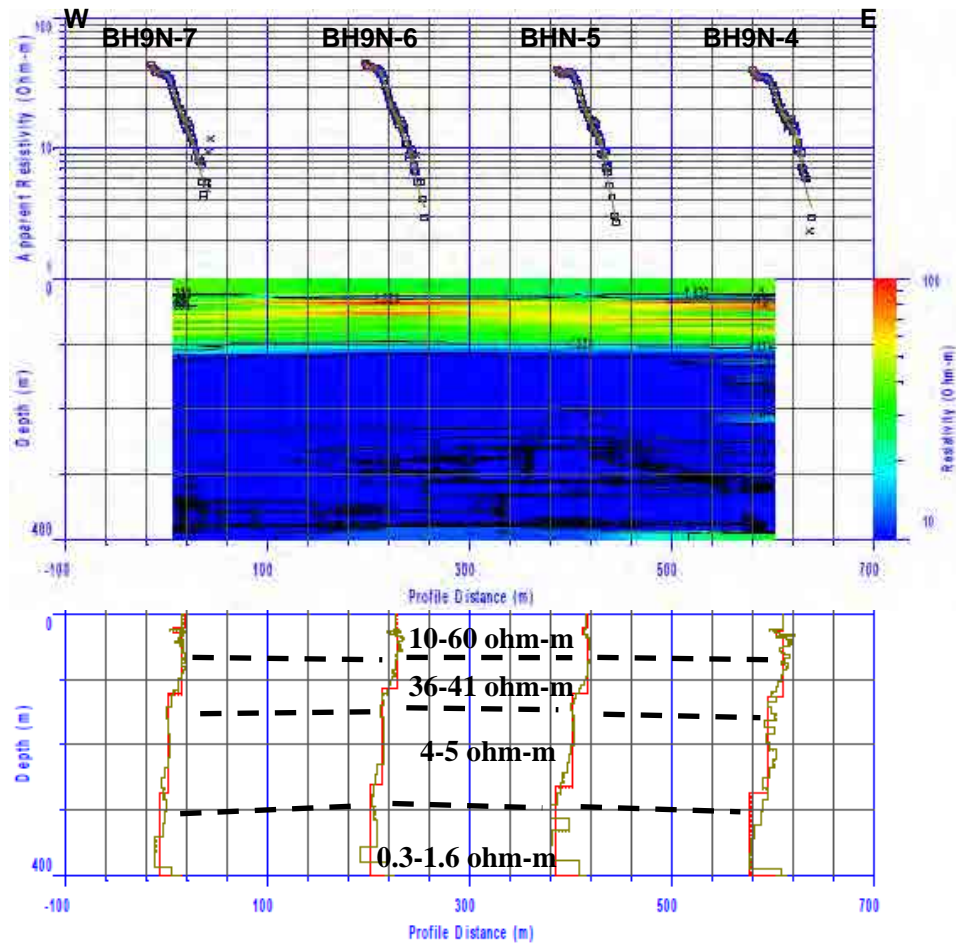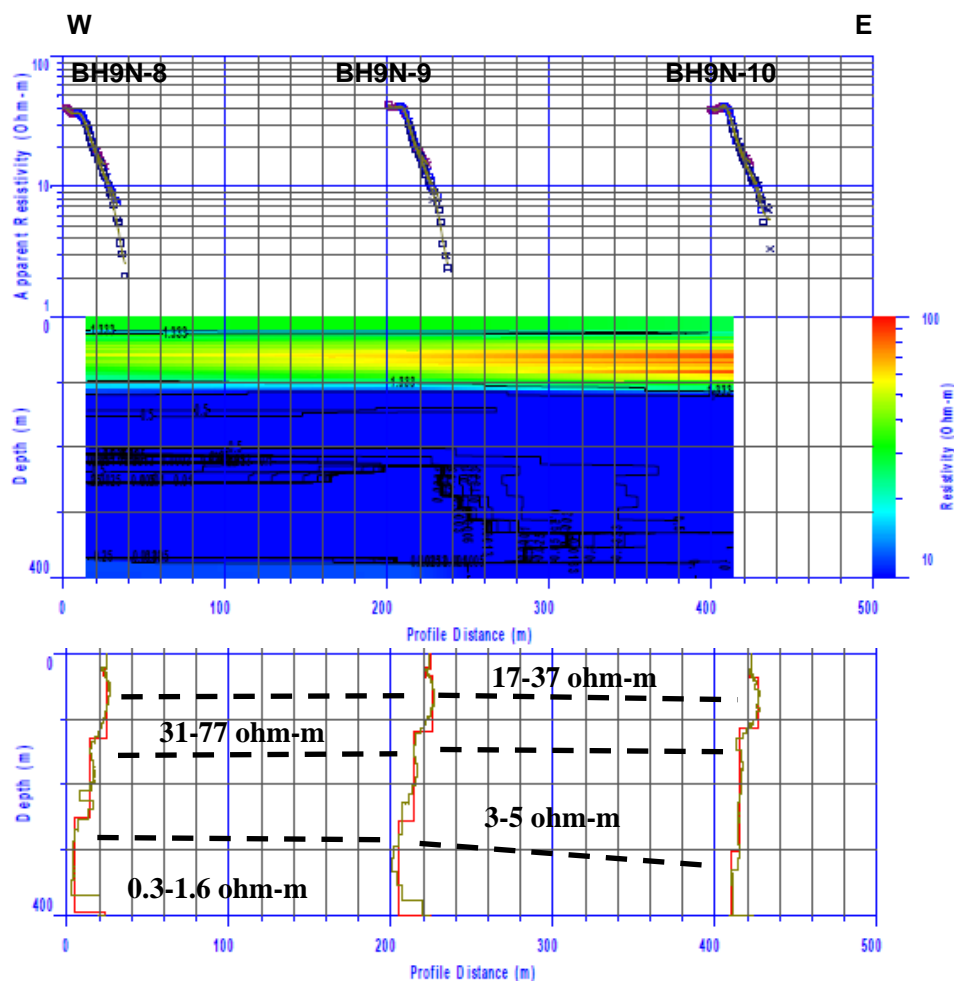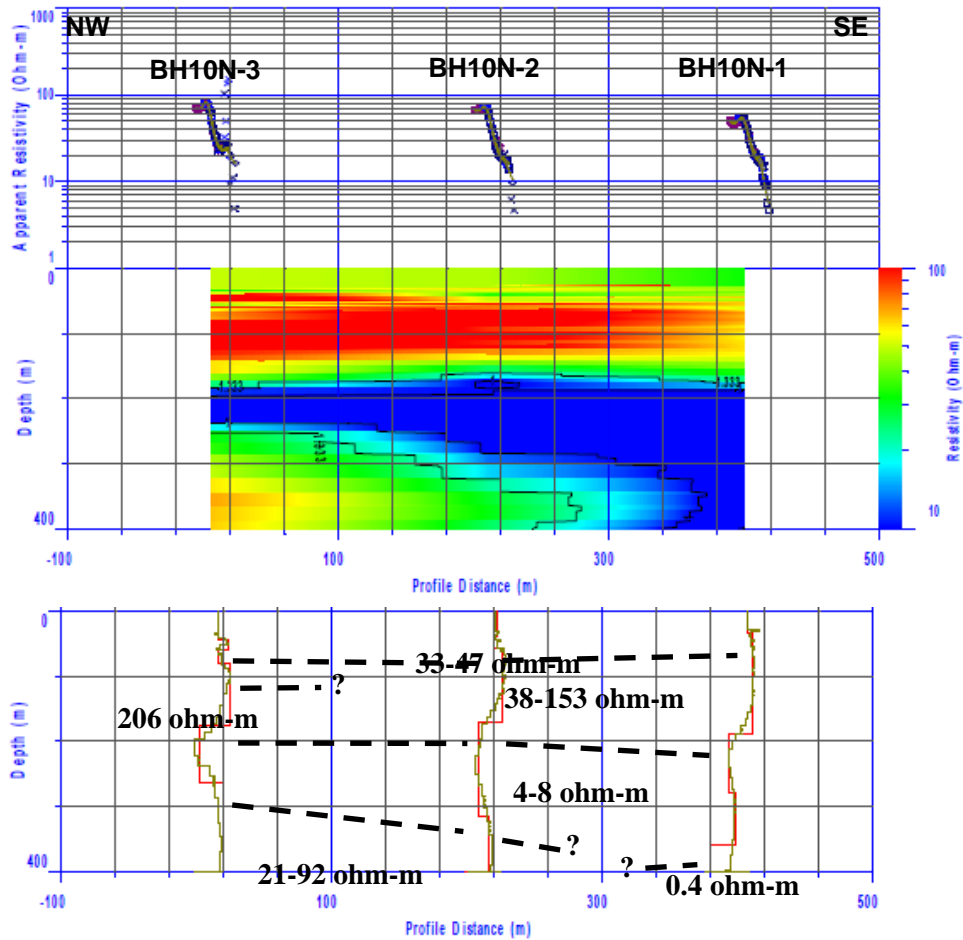

Figure 4.22: Cross-section of Smooth Imaging Resistivity and Layered Structure Analysis (BH9N line 1)

The resistivity structure shows 4 layers. From the surface down to about 100m, the resistivity is somewhat high, but in layers below that it is low, especially at depths below 300m.
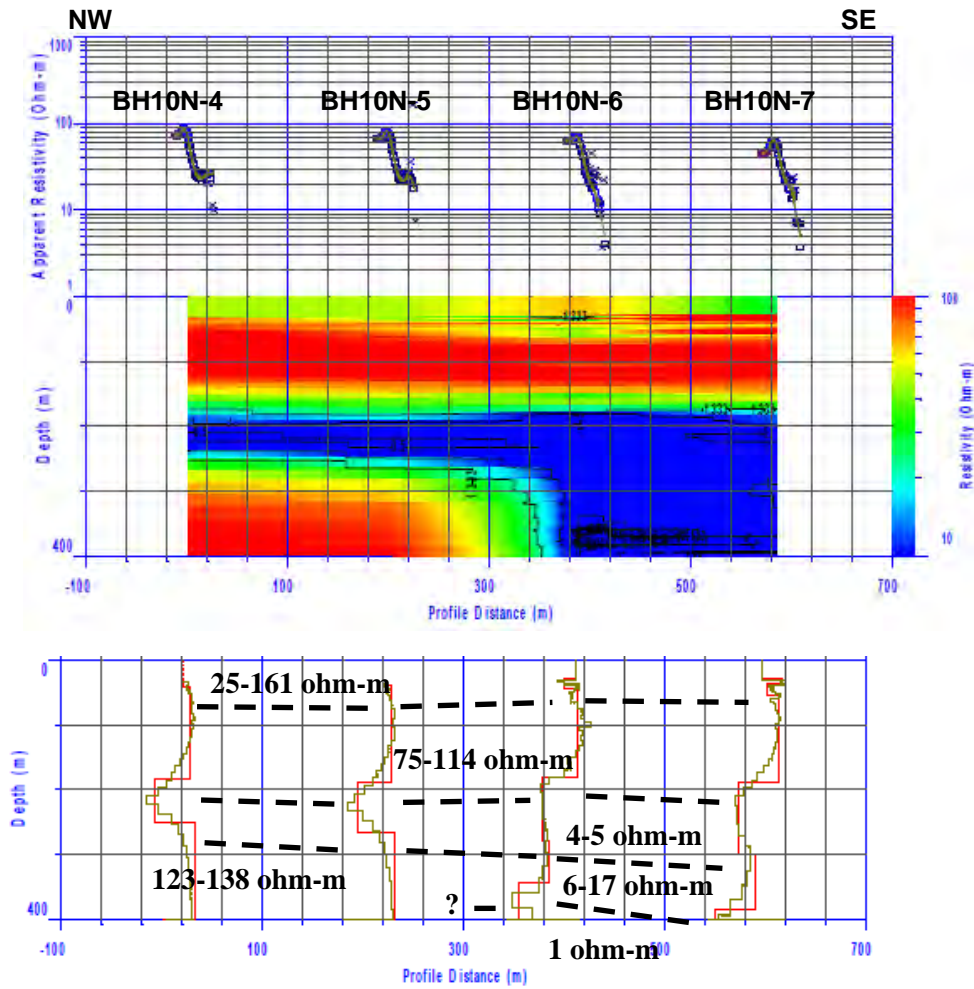
Figure 4.23: Cross-section of Smooth Imaging Resistivity and Layered Structure
Analysis (BH-9N line 2)

As with measuring line 1, the resistivity structure shows 4 layers. From the surface down to about 100m, the resistivity is somewhat high, but in layers below that it is low, especially at depths below 300m.
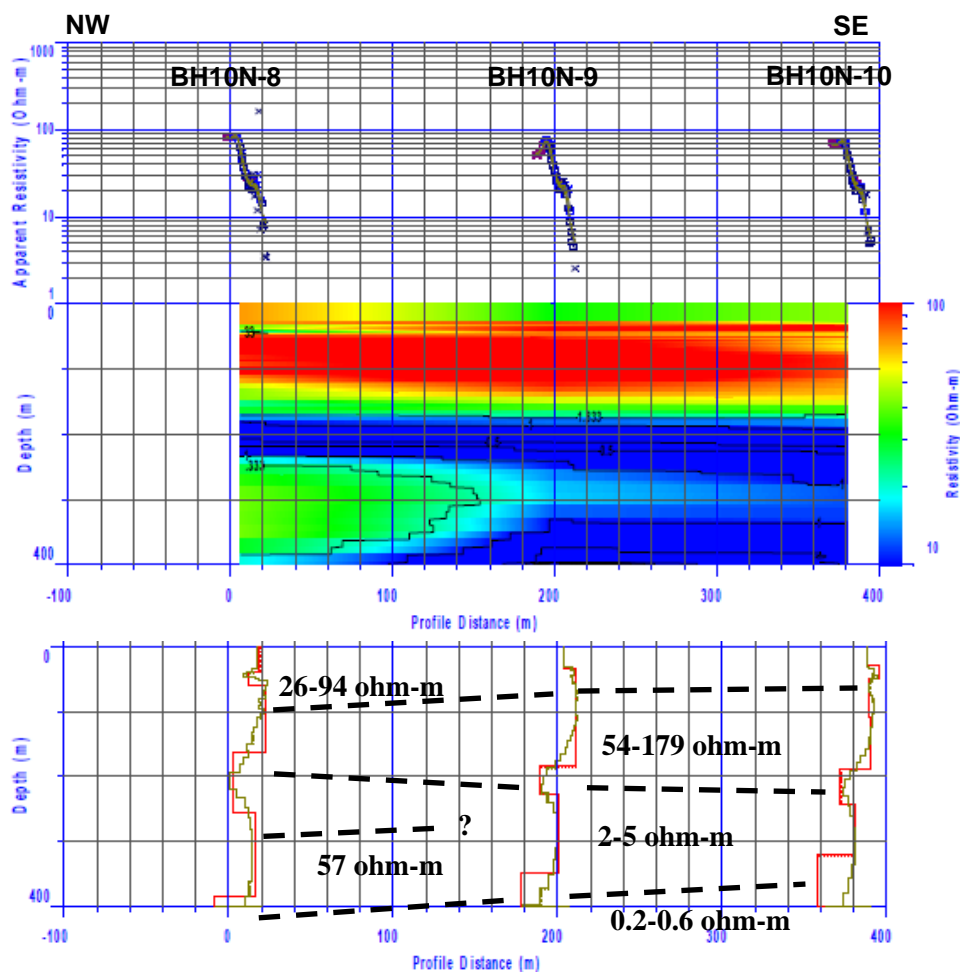
Figure 4.24: Cross-section of Smooth Imaging Resistivity and Layered Structure
Analysis (BH-9N line 3)

This longitudinal profile shows a resistivity structure that is similar to that of measuring lines 1 and 2.

The geology of this region mainly distributed the volcanic materials. Because these sediments are considered to be indicative of a weakly consolidated geology, it is easy for them to contain an adequate amount of water. This is especially the case for depths of 100m or greater below the surface, where groundwater saturation appears to be the cause of declining resistivity. Moreover, this area is between dislocated groups running N-S. So as a result of these dislocations, deep underground geological structures are imagined to be highly permeable and hold layers of accumulated water.

c.2   BH-10N Ubo Bericca/Ogolcho)

This point is located in a flat area 8km to the northeast of Lake Zway. It is a rural village that is about 1,700m above sea level, and about 100m above the surface of the lake. Measurements were taken at 10 TEM measuring points which were spaced about 200m apart (see to Data book). This region is slated for drilling down to a depth of 150m. Three cross sections of resistivity were also created for this point, and a resistivity structure similar to the above structures was obtained. The following is a description of its main characteristics.
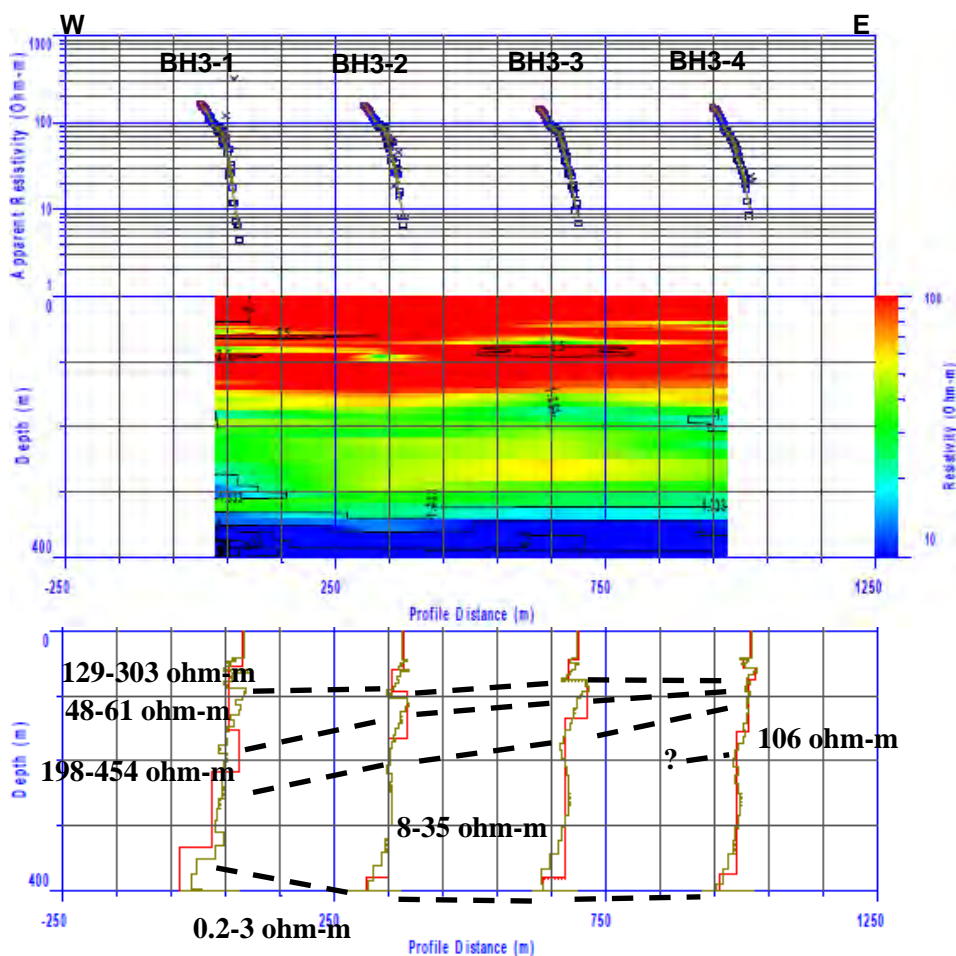
Figure 4.25: Cross-section of Smooth Imaging Resistivity and Layered Structure
Analysis (BH-10N No1)

The resistivity structure of this profile shows mainly 4 layers. From the top layer down to a depth of about 300m, the resistivity repeatedly alternates from medium to high to low. However, below 300m the resistivity differs. At measuring points BH-10N-3 and BH-10N-2, resistivity is high in the deepest layer, but at point BH-10N-1 it is remarkably low. It appears than an anomaly exists in the resistivity structure between these points.

The Study on Groundwater Resources Assessment
in the Rift Valley Lakes Basin in Ethiopia, Final Report (Supporting Report)

JICA
KOKUSAI KOGYO CO., LTD.

Figure 4.26: Cross-section of Smooth Imaging Resistivity and Layered Structure Analysis (BH-10N No2)

As with the previous measuring line (1), the resistivity repeatedly alternates from medium to high to low from the top layer down to a depth of about 300m, and the lowest parts show the same trends. In particular, differences in resistivity structure were found between measuring points BH-10N-5 and BH-10N-6.

Figure 4.27: Cross-section of Smooth Imaging Resistivity and Layered Structure
Analysis (BH-10N line 3)

This profile shows a resistivity structure that is similar to the other two profiles. As well, there are differences in structure between measuring points BH-10N-8 and BH-10N-9.

To summarize the above, the areas of anomalies in each resistance profile ran N-S on the east-central side of the region, and it was estimated that there was a non-continuous line in the vicinity.

The geology of this region shows a distribution of Holocene Q1, which consists of lacustrine sediments, as well as sandy, silty, and pyroclastic sediments. In addition, because there is an indeterminate number of faults running NNE-SSW, the geology is reflected in these faults, suggesting a high possibility of differences in resistivity.

c.3   BH-3 (Meja Dema)

This point is located in a farming area about 5km to the west of Shashemene (refer to Annex 5.4). It is at an elevation of about 1,810m. The drilling of observation wells is being finished at points selected based on the results of electromagnetic prospecting conducted in the first year. First, the following shows a cross section of resistivity structure based on the results of electromagnetic prospecting (see Figure 4.28).

Table 4.12 to Table 4.14 show in contrast the geological data extracted from the results of the electrical survey in the first year and the results of the electromagnetic survey just carried

out. Figure 4.29 shows the synthesized results.

Figure 4.28: Cross-section of Smooth Imaging Resistivity and Layered Structure Analysis (BH3)

The resistivity structure of this cross section is mainly 5-layer. From the surface, resistivity is high-medium-high-medium-low, and deep underground it tends to be low. Discontinuity in resistivity structure between measuring points was not found.

Table 4.12: Comparison between TEM and VES Result（BH-3, No1）

Measurement	Parameter	TEM3-3/VES3-8					
		─	L1	L2	L3	L4	L5
T E M	Resistivity (ohm-m)	─	158.2	55.8	454	34.9	2.8
	Thickness (m)	─	43.1	33.3	57.4	248	─
	Undersurface depth (m)	─	43.1	76.4	133.8	382	─
		L1	L2	L3	L4	L5	─
V E S	Resistivity (ohm-m)	280	13537	124	839	45	─
	Thickness (m)	0.1	1.2	25.0	98.0	─	─

The Study on Groundwater Resources Assessment
in the Rift Valley Lakes Basin in Ethiopia, Final Report (Supporting Report)

JICA
KOKUSAI KOGYO CO., LTD.

	Undersurface depth (m)	0.1	1.3	26.3	124.3	—	—
Geologic column (247m)	—	pumice, tuff →welded tuff(weathering alteration in a part)→tuff breccia				—	—

＊ The gray section denotes a correlation between the resistivity and undersurface depth.

According to the results of the electromagnetic survey, resistivity is high down to 43 meters, decreases below this structure, then rises again, and finally decreases again below layer number four. Comparing this resistivity structure with the results of the electrical survey, we see a discrepancy in the electrical survey and underside depth down to 125 meters, below which they are uniform.

Table 4.13: Comparison between TEM and VES Result（BH-3, No2）

Measurement	Parameter	TEM3-4/VES3-10						
		—	L1	L2	L3	L4	L5	L6
ＴＥＭ	Resistivity (ohm-m)	—	129.0	61.3	213.5	106.3	27.1	4.1
	Thickness (m)	—	42.3	14.6	18.7	79.2	220.9	—
	Undersurface depth (m)	—	42.3	56.9	75.6	154.8	375.8	—
		L1	L2	L3	—	L4	L5	—
ＶＥＳ	Resistivity (ohm-m)	837	10164	139	—	908	76	—
	Thickness (m)	0.3	1.3	45.0	—	99.0	—	—
	Undersurface depth (m)	0.3	1.6	46.6	—	145.6	—	—
Geologic column (247m)	—	pumice, tuff →welded tuff(weathering alteration in a part)→tuff breccia					—	—

＊ The gray section denotes a correlation between the resistivity and undersurface depth.

A comparison between electromagnetic prospecting and electric prospecting showed that the resistivity values derived from the analysis of the electric prospecting tended to be higher overall than those derived from the electromagnetic prospecting analysis.

According to the results of electric prospecting, the relative resistivity structure was subdivided down to about 40m below the ground surface, while these layers were analyzed as one layer in the electromagnetic prospecting. Yet in both cases, there was high relative resistivity, and the overall depth appeared to be the same. In the middle depths, differences were found in the number of layers, but there was good agreement about the depth of low resistivity in the deepest areas. The values for low resistivity are also generally consistent.

The electric prospecting went down to a depth of about 200m, while the electromagnetic prospecting went deeper than that, to a depth of about 400m. There was remarkably low relative resistivity below 300m; this low resistivity may have been due to the salinity of the groundwater.

Table 4.14: Comparison between the Results of Observation Well and
Electromagnetic Prospecting Analysis (BH3)

Measurement	Parameter	TEM3-1/Observation well				
		L1	L2	L3	L4	L5
TEM	Resistivity (ohm-m)	302.5	59.3	198.2	8.3	0.2
	Thickness (m)	55.4	96.7	65.2	116.7	–
	Undersurface depth (m)	55.4	152.1	217.3	334.0	–
Geologic column (247m)	–	pumice, tuff →welded tuff(weathering alteration in a part)→tuff breccia			–	–
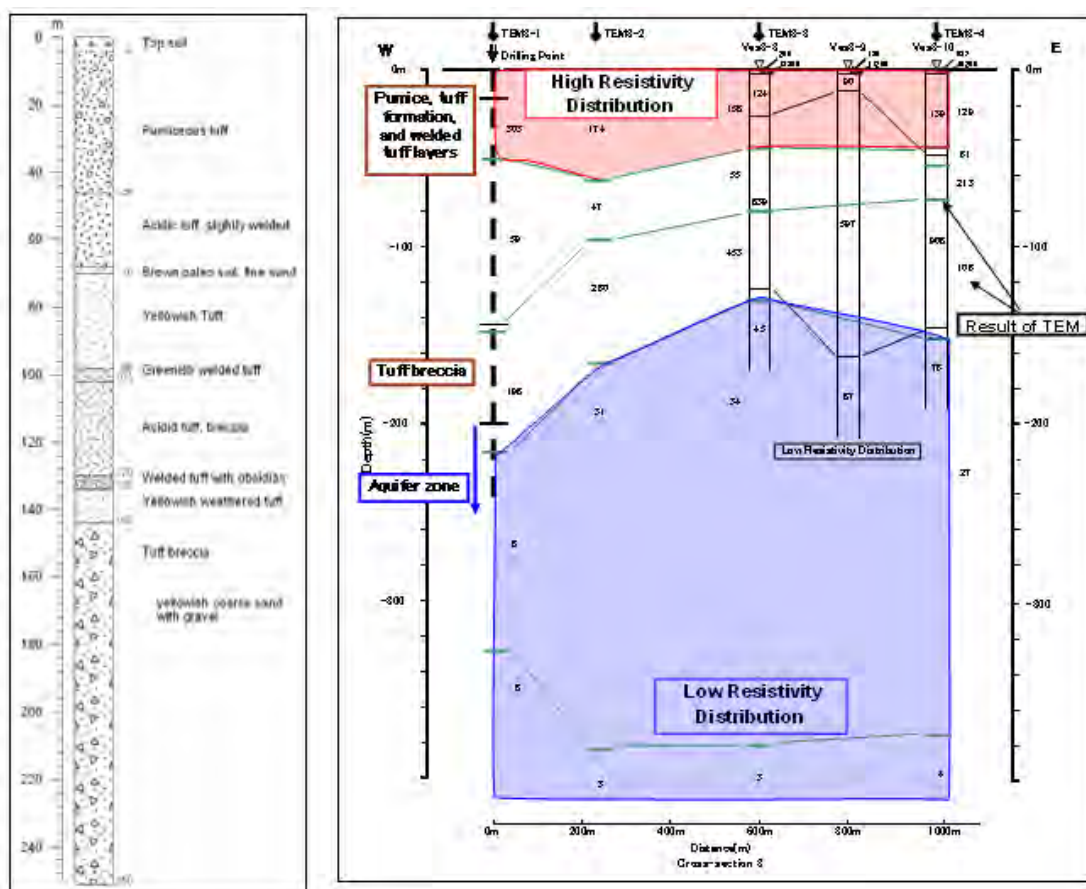
Figure 4.29: Comprehensive Cross-sectional Diagram of the Analysis (BH3)

According to the drilling results, the rock facies of this area consists of pumice, tuff, and welded tuff layers. At around 70m, silt sediments, perhaps from tuff transformed by weathering, were found. Starting at about 140m, there were fragments of volcanic rocks, which were determined to be gravels of unconsolidated to semi-consolidated tuff breccia. In addition, the depth of the aquifer zone was from 200m to the bottom of the borehole (247m).

A comparison with the results of TEM analysis showed that resistivity in the top layers was high, and compared with the pumice, tuff formation, and welded tuff layers, there didn't appear to be any water content. The resistivity of the middle depths was somewhat low, corresponding to the tuff breccia. Furthermore, because resistivity became noticeably lower at

around -200m, and the rocks were pumice, tuff breccia, and gravels of basaltic rock, it became a high-quality aquifer, roughly corresponding with the depth of the aquifer zone.

Therefore, the analytical results of the TEM method were compared with the electric prospecting results of the first year. As a result, it was found that they were somewhat harmonious with the general results of the resistivity structure, and also agreed with the geological conditions determined from the drilling.

c.4 BH10 (Brindar)

This site is in lowland, at an elevation of about 890m located about 35km SW of Konso. There is a stream flowing in the vicinity, which floods when there are heavy rains during the rainy season, and the surrounding area is often inundated. Electric prospecting was conducted in this zone in the first year, and electromagnetic prospecting was conducted to make comparisons with electric prospecting results and to better understand the resistivity data from the deep underground area (see to Data book).
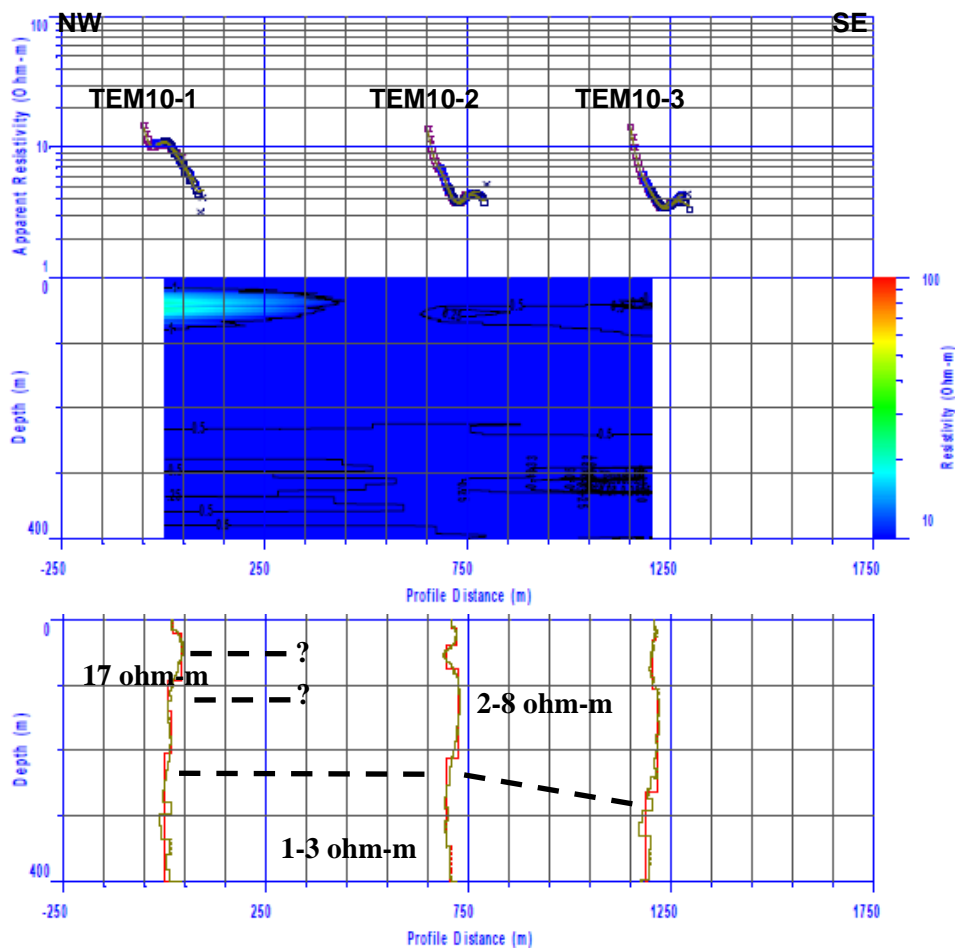
Figure 4.30: Cross-section of Smooth Imaging Resistivity and Layered Structure Analysis (BH-10)

At measuring point TM10-1, there is somewhat high resistivity between 20m and 90m, and while its resistivity structure differs from that of the other two points, there is not a major difference in resistivity values, which generally do not exceed 10ohm-m.

The Study on Groundwater Resources Assessment
in the Rift Valley Lakes Basin in Ethiopia, Final Report (Supporting Report)

JICA
KOKUSAI KOGYO CO., LTD.

This area is covered with alluvial deposits, and the Teltele basalt bedrock is distributed under the surface. The low resistivity from the surface to the deep section is considered to be due to sediments and/or weathered layers, and it appears that there is abundant groundwater here. The somewhat high resistivity of measuring point TM10-1 is believed to be due to the basalt bedrock.

The following Table 4.15 to Table 4.17 show comparisons between the results of electromagnetic and electric prospecting.

Table 4.15: Comparison between the Results of Electromagnetic and Electric Prospecting (BH 10, No.1)

Measurement	Parameter	TEM10-1/VES10-1						
		—	—	L1	L2	L3	L4	L5
T E M	Resistivity (ohm-m)	—	—	6.1	17.6	3.7	5.3	2.3
	Thickness (m)	—	—	21.5	71.4	46.0	66.2	—
	Undersurface depth (m)	—	—	21.5	93.0	139.0	205.1	—
		L1	L2	L3	L4	L5	L6	—
V E S	Resistivity (ohm-m)	2.8	86	2.5	68.0	5.0	14.0	—
	Thickness (m)	0.2	1.4	5.8	28.0	78.0	—	—
	Undersurface depth (m)	0.2	1.6	7.4	35.4	113.4	—	—

∗   The gray section denotes a correlation between the resistivity and undersurface depth.

The results of electromagnetic prospecting show low resistivity down to about 22m below the surface, but from there down to about 93m it is high. Then, from the 3rd layer to the bottom layer, it becomes low again.

A comparison with the results of electric prospecting show low resistivity values for both down to the 3rd layer, but the depth is greater than 10m. Furthermore, while high resistivity was found in lower layers, the results of electromagnetic prospecting were deeper. Each of the high resistivity lower layers tends to decrease in resistivity, but the resistivity values are roughly the same.

Table 4.16: Comparison between the Results of Electromagnetic and Electric Prospecting (BH-10, No. 2)

Measurement	Parameter	TEM10-2/VES10-4						
		—	L1	L2	L3	L4	L5	L6
T E M	Resistivity (ohm-m)	—	3.7	6.5	2.1	8.2	2.0	3.3
	Thickness (m)	—	12.7	25.9	36.4	138.3	134.7	—
	Undersurface depth (m)	—	12.7	38.6	75.0	213.3	348.1	—
		L1	L2	L3	L4	L5	—	—
V E S	Resistivity (ohm-m)	7.1	3.0	9.9	2.8	9.6	—	—
	Thickness (m)	5.3	9.3	18.0	26.0	—	—	—
	Undersurface depth (m)	5.3	14.6	32.6	58.6	—	—	—

∗   The gray section denotes a correlation between the resistivity and undersurface depth.

The results of the electromagnetic prospecting showed a low resistivity that generally did not exceed 10ohm-m. The 4th layer of the analyzed structure showed a somewhat high

relative resistivity.

As with the electric prospecting results, resistivity was 10ohm-m or less, and while there were some differences seen in the bottom parts of layers the resistivity and lower boundary depths showed good agreement.

Table 4.17: Comparison between the Results of Electromagnetic and Electric Prospecting (BH-10, No. 3)

Measurement	Parameter	TEM10-3/VES10-8						
		−	−	L1	L2	L3	L4	L5
T E M	Resistivity (ohm-m)	−	−	3.8	4.6	2.7	5.6	1.3
	Thickness (m)	−	−	13.3	18.7	73.7	157.3	−
	Undersurface depth (m)	−	−	13.3	31.9	105.6	262.9	−
		L1	L2	−	L3	L4	L5	−
V E S	Resistivity (ohm-m)	14.0	1.4	−	7.8	2.6	1010	−
	Thickness (m)	3.1	3.5	−	20.0	100.0	−	−
	Undersurface depth (m)	3.1	6.6	−	26.6	126.6	−	−

＊   The gray section denotes a correlation between the resistivity and undersurface depth.

The results of electromagnetic prospecting at this measuring point also were showed a low resistivity of 10ohm-m or less.

A comparison with the results of electric prospecting shows similarly low values for resistivity and the depths of bottom sides of layers also coincide with one another. However, the resistivity of the 4th layer in the electric prospecting is a remarkably high 100ohm-m, which is different from the value from the electromagnetic prospecting.

The Study on Groundwater Resources Assessment
in the Rift Valley Lakes Basin in Ethiopia, Final Report (Supporting Report)

JICA
KOKUSAI KOGYO CO., LTD.
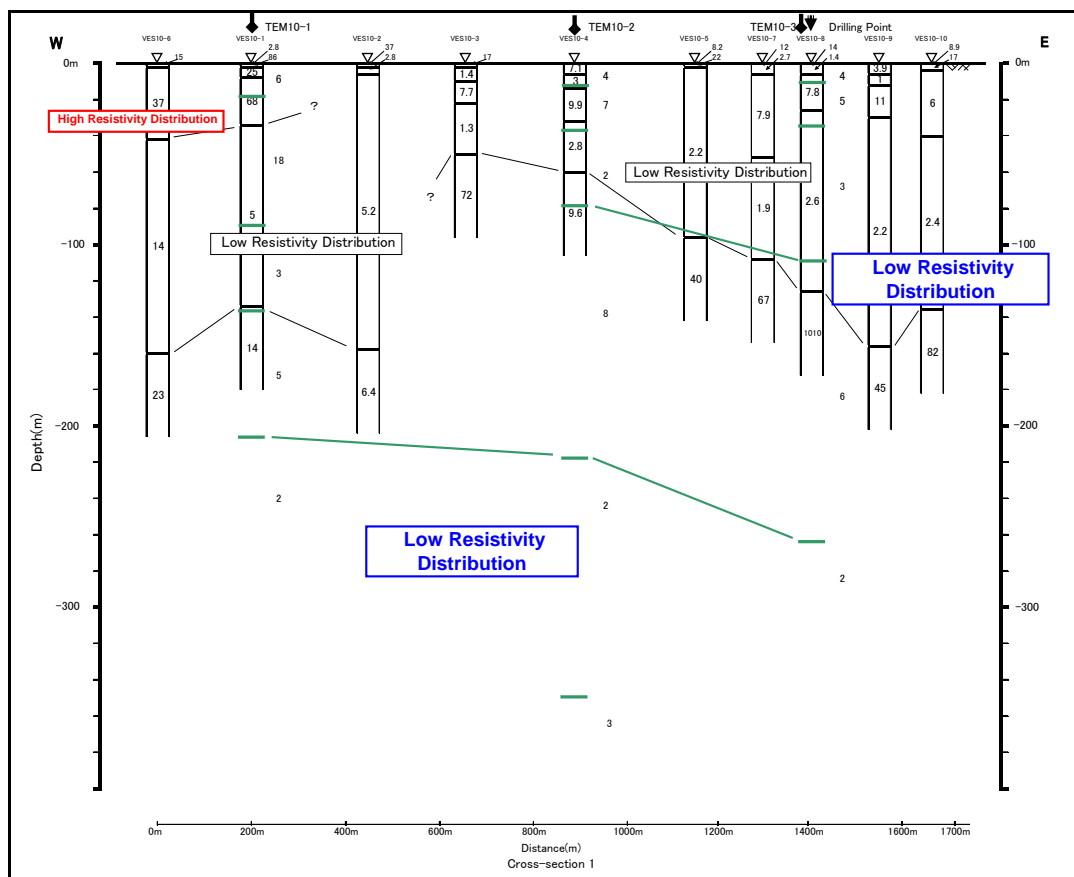
Figure 4.31: Comprehensive Cross-sectional Diagram of the Analysis（BH-10）

The above Figure 4.31 is a juxtaposition of the results of the electric and electromagnetic prospecting. Except for the high resistivity that was found in the top layer by the results of electrical prospecting (on the west side of the diagram), there are no major differences in resistivity, which was generally 10ohm-m or less. Regarding trends in the structure, from the surface down to a depth of about 100m, there was low resistivity, which increased somewhat below that until about 200m below the surface, where it decreased remarkably.

The Teltele basalt formation underlies this region, and the low resistivity from the surface down to the deep layers is believed to correspond to sediments and/or weathered layers which show high potential for the existence of groundwater. In addition, the somewhat high resistivity at measuring sites VES10-6 and TEM10-1 on the west side of the cross sections to be due to the basaltic base rock.

c.5 Tora (Meded Gagebo/Anshebeso Kuchi)

Electromagnetic prospecting was conducted at this point to acquire data for creating a longitudinal geological map. The study area is a plain lying at 1,880m above seal level about 35km south of Butajira and about 20km NW of Lake Abija. According to the geological map, it is easily flooded, and the surrounding area is dotted with numerous small lakes and water wells or water holes.

In addition, there are existing wells in Tora, about 10km to the NE of this area, and we were able to obtain columnar sections of the geology. Here, we report on the results of comparisons between the electromagnetic prospecting results and the geological columnar

sections. It should be noted that there were 3 TEM measuring points (see to Data book).
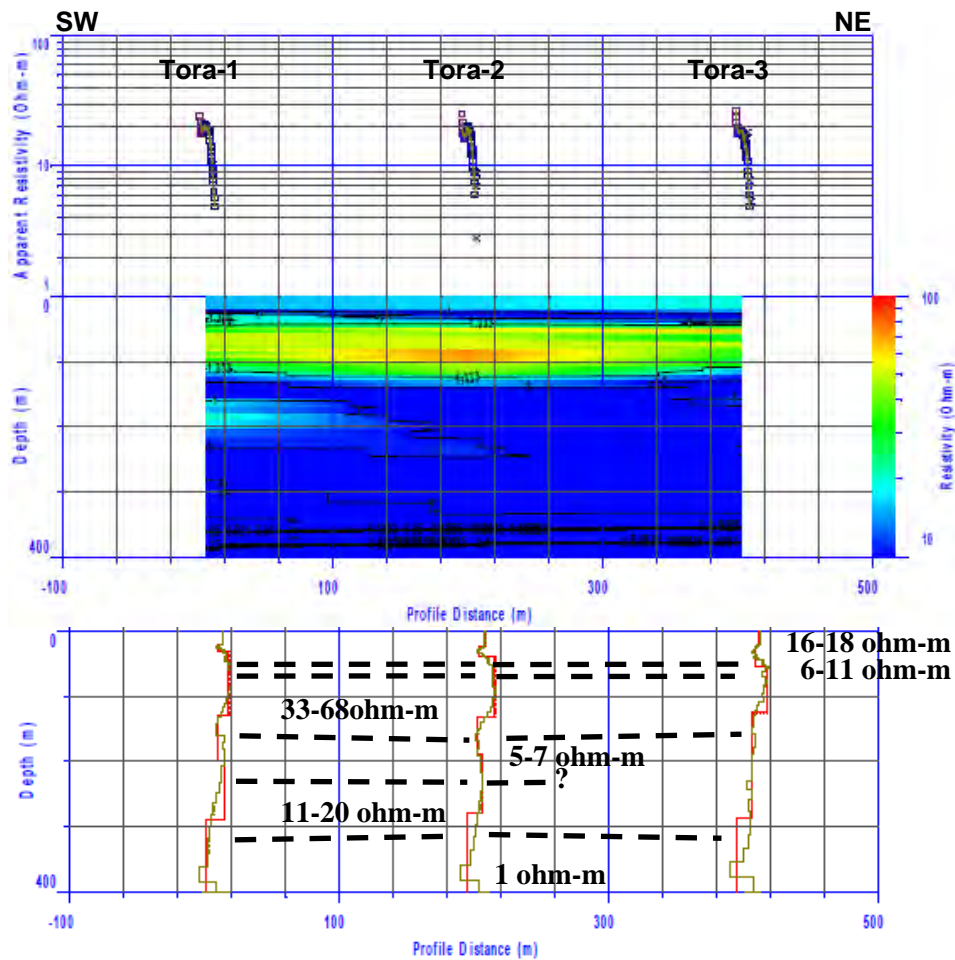
Figure 4.32: Cross-section of Smooth Imaging Resistivity and Layered Structure
Analysis (Tora area)

The resistivity structure of this area shows 5-6 layers, which show a continuous pattern of low-high-low resistivity. About 30m to130m below the surface, a somewhat high resistivity of 33ohm-m to 68ohm-m was found. In addition, there were no areas of noncontiguous resistivity found in the structure between measuring points.
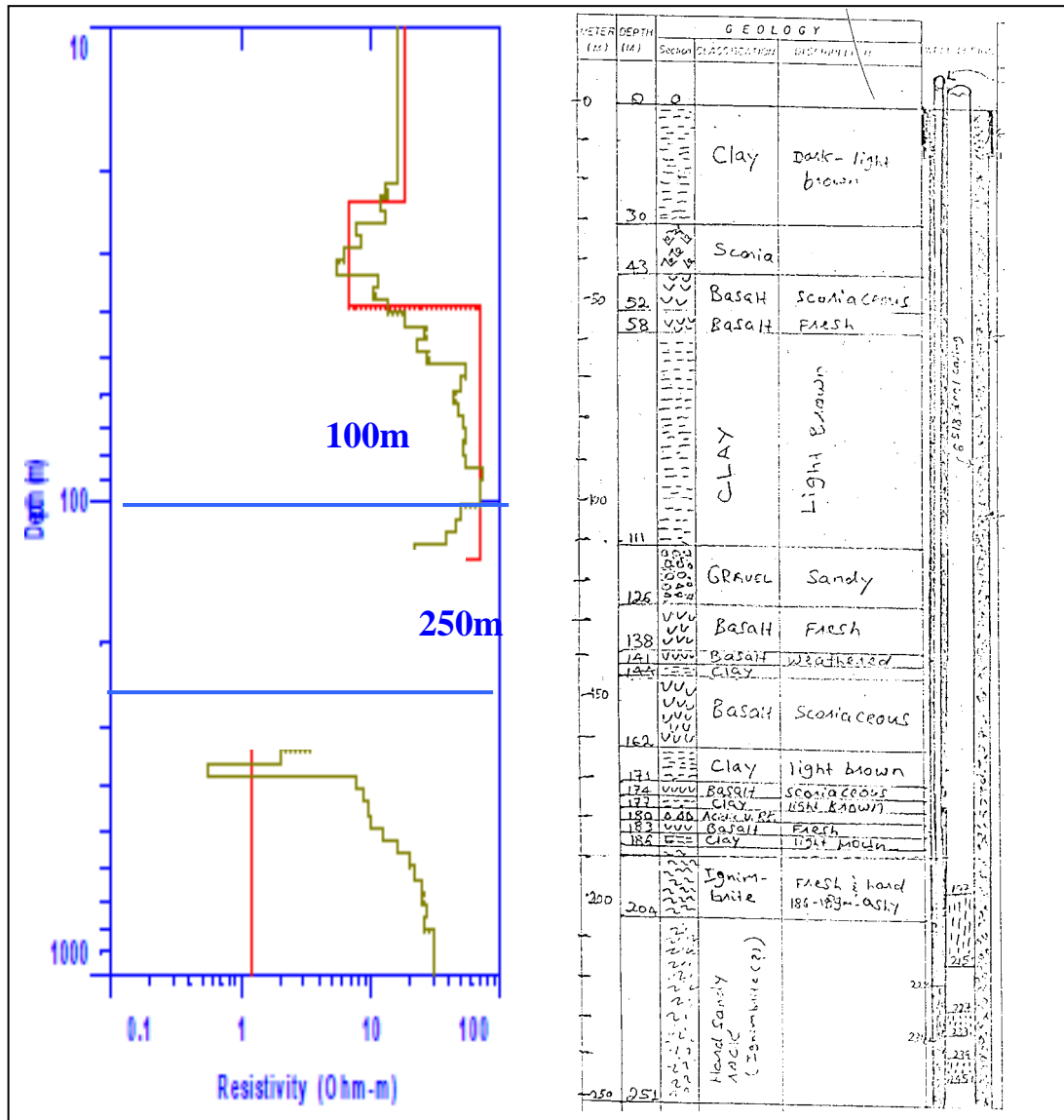
Figure 4.33: Comparison with the Analysis and the Geological Columnar Section

The geological columnar section is located in the distributed area of Recent Basalt. The geology of the electromagnetic survey points are not able to correlate with the columnar section in judgment of geological map. The geology of columnar section consists of, from surface, Recent Basalt up to 138m in depth, below that, at a depth of 138m-186m are layers of poorly welded tuff or pyroclastics (so called "White"). Between 186m and 204m is strongly welded tuff, and between 204m and 251m is rhyolite. SWL is 189.1m.

The results of electromagnetic prospecting showed low resistivity down to 40m below the surface, high resistivity between 40m and 130m, and remarkably low resistivity from about 130m to about 280m.

In terms of geology, the low resistivity of the upper layers corresponds to the pyroclastics (so called "White"), the high resistivity is not divided completely, but may correlate with the strongly welded tuff or rhyolite. The aquifer may exist in this welded tuff below, but is not able to decide because it is difficult with comparing between electromagnetic data and the columnar section.

c.6   Yirgachefe (Budukisa/Worago)

At this site, electromagnetic prospecting was conducted to obtain data for the creation of a geological longitudinal map. The site is located at an elevation of 1,870m in a coffee plantation in highly undulating terrain about 4km north of the center of Yirgachefe. There were 3 TEM measuring points (see to Data book).
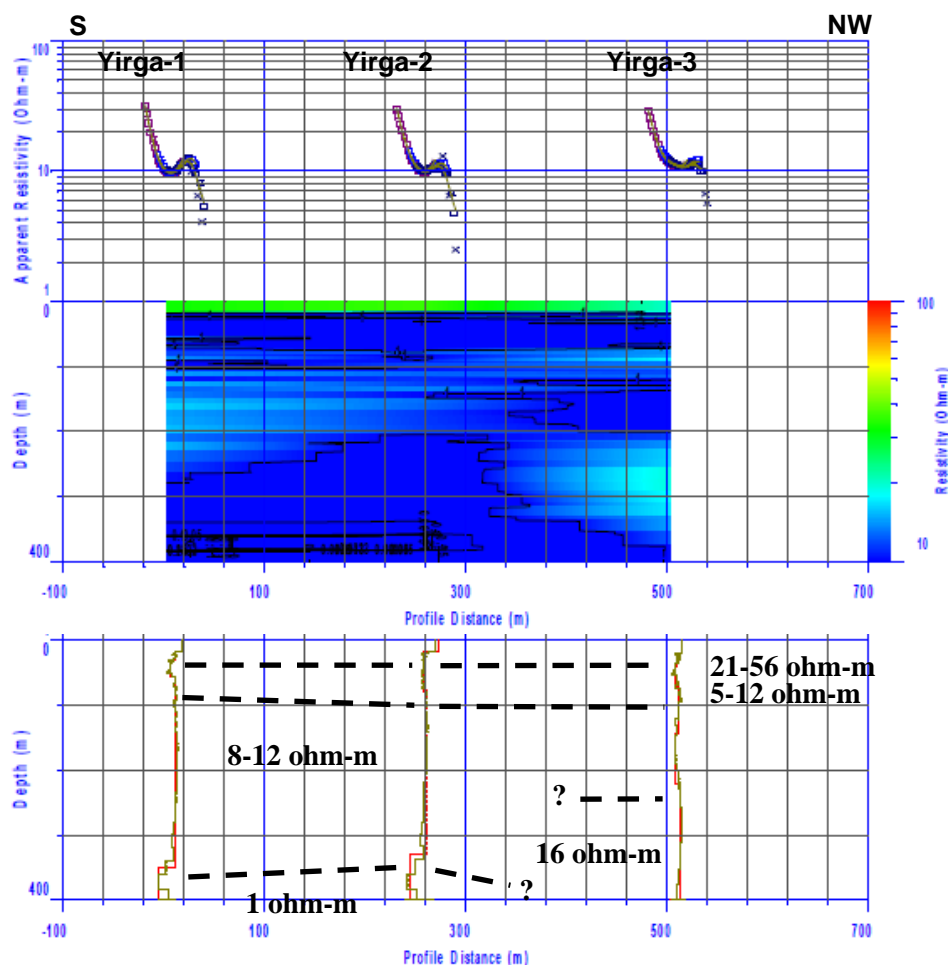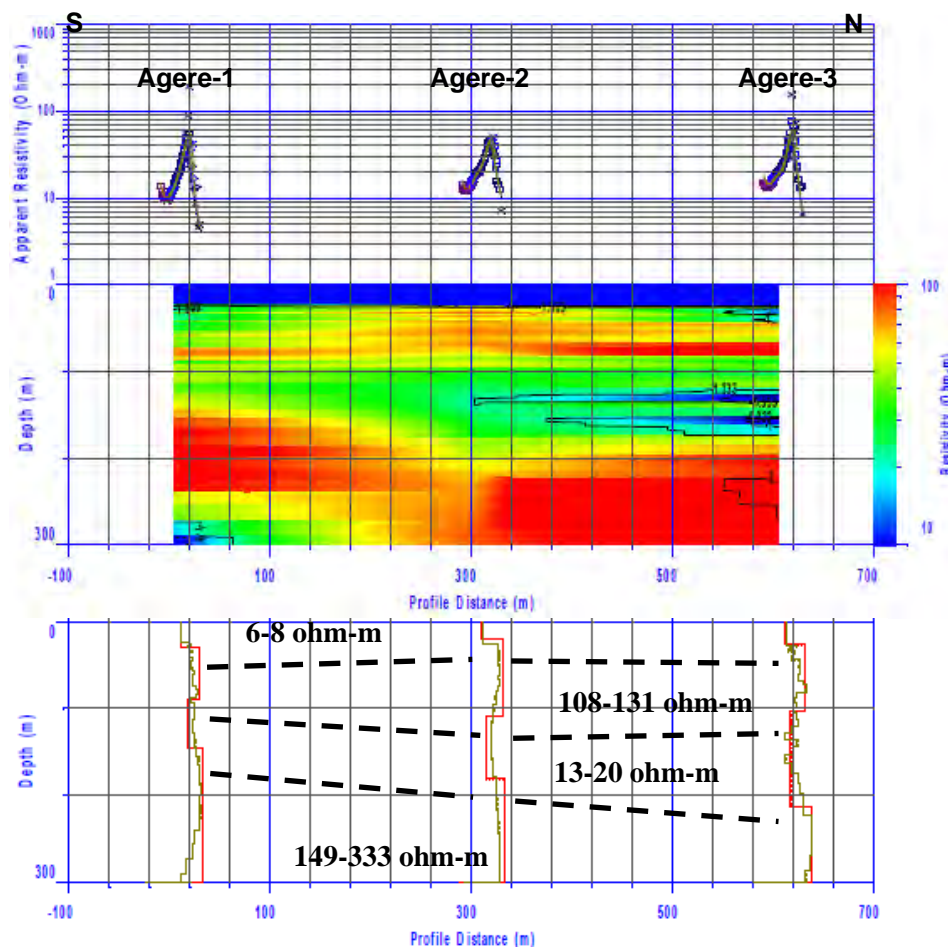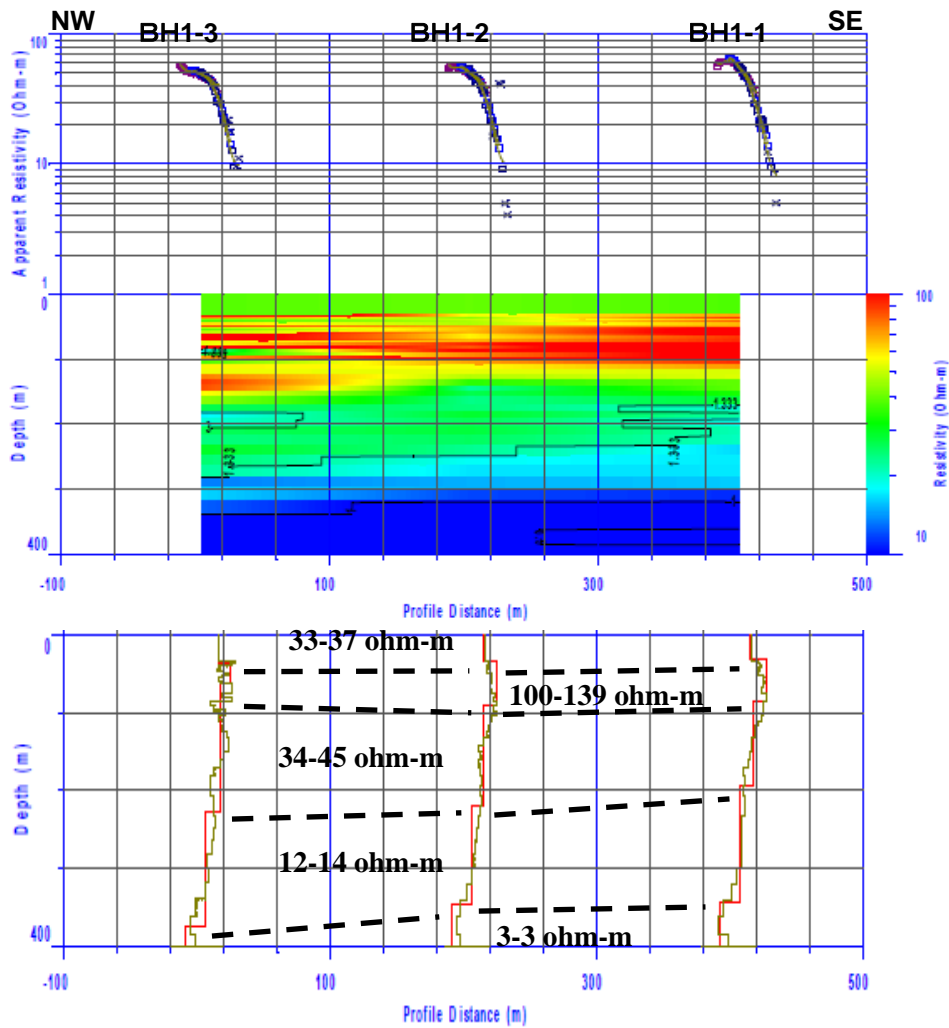

Figure 4.34: Cross-section of Smooth Imaging Resistivity and Layered Structure analysis (Yirgachefe area)

The resistivity structure at this site shows 4 layers, which show high-low-remarkably low resistivity from the surface downwards. However, somewhat high resistivity was found at -220m at measuring point Yirga-3.

The geology of this area consists of lacustrine sediments of rhyolite, trachyte, tuff and basalt dating from the Oligocene to the Miocene with distributions of PNv and/or Pv. This area is covered by thick lacustrine sediments, and there are several fault groups that have developed along an N-S axis. Due to the extensive faulting, weathered rhyolite, fissure water, etc., have penetrated deep underground, and the resistivity appears to be low.

c.7   Agere Maryam (Bule Kagna)

At this site, electromagnetic prospecting was conducted to obtain data for the creation of a geological longitudinal map. The site, which is surrounded by hills, is located at an elevation of 1,760m about 5km west of Agere Maryam. TEM measurements were taken at 3 points that were spaced 300m apart (see to Data book).

The Study on Groundwater Resources Assessment
in the Rift Valley Lakes Basin in Ethiopia, Final Report (Supporting Report)

JICA
KOKUSAI KOGYO CO., LTD.

Figure 4.35: Cross-section of Smooth Imaging Resistivity and Layered Structure
Analysis (Agere Maryam area)

Unlike the resistivity structures that have been described so far, this is an area where resistivity is high. While there is low resistivity from the surface down to 30m and between 100m and 200m, other layers tend to show high resistivity.

Note: There were many anomalies in the L frequency measurement data acquired from this region, which made precise depth analysis difficult. Accordingly, the depth was assessed to be 300 meters.

The geology in this area consists of lacustrine Pv sediments from the Oligocene to Miocene. In the middle of this is a narrow Qa alluvial area from the Holocene.

The surface layer is composed of deposits of sand, mud, gravel, etc. and from the surface down to about 100m is basalt rock that does not contain groundwater. However, the low resistivity from about -100m to -200m seems to indicate basalt that is saturated with groundwater.

d.   SNNPRS

d.1   BH-1 (Abaya Chokane)

This area is located at an elevation of about 1,240m above sea level in a forested region about 3km from the northern shore of Lake Abaya. There appears to be about a 10m difference in relief between the lake and the site (see to Data book).

The results of electromagnetic prospecting are shown below.

Figure 4.36: Cross-section of Smooth Imaging Resistivity and Layered Structure Analysis (BH-1)

The relative resistivity structure of this site shows 5 layers, with values of medium-high-medium-low in descending order. The surface layer, which is 30m thick, has a resistivity of 40ohm-m or less, while the layer below that has high resistivity and continues to about 90m below the surface. From there to about 200m below the surface, the resistivity is 40ohm-m more or less. Below that, down to a depth of 350m, the resistivity decreases, and becomes remarkably low in the bottom layer.

Table 4.18 shows the results of electric prospecting analysis conducted in the 1st year, and the recently conducted electromagnetic prospecting analysis. There is also a comparison with the geology derived from the drilling results. It should be noted that measuring point TEM1-2 lies in-between points VES1-3 and VES1-2, so there is no comparison with their results and TEM1-2.

Table 4.18: Comparison between the Results of Electric and Electromagnetic
Prospecting Analyses (BH-1, No. 1)

Measurement	Parameter	TEM1-3/VES1-4					
		—	L1	L2	L3	L4	L5
TEM	Resistivity (ohm-m)	—	37.5	100.8	42.1	11.5	2.1
	Thickness (m)	—	37.7	24.1	166	148.5	—
	Undersurface depth (m)	—	37.7	61.8	228	376	—
		L1	L2	L3	L4	—	—
VES	Resistivity (ohm-m)	34	17	291	48	—	—
	Thickness (m)	6.9	5.6	31	—	—	—
	Undersurface depth (m)	6.9	12.5	43.5	—	—	—
Geologic column (150m)		—	pumice→welded tuff→Rhyolite			—	—

＊   The gray section denotes a correlation between the resistivity and undersurface depth.

The electromagnetic results show that except for an area of high resistivity that exists in Layer 2, 38m to 62m below the surface, resistivity of each layer is low. Particularly low resistivity is found around 380m below the surface.

In contrast, the results of electric prospecting show high resistivity within a range of 13m to 44m below the surface, while the electromagnetic results indicated it went deeper. However, both sets of data showed roughly the same values for the low resistivity area below this area of high resistivity.

According to the drilling results, the rock facies of this area consists of a pumice layer down to about -42m, with a welded tuff layer below that, and starting at about -126m beneath that there appears to be a hard rhyolite layer. Between 10m and 60m below the surface, there are confirmed layers of pumice-rich volcanic ash, gravel and welded tuff. In addition, the aquifer zone has been determined to be between -67m and -130m.

In terms of geology, the areas of high resistivity indicate a volcanic ash layer, pumice layer and welded tuff layer which do not appear to contain water. The area of low resistivity below that appears to be comprised of welded tuff that formed in fissures and a rhyolite layer. Furthermore, the aquifer zone has been determined to start at -67m, and this roughly agrees with the bottom depth of the high resistivity area in the electromagnetic prospecting.

Table 4.19: Comparison between the Results of Electric and Electromagnetic
Prospecting Analyses (BH-1, No.2)

Measurement	Parameter	TEM1-1/VES1-6(Near the drilling site)					
		—	L1	L2	L3	L4	L5
TEM	Resistivity (ohm-m)	—	33.2	139.0	45.4	13.6	2.6
	Thickness (m)	—	30.4	56.2	107	151	—
	Undersurface depth (m)	—	30.4	86.8	194	345	—
		L1	L2	L3	L4	—	—
VES	Resistivity (ohm-m)	62	10	1330	17	—	—

	Thickness (m)	0.5	8.0	53	–	–	–
	Undersurface depth (m)	0.5	8.5	61.5	–	–	–
Geologic column (150m)	–	pumic→welded tuff→Ryolite				–	–

＊ The gray section denotes a correlation between the resistivity and undersurface depth.

The results of electromagnetic prospecting resemble the resistivity structure shown in Table 4.19. The depth of the bottom of the high resistivity layer No.2 is deepest at measuring point TEM1-1, and the depth of the aquifer zone is about 20m, starting at -67m.
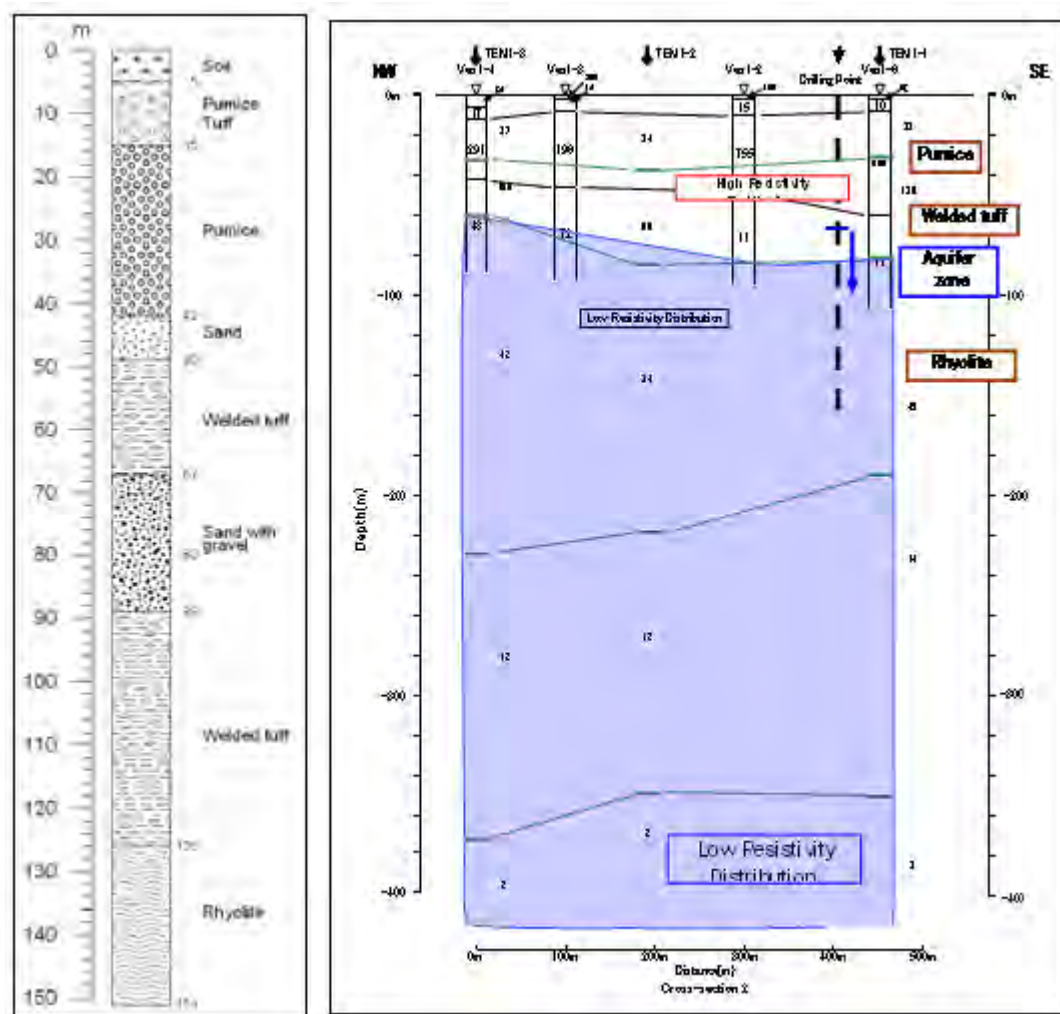
Figure 4.37: Comprehensive Cross-sectional Diagram of the Analysis（BH-1）

Figure 4.37 is a cross section of the comprehensive analysis of BH-1.

The depth of the bottom part of the high resistivity area is about -62m to -87m, while that for the electric prospecting is 44m to 62m. This is roughly the same as the general aquifer zone of -67m.

In terms of geology, the area of high resistivity in the top layer down to about -90m consists of a volcanic ash layer, gravel, and a welded tuff layer, and does not appear to

contain water. The resistivity in the layer below that is low and corresponds to a gravel layer, welded tuff that appears to have developed fissures, and a rhyolite layer, and is at roughly the depth of the aquifer zone.

Therefore, the resistivity structure of the electromagnetic prospecting roughly agrees with that of the electric prospecting, and it also conforms with the geological conditions determined from the drilling results.

d.2   BH-6 (Yeye Alaba/Lajo)

This site is located in a farming area about 35km west of Shashemane (see to Data book). Electrical prospecting was conducted in the 1st year, and plans call for drilling as well, which would be to a depth of 400m. There are 3 measuring points for the electromagnetic prospecting, but this site was a training site for the EWTEC groundwater survey short course, so the measurement data that were obtained through participation in the course were also analyzed. The following is a description of the resistivity structure of the three measuring points.
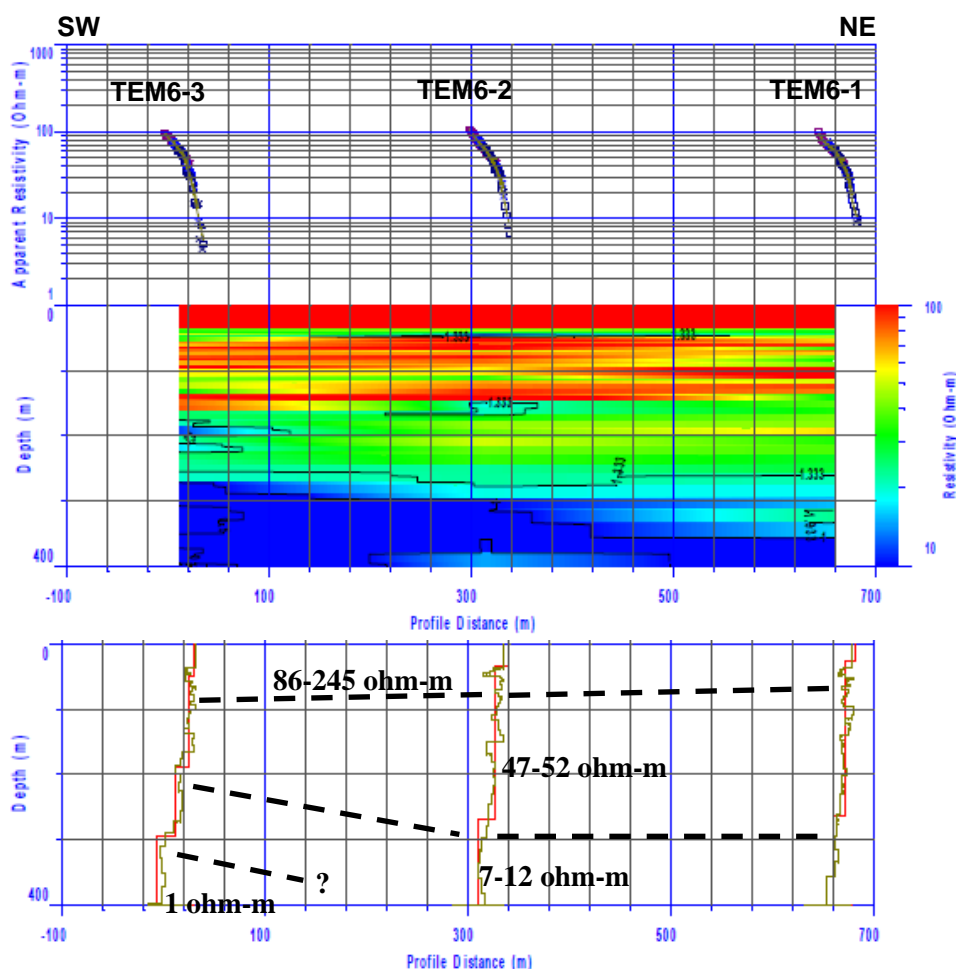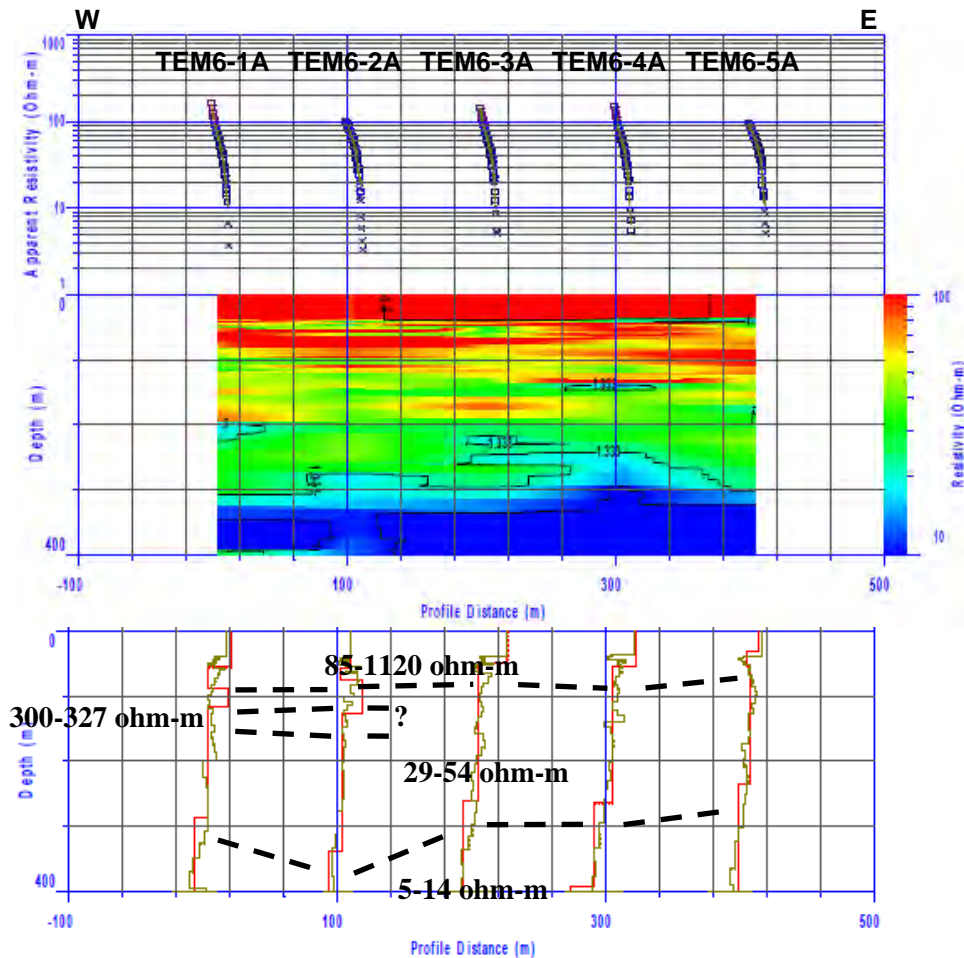

Figure 4.38: Cross-section of Smooth Imaging Resistivity and Layered Structure Analysis (BH-6 line 1)

The resistivity of this profile is 3-4 layers. A shallow area below the surface shows a high resistivity at a depth of 200m – 300m. Layer below 300m in depth show low resistivity, especially at TEM6-3, where it decreases dramatically at around -300m.

The geology of the study area is Quaternary consisting of Qdp belonging to Dino of the Wonji Group. There is wide distribution of coarse, pumice-like pyroclastic materials. The high-to-medium resistivity at 200m and deeper below the surface may be due to weathered pyroclastic materials and/or the existence of crushed rock. In addition, there is a deep (360m) water well 3km SW of the site and the SWL is 273m, so it appears that the low resistance of the bottom layer would indicate that it is saturated with groundwater.

The following charts show the analytical results of electromagnetic prospecting That EWTEC conducted during the training course.

Figure 4.39: Cross-section of Smooth Imaging Resistivity and Layered Structure Analysis (BH-6 line 2)

The measuring points in this profile, TEM6-1A and TEM6-2A, each have a 5-layered structure with a 30-50m thick layer of high resistivity at around 100m below the ground surface. The other measuring point shows a 3-layered structure which generally is similar to the low resistivity structure described earlier.

The following chart shows a comparison between the results of the electromagnetic (TEM) and electric (VES) prospecting.

The Study on Groundwater Resources Assessment
in the Rift Valley Lakes Basin in Ethiopia, Final Report (Supporting Report)

JICA
KOKUSAI KOGYO CO., LTD.

Table 4.20: Comparison between TEM and VES results（BH6 No1）

Measurement	Parameter	TEM6-3/VES6-8						
		—	—	L1	L2	L3	L4	—
TEM	Resistivity (ohm-m)	—	—	85.9	52.1	10.8	1.4	—
	Thickness (m)	—	—	48.8	139.7	106.9	—	—
	Undersurface depth (m)	—	—	48.8	188.4	295.4	—	—
		L1	L2	L3	L4	L5	—	—
VES	Resistivity (ohm-m)	393.0	33.0	410.0	256.0	48.0	—	—
	Thickness (m)	1.2	2.4	18.0	243.0	—	—	—
	Undersurface depth (m)	1.2	3.6	21.6	264.6	—	—	—

＊   The gray section denotes a correlation between the resistivity and undersurface depth.

The resistivity in the 1st layer of the TEM is high, but in lower layers it gradually decreases. On the other hand, the VES showed a thin layer of low resistivity in the 2nd layer, but overall the resistivity was high in the 1st through 3rd layers. While the trend was similar to that of the TEM, the depth was shallower. While resistivity is still high in the 4th layer, it is lower than that of the 3rd layer, and it decreases even further below the 4th layer.

A comparison of the results of the two prospecting methods shows a large difference between the low resistivity of the 4th layer in the TEM and the 5th layer of the VES, but the depths roughly coincide with one another.

Table 4.21: Comparison between TEM and VES Results（BH-6, No2）

Measurement	Parameter	TEM6-2/VES6-3						
		—	—	L1	L2	L3	—	—
TEM	Resistivity (ohm-m)	—	—	245.1	46.5	7.3	—	—
	Thickness (m)	—	—	34.0	235.5	—	—	—
	Undersurface depth (m)	—	—	34.0	269.5	—	—	—
		L1	L2	L3	L4	L5	—	—
VES	Resistivity (ohm-m)	218.0	29.0	191.0	256.0	57.0	—	—
	Thickness (m)	1.2	2.2	45.0	226.0	—	—	—
	Undersurface depth (m)	1.2	3.4	48.4	274.4	—	—	—

＊   The gray section denotes a correlation between the resistivity and undersurface depth.

At this measuring point as well, the resistivity in the 1st layer is high, but decreases below that.

In the VES, a thin layer of low resistivity was found in the 2nd layer, but except for this section the resistivity was high from the surface down to the 4th layer, continuing to a depth of about -270m. However, resistivity decreased at depths below that.

A comparison of the two sets of results shows some differences in the stratification of the respective resistivity structures, but in both cases, the bottommost layer has low resistivity, and it is about at the same depth.

Table 4.22: Comparison between TEM and VES Results（BH-6, No3）

Measurement	Parameter	TEM6-1/VES6-7						
		—	—	L1	L2	L3	—	—
T E M	Resistivity (ohm-m)	—	—	157.0	50.1	12.3	—	—
	Thickness (m)	—	—	26.9	238.1	—	—	—
	Undersurface depth (m)	—	—	26.9	265.0	—	—	—
		L1	L2	L3	L4	L5	—	—
V E S	Resistivity (ohm-m)	185	29.0	386.0	244.0	59.0	—	—
	Thickness (m)	1.8	2.7	22.0	197.0	—	—	—
	Undersurface depth (m)	1.8	4.5	26.5	223.5	—	—	—

　＊　The gray section denotes a correlation between the resistivity and undersurface depth.

At this measuring point as well, there is a rough similarity with the other resistivity structures discussed so far, and the depths of the high RR of the TEM and VES, as well as the depths of the low resistivity of the bottommost layer, are about the same.

The following longitudinal diagram depicts the results of both the TEM and VES analyses.
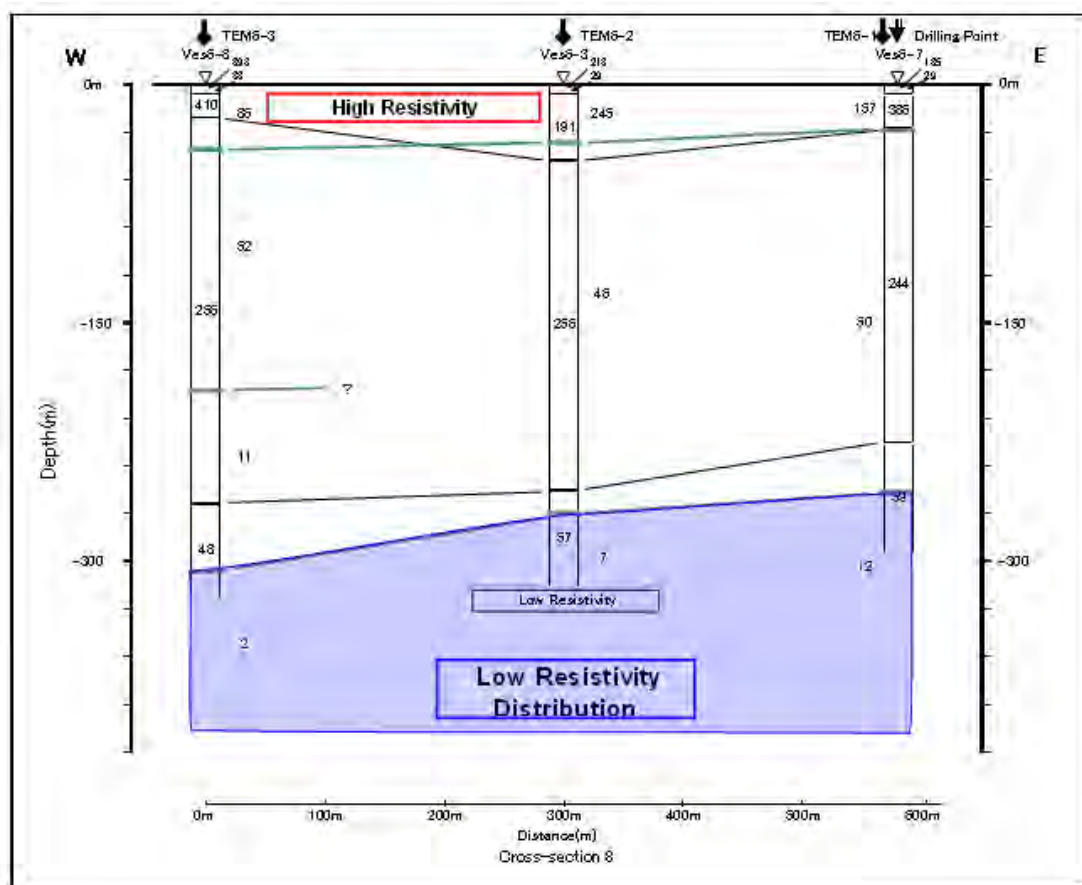
Figure 4.40: Comprehensive Cross-sectional Diagram of the Analysis（BH-6）

The resistivity structure has roughly 3 layers, with high resistivity of 80ohm-m or greater down to a depth of 50m; low resistivity of 50ohm-m from -50m down to about -260m, and a

very low resistivity of 10ohm-m or less from -260m to -300m. The depth of this low resistivity roughly coincides with the depth of a water well SWL273m to the southwest of this site.

The geology of the study area is Quaternary consisting of Qdp belonging to Dino of the Wonji Group. There is deposition of coarse, pumice-like pyroclastic materials. The high-to-medium resistivity at 200m and deeper below the surface may correspond to weathered pyroclastic materials and/or crushed rock.

d.3   BH-7 (Weze / Hare)

This site is at an elevation of 1,200m in a farming area facing Arbaminch University. Vertical electric sounding (VES) was conducted in the 1st year, and plans call for drilling (down to a depth of 200m) in this area. There were 3 TEM measuring points here (see to Data book)
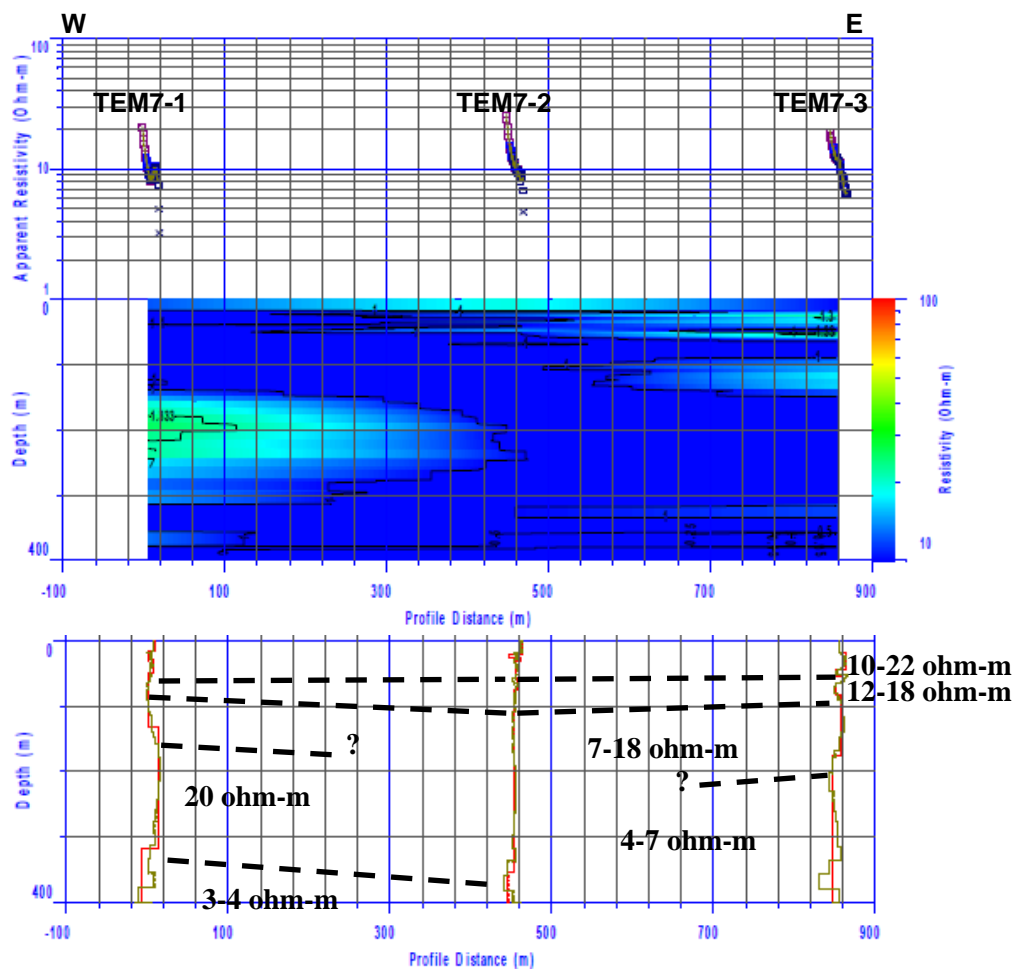
Figure 4.41: Cross-section of Smooth Imaging resistivity and layered structure analysis (BH-7)

The resistivity structure of this site has 5 general layers. The resistivity of the surface is 10ohm-m or less, and below that it decreases somewhat until it becomes remarkably low in

The Study on Groundwater Resources Assessment
in the Rift Valley Lakes Basin in Ethiopia, Final Report (Supporting Report)

JICA
KOKUSAI KOGYO CO., LTD.

the bottom layer. At a depth of 130m-320m at measuring point TEM7-1, the resistivity is a somewhat high 20ohm-m.

The geology of this area is Holocene Q1 consisting of lacustrine sediments, as well as sandy, silty and pyroclastic sediments. Because these sediments are considered to be loosely consolidated geology, they may easily contain a sufficient amount of groundwater, and the resistivity may be low due to saturation by groundwater.

The following is a comparison between the results of TEM and VES.

Table 4.23: Comparison between TEM and VES Results（BH-7 No1）

Measurement	Parameter	TEM7-1/VES7-5						
		—	L1	L2	L3	L4	L5	L6
TEM	Resistivity (ohm-m)	—	13.3	6.4	12.3	6.2	20.3	3.0
	Thickness (m)	—	16.7	13.5	18.2	84.7	185.3	—
	Undersurface depth (m)	—	16.7	30.2	48.4	133.1	318.5	—
		L1	L2	L3	L4	L5	L6	—
VES	Resistivity (ohm-m)	13.0	36.0	7.5	38.0	4.9	17	—
	Thickness (m)	1.4	2.7	6.7	20.0	70.0	—	—
	Undersurface depth (m)	1.4	4.1	10.8	30.8	100.8	—	—

＊　The gray section denotes a correlation between the resistivity and undersurface depth.

The TEM showed a resistivity structure that repeatedly cycled from high to low from the ground surface, and, while the VES starts with low resistivity, it shows the same sort of repeating resistivity structure. A comparison with each of these resistivity layers and depth shows that down to about -30m, depths and resistivity values are different, but in lower layers, both RR values and depth apparently coincide with one another. There was particular correlation between the resistivity values and depth readings in layer four of the electromagnetic survey and layer five of the electric survey, and between the resistivity values in layer five of the electromagnetic survey and layer six of the electric survey.

Table 4.24: Comparison between TEM and VES Results（BH-7, No2）

Measurement	Parameter	TEM7-2/VES7-6						
		L1	L2	L3	L4	L5	L6	L7
TEM	Resistivity (ohm-m)	20.7	4.4	17.7	10.0	10.6	7.7	4.0
	Thickness (m)	21.7	4.6	5.3	24.8	18.2	280.5	—
	Undersurface depth (m)	21.7	26.4	31.7	56.5	74.7	355.2	—
		L1	L2	L3	L4	L5	—	—
VES	Resistivity (ohm-m)	6.3	88.0	4.6	27.0	11.0	—	—
	Thickness (m)	1.3	18.0	18.0	63.0	—	—	—
	Undersurface depth (m)	1.3	19.3	37.3	100.3	—	—	—

＊　The gray section denotes a correlation between the resistivity and undersurface depth.

The TEM showed a resistivity structure that repeatedly cycled from high to low and back to high from the ground surface down to 30m, but below this is a low resistivity of 10ohm-m, and a remarkably low resistivity in the bottom layer. The VES also showed a repeating

resistivity structure.

A comparison of the two sets of results suggests that the layers from No. 3 to the bottom of the TEM correspond to the layers from No. 4 downward in the VES, but it is difficult to make a clear comparison. However, the low resistivity layers (No. 6 in the TEM and No. 5 in the VES) are both considered to be the depth of the low resistivity boundary.

Table 4.25: Comparison between TEM and VES Results（BH-7, No3）

Measurement	Parameter	TEM7-3/VES7-7						
		L1	L2	L3	L4	L5	L6	L7
TEM	Resistivity (ohm-m)	9.6	21.9	6.8	15.3	6.7	11.8	4.1
	Thickness (m)	19.3	23.8	10.3	11.6	18.0	92.3	—
	Undersurface depth (m)	19.3	43.1	53.4	65.0	83.0	175.4	—
		L1	L2	L3	L4	L5	—	—
VES	Resistivity (ohm-m)	9.4	167	1.1	64	1.3	—	—
	Thickness (m)	12.0	6.8	18.0	73.0	—	—	—
	Undersurface depth (m)	12.0	18.8	36.8	109.8	—	—	—

＊ The gray section denotes a correlation between the resistivity and undersurface depth.

The resistivity structure of the TEM repeatedly cycles from low to high, but it becomes remarkably low in the bottom layer (No. 7). The VES also shows a cyclical pattern of low to high, and resistivity is particularly low in the No. 5 layer. A comparison of the respective analytical results shows many cases where depths and values of resistivity do not coincide with one another, but it appears at least that the depth of low resistivity in layer No. 5 of the TEM and in layer No. 5 of the VES are identical.

The following longitudinal diagram shows the analytical results of both the TEM and VES.
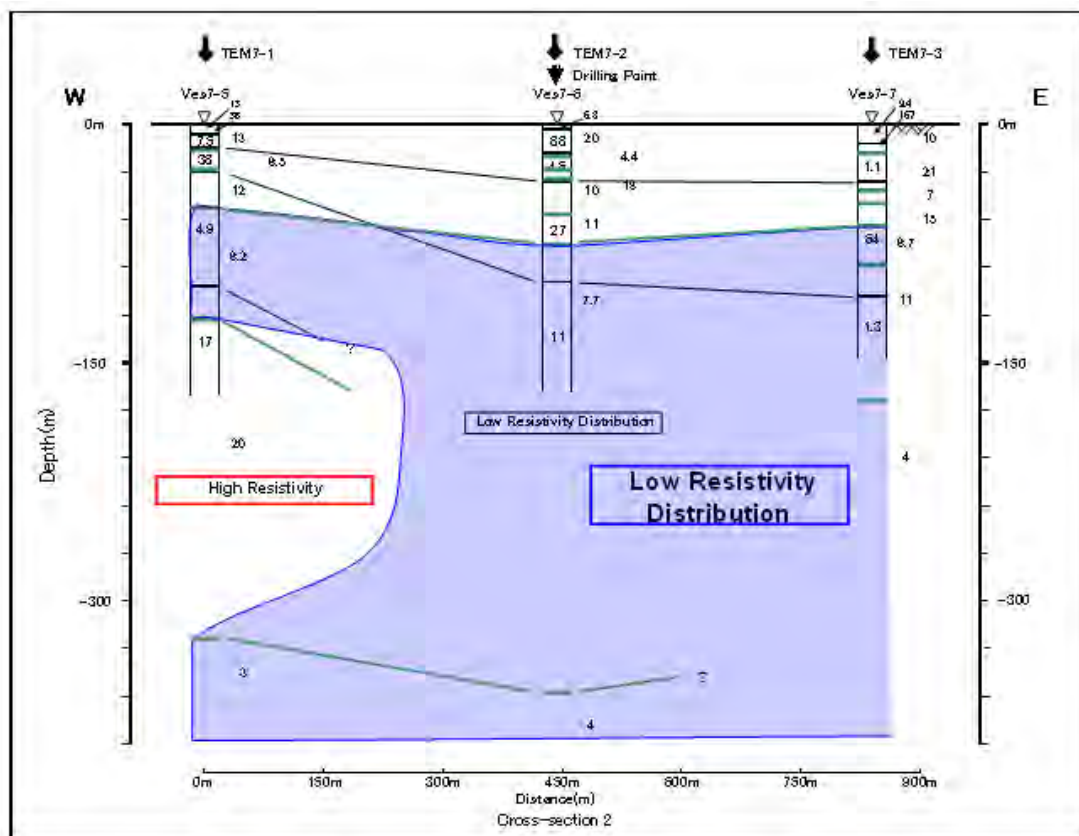
Figure 4.42: Comprehensive Cross-sectional Diagram of the Analysis（BH-7）

From the ground surface to -60m, the resistivity structure can be divided into 4 or 5 layers which repeat a cycle of high-low-high. In the shallow layer just below the surface, there are some differences in depth and resistivity values, but there are no major differences. In addition, low resistivity has been found in a section 60-90m below the surface. There is a close correspondence in resistivity values and boundary depths between -120m at electromagnetic measuring point TEM7-1, and around -115m at electric measuring point VES7-5.

The geology of this area is Holocene Q1 consisting of accumulations of lacustrine sediments, as well as sandy, silty and pyroclastic sediments. The low resistivity that extends from -60m downwards indicates that groundwater may be permeated through these sediments and that resistivity becomes low when there is groundwater saturation.

d.4　　BH-8 (Walesa / Kolta)

This site is located at an elevation of approximately 1,150m about 40km south of Arbaminch and 3km from the southern shore of Lake Abaya. The difference in relief between the site and the lake is apparently a few tens of meters. Electric prospecting was conducted here in the first year, and plans call for drilling down to a depth of 200m. There were 3 TEM measuring points (see to Data book).

The Study on Groundwater Resources Assessment
in the Rift Valley Lakes Basin in Ethiopia, Final Report (Supporting Report)

JICA
KOKUSAI KOGYO CO., LTD.
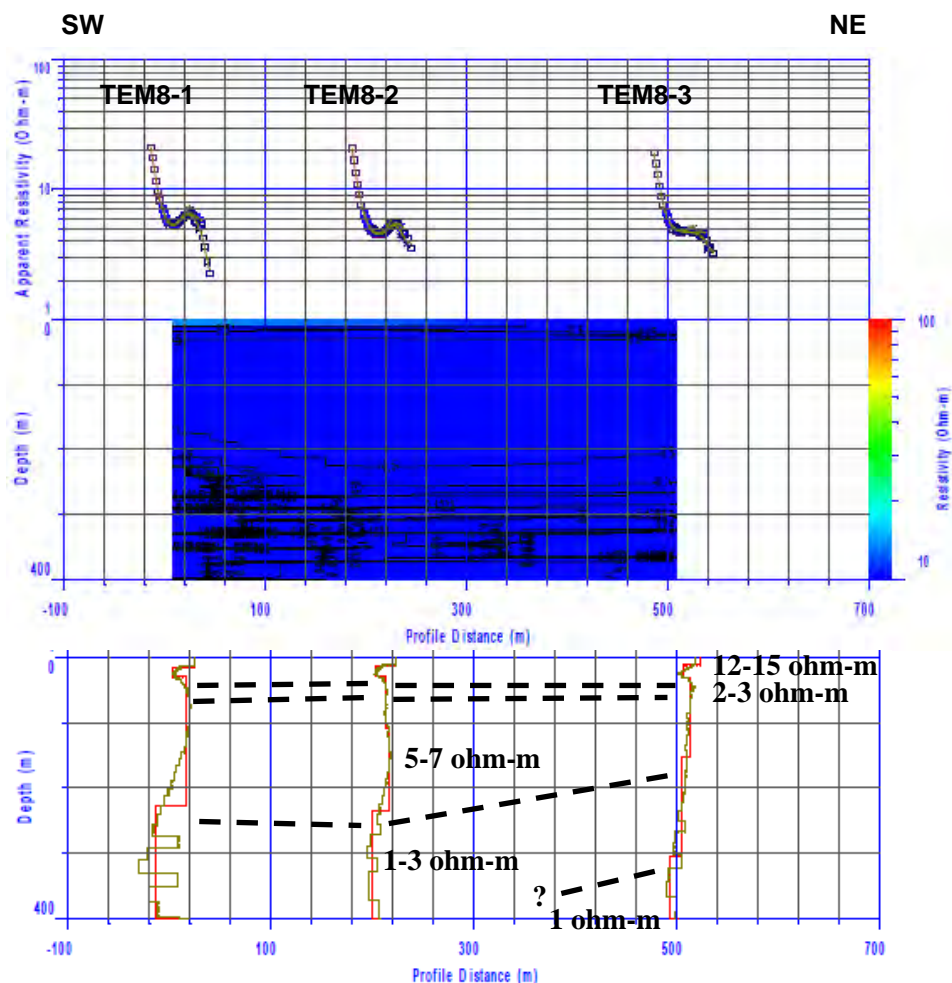
Figure 4.43: Cross-section of Smooth Imaging Resistivity and Layered Structure Analysis (BH-8)

The resistivity structure of this area shows 4 or 5 layers, with the resistivity of the surface layer registering 10ohm-m or higher. However, in all layers below that, the resistivity becomes low, at 10ohm-m or less.

The geology of this area is Holocene Q1 consisting of accumulations of lacustrine sediments, as well as sandy, silty and pyroclastic sediments. The low resistivity that extends from -60m downwards indicates that groundwater may be permeated through these sediments and that resistivity becomes low when there is groundwater saturation.

The following chart shows a comparison between the results of the electromagnetic (TEM) and electric (VES) prospecting.

Table 4.26: Comparison between TEM and VES Result（BH-8 No1）

Measurement	Parameter	TEM8-1/VES8-2						
		—	L1	L2	L3	L4	—	—
TEM	Resistivity (ohm-m)	—	14.8	2.3	6.7	0.5	—	—
	Thickness (m)	—	15.4	14.7	196.8	—	—	—
	Undersurface depth (m)	—	15.4	30.1	226.9	—	—	—
		L1	L2	L3	L4	—	—	—

	Resistivity (ohm-m)	14.0	47.0	3.0	11.0	—	—	—
VES	Thickness (m)	3.2	5.6	37.0	—	—	—	—
	Undersurface depth (m)	3.2	8.8	45.8	—	—	—	—

＊　The gray section denotes a correlation between the resistivity and undersurface depth.

The resistivity structure of the TEM shows high-low-high from the surface, but is remarkably low in the bottom layer. The resistivity of the VES also shows a repeated cycle of high-low.

A comparison of these resistivity structures shows differences in resistivity values and depths down to -15m, but below that they show good correspondence with one another.

Table 4.27: Comparison between TEM and VES Results（BH-8, No2）

Measurement	Parameter	TEM8-2/VES8-3						
		—	L1	L2	L3	L4	L5	—
TEM	Resistivity (ohm-m)	—	12.0	2.2	5.0	7.2	1.6	—
	Thickness (m)	—	14.3	14.0	88.9	125.4	—	—
	Undersurface depth (m)	—	14.3	28.3	109.1	234.5	—	—
		L1	L2	—	L3	L4	—	—
VES	Resistivity (ohm-m)	5.6	38.0	—	5.7	45	—	—
	Thickness (m)	0.4	9.6	—	197.0	—	—	—
	Undersurface depth (m)	0.4	10.0	—	207.0	—	—	—

＊　The gray section denotes a correlation between the resistivity and undersurface depth.

The resistance in both the TEM and VES is high down to a depth of -15m, but decreases below that. In the TEM, there are no major changes in resistivity between -15m and -235m and this could be said to be a single layer. However, the resistivity becomes remarkably low in layers below that. In the VES, the resistivity values between -10m and -210m are roughly the same as those of the TEM. The bottom layer shows high resistivity, and this layer might correspond to layer No. 4 in the TEM.

Table 4.28: Comparison between TEM and VES Results（BH-8, No3）

Measurement	Parameter	TEM8-3/VES8-5						
		—	L1	L2	L3	L4	L5	—
TEM	Resistivity (ohm-m)	—	12.5	2.8	4.9	2.5	0.9	—
	Thickness (m)	—	11.7	18.8	123.2	152.2	—	—
	Undersurface depth (m)	—	11.7	30.5	153.7	305.9	—	—
		L1	L2	L3	L4	L5	—	—
VES	Resistivity (ohm-m)	14.0	34.0	5.5	1.1	83	—	—
	Thickness (m)	2.4	4.4	50.0	49.0	—	—	—

＊　The gray section denotes a correlation between the resistivity and undersurface depth.

In both cases, the resistivity of the surface layer is high, but decreases in the lower layers. However, while the low resistivity zone in the TEM continues down to below -300m, in the VES this zone is shallower, extending down to only -100m. In addition, the resistivity in the

The Study on Groundwater Resources Assessment
in the Rift Valley Lakes Basin in Ethiopia, Final Report (Supporting Report)

JICA
KOKUSAI KOGYO CO., LTD.

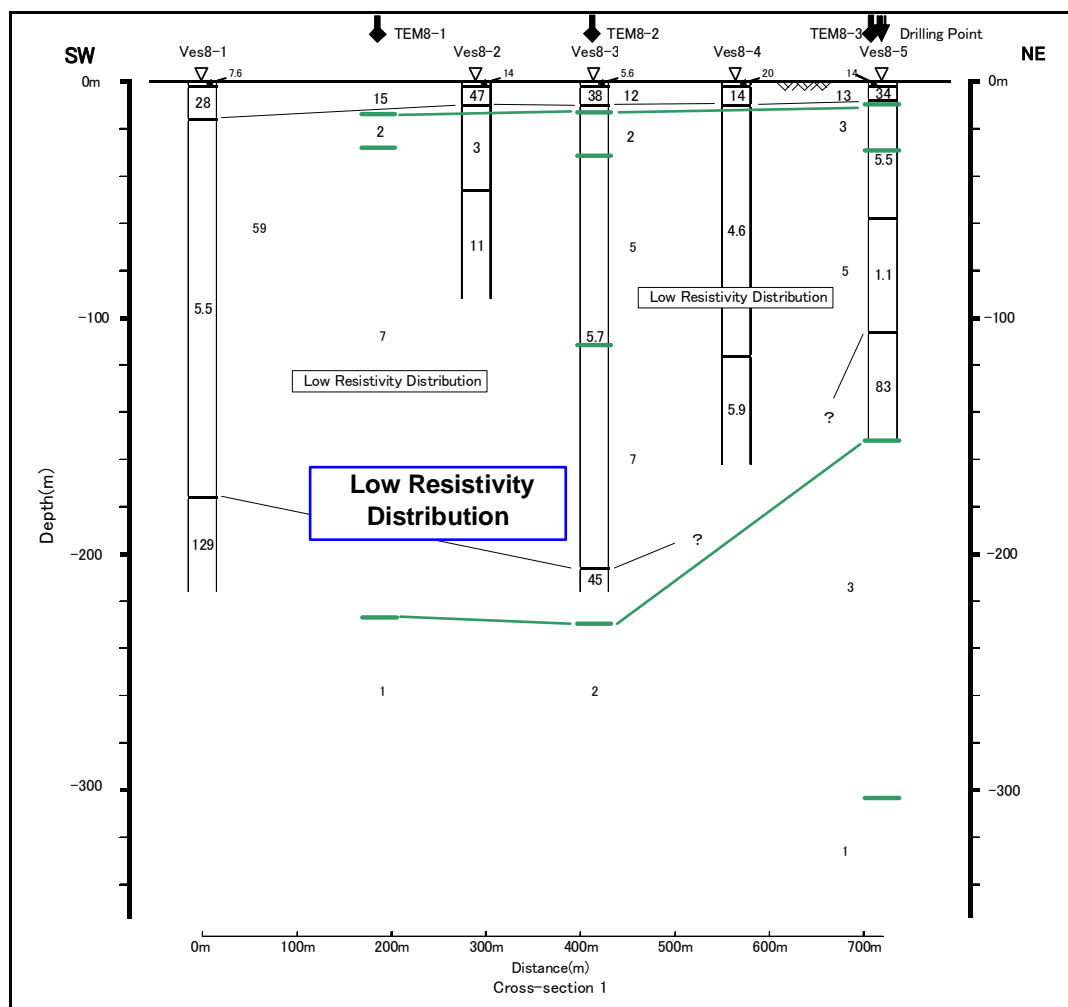bottom layer of the VES is high, which doesn't agree with the result of the TEM.

Figure 4.44: Comprehensive Cross-sectional Diagram of the Analysis（BH-8）

Figure 4.44 is a summary of the results of the TEM and VES analyses. In both cases, the resistivity from the surface down to 20m was high and uniform. Below that was low resistivity, the layer thickness was 100m to 200m, and there were many changes. Furthermore, regarding the bottom layer, the results of the VES analysis showed high resistivity, while the TEM analysis indicated that it was remarkably low. As a result of rechecking the VES curve, the depth AB/2 of this zone increased the resistivity value in nearly all cases.

On the other hand, the apparent resistivity curve of the TEM showed a decreasing value for resistivity as the sampling time increased. In all cases, there was no conformity in the lowest layer, and it could not be determined which set of results was appropriate. However, in the VES measurements, the transmission current was too weak and the electric potential of the receiver was very small, so there is a possibility that true apparent resistivity values were not obtained for the deep sections using this method. At the same time, there was no variability in the TEM data, which was highly accurate, so the overall conclusion is that the TEM results for relative resistivity structure in the deep section are reasonable.

d.5   Mirab Abaya (Fetle Doronje)

This site was subjected to electromagnetic prospecting to obtain information about the resistivity structure in order to create a geological longitudinal map. The site is located at an

The Study on Groundwater Resources Assessment
in the Rift Valley Lakes Basin in Ethiopia, Final Report (Supporting Report)

JICA
KOKUSAI KOGYO CO., LTD.

elevation of 1,320m in a farming zone about 10km north of Mirba Abaya and about 5km west of Lake Abaya. The difference in relief between the site and the lake appears to be at least 100m. There were 3 TEM measuring points, which were spaced 300m apart (see to Data book)
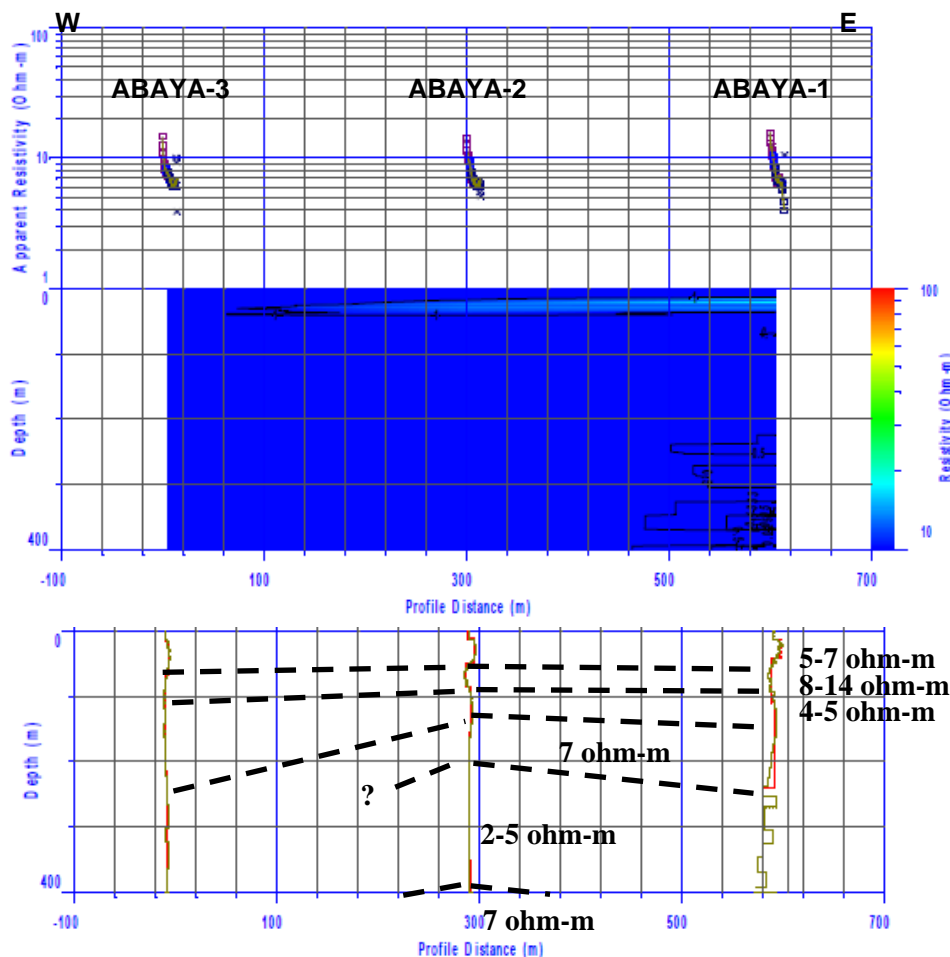
Figure 4.45: Cross-section of Smooth Imaging Resistivity and Layered Structure Analysis (Mirab Abaya area）

The resistivity structure at this site can be divided into 4 to 6 layers, which overall have a low resistivity. While the bottom layer of ABAYA-2 shows a slightly higher value, there is almost no difference with other resistivity values. Furthermore, since a noncontiguous resistivity structure was not found between measuring points, it is considered to be a stratified structure.

The geology of this region dates from Holocene Q1, and there are accumulations of lacustrine sediments, as well as sandy, silty and pyroclastic sediments. Because these sediments are considered to be indicative of a weakly consolidated geology, it is easy for them to contain an adequate amount of water, and it appears that the low resistivity can be attributed to saturation with groundwater.

e.   Other layer structure analysis

A longitudinal profile of the resistivity structure in the E-W direction was compiled based on the results of the TEM analysis. This profile was created based on the analytical results of one measuring point at each site. Criteria for selecting data sites included a low amount of

4-62

noise in the data, and a high degree of analytical accuracy. If the data from different points in a site or the analytical results were similar, then the point in the center of the site was chosen.

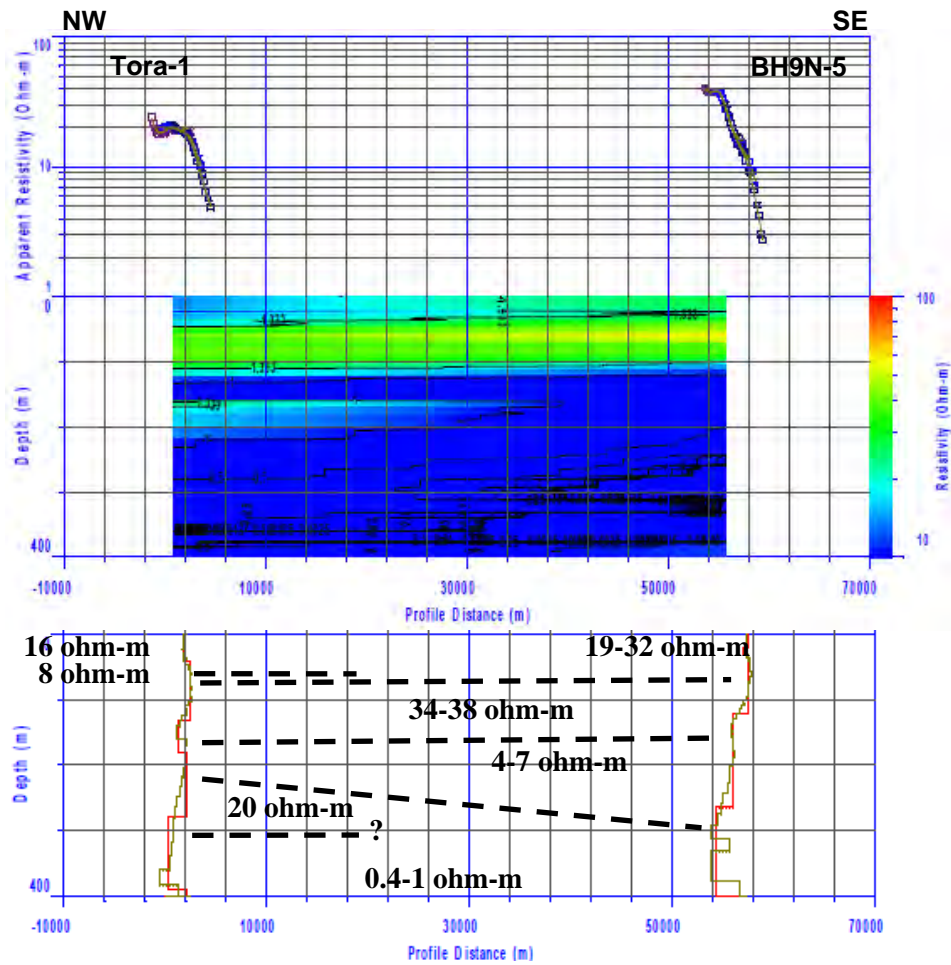The following is a description of the characteristics of each profile.

e.1   Tora – BH10N
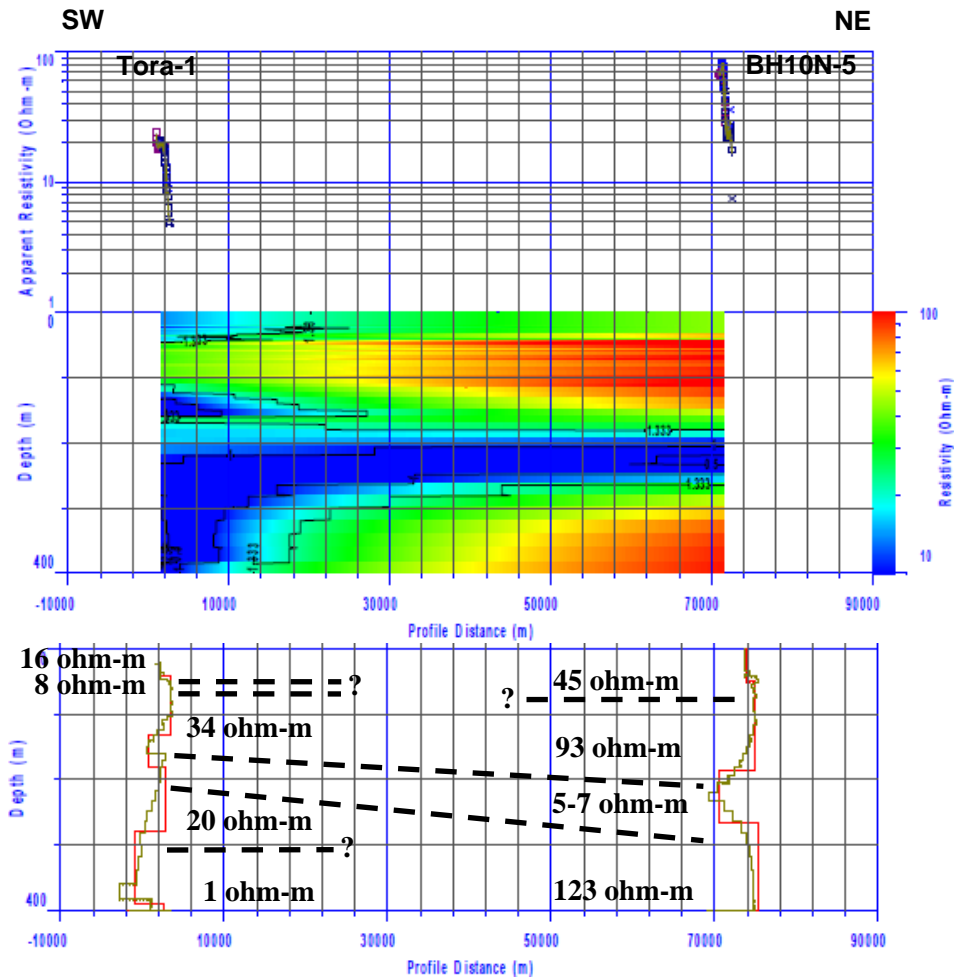
Figure 4.46: Cross-section of Smooth Imaging Resistivity and Layered Structure Analysis（Tora-BH-10N）

This profile is oriented SW-NE with a spacing of about 70km between measuring points. There is low resistivity at measuring point Tora-1, while the overall resistivity at point BH-10N-5 is high, and it is estimated that the resistivity structure between these points is noncontiguous.

In addition, at -200m below the surface there exists low resistivity. In the geological columnar section of the Tora site, there is strongly welded tuff (so called "green") at -186m to -204m, and rhyolite from -204m to -251m. At measuring point BH-10N, there are accumulated sandy, silty, and pyroclastic lacustrine sediments. The low resistivity of the deep area below the surface strongly indicates the presence of an aquifer. On the other hand, the high resistivity of the surface at BH-10N-5 corresponds to lacustrine sediments, while the high resistivity of the deep sections suggests the existence of ignimbrite and/or welded tuff.

e.2   Tora – BH9N

The Study on Groundwater Resources Assessment
in the Rift Valley Lakes Basin in Ethiopia, Final Report (Supporting Report)
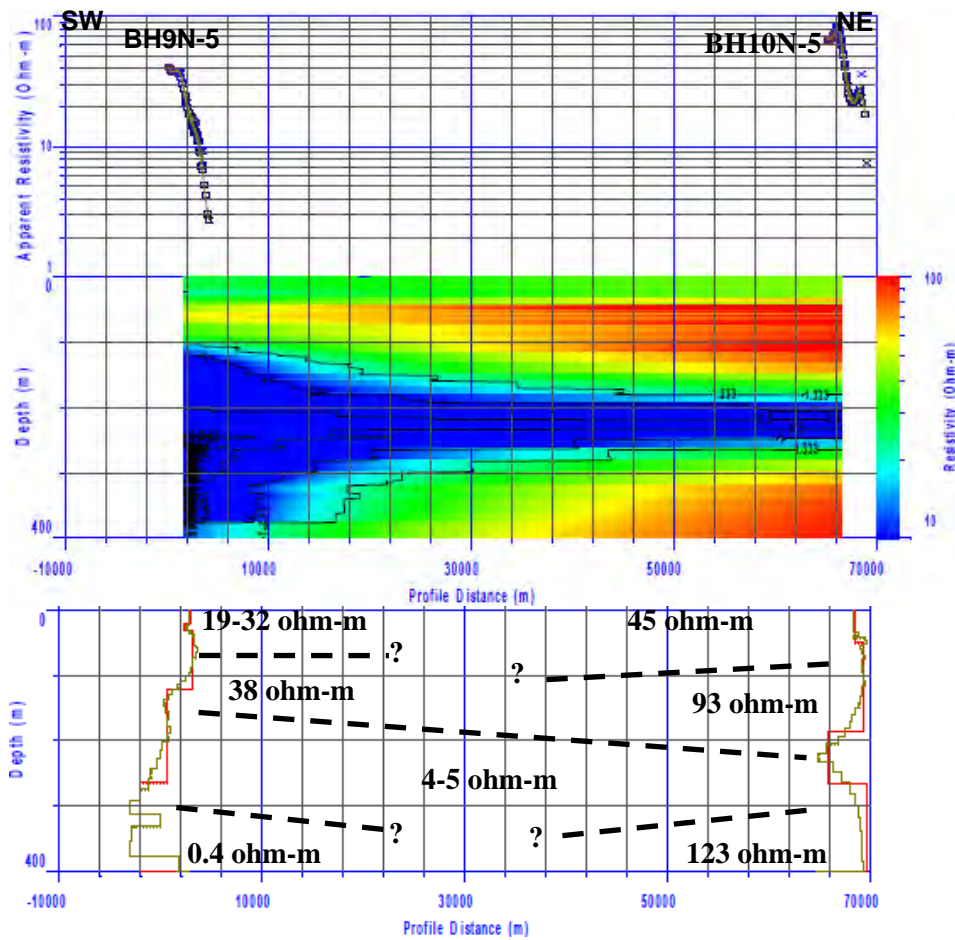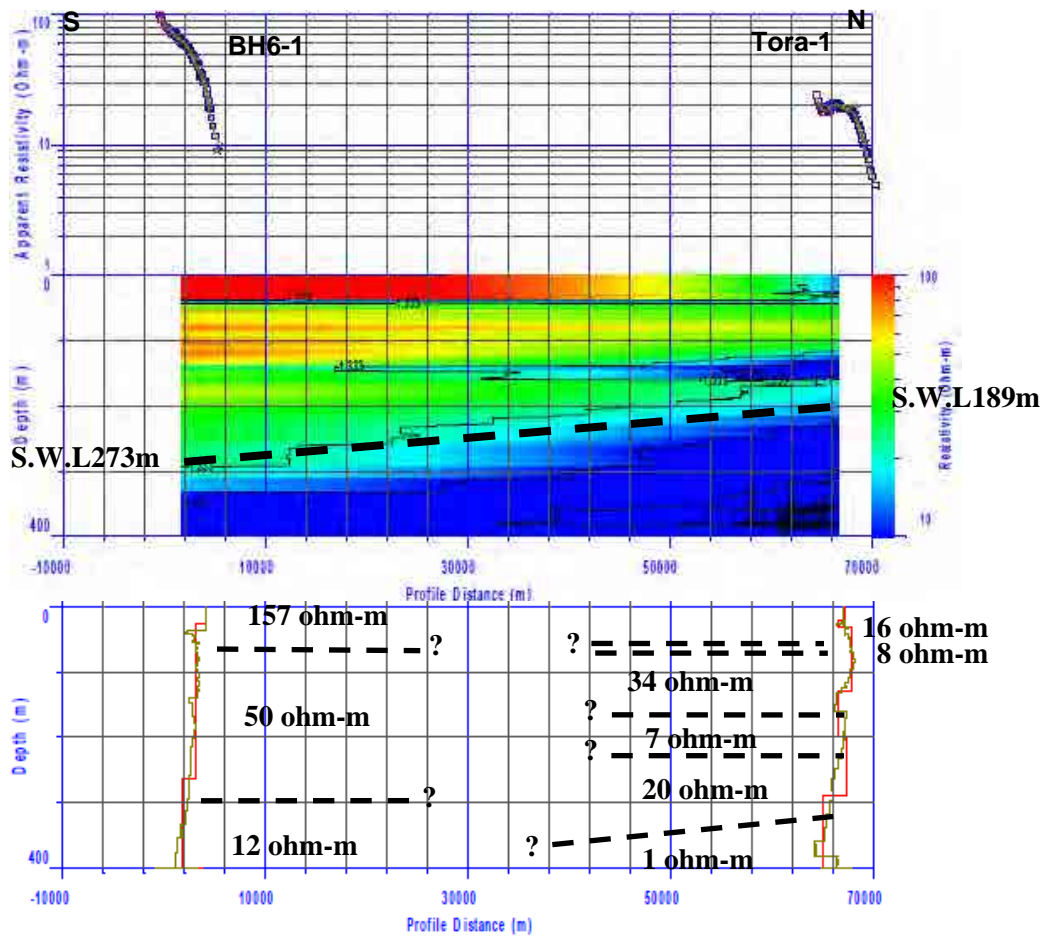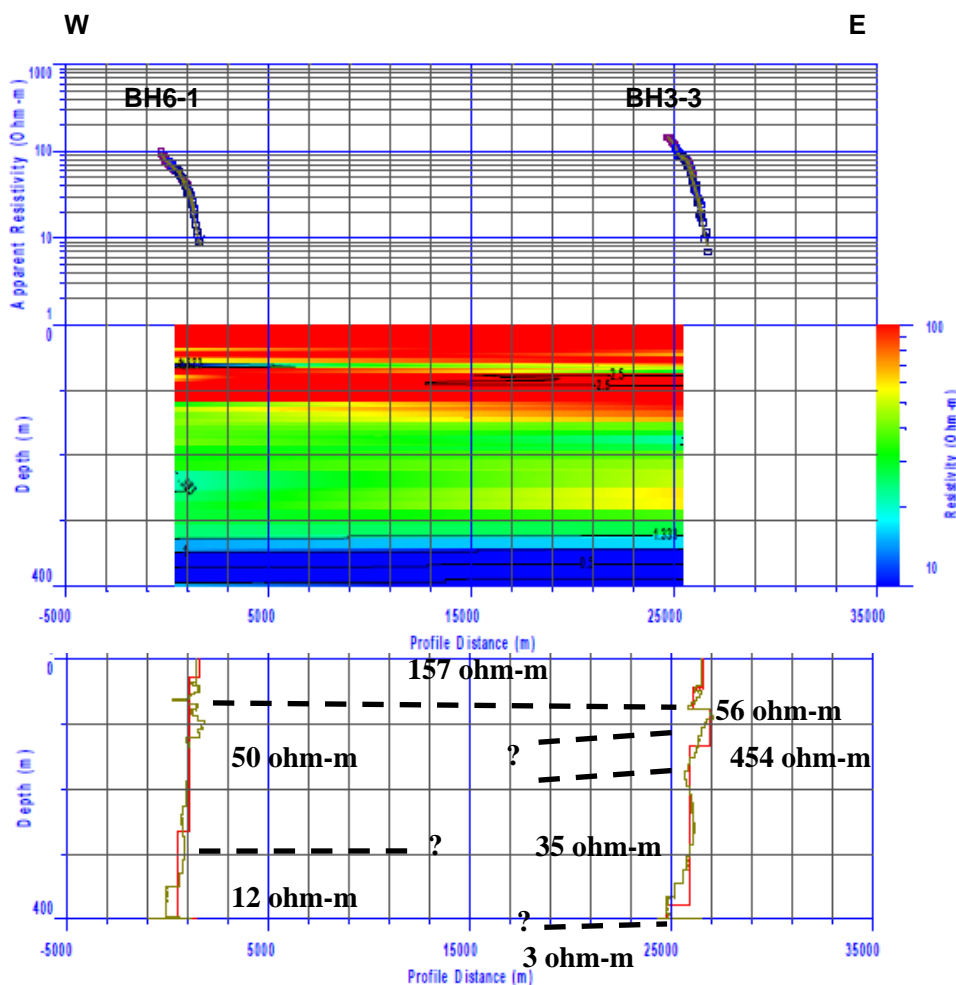
JICA
KOKUSAI KOGYO CO., LTD.

Figure 4.47: Cross-section of Smooth Imaging Resistivity and Layered Structure Analysis（Tora-BH9N）

This profile is oriented in the NW-SE direction, with measuring points spaced 55km apart. From the surface down to 100m, the resistivity is somewhat high, but it decreases in the lower layers. There is welded tuff between -186m and -204m at the Tora site, and between 204m and 251m there is rhyolite.

In addition, at BH9N there are deposits of sandy, silty and pyroclastic lacustrine sediments. In the layer below that are distributions of ignimbrite, tuff, etc., and below that, starting at depth of 100m, there appears to be low resistivity due to saturation by groundwater.

The Study on Groundwater Resources Assessment
in the Rift Valley Lakes Basin in Ethiopia, Final Report (Supporting Report)

JICA
KOKUSAI KOGYO CO., LTD.

e.3   BH-9N – BH-10N

Figure 4.48: Cross-section of Smooth Imaging Resistivity and Layered Structure Analysis（BH9N–BH10N）

This profile is oriented in the NE-SW direction, with low resistivity seen at depths of 100m and lower at measuring point BH9N, and at depths between -200m and -270m at BH10N. The geology of this area is Holocene Q1, and there are deposits of sandy, silty and pyroclastic lacustrine sediments. In addition, at the BH-10N site there are numerous faults running NNE-SSW, and there is a possibility that the low resistivity might be a reflection of these faults.

The Study on Groundwater Resources Assessment
in the Rift Valley Lakes Basin in Ethiopia, Final Report (Supporting Report)

JICA
KOKUSAI KOGYO CO., LTD.

e.4   BH-6 - Tora

Figure 4.49: Cross-section of Smooth Imaging Resistivity and Layered Structure Analysis（BH-6-Tora）

This profile is oriented in the N-S direction with measuring points spaced 65km apart. The relative resistivity of point BH-6-1 is high, while it is low at Tora-1. The geology of BH-6 consists of expansive coarse pumice-like pyroclastic materials. From the surface down to about -200m or lower, there apparently exists crushed rock and/or weathered pyroclastic materials in the areas with high to medium resistivity. Furthermore, the low resistivity in the lower layer may indicate an aquifer (water well SWL273m exists 3km southwest of this site).

The Study on Groundwater Resources Assessment
in the Rift Valley Lakes Basin in Ethiopia, Final Report (Supporting Report)

JICA
KOKUSAI KOGYO CO., LTD.

e.5 BH-6 – BH-3
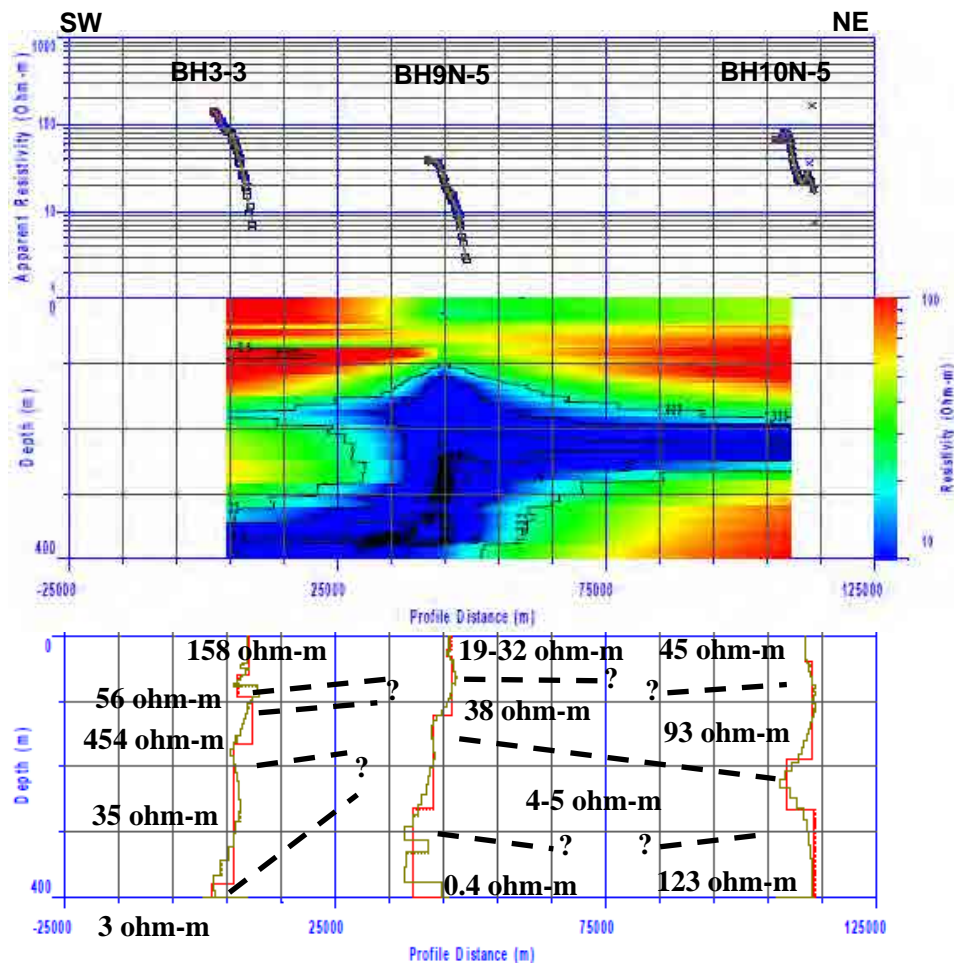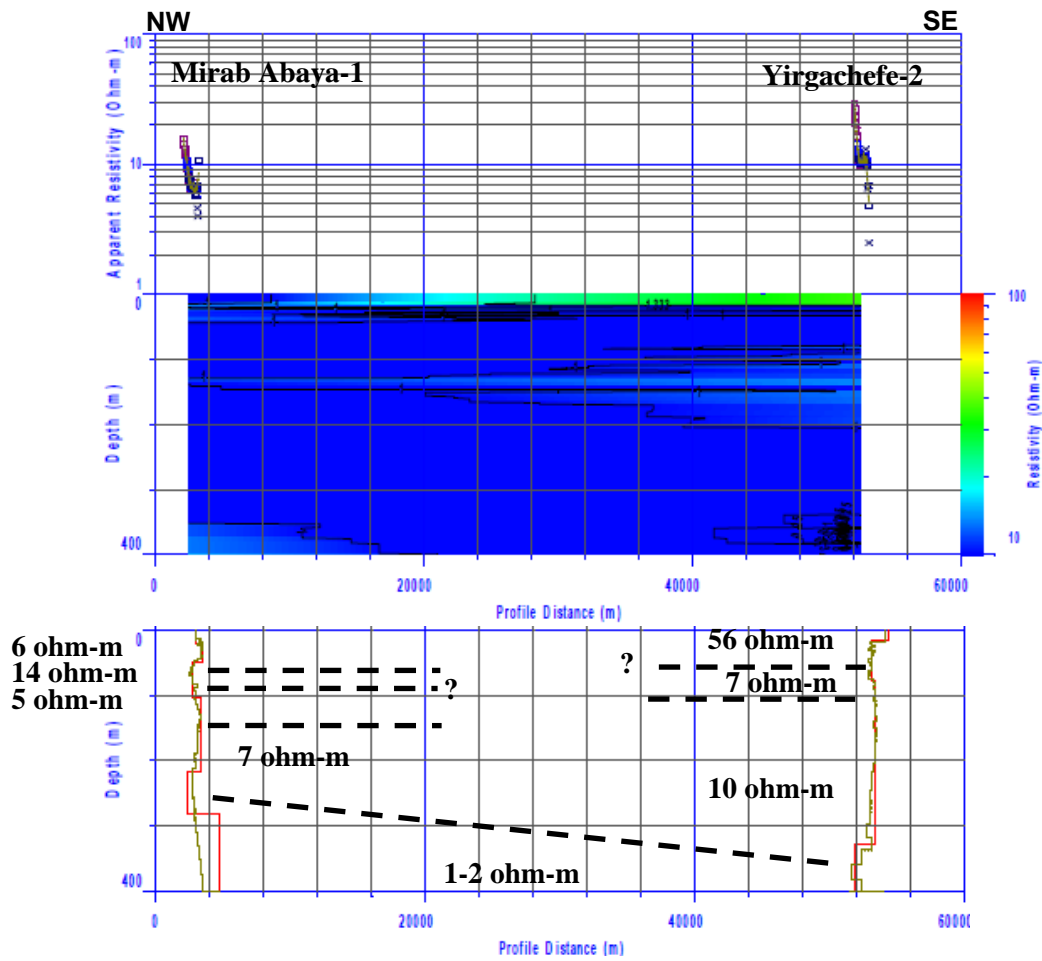

Figure 4.50: Cross-section of Smooth Imaging Resistivity and Layered Structure Analysis（BH-6-BH-3）

This profile is oriented in an E-W direction, with measuring points spaced 25km apart. There are some differences in resistivity and thickness between the two points and the resistivity structure between these points is believed to be noncontiguous. The geology of measuring point BH6 consists of widely distributed coarse pumice-like pyroclastic materials. The high-to-medium resistivity from the surface to -265m may be due to weathered pyroclastic materials and/or the existence of crushed rock. In addition, there is low resistance from -265m downward, which closely corresponds with an adjacent existing well, SWL273m, and it appears that the decreasing resistivity is due to saturation by groundwater.

On the other hand, the geology of measuring point BH3 consists of pumice, tuff layer, welded tuff layer, etc., and weathered tuff and silty sediments have been found around -70m. Furthermore, at around -140m, there is debris from pyroclastic rock, which has been determined to be unconsolidated and semi-consolidated tuff breccia gravel. In addition, the depth of the aquifer zone is -200m or lower. Since the resistivity around that depth is low, this would appear to correspond to the aquifer zone.

4-67

The Study on Groundwater Resources Assessment
in the Rift Valley Lakes Basin in Ethiopia, Final Report (Supporting Report)

JICA
KOKUSAI KOGYO CO., LTD.

e.6 BH-3 – BH-9N – BH-10N

Figure 4.51: Cross-section of Smooth Imaging Resistivity and Layered Structure Analysis（BH-3–BH-9N-BH-10N）

This profile is oriented in an NE-SW direction, with measuring points BH-3 and BH-10N spaced 105km apart. There are some differences in resistivity values between the two points, but between -100m and -200m the resistivity is generally high, but it decreases in layers below that. The resistivity structure between points BH-3 and BH-9 is estimated to be particularly noncontiguous. Between these points are numerous streams that flow NW-SE into Lake Shala. In addition, there are many faults that are oriented in a NW direction. Thus, the area between these points, which is an anomalous resistivity area, is believed to consist of pyroclastic rock that has either been weathered or crushed and/or tuff layer, welded tuff layer, etc., that appear to be saturated with groundwater.

The Study on Groundwater Resources Assessment
in the Rift Valley Lakes Basin in Ethiopia, Final Report (Supporting Report)

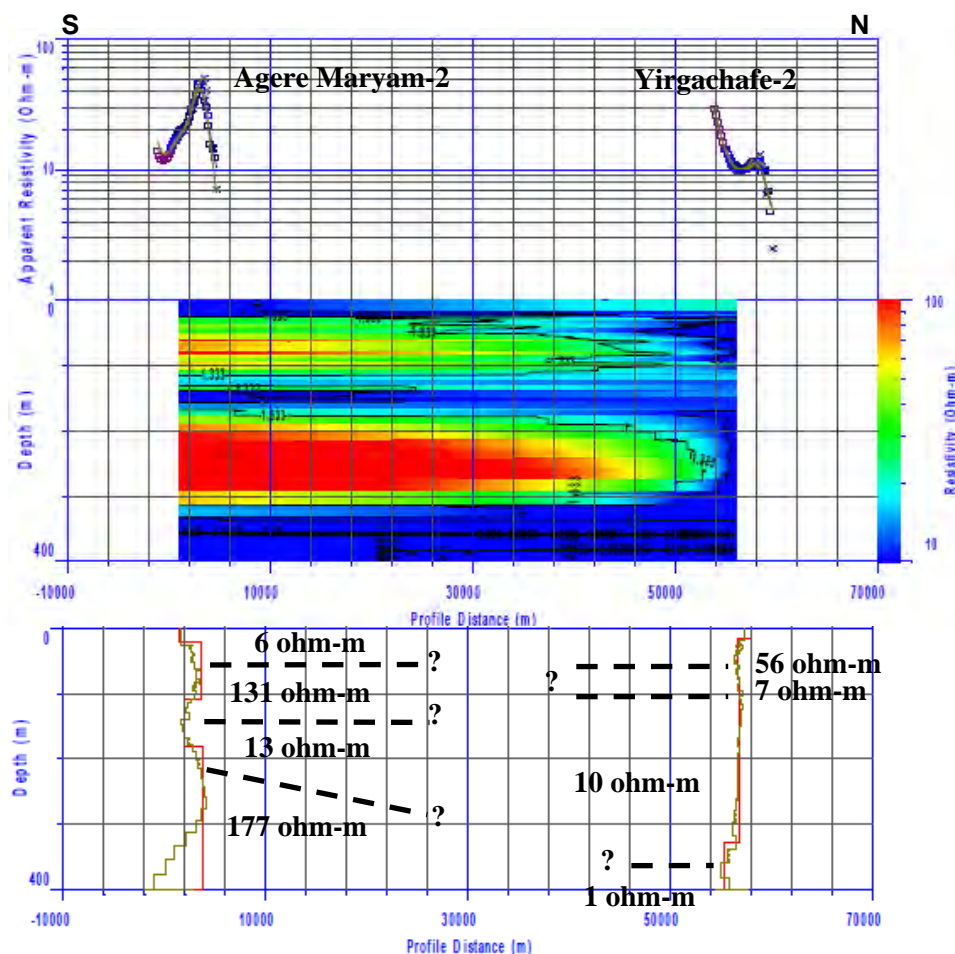JICA
KOKUSAI KOGYO CO., LTD.

e.7　　　Mirab Abaya - Yirgachafe

Figure 4.52: Cross-section of Smooth Imaging Resistivity and Layered Structure Analysis（Mirab Abaya-Yirgachefe）

This profile is oriented NW-SE and encompasses Lake Abaya. The distance between measuring points is about 50km. Except for the high resistivity that was found in the top layer of the Yirgachafe site, nearly all of the layers show low resistivity. The geology of the Mirab Abaya site is Holocene Q1 consisting of lacustrine sediments, as well as sandy, silty and pyroclastic sediments. It appears that these sediments have a high volume water content, the groundwater is saturated, and relative resistivity is decreasing.

Similarly, the geology of Yirgachefe consists of distributions of lacustrine sediments PNv and/or Pv from the Oligocene to Miocene. In addition, there are numerous fault groups in this area, so there is a high possibility that weathered and/or crushed rock is saturated with groundwater.

e.8   BH-7 - Yirgachefe
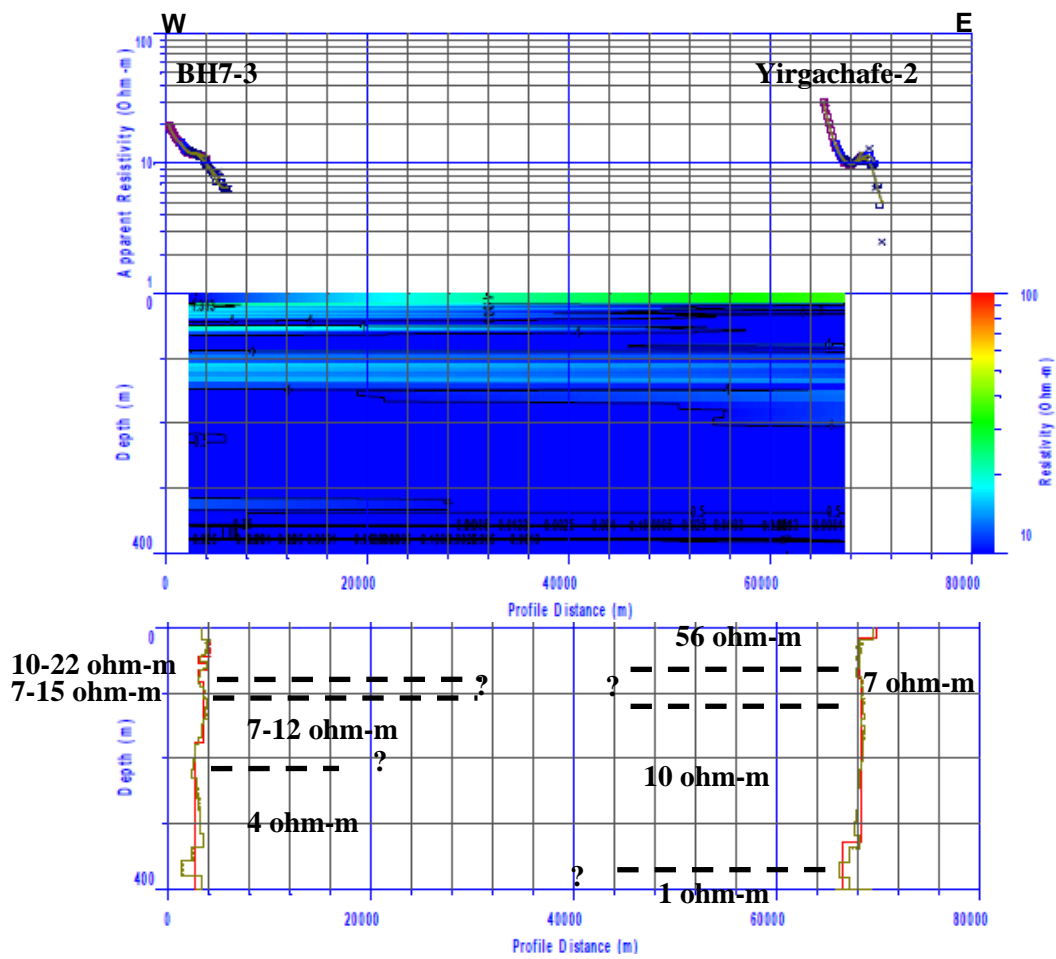
Figure 4.53: Cross-section of Smooth Imaging Resistivity and Layered Structure Analysis（BH-7-Yirgachafe）

This profile also traverses Lake Abaya, in an E-W direction, and the distance between measuring points is 65km. Overall, the relative resistivity is low.

The geology of BH-7 is Holocene Q1 consisting of lacustrine sediments, as well as sandy, silty and pyroclastic sediments. The geology of the Yirga site consists of distributions of lacustrine sediments of rhyolite, trachyite, tuff, basalt, etc. These sediments are considered to be loosely consolidated geology. It appears that they can easily hold sufficient amounts of water, and that the groundwater is saturated.

The Study on Groundwater Resources Assessment
in the Rift Valley Lakes Basin in Ethiopia, Final Report (Supporting Report)

JICA
KOKUSAI KOGYO CO., LTD.
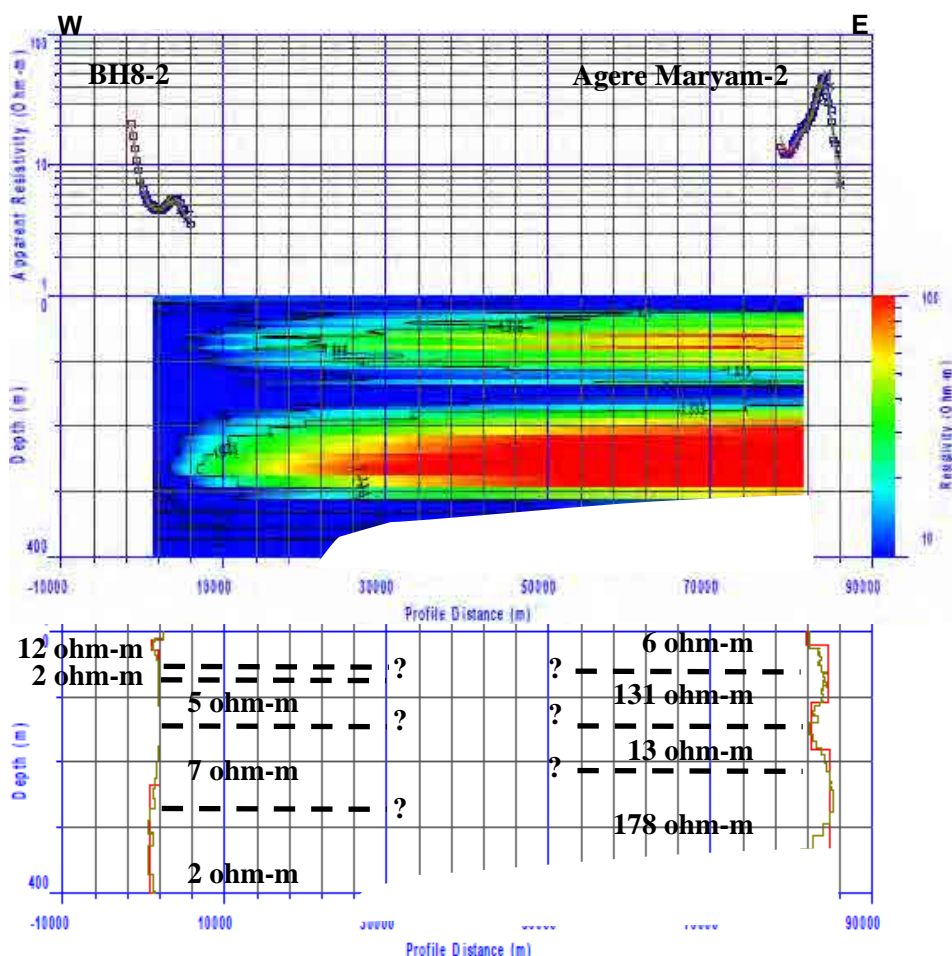
e.9   Agere Maryam - Yirgachefe

Figure 4.54: Cross-section of Smooth Imaging Resistivity and Layered Structure Analysis（Agere Maryam- Yirgachafe）

This profile is oriented in a N-S direction and the measuring points are spaced 55km apart. The resistivity structure between the two points is different, and there is a possibility that it is noncontiguous. The resistivity structure at the Agere Maryam site shows low-high-low-high, with high resistivity between -20m and -110m, and below -180m. At the Yirgachafe site, the resistivity is high only in the surface layer, while in lower layers it shows low values of 10ohm-m or less.

The geology of the Agere Maryam site consists of an alluvial layer of Holocene Qa, with the upper layer consisting of deposits of sand, silt and gravel, while down to -100m below the surface there is what appears to be basalt that has high resistivity and does not contain groundwater. The low resistivity between -100m and -200m indicates basalt that is saturated with groundwater, while the high resistivity below -200m seems to indicate bedrock. The Yirgachafe site is covered with thick deposits of lacustrine sediments PNv and/or Pv, and it appears that weathered rhyolite, fissure water, etc., have permeated down to the deep underground.
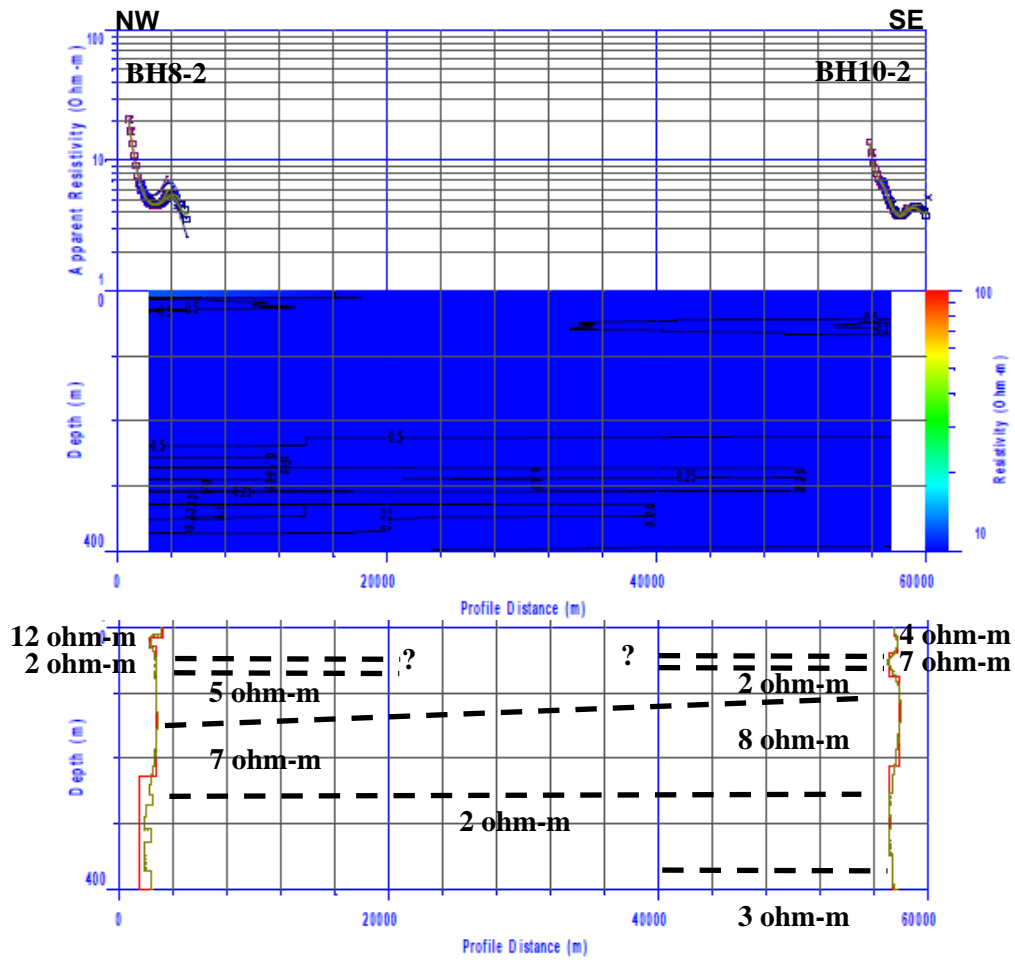
e.10   BH-8 - Agere Maryam

Figure 4.55: Cross-section of Smooth Imaging Resistivity and Layered Structure analysis（BH8-Agere Maryam）

This profile is oriented in an E-W direction and the measuring points are spaced about 80km apart. Measuring point BH-8 generally has low resistivity, while the Agere Maryam site shows high resistivity, and it appears that the area between these points has a noncontiguous resistivity structure. The L frequency of the measurement data from the Agere Maryam site show a lot of variation, and the accuracy of the deep section analysis is not vey good. Therefore, it appears that the depth of the analysis is about 300m.

The geology of BH-8 is Holocene Q1, and there are deposits of lacustrine sediments, as well as sandy, silty and pyroclastic sediments. The geology of the Agere Maryam site consists of an alluvial layer of Holocene Qa. In the surface layer are sand, silt, and gravel deposits. The high resistivity down to about -100m below the surface indicates basalt that does not contain groundwater, but the low resistivity layer below that (-100m to -200m) appears to be basalt that is saturated with groundwater. In addition, the high resistivity at -200m and below is believed to be bedrock.

e.11   BH-8 – BH-10

The Study on Groundwater Resources Assessment
in the Rift Valley Lakes Basin in Ethiopia, Final Report (Supporting Report)

JICA
KOKUSAI KOGYO CO., LTD.
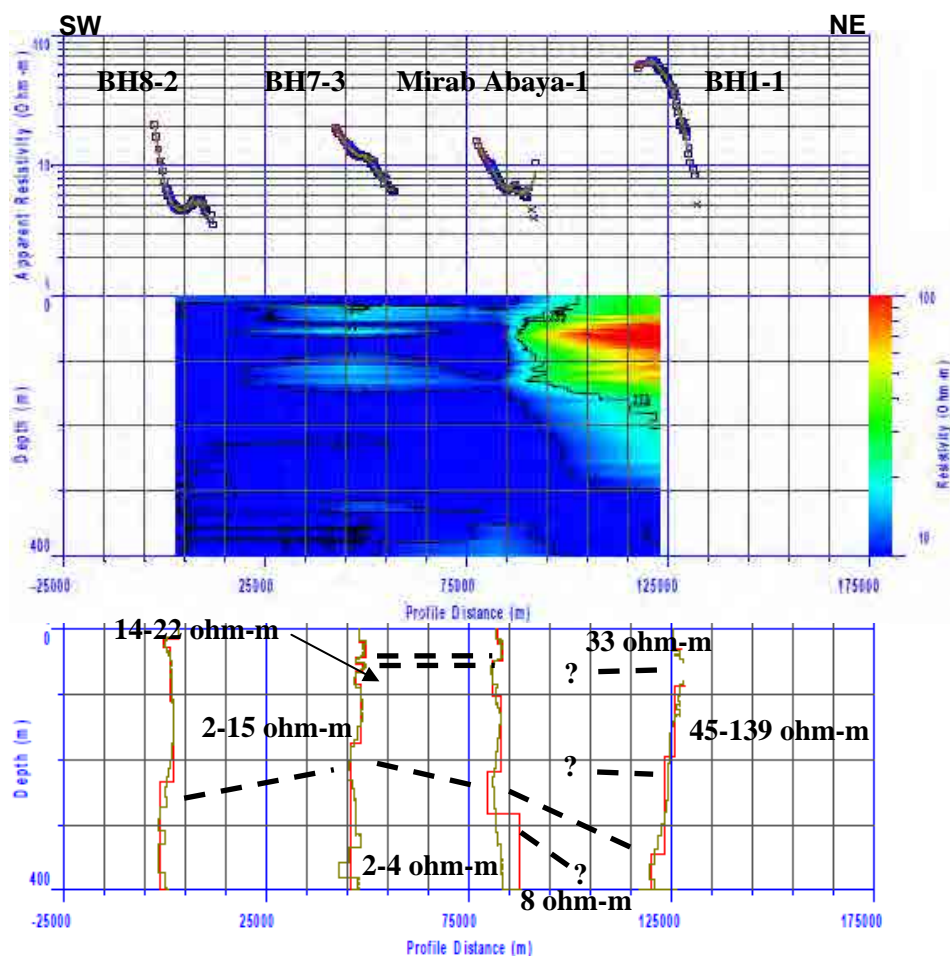
Figure 4.56: Cross-section of Smooth Imaging Resistivity and Layered Structure Analysis（BH-8-BH-10）

This profile is oriented in a NW-SE direction and the measuring points are spaced about 55km apart.

The geology of BH8 is Holocene Q1, and there are deposits of lacustrine sediments, as well as sandy, silty and pyroclastic sediments. It appears that these sediments can contain sufficient amounts of groundwater, and that the resistivity is low due to saturation by groundwater. In addition, point BH10 is covered by alluvial deposits such as basaltic gravel, sand and silt, and they are believed to contain rich amounts of groundwater.

e.12   BH-8 – BH-7 – Mirab Abaya – BH-1

Figure 4.57: Cross-section of Smooth Imaging Resistivity and Layered Structure Analysis（BH-8-BH-7-Mirab Abaya-BH-1）

This profile is oriented in a NE-SW direction and runs along the western sides of lakes Abaya and Chamo. The distance between points BH-8 and BH-1 is about 120km. From the Mirab Abaya site to the SW side there is generally low resistivity, but it is high on the NE side. It is estimated that the resistivity structure between these points is noncontiguous.

The geology from BH-8 to Mirab Abaya is Holocene Q1 consisting of lacustrine sediments, as well as sandy, silty and prelatic sediments, and it appears that there is groundwater saturation down to the deep section.

In addition, the results of drilling at BH-1 indicate that there is a pumice layer from the surface down to -42m. Below that is a welded tuff layer, and below that, starting at -126m is a hard rhyolite layer. In addition, the depth of the aquifer zone is determined to be between -67m and -130m. The high resistivity indicates a volcanic ash layer, a pumice layer, and a welded tuff layer, while the low resistivity below that appears to be welded tuff that has developed fissures and a rhyolite layer.

The Study on Groundwater Resources Assessment
in the Rift Valley Lakes Basin in Ethiopia, Final Report (Supporting Report)

JICA
KOKUSAI KOGYO CO., LTD.

e.13   BH-10 - Agere Maryam
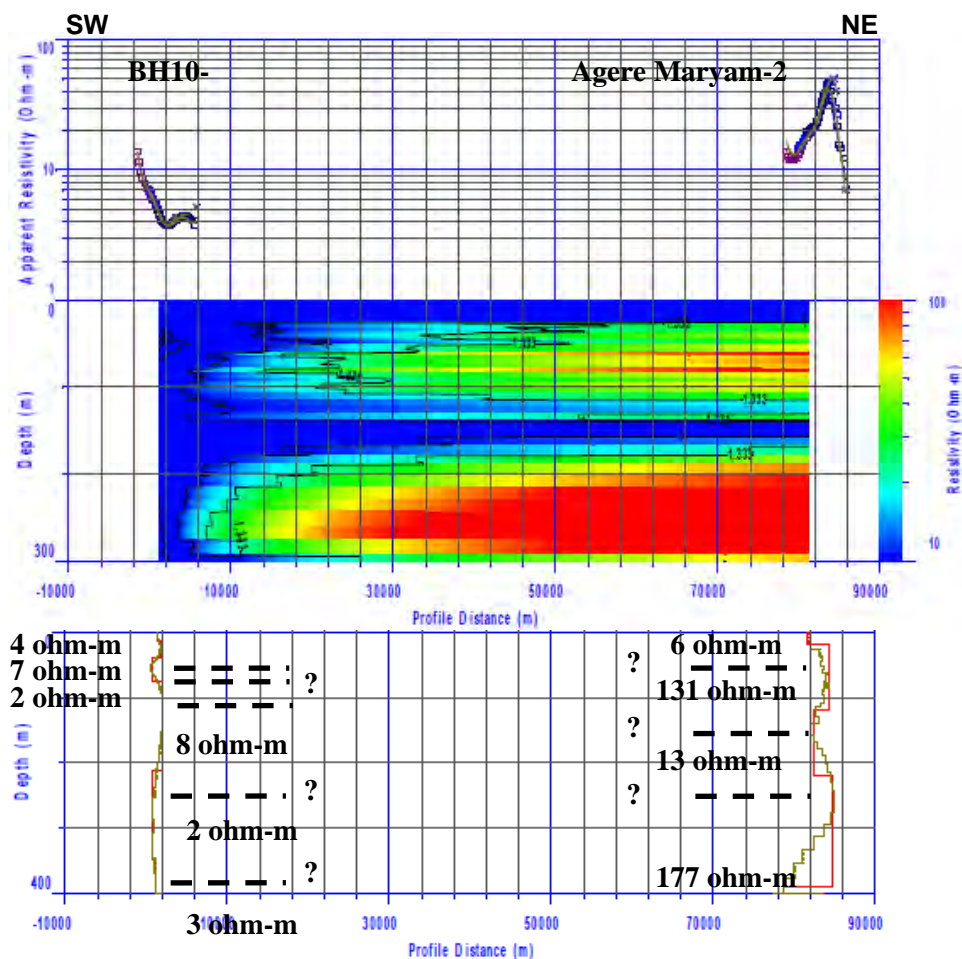

Figure 4.58: Cross-section of Smooth Imaging Resistivity and Layered Structure Analysis（BH-10-Agere Maryam）

This profile is oriented in an NE-SW direction and the measuring points are spaced about 80km apart. Measuring point BH-10 generally has low resistivity, while the Agere Maryam site shows high resistivity, and it appears that the area between these points has a noncontiguous resistivity structure.

The geology of BH-10 is covered in alluvial sediments such as basalt pebbles, sand, and mud, the underground structure is thought to be weathered layers and low resistivity sediments with abundant underground water. The geology of the Agere Maryam site consists of an alluvial layer of Holocene Qa. In the surface layer are sand, silt, and gravel deposits. The high resistivity down to about -100m below the surface indicates basalt that does not contain groundwater, but the low resistivity layer below that (-100m to -200m) appears to be basalt that is saturated with groundwater. In addition, the high resistivity at -200m and below is believed to be bedrock.

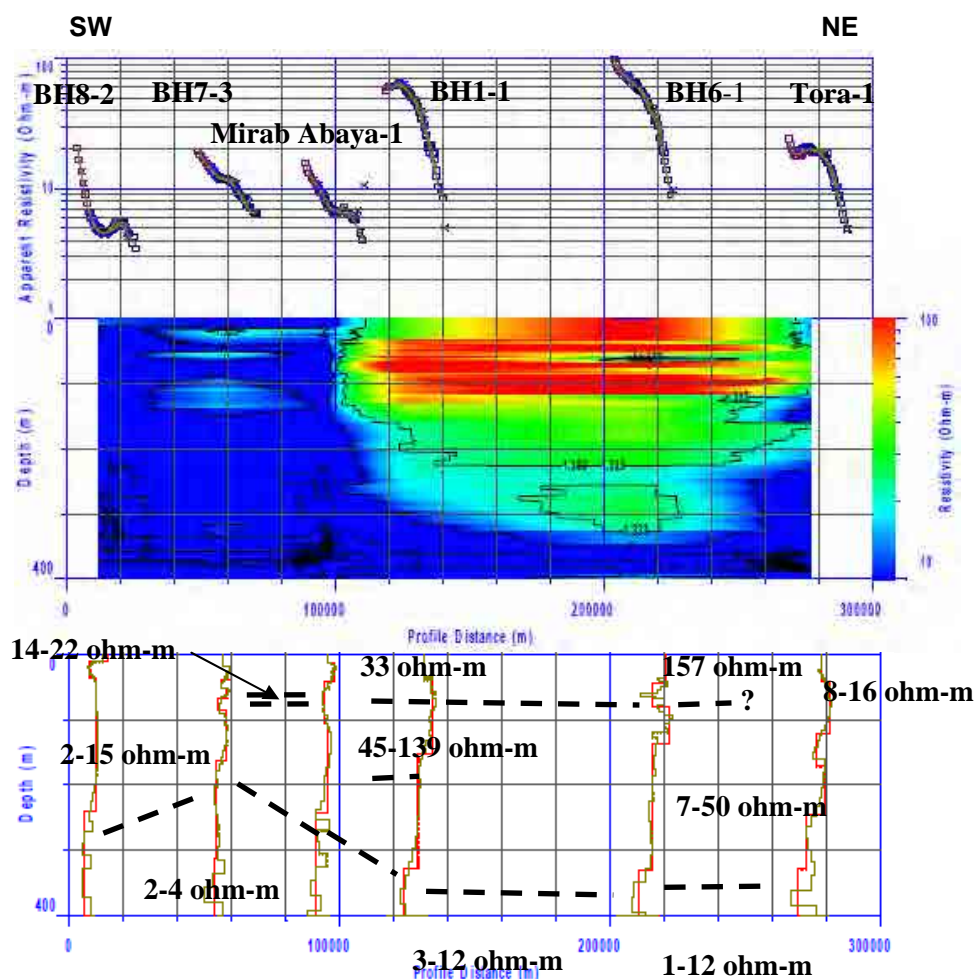### e.14   BH-8 – BH-7 – Mirab Abaya – BH-1 – BH-6 - Tora

Figure 4.59: Cross-section of Smooth Imaging Resistivity and Layered Structure Analysis（BH-8–BH-7–Mirab Abaya–BH-1–BH-6-Tora）

This profile is oriented in an SW-NE direction on the west side of the Rift Valley Lakes area. The distance between the first measuring point and the last measuring point is about 265km.. Measuring points BH-1-BH-6 generally show high resistivity down to 250 meters. However, other regions show low resistivity. A noncontiguous low resistivity structure is presumed to exist between Mirab Abaya and measuring point BH-1.

The geology between BH-8 and Mirab Abaya is Holocene Q1, consisting of deposits of lacustrine sediments, as well as sandy, silty, and pyroclastic sediments. This loosely consolidated geology makes it easy for groundwater to exist in sufficient quantity, and it appears that it is saturated with groundwater.

At measuring point BH-1, there is a layer of pumice rock down to 42 meters, and below that a layer of welded tuff.. Starting at -126m there is a hard rhyolite layer. High resistivity is found in the volcanic ash, pumice and welded tuff layers, while below them are what appear to be low-resistivity areas of welded tuff that has developed fissures and a rhyolite layer.

4-76

Measuring point BH-6 consists of distributions of coarse pumice-like pyroclastic materials. From the surface down to about 200m there is high-to-medium resistivity which may indicate the existence of weathered pyroclastic materials and/or crushed rock. Below that is low resistivity that may indicate an aquifer (there is information about an existing well, SWL273m, that is in the vicinity).

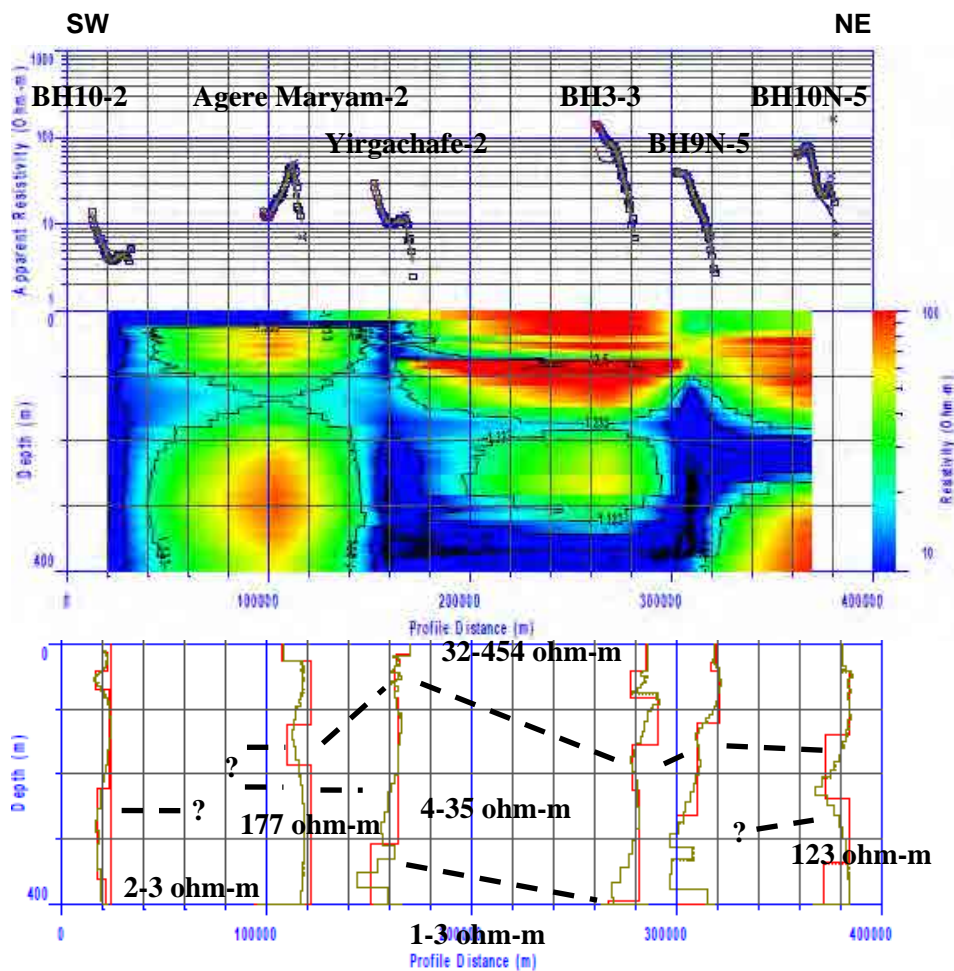### e.15   BH-10 - Agere Maryam – Yirgachafe – BH-3 – BH-9N – BH-10N

Figure 4.60: Cross-section of Smooth Imaging Resistivity and Layered Structure
Analysis（BH-10-Agere Maryam–Yirgachafe–BH-3–BH-9N–BH-10N）

This profile is oriented in a SW-NE direction and shows the eastern side of the Rift Valley Lakes area. The distance between the first measuring point and the last measuring point is about 350km. This profile shows a wealth of variation, and discontinuity of the resistivity structure is estimated to exist between BH-10 and Agere Maryam, between Agere Maryam and Yirgachafe, and between measuring points BH3and BH9N.

Comparing the resistivity with the geology of each region, we find that measuring point BH-10 contains distributions of basaltic gravel and sandy, silty, and other sediments, and that the low resistivity suggests sediments, weathered layers, etc., that have high potential for containing groundwater.

The geology of the Agere Maryam area is Holocene Q1, consisting of deposits of lacustrine sediments, as well as sandy, silty, and pyroclastic sediments. From the surface down to -100m, there is highly resistive basalt that does not contain water. From -100m down to -200m, there is low-resistivity basalt that may be saturated with groundwater. Below that is a highly resistive layer that is believed to be bedrock. Those measurement points indicated the high resistivity, due to the topography and geology compare to other points.

The Yirgachafe area consists of thick distributions of lacustrine sediment PNv and/or Pv. The low resistivity appears to be caused by weathered rhyolite, fissure water, etc. that has permeated to deep underground areas.

The high resistivity of the upper layer of measuring point BH-3 consists of pumice, a tuff layer and a welded tuff layer. The somewhat low resistivity of the middle depths is believed to be tuff breccias but that it is difficult for this layer to become a groundwater layer. Furthermore, around -200m below the surface, because the decreasing resistivity appears to correspond to pumice, welded tuff, gravels of basaltic tuff, etc., it may be an aquifer layer.

Measuring point BH-9N contains distributions of Holocene Q1 and deposits of lacustrine sediments, as well as sandy, silty, and pyroclastic sediments. This loosely consolidated geology makes it easy for groundwater to exist in sufficient quantities, especially starting at -100m below the surface, where it appears that resistivity is decreasing due to saturation by groundwater.

The geology of measuring point BH-10N contains distributions of Holocene Q1 and deposits of lacustrine sediments, etc. From the surface down to a depth of around -300m there is a repetitive cycle of medium-high-low resistivity. There are numerous faults that run along a NNE-SSW axis, and there is a possibility that the low resistivity is a reflection of these faults.

4.3   Technology transfer

4.3.1   TEM workshop

The TEM Electromagnetic Prospecting Workshop was held at EWTEC on December 23 and 24, 2010. The purposes of the workshop were to understand the basic theory of electromagnetic prospecting, to learn measurement methods and acquire and analyze measurement data through practical training, and to learn how to interpret the data. In all there were 14 participants from such organizations as the GSE, the Ministry of Water and Energy, Addis Ababa University, private sector consultants, and EWTEC, among others.

The lecture on the first day mainly consisted of explanations of the purposes of the study, an overview of the electric prospecting that was conducted in the 1st year and study results, an overview of the electromagnetic prospecting and study results, and comparisons between drilling results and relative festivity structure. On the 2nd day, practical training was given on the grounds of EWTEC in TEM prospecting, and participants were given hands-on instruction in the installation of everything from transmission loops to survey equipment, taking measurements, and removing equipment. Because the transmission loop used in the practical training at EWTEC was only 50 meters on each side, it appeared that resistivity data could be obtained from a maximum depth of -200m. It should be noted that the central loop method was used for the measurements. After that, the acquired data were analyzed, and a discussion was held using existing geological columnar sections to compare with the data.

Sentiments of the participants were wide-ranging, and included: first time to hear a lecture about TEM electromagnetic prospecting; first time to receive practical training; ability to gain

an understanding about TEM; ability to thoroughly understand data on resistivity structure down to several hundred meters below the aground surface, and the ability to gain a certain degree of confidence in the accuracy of electromagnetic prospecting through comparisons with examples of actual TEM and drilling results.

The following diagrams show the results of analyses, and the results of drilling in the grounds of EWTEC. However, the drilling site was several tens of meters away from the practical training site, and there was a difference in relief between the two sites, with the training site being about 10m higher.
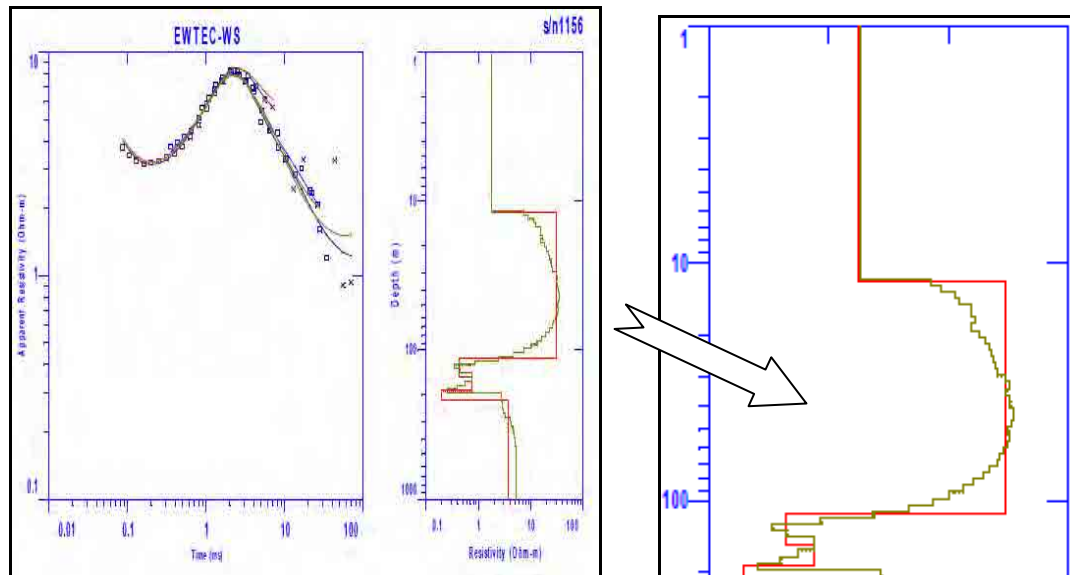

Figure 4.61: Resistivity analytic result of the EWTEC site

The geology of this practical training site consists mostly of basaltic materials. The surface consists of clayey soil and below that is basalt that is cross-crossed with fissures. Large-scale fissures were confirmed to exist from about -92m downward.

The analyzed relative resistivity structure shows low resistivity from around -100m, which is believed to be due to the influence of the fissures and saturation with groundwater. It should be noted that SWL was 29m.
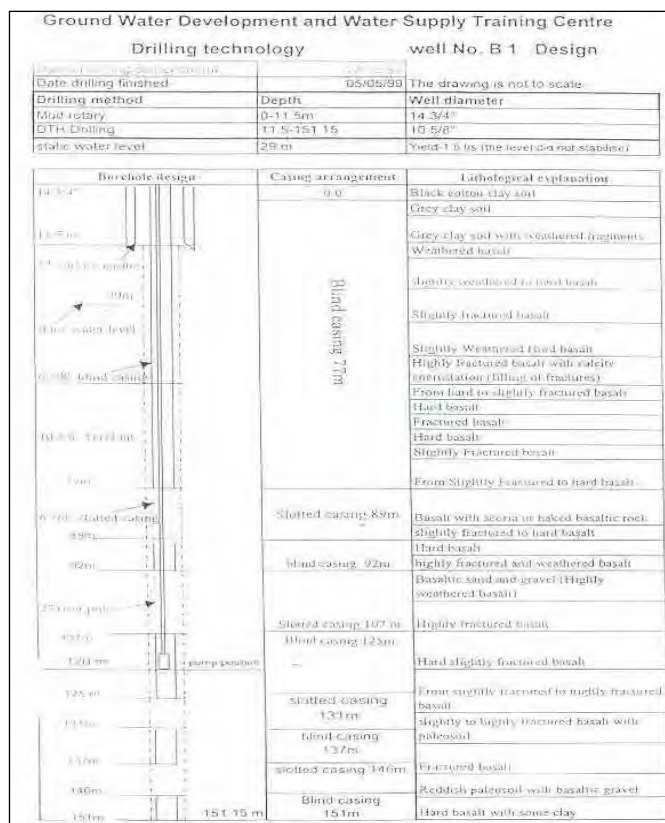
Figure 4.62: Geologic Columnar Section of the EWTEC Site

4.3.2 Technology transfer and the results of collaboration work with counterpart personnel

TEM workshop is one of the components of technology transfer to counterpart (C/P) personnel. The current ability of C/P personnel and the contents of technology transfer for TEM electromagnetic survey in the workshop are presented in the following sections:

a.1   Current capacity of C/P personnel with regard to TEM survey

- They have the basic knowledge on the method and operations of the TEM measurement
- They have no know-how about choice of appropriate size of transmitter loop for a targeted depth.
- They are not totally proficient in data analysis procedure

a.2   Major points of technology transfer

- The know-how on actual survey and data analysis have been transferred to the C/P personnel although the collaborated survey was limited to an area and, thus, could not cover various types of geology. They are expected to acquire more survey experience in different geological settings (e.g. alluvial terrain, volcanic terrain, fault and fractured zones) to enhance their capacity of survey operation and data analysis.
- The survey was only done with the fixed size of transmission loop in the workshop. In the future, different sizes of transmission loop should be employed to get the survey data

in order to analyze the relation between the survey depth and analytical resolution. Through this analysis, they should lean the limitation in survey depth and resolution for different frequency bands to be employed.

・ The data obtained through the collaborative survey was analyzed and discussed among the participants.

・ Data visualization method was explained to the participants.

a.3   Result of collaborative work with EWTEC

The collaborative work was conducted in the area of borehole 6 of this study (RVS BH-6) where EWTEC was conducting training on geophysical survey to participants. The work mainly covered instruction on field survey methods and operation of the survey equipment. The instructor was found to have the following advantages and disadvantages.

・ Although the instructor gives instructions on how to make preparations for the survey (survey line setting, survey points determination, laying out the transmission loop) as necessary, the participants did not sometimes clearly understand the instructions and the instructor had to do it by himself. Also, the group wasted some time owing to the mistake in survey of length when laying out the transmission loop.

・ The instructor has satisfactory understanding of the operation of the transmitter. On the other hand, as for the operation of the receiver, the instructor can somehow used to its routine operations, but did not have sufficient understanding of the various information shown on the display. The instructor could not properly adjust the noise level according to different intensity of signals by the use of the amplifier. Another thing observed was that he could not set the proper value for stacking (data collection frequency).

・ The instructor has understanding of series of necessary operations for the survey but he could not really evaluate the obtained data: he could not properly determine which obtained data should be employed for analysis.